Molecular and functional characterization of the HP1c complex in *Drosophila melanogaster*

Roman Kessler

TESI DOCTORAL UPF / 2014

Director de la tesi: Dr. Ferran Azorín Marín

Institut de Recerca Biomèdica de Barcelona i

Institut de Biologia Molecular de Barcelona (CSIC)

Tutora: Dra. Elena Hidalgo

Departament de Ciències Experimentals i de la Salut

Universitat Pompeu Fabra

ACKNOWLEDGEMENTS

After five years of work on this project, the thesis is written and an important and exciting period of my life is coming to an end. The development of this project would have been impossible without the help and support of many people.

First of all, I want to thank to Ferran, my thesis director, for offering me the possibility to carry out my PhD in his lab. He was always giving me efficient support during my thesis and his fascination for science helped to keep me motivated. I appreciated the way how he guided my thesis, being always there for discussing the project when I had some doubts, but on the same time leaving me plenty of freedom to develop my work independently.

Joan Font did an invaluable job in passing me over his project, introducing me to new techniques, helping to design the experiments and teaching me about HP1 proteins. It is largely thanks to Joan that my work in the lab started smoothly. During four years of my thesis Sergi accompanied me as desk neighbor and above all as a good friend. Thanks Sergi for all the good moments we have spent in the lab and for the many discussions about science, life and politics. I thank Johan, who joined the lab towards the end of my thesis, for the excellent contribution to the project and for helping to develop it further. Oscar Reina, thanks for making sense out of the experimental data and for all the time and effort you have invested related to my project. I really liked collaborating with you. I am very happy having Milos as a lab mate and as a friend, thanks for all the good times inside and outside the lab. Alicia, Esther, Estefania and Gemma did a great job in managing the lab, preparing reagents, helping with fly work and in general facilitating work in the lab. Thanks to all the past and present lab members for contributing to a lively atmosphere that made working there a pleasure. You were always very

open to help with protocols, advice on the project or whatever was necessary.

I am thankful to my tutor Elena Hidalgo and the other members of my thesis advisory committee, Marian Martinez and Andreu Casali. Thanks for the critical feedback during our annual meetings that helped develop my project further. My acknowledgement also goes to the facilities of the institute for invaluable support and assistance to my work.

Special thanks to all my running and cycling colleagues for the many wonderful trainings and races together all across Catalonia. The initial IRB marathon team to make me join them and to all the runners that helped to maintain the weekly training during all these years and for enjoying the hills of Collserola together.

Finally, I am very grateful to my mother, father, sister and grandparents for their continuous support and encouragement. Thanks as well for all the memorable moments we could spend together during the visits in Barcelona and in Switzerland.

ABSTRACT

Unlike characteristic HP1 proteins, the HP1c isoform of *Drosophila melanogaster* is a euchromatic protein. HP1c forms a complex with the zinc finger proteins ROW and WOC, which are crucial for HP1c function. In the present work, we aimed to further characterize the HP1c complex. We purified several novel factors that are associated with the complex. In particular, we characterize the ubiquitin receptor Dsk2 as an intrinsic subunit of the HP1c complex. Further, we show that the HP1c complex binds to TSS of actively transcribed genes and contributes positively to their transcription. The HP1c complex promotes an active chromatin state at target genes. We show evidence that this role involves regulation of H2Bub1 levels through Dsk2.

Al contrario de proteinas HP1 características, la isoforma HP1c de *Drosophila melanogaster* es una proteína eucromatica. HP1c se encuentra en un complejo con las proteínas "zinc finger" ROW y WOC, que son esenciales para la función de HP1c. En este trabajo, quisimos caracterizar el complejo HP1c en más detalle. Purificamos varios factores nuevos que se unen al complejo. En particular, caracterizamos el receptor de ubiquitina Dsk2 como una unidad principal del complejo HP1c. Además, demostramos que el complejo HP1c se une a TSS de genes que se transcriben activamente y que influye positivamente en su transcripción. El complejo HP1c favorece un estado activo de cromatina en los genes donde se encuentra. Nuestros resultados indican que este mechansimo incluye una regulación de los niveles de H2Bub1 a través de Dsk2.

PROLOGUE

The first member of the HP1 protein family was discovered in 1986 in *Drosophila*. Thereafter, extensive research efforts made HP1 one of the best characterized chromosomal proteins. Numerous studies on this protein gave important insights into the mechanisms of chromatin biology.

The HP1 protein family is highly conserved in eukaryotes and in most species several HP1 isoforms are present. It has emerged that HP1 proteins are involved in a tremendous variety of mechanisms, which involve heterochromatic gene silencing, active gene expression and regulation of genome integrity. While the heterochromatic functions of HP1 proteins have been described in great detail, other aspects of HP1 functions remain poorly understood.

In this thesis we used the model organism *Drosophila melanogaster* and its HP1c isoform to study its functions in euchromatin and gene regulation. The HP1c isoform is an excellent representative to address these aspects, as it is uniquely found in euchromatin. Previously, HP1c has been shown to occur in a complex with the zinc finger proteins ROW and WOC. This HP1c complex has also been suggested to regulate gene expression by a mechanism that remained vague.

We have determined the genome-wide binding profiles of subunits of the HP1c complex in S2 cells, showing that it binds to the TSS of actively transcribed genes. Further, we demonstrate that a functional HP1c complex contributes positively to target gene expression and is required for an active chromatin signature at target genes. In addition, we have obtained an extended understanding of the interaction partners of the HP1c complex.

Strikingly, we found that the ubiquitin receptor Dsk2 is a core subunit of the HP1c complex. Dsk2 is crucial for a functional HP1c complex, as it is required for recruitment to chromatin and for the transcriptional output of

target genes. Dsk2 is a member of the UbL/UBA family of ubiquitin receptors and has been described to regulate protein degradation by the proteasome. Our work reveals a novel function of Dsk2 at chromatin as a transcription factor that is independent of the proteasome. Dsk2 is evolutionarily conserved and has several homologs in humans, where they are known as Ubiquilins. Recently, some of these homologs have gained major interest, because of their association with neurodegenerative diseases. Currently it is not known whether the role of Dsk2 in transcription is conserved in other species. Nevertheless, our results might indicate a broader role for ubiquitin receptors as important players in chromatin regulation and transcription.

TABLE OF CONTENTS

Acknowledgements i

Abstract v

Prologue ix

Table of contents xiii

List of figures xxi

1. Introduction 1

1.1. Chromatin 3

1.1.1. The nucleosome 3

1.1.2. Higher order structure 5

1.1.3. Types of chromatin 7

1.1.3.1. Euchromatin and heterochromatin 7

1.1.3.2. Five colors chromatin 8

1.1.3.3. Insulators 10

1.1.4. Chromatin regulation 11

1.1.4.1. Histone variants 12

1.1.4.2. Post-translational histone modifications 14

1.1.4.3. Chromatin remodeling 17

1.1.4.4. DNA methylation 19

1.1.4.5. RNA 21

1.2. Transcription by RNA polymerase II 23

1.2.1. Initiation 23

1.2.2. Promoter proximal pausing 26

1.2.3. Elongation 29

1.2.4. Termination 30

1.3. HP1 proteins 32
1.3.1. Domain organization 33
1.3.1.1. The chromo domain 35
1.3.1.2. The chromo shadow domain 37
1.3.1.3. The hinge region 40
1.3.2. HP1 functions and recruitment 41
1.3.2.1. Heterochromatic functions 43
1.3.2.2. Euchromatic functions 49
1.3.2.3. DNA damage response 55
1.3.2.4. Telomeres 60
1.4. Extra-proteasomal ubiquitin receptors 62
1.4.1. Proteasomal functions 64
1.4.2. Rad23 in DNA damage response 67
1.4.3. Rad23 in transcriptional control 69
1.4.4. Dsk2 in neurodegenerative diseases 71
2. Objectives 73
3. Results 77
3.1. Analysis of the HP1 – H3K9me3 interaction 79
3.1.1. Conservation of the HP1 chromo domain 80
3.1.2. Specific binding to methylated H3K9me3 peptides 83
3.1.3. Abolishing H3K9me3 binding by point mutations 85
3.1.4. HP1c localization is independent of a functional methyl-binding cage 86
3.2. Purification of ROW and WOC complexes 91

3.2.1. Establishing the system 92

3.2.2. The purifications 94

3.2.3. Identification of ROW and WOC associated proteins 96

3.2.4. Validation by co-immunoprecipitation 99

3.3. The interaction with Dsk2 101

ABSTRACT 103

INTRODUCTION 104

RESULTS 106

dDsk2 interacts with the dHP1c/WOC/ROW transcription complex 106

The dHP1c-complex localizes at promoters of active genes and is required for transcription 108

dDsk2 is required for binding of the dHP1c-complex 110

dDsk2 regulates H2Bub1 114

DISCUSSION 118

SUPPLEMENTARY DATA 123

ACKNOWLEDGEMENTS 130

3.4. The interaction with Z4 and Chromator 131

3.4.1. Localization to polytene chromosomes 131

3.4.2. Genome-wide localization 135

3.4.3. Effects on target gene expression 139

3.5. Co-localization of BEAF-32 and the HP1c complex 142

4. Discussion 145

4.1. The function of the HP1 chromo domain 147

4.2. Genome-wide localization of the HP1c complex 151
4.3. Dsk2 is an intrinsic component of the HP1c complex 154
4.4. Interaction partners of the HP1c complex 158
4.5. The role in transcription 162
4.6. HP1 isoforms 167
4.7. Recruitment to chromatin 173
5. Conclusions 179
6. Materials and methods 183
6.1. Materials 185
6.1.1. Oligos 185
6.1.1.1. Designed oligos 185
6.1.1.2. Other oligos used 193
6.1.2. Plasmids 194
6.1.2.1. Generated plasmids 195
6.1.2.2. Other plasmids used 199
6.1.3. Antibodies 201
6.1.4. Fly lines 202
6.1.5. Stable S2 cell lines 206
6.2. Methods 207
6.2.1. Induction and purification of His-tagged proteins 207
6.2.2. Induction and purification of GST-tagged proteins 210
6.2.3. Immunostainings of polytene chromosomes 213
6.2.4. Histone peptide pull-down 215
6.2.5. Cellular fractionation 217

6.2.6. Histone acid extraction 218

6.2.7. RNAi in S2 cells by long double-stranded RNA..... 220

6.2.8. Transfection of S2 cells 222

6.2.9. RNA extraction from S2 cells 223

6.2.10. RT-qPCR 224

6.2.11. Co-immunoprecipitation 226

6.2.12. Chromatin-immunoprecipitation in S2 cells 230

6.2.13. Protein complex purification 235

6.2.14. Bioinformatics and Biostatistics analysis 241

7. Bibliography 245

LIST OF FIGURES

Figure 1. The structure of the nucleosome core particle. 4
Figure 2. Solenoid vs. zigzag model for chromatin secondary structure. .. 6
Figure 3. Five principal types of chromatin. 9
Figure 4. Readers of post-translational histone modifications. 16
Figure 5. Histone chaperones mediate replication-coupled and replication-independent nucleosome assembly. 18
Figure 6. Distribution of DNA methylation and hydroxymethylation in mammals. 20
Figure 7. Average enrichment profile of phosphorylation marks of the RNA pol II CTD..... 24
Figure 8. H2B ubiquitylation in gene activation. 26
Figure 9. Establishment and release of paused RNA pol II. 28
Figure 10. HP1 proteins are characterized by a chromo and a chromo shadow domain..... 34
Figure 11. Examples of direct HP1 interacting partners. 40
Figure 12. *Drosophila* HP1 isoforms. 42
Figure 13. Model for HP1 spreading in heterochromatin. 44
Figure 14. Model for HP1 (Swi6) oligomerization. 46
Figure 15. Models for *Drosophila* HP1 functions in the Piwi pathway... 48
Figure 16. ROW and WOC are required for mutual and for HP1c recruitment. 55
Figure 17. Model for the role of HP1β release in ATM activation. 57
Figure 18. Model for the role of HP1 in recruitment of DNA damage response proteins. 59
Figure 19. Proteasome associated ubiquitin receptors. 63
Figure 20. UbL/UBA proteins regulate proteasomal degradation..... 66
Figure 21. Functions of Rad23 at chromatin. 70
Figure 22. The HP1 chromo domain. 81
Figure 23. Histone peptide pull-down. 84

Figure 24. HP1c localization to polytene chromosomes is independent of a functional methyl-binding cage. 88
Figure 25. A hypomorphic *HP1b* allele. 90
Figure 26. Induction of TAP tagged ROW and WOC in S2 cells. 93
Figure 27. Purification of ROW and WOC protein complexes. 95
Figure 28. Proteins identified in ROW and WOC complex purifications. 98
Figure 29. Validation of interactions by co-immunoprecipitation. 100
Figure 30. The dHP1c-complex interacts with dDsk2. 107
Figure 31. The dHP1c-complex localizes at TSS. 109
Figure 32. dDsk2 does not mediate proteolytic degradation of the dHP1c-complex. 111
Figure 33. dDsk2 is required for binding of the dHP1c-complex and *vice versa*. 113
Figure 34. The UBA domain of dDsk2 binds H2Bub1. 115
Figure 35. dDsk2 regulates H2Bub1. 117
Figure 36. A model of the contribution of the dHP1c-complex to transcription regulation. 119
Figure 37. Co-localization of Z4 and the HP1c complex at polytene chromosomes. 132
Figure 38. HP1c localization is independent of Z4 and Chromator. 133
Figure 39. Z4 localization is independent of the HP1c complex. 134
Figure 40. Number of peaks identified in ChIP-seq experiments. 136
Figure 41. Enrichment of Z4 and the HP1c complex at TSS. 137
Figure 42. Comparison with ChIP-chip data for HP1c and Chromator. 138
Figure 43. Target gene overlap between Z4, Chromator and the HP1c complex. 139
Figure 44. Z4 and the HP1c complex affect target gene expression differently. 141
Figure 45. Comparison with BEAF-32 ChIP-chip data. 143

1. INTRODUCTION

1.1. Chromatin

The DNA in the nucleus of eukaryotic cells is not naked, but instead is associated with histones and other chromosomal proteins, a structure called chromatin. Chromatin mediates compaction of the DNA within the nucleus and plays an important role in all processes that involve DNA, such as replication, transcription, damage repair and cell division. Dynamic regulation of chromatin structure occurs on different levels. Below I describe how chromatin is organized and outline some regulatory mechanisms that act on chromatin.

1.1.1. The nucleosome

Major advance in the understanding on how DNA packaging is achieved was obtained from a series of studies performed in the 1970s. Nuclease digestion experiments of purified chromatin revealed that histone proteins are regularly spaced along the DNA (Clark & Felsenfeld, 1974; Kornberg, 1974; Noll, 1974). These experiments took advantage of the fact that DNA associated with proteins is protected from digestion. When digestion was done under limited conditions, the chromatin was cut into DNA fragments of approximately 200bp and multiples thereof. When the chromatin was digested to completion the resulting fragments were of 146bp. These experiments suggested that chromatin consists of evenly spaced units of approximately 150bp of DNA that is associated with histones and is separated by 50-70bp of linker DNA. By electron microscopy, a 10nm fiber can be observed, a structure known as beads on a string (Olins & Olins, 1974). Each of these beads is a nucleosome made

up of an octamer containing two of each core histones: H2A, H2B, H3 and H4 (Kornberg, 1977). The core histones are small and basic proteins that consist of a globular domain and flexible terminal extensions that protrude from the nucleosome. Further, a histone H1, the linker histone, is attached to each nucleosome forming a chromatosome. In 1997 Luger et al. solved the X-ray crystal structure of the nucleosome at a resolution of 2.8 Å (Luger *et al.*, 1997) (Figure 1). The structure reveals the protein-protein and the protein-DNA interactions within the nucleosome. The globular domains of the histones make multiple contacts with the DNA, which is wrapped 1.65 times around the octamer. The interactions with the DNA involve mainly the phoshpodiester backbone of the double helix, which allows that the octamer can bind DNA largely independent form its sequence all over the genome.

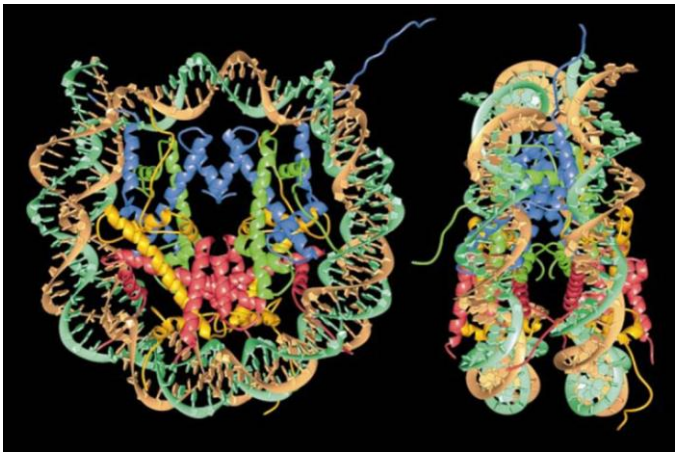

Figure 1. The structure of the nucleosome core particle.
Two different views of the core nucleosome particle are depicted. Shown are the ribbon traces for the DNA phosphodiester backbones (brown and turquoise) and the main chains of the eight histone proteins (H2A, yellow; H2B, red; H3, blue; H4, green). Extracted from (Luger *et al.*, 1997).

1.1.2. Higher order structure

The primary structure, the 10nm fiber, is further folded and adopts a complex condensed conformation that is still poorly understood. The linker histone H1 is thought to promote the formation of such structures by shielding negative charges of the linker DNA (McGhee & Felsenfeld, 1980). Chromatin has been observed as a 30nm fiber and has been suggested to be the main conformation during interphase (Widom & Klug, 1985; Williams *et al.*, 1986). Two different models to explain the formation of the 30nm fiber are usually considered: the solenoid and the zigzag model (reviewed in Luger *et al.*, 2012) (Figure 2). The solenoid conformation is a one-start helix, where consecutive nucleosomes interact with each other and involves bending of the linker DNA. The zigzag model describes a two-start helix that involves interactions of alternate nucleosomes and relatively straight linker DNA. There is experimental evidence that both of them might actually occur (Grigoryev *et al.*, 2009). The length of the linker DNA might have an influence on the conformation (Luger *et al.*, 2012). Shorter linker DNA energetically favors the zigzag structure, while longer linker DNA favors the solenoid structure.

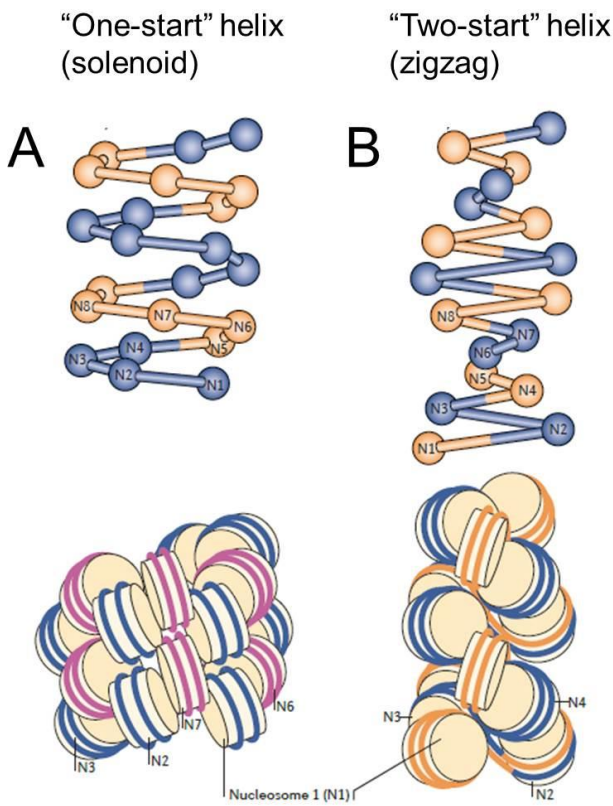

Figure 2. Solenoid vs. zigzag model for chromatin secondary structure.
(A) In the solenoid model, consecutive nucleosomes (n, n+1) interact with each other. The result is a one-start helix. At the bottom, alternative helical turns are colored in blue and magenta. **(B)** In the zigzag model, alternated nucleosomes (n, n+2) interact with each other. The outcome of this folding is a two-start helix. At the bottom, alternative nucleosome pairs of the helices are shown in blue and orange. Extracted from (Luger *et al.*, 2012).

Recently, evidence against the existence of a 30nm chromatin fiber has been obtained (Fussner *et al.*, 2011; Nishino *et al.*, 2012). The 10nm fiber might instead fold into more diverse and irregular higher order structures than previously anticipated. These fibers, independently of their exact nature, fold into larger chromatin loops thereby reaching a higher level of condensation. The most condensed state is reached in metaphase

chromosomes, which are approximately 1.5 µm in diameter and represent a 10'000 fold compaction. This high degree of condensation involves hyperphosphorylation of histones and depends on condensins, cohesins and topoisomerases (reviewed in Allis *et al.*, 2007).

1.1.3. Types of chromatin

1.1.3.1. Euchromatin and heterochromatin

The chromatin of non-dividing cells is traditionally classified into two main types of chromatin states that can be distinguished by light microscopy: a light staining area that represents a more open type of chromatin called euchromatin and a dark staining area that results from a more condensed form of chromatin known as heterochromatin (Heitz, 1928). Heterochromatin localizes mainly to the periphery of the nucleus, replicates late in S phase and has a low meiotic recombination rate (reviewed in Elgin, 1996; Elgin & Grewal, 2003). Heterochromatin can be subdivided into constitutive and facultative heterochromatin. Constitutive heterochromatin at centromeres and telomeres is poor in coding genes and its underlying DNA sequence is repetitive. These regions contribute to genome integrity by ensuring proper chromosome segregation during mitosis and meiosis and by protecting the chromosome ends (Yunis & Yasmineh, 1971). Notable cases are the Y chromosomes of mammals and *Drosophila* and the fourth chromosome of *Drosophila*, which are mostly heterochromatic and show some peculiar features (reviewed in Brown, 2002; Riddle *et al.*, 2009). Facultative heterochromatin on the other hand are regions that are not permanently in a silenced state, but where a more condensed type of chromatin can be developmentally induced. Examples

of facultative heterochromatin are the inactivation of one female X chromosome in mammals and the developmentally induced silencing of gene promoters (reviewed in Craig, 2005). Euchromatin represents a more open and accessible state of chromatin that contains mainly actively transcribed genes and only represents a relative small fraction of the genome. By electron microscopy the euchromatic regions can be observed to form loops of 40–100kb in length, which are attached to the nuclear matrix (Comings, 1967).

1.1.3.2. Five colors chromatin

Recently, the advent of techniques that permit the generation of genome-wide binding patterns of a large number of chromosomal proteins led to the proposition of more sophisticated classifications of chromatin. Filion et al. determined the binding profiles of 53 chromatin proteins in *Drosophila* Kc167 cells using the DamID technique (Filion *et al.*, 2010). By applying computational methods to analyze the differential binding patterns of these 53 proteins, the authors observed that chromatin can be subdivided into five main types. A color code is used to denominate these chromatin types: GREEN, BLUE, BLACK, YELLOW and RED chromatin (Figure 3). Most of the proteins are found in more than one chromatin type, it is the combination of different proteins that defines each group. The median length of the chromatin domains is 6.5kb and the longest ones reach an extension of several hundreds of kilobases. GREEN and BLUE are known heterochromatic chromatin types. GREEN is bound by HP1a and Su(var)3-9, contains H3K9me2 and is mainly found at pericentromeres and on the fourth chromosome. BLUE is bound by Polycomb-group proteins and is enriched in H3K27me3.

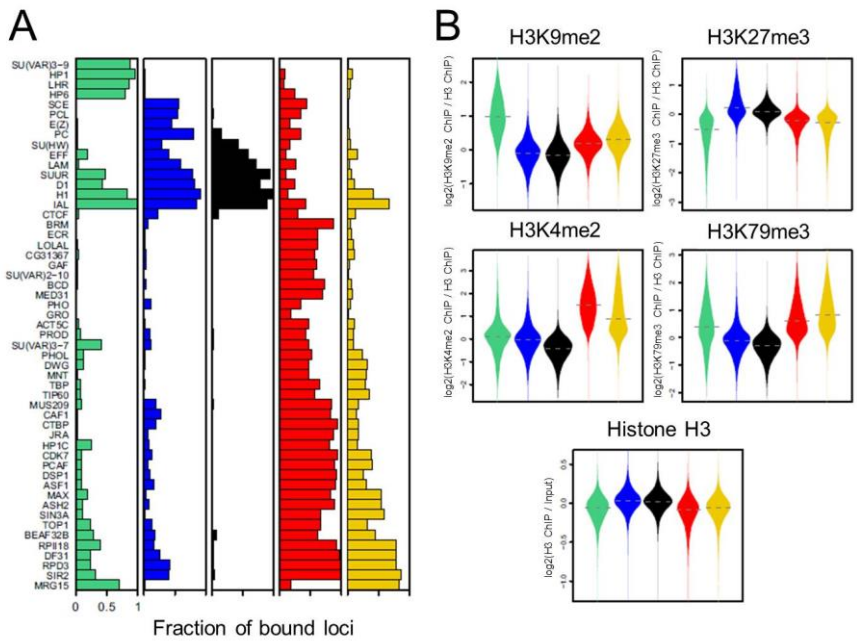

Figure 3. Five principal types of chromatin.
(A) The genome-wide binding profiles for 53 chromosomal proteins were determined by DamID in *Drosophila* cells. A principal component analysis revealed five main chromatin types (color coded) that are characterized by the combination of bound proteins. GREEN, BLUE and BLACK are silenced loci, while RED and YELLOW are actively transcribed loci. **(B)** The enrichment of known heterochromatic (H3K9me2 and H3K27me3) and euchromatic (H3K4me2 and H3K79me3) histone modifications in the five different chromatin types is shown. The levels of histone modifications were determined by genome-wide ChIP and normalized with respect to histone H3. Extracted from (Filion *et al.*, 2010).

Interestingly, almost half of the probed genome is BLACK chromatin that is a different state of silenced chromatin enriched in histone H1, D1, IAL and SUUR. BLACK is relatively gene-poor and the expression of these genes is either not detectable or very low. The remaining YELLOW and RED chromatin are both euchromatic and the genes residing in these domains are actively transcribed at similar levels. YELLOW and RED share a set of proteins, such as the histone deacetylases RPD3 and SIR2,

but also exhibit several differences. RED specific proteins are the remodeler Brahma, GAGA factor and subunits of the Mediator and the CAF1 complexes. YELLOW on the other hand is specifically enriched in MRG15, a chromo domain protein that is known to bind H3K36me3 in humans (Zhang *et al.*, 2006). Indeed, H3K36me3 is enriched along genes in YELLOW but not RED chromatin (Filion *et al.*, 2010).

1.1.3.3. Insulators

Specialized sequences called insulators that can act as boundaries between chromatin types have been described initially in *Drosophila* and later in other eukaryotes (Kellum & Schedl, 1991; Bushey *et al.*, 2008). Insulators have been shown to function both as barriers that impede the spreading of heterochromatin and as enhancer blockers that interfere with the crosstalk between an enhancer and its promoter. In *Drosophila* several classes of insulators have been described that differ in the DNA binding proteins recognizing the respective boundary sequences, but all of them share the recruitment of CP190 and Mod(mdg4) (reviewed in Yang & Corces, 2012). Striking similarities have been observed between insulators and promoters, which led to the proposition that insulators may have evolved from a class of promoters (reviewed in Raab & Kamakaka 2010). Mainly in yeast it has been described that promoters can act as insulators and that this function is independent of ongoing transcription. Transcription factors recruited by promoters might promote an open chromatin conformation that impedes heterochromatin spreading. Interestingly, in *Drosophila* several boundary proteins, such as CTCF, BEAF-32 and CP190 have been shown to localize also to promoters. An important principle of insulator function appears to be the occurrence of long range interactions and

chromatin loops (reviewed in Raab & Kamakaka, 2010; Phillips-Cremins & Corces, 2013). Thus, it seems that insulators determine chromatin domains via a role in the organization of higher order chromatin structure. Insulators not only interact with each other but also with regulatory elements and with promoters. Such interactions are thought to play a role in the targeting of enhancers to their appropriate promoters and loop formation appears to facilitate the formation of distinct chromatin domains (Yang & Corces, 2012). Furthermore, insulators have been described to cluster at so-called insulator bodies (Raab & Kamakaka, 2010).

1.1.4. Chromatin regulation

As described above, DNA within the eukaryotic nucleus is highly compacted in the context of chromatin. Nevertheless, the underlying DNA needs to be accessible, so that fundamental processes such as transcription, replication and repair can be carried out. The nucleosome can be seen as an obstacle that obstructs the access of machineries that work on the DNA molecule. The cell features a set of mechanisms that dynamically regulate the chromatin structure and that play an important role in all processes that involve DNA. These functions do not merely make the DNA exposed and more accessible, but also are contributing more directly to these processes, such as by mediating recruitment of chromatin factors. In the following paragraphs I review a few aspects that are important in the regulation of chromatin structure.

1.1.4.1. Histone variants

Histones can be broadly classified into two groups, the canonical histones and the histone variants. The genes encoding the canonical histones are found in repeat arrays in the histone cluster and their transcription is coupled to replication. The histone variants on the other hand are constitutively expressed from single genes. While the canonical histones make up the nucleosomes that have a general function in genome packaging and gene regulation, the nucleosomes that contain histone variants are typically associated with more specific functions. Histone variants have been implicated in DNA damage repair, meiotic recombination, chromosome segregation, sex chromosome condensation, packaging of sperm chromatin and transcription initiation and termination (reviewed in Talbert & Henikoff, 2010). Histone variants differ from their canonical counterparts mainly in the terminal domains, while the histone fold domain is more conserved. Differences in the amino acid sequence can affect nucleosome structure and stability, susceptibility to modifications and interactions with other proteins. A large number of histone variants have been described and functionally studied (Talbert & Henikoff, 2010; Yuan & Zhu, 2012). Below, I describe some of the various functions of histone variants by means of a few examples.

CenH3 is an H3 variant that is incorporated into centromeric nucleosomes and is crucial for centromere identity and kinetochore assembly. It was suggested that CenH3 containing nucleosomes might wrap the DNA right-handed, while the nucleosomes containing canonical H3 wrap the DNA left-handed (Furuyama & Henikoff, 2009). Furthermore, some studies indicate that centromeric nucleosomes containing CenH3 might not be octameric. In *Drosophila*, centromeric nucleosomes were proposed to be hemisomes that contain one molecule of each H2A, H2B, CenH3 and H4

(Dalal *et al.*, 2007). Unconventional centromeric nucleosomes might also exist in yeast, where hexamers were reported (Mizuguchi *et al.*, 2007). However, the nature of CenH3 containing nucleosomes is controversial and requires further experimental clarification (Lavelle *et al.*, 2009).

Another well studied H3 variant that is widely conserved in eukaryotes is H3.3. In most species H3.3 only differs in four amino acids from the canonical variant (reviewed in Elsaesser *et al.*, 2010). The H3.3 variant is assembled into chromatin by the HIRA complex, in contrast to the canonical H3 that is assembled by the CAF1 complex (Tagami *et al.*, 2004). H3.3 replaces the canonical H3 in transcribed genes, promoters and regulatory elements. Nucleosomes that contain H3.3 were found to be less stable and might thereby contribute to a chromatin structure that facilitates transcription.

In mammals and yeast, the histone H2A.Z has also been described to be related to active transcription. H2A.Z is enriched at promoter regions, where it is promoting RNA pol II recruitment (Adam *et al.*, 2001; Hardy *et al.*, 2009). The H2A.Z variant was also found to function in the DNA damage response pathway, where it seems to promote efficient repair and is incorporated in the flanking regions of DNA break sites (reviewed in Ransom *et al.*, 2010). Both in transcription and damage repair the assembly of histone variants was suggested to partially function by making the chromatin more accessible for the machineries. In addition, the variants might index the chromatin for these functions and recruit partners that bind specifically to the variant (reviewed in Allis *et al.*, 2007). Curiously, H2A.Z is also associated with heterochromatin. A common function of H2A.Z in these different environments appears to be its tendency to form stably positioned nucleosomes. The *Drosophila* histone H2Av is a H2A.Z-like variant, but interestingly it shares a C-terminal phosphorylation motif with another mammalian H2A variant,

H2A.X (Talbert & Henikoff, 2010). ATM mediated phosphorylation of H2A.X (γ-H2A.X) is an early event in the DNA damage response (Rogakou *et al.*, 1998).

1.1.4.2. Post-translational histone modifications

Histones are subject to a large variety of post-translational modifications. This growing number of modifications includes phosphorylation, acetylation, methylation, ubiquitylation, sumoylation, ADP-ribosylation, biotinylation, deimination and proline isomerization (reviewed in Kouzarides, 2007). Lysines can be mono-, di- or trimethylated and arginines can be mono-, symmetrically di- or asymmetrically dimethylated. Mainly the terminal histone tails that protrude from the nucleosome serve as a platform for modifications. Histone modifications correlate with biological functions and most of them correlate with either repressed or active chromatin (reviewed in Allis *et al.*, 2007). Acetylation is correlating with active transcription and phosphorylation is generally associated with condensed chromatin. Methylation in contrast can be associated both with activation or repression, depending on the residue that is modified and where in the genome it is found (Kouzarides, 2007). Methylated histone lysines show specific profiles at active and inactive genes. Histone modifications also have been described to function in other processes such as DNA repair and replication. Furthermore, histone modifications are also regulated during the cell cycle (reviewed in Black *et al.*, 2012; Wang & Higgins, 2013). For most histone modifications, chromatin associated enzymes have been described that mediate, often with high substrate specificity, the establishment or removal of the mark. This suggests that histone modifications are much more dynamic than

initially anticipated. Numerous examples of crosstalk between different modifications have been described, which can be both of synergistic or antagonistic nature (reviewed in Bannister & Kouzarides, 2011). Modified histones regulate chromatin function via two main mechanisms: by directly altering the chromatin structure and by affecting binding of effector proteins. Acetylation and phosphorylation reduce the positive charge of histones and might therefore affect the interaction with DNA, leading to less compacted chromatin. Apart from this direct structural effect, modifications can positively or negatively affect binding of chromosomal proteins. For many of the modifications, binding proteins have been described that can interact specifically (reviewed in Bycroft, 2011; Musselman *et al.*, 2012) (Figure 4). Typically, chromosomal complexes comprise several binding domains for histone modifications. Thus, it seems that modifications are recognized in a combinatorial way (Musselman *et al.*, 2012). It has been hypothesized that a histone code or epigenetic code might exist, in analogy to the genetic code (reviewed in Strahl & Allis, 2000). In this scenario, the combination of post-translational histone modifications is translated into a functional output, by the action of readers, which can recognize this code. Recent studies however suggest that the situation is much more complicated, as the readout of histone modifications appears to depend on many other variables (reviewed in Smith & Shilatifard, 2010). Instead, modifications of histones might function in a way not much different from post-translational modifications of any other protein.

A

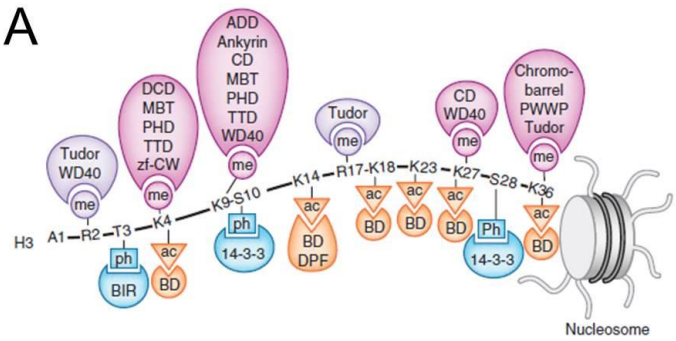

B

Recognition of	Reader	Histone PTM
Methyllysine	ADD	H3K9me3
	Ankyrin	H3K9me2, H3K9me1
	BAH	H4K20me2
	Chromo-barrel	H3K36me3, H3K36me2, H4K20me1, H3K4me1
	Chromodomain	H3K9me3, H3K9me2, H3K27me3, H3K27me2
	DCD	H3K4me3, H3K4me2, H3K4me1
	MBT	H3Kme1, H3Kme2, H4Kme1, H4Kme2
	PHD	H3K4me3, H3K4me2, H3K9me3
	PWWP	H3K36me3, H4K20me1, H4K20me3, H3K79me3
	TTD	H3K4me3, H3K9me3, H4K20me2
	Tudor	H3K36me3
	WD40	H3K27me3, H3K9me3
	zf-CW	H3K4me3
Methylarginine	ADD	H4R3me2s
	Tudor	H3Rme2, H4Rme2
	WD40	H3R2me2
Acetyllysine	Bromodomain	H3Kac, H4Kac, H2AKac, H2BKac
	DBD	H3KacKac, H4KacKac
	DPF	H3Kac
	Double PH	H3K56ac
Phosphoserine or phosphothreonine	14-3-3	H3S10ph, H3S28ph
	BIR	H3T3ph
	Tandem BRCT	H2AXS139ph
Unmodified histone	ADD	H3un
	PHD	H3un
	WD40	H3un

Figure 4. Readers of post-translational histone modifications.
(A) The N-terminal tail of histone H3 and post-translational modifications with their respective reader domains are shown. methylation, me; phosphorylation, ph; acetylation, ac. **(B)** The table specifies the variety of histone reader domains and the post-translational modifications that are known to be their targets. Extracted from (Musselman *et al.*, 2012).

Histone modifications are often referred to as epigenetic marks. However, this annotation is somewhat misleading, as there is little evidence to date that they are truly epigenetic (reviewed in Campos & Reinberg, 2009; Henikoff & Shilatifard, 2011). Epigenetic marks in its basic definition are chromatin components on top of the DNA sequence that affect transcription and are inherited and self-propagated through cell divisions (Campos & Reinberg, 2009).

1.1.4.3. Chromatin remodeling

Chromatin can be remodeled in different ways, which includes regulation of nucleosome positioning as well as nucleosome assembly and disassembly. One mechanism to remodel chromatin is the action of ATP-dependent enzymes that belong to the SWI/SNF family (reviewed in Narlikar *et al.*, 2013). These complexes possess a translocase activity that allows them to move along the DNA and to reposition nucleosomes. Another group of proteins that play an important role in regulating chromatin structure are histone chaperones (Figure 5). Histone chaperones can bind histones and function in nucleosome assembly. During replication, histone chaperones are disassembling nucleosomes in front of the replication fork and after passage mediate reassembly of both parental and newly synthesized histones. Histone chaperones also mediate replacement of canonical histones with variants and promote the mobilization of nucleosomes during transcription and DNA repair (reviewed in Ransom *et al.*, 2010; Burgess & Zhang, 2013). Many relations between histone chaperones and post-translational histone modifications have been described. Histone chaperones can mediate both establishment and removal of certain histone modifications (reviewed in

Avvakumov *et al.*, 2011). The action of histone chaperones has been proposed to be an elegant mechanism to reset the modification state of histones (reviewed in Allis *et al.*, 2007).

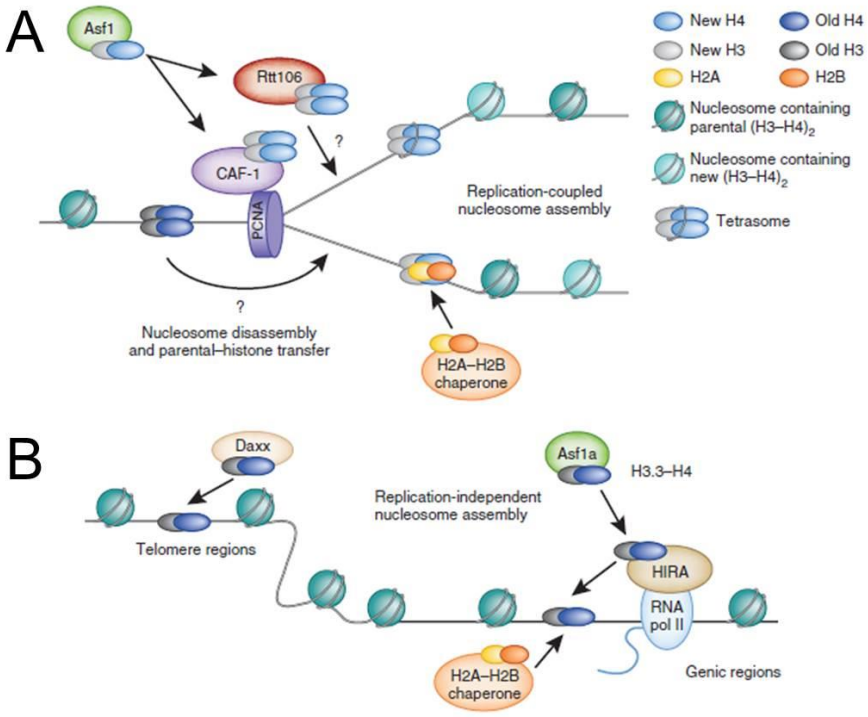

Figure 5. Histone chaperones mediate replication-coupled and replication-independent nucleosome assembly.
(A) Histone chaperones are involved in replication-coupled disassembly and assembly of nucleosomes. Asf1 transfers newly synthesized H3-H4 to CAF-1 and Rtt106 for tetrasome formation and deposition onto the replicated DNA. Specialized chaperones mediate the assembly of H2A-H2B dimers to complete the nucleosome. The mechanisms that are involved in reassembly of parental histones are less well understood. **(B)** Histone chaperones regulate also the exchange and mobility of histones independently from replication. For example, Daxx and HIRA assist the assembly of H3.3-H4 dimer variant into telomeric and transcribed regions, respectively. Extracted from (Burgess & Zhang, 2013).

1.1.4.4. DNA methylation

DNA can be methylated at carbon 5 of cytosines and is occurring mainly as symmetrical mark at CpG dinucleotides (reviewed in Guibert & Weber, 2013). DNA methylation has been mainly studied in mammals and is enriched in non-coding regions and transposons. It has been proposed that DNA methylation functions as a defense mechanism to silence sequences of foreign origins. Methylated cytosines have a highly increased rate of C-T transitions, as a result of a deamination reaction. This might contribute to the deactivation of parasitic DNA sequences. In highly repetitive sequences on the other hand, DNA methylation contributes to genome integrity (reviewed in Allis *et al.*, 2007). As indicated above, DNA methylation has been related to silencing. One silencing mechanism involves methyl-binding proteins such as MeCP2, which then mediate the recruitment of histone deacetylases. Another mechanism of DNA methylation might be the disruption of binding sites for transcription factors (Allis *et al.*, 2007). However, also positive correlations between DNA methylation and gene expression have been described (reviewed in Hellman & Chess, 2007; Guibert & Weber, 2013). DNA methyltransferases are responsible for de novo methylation and maintenance after replication, when DNA is found hemimethylated. Thereby, DNA methylation can be self-propagated through cell divisions and thus represents a true epigenetic mark. CpG dinucleotides are depleted from vertebrate genomes, occurring at less than 25% of the expected frequency. The explanation for this depletion are deamination events of methylated cytosines into thymines (Guibert & Weber, 2013). However, exceptions are the so-called CpG islands that are regions with high CpG density that are found in the promoter region of approximately two thirds of mammalian genes. CpG islands are mostly unmethylated,

while the CpG-poor sequences are heavily methylated (Guibert & Weber, 2013) (Figure 6). It is not well known, what are the determinants that cause the reduced methylation levels at CpG islands. CpG-rich promoter regions however can be de novo methylated, which induces silencing (reviewed in Beisel & Paro, 2011).

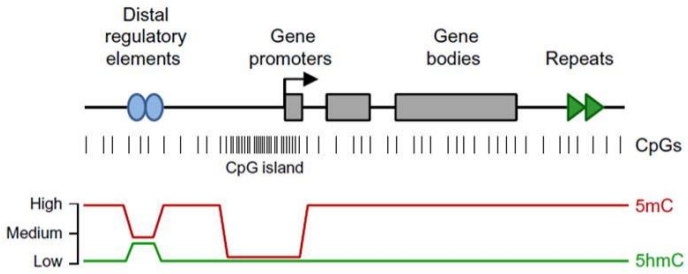

Figure 6. Distribution of DNA methylation and hydroxymethylation in mammals.
Different genomic features and the frequency of CpG dinucleotides are indicated. CpGs are frequent at gene promoters (CpG islands) and depleted from the rest of the genome. CpGs tend to be highly methylated (5mC), except for CpG islands that are mostly unmethylated and for regulatory elements that are only moderately methylated. Levels of hydroxymethylation (5hmC) are low compared to methylation and are found enriched at regulatory elements. Extracted from (Guibert & Weber, 2013).

Recent studies have described hydroxymethylated cytosines, which are converted from methylated cytosines by the action of TET enzymes. Unlike DNA methylation, hydroxymethylation levels vary a lot between different cell types, being most abundant in ES cells and the nervous system (Guibert & Weber, 2013). Hydroxymethylation might be an intermediate step in a replication independent DNA demethylation process. Hydroxymethylation was found to be enriched at CpG-poor

enhancers, suggesting a possible role in gene regulation (Guibert & Weber, 2013) (Figure 6).

In *Drosophila*, DNA methylation is largely absent (Allis *et al.*, 2007). This is in agreement with the observation that CpG dinucleotides are not depleted in the *Drosophila* genome (Guibert & Weber, 2013). However, DNA methylation does not appear to be completely lost in *Drosophila*. The *Drosophila* genome encodes a DNA methyltransferase and a methylcytosine binding protein. Further, DNA methylation has been detected in *Drosophila*, with higher levels in the embryo and very little methylation in the adult fly (Mandrioli & Borsatti, 2006).

1.1.4.5. RNA

RNAi is a conserved mechanism to mediate post-transcriptional gene silencing by using short antisense RNA to inhibit translation or to induce mRNA degradation. An interesting link between the RNAi machinery and chromatin structure was found in yeast, where components of the RNAi machinery are involved in heterochromatin formation (Volpe *et al.*, 2002). Recent studies showed that gene silencing by RNAi is a conserved mechanism in plants, fungi and metazoans. RNAi dependent silencing can be mediated through H3K9me3 or DNA methylation (reviewed in Castel & Martienssen, 2013). It also has become clear that noncoding RNAs appear to play a broader function in chromatin regulation. RNA has been shown to be an important factor for the action of chromatin modifiers (reviewed in Nagano & Fraser, 2011; Wang & Chang, 2011). Long noncoding RNAs (lncRNAs) can mediate the recruitment of chromatin modifiers, which in some cases was shown to occur co-transcriptionally. lncRNAs might also function as scaffolds for the assembly of chromatin

modifying complexes. Another role of lncRNA appears to be the formation of chromatin loops, in concert with CTCF and cohesin (Nagano & Fraser, 2011). A RNA component has also been described to contribute to various aspects of HP1 function (see chapter 1.3).

1.2. Transcription by RNA polymerase II

Eukaryotes possess three different RNA polymerases (RNA pol) for the transcription of nuclear genes. These polymerases are multi-subunit proteins that transcribe different non-overlapping sets of genes. Here, I focus on RNA pol II, which transcribes all protein coding genes and a large fraction of non-coding RNAs. RNA pol I transcribes ribosomal RNAs and RNA pol III transcribes transfer RNAs and some other non-coding RNAs (reviewed in Brown, 2002).

1.2.1. Initiation

The first step in transcription initiation involves general transcription factors (GTFs) that make contact with the promoter sequence of the gene to be transcribed. There are different types of promoters that vary in having different combinations of sequences, including an AT-rich TATA box upstream of the transcription start site (TSS), an initiator sequence overlapping with the TSS and CpG islands (reviewed in Brown, 2002; Lenhard *et al.*, 2012). An initial contact with the core promoter is made by the GTF TFIID, which is a complex that contains the TATA-binding protein and associated proteins. Subsequently, the other GTFs and RNA pol II are recruited and make up the pre-initiation complex (PIC). In order to efficiently initiate transcription by RNA pol II, the action of co-activators and chromatin remodelers is required to overcome the nucleosome barrier. Co-activators include DNA binding proteins that bind to upstream promoter elements or enhancer sequences and that contact the PIC and thereby help stabilizing it. Some co-activators such as the

mediator complex do not bind directly to DNA, but rather act as a scaffold or platform that communicates between other activators and RNA pol II, to which the mediator complex can directly bind. Also the SAGA complex has been suggested to function as a scaffold to assist assembly of GTFs and RNA pol II. Further, ATP-dependent nucleosome removal by SWI/SNF from the promoter region also facilitates PIC formation (reviewed in Weake & Workman, 2010). Once the PIC is assembled a series of further events is required, which involves several modifications of histones and RNA pol II. A central role plays the C-terminal domain (CTD) of the largest subunit, RBP1, of RNA pol II. In mammals, the CTD consists of 52 repeats of the heptapeptide Tyr-Ser-Pro-Thr-Ser-Pro-Ser, which is subject to various modifications and in particular to phosphorylation (reviewed in Brookes & Pombo, 2009) (Figure 7).

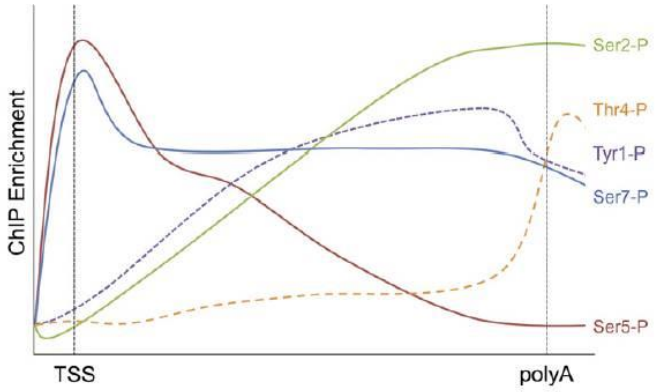

Figure 7. Average enrichment profile of phosphorylation marks of the RNA pol II CTD.
The CTD repeats of RNA pol II can be phosphorylated (P) at several residues. The scheme shows the average enrichment profiles of these modifications, which have been determined in ChIP experiments, with respect to the transcription start site (TSS) and the polyadenylation site (polyA) of genes. Ser5-P and Ser7-P peak at the TSS, while Tyr1-P, Ser2-P and Thr4-P are more enriched towards the 3'-end of the average gene. Extracted from (Heidemann *et al.*, 2013).

Recruitment of RNA pol II to promoters occurs in a hypo-phosphorylated state and then the CTD gets phosphorylated at Ser5 by the GTF TFIIH. This phosphorylation event is required for promoter clearance and for the recruitment of the RNA capping machinery. In yeast, Ser5 phosphorylation also stimulates methylation of H3K4 by the histone methyltransferase Set1.

Another mechanism that appears to contribute to H3K4 methylation at promoters is an activator dependent recruitment of the E2 and E3 enzymes Rad6 and Bre1, which are responsible for H2B monoubiquitylation (H2Bub1) (Kao *et al.*, 2004; Kim, Hake, *et al.*, 2005; Wood *et al.*, 2005) (Figure 8). The target of this ubiquitylation mark in H2B is K120 in mammals, K123 in *S. cerevisiae* and K118 in *D. melanogaster*. In yeast, this ubiquitylation is dependent the BUR complex. The requirement of the BUR complex for H2Bub1 involves a phosphorylation event in Rad6 and the recruitment of the PAF complex (Laribee *et al.*, 2005; Wood *et al.*, 2005). H2Bub1 is involved in a histone crosstalk that stimulates methylation of both H3K4 and H3K79 (Lee *et al.*, 2007). Interestingly, H2Bub1 has also a negative effect on transcription, at least in yeast. The Ubp8 subunit of the SAGA complex deubiquitylates H2Bub1 and is required for Ctk1 dependent phosphorylation of Ser2 of the RNA pol II CTD, and thus for release into elongation (Wyce *et al.*, 2007). Promoter clearance is an inefficient step, as transcription is frequently aborted after a few nucleotides, which leads to truncated transcripts (Brown, 2002).

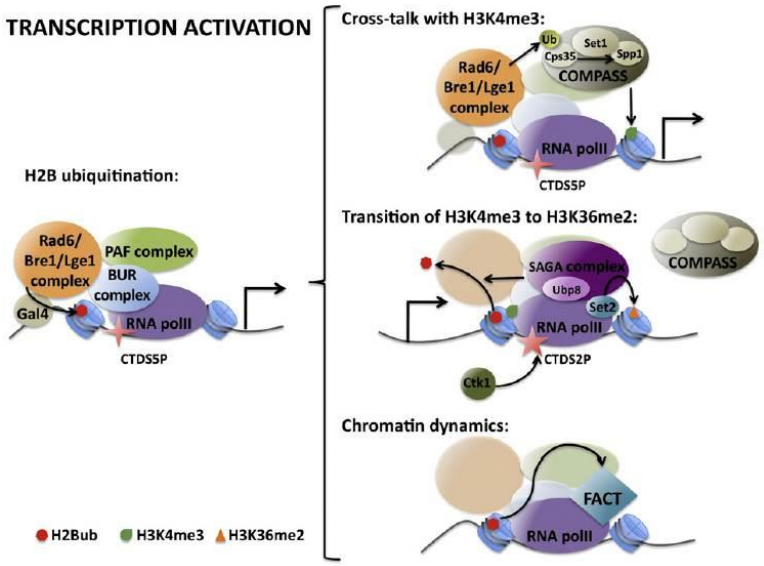

Figure 8. H2B ubiquitylation in gene activation.
Rad6 and Bre1 can be recruited to promoters by activators, such as GAL4 in yeast and p53 in humans. Shown is the situation in yeast. Rad6/Bre1 ubiquitylates H2B, an event that is also dependent on the PAF complex and the BUR complex. H2Bub1 mediates crosstalk with H3K4me3 through the COMPASS complex. Later, deubiquitylation by the SAGA subunit Ubp8 is required for efficient transition into elongation and enables establishment of CTD Ser2 phosphorylation and H3K36me2. In addition, H2Bub1 plays a role in stimulating chromatin remodeling by the FACT complex in transcribed genes. Extracted from (Hammond-Martel *et al.*, 2012).

1.2.2. Promoter proximal pausing

Experiments performed in *Drosophila* in the 1980s showed that RNA pol II is associated with the *hsp70* gene already before induction by heat-shock (Rougvie & Lis, 1988). RNA pol II in this situation has left the promoter and started RNA synthesis, but it is stalled 20-40 nucleotides downstream of the promoter, a state known as promoter proximal pausing.

Upon heat-shock, transcription is rapidly resumed. A large quantity of reports suggest that pausing of RNA pol II is a wide-spread phenomena at inducible and developmental genes and that it is conserved also in mammalian cells, but not in yeast (reviewed in Adelman & Lis, 2012). These studies also gave detailed insights into the regulatory mechanisms of this process (Figure 9). Establishment of paused RNA pol II requires the two factors DSIF and NELF. The negative effects of these factors on elongation are relieved by the action of P-TEFb, which results in release of RNA pol II into productive elongation. P-TEFb phosphorylates Ser2 of the CTD of RNA pol II, NELF and DSIF. These phosphorylation events lead to the dissociation of NELF and transform DSIF into a stimulator of elongation (Marshall *et al.*, 1996; Wada *et al.*, 1998; Weake & Workman, 2010). Genome-wide studies in *Drosophila* and human cells suggest that RNA pol II pausing is a wide-spread feature occurring at many gene promoters, which allows transcriptional regulation at a post-initiation step (Kim, Barrera, *et al.*, 2005; Muse *et al.*, 2007; Zeitlinger *et al.*, 2007). Several possible functions, which are mutually not exclusive, have been proposed for promoter proximal pausing. Pausing might be a mechanism to allow fast and synchronous response to an inducing signal. Further, it might allow enough time for the mRNA processing machinery to cap the nascent RNAs. In another model, paused RNA pol II helps maintaining an open chromatin structure that facilitates the initiation of further rounds of transcription. Even though there are several independent observations that suggest that pausing is a widely used regulatory mechanism, it should be noted that promoter proximal peaks of RNA pol II could also occur in absence of pausing (Ehrensberger *et al.*, 2013). Therefore, from RNA pol II density profiles alone, pausing cannot be deduced unequivocally.

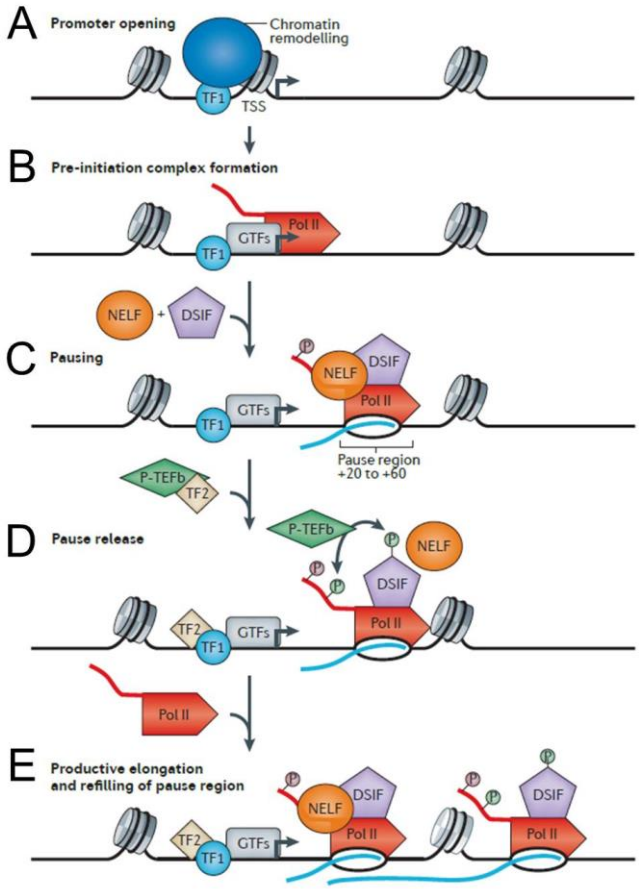

Figure 9. Establishment and release of paused RNA pol II.
(A) The TSS is made accessible for the transcription machinery by binding of sequence specific transcription factors (TF1) and the action of chromatin remodeling complexes. **(B)** General transcription factors (GTFs) and RNA pol II are recruited to the promoter region and form the pre-initiation complex. **(C)** Shortly after transcription has set in, the RNA pol II gets paused, which involves the action of the negative elongation factors NELF and DSIF. The CTD of paused RNA pol II is phosphorylated at Ser5. **(D)** The P-TEFb kinase is recruited and phosphorylates DSIF, NELF and CTD Ser2, whereby it induces pause release. Phosphorylation leads to disassociation of NELF and to the transformation of DSIF into a positive elongation factor. **(E)** After RNA pol II has escaped into elongation, the pause site is rapidly reoccupied by a new RNA pol II. Extracted from (Adelman & Lis, 2012).

1.2.3. Elongation

As described above, the CTD of RNA pol II gets phosphorylated first at Ser5 during initiation and then at Ser2 during the transition to elongation. While Ser5 phosphorylation gets gradually removed by phosphatases during elongation, Ser2 phosphorylation further increases during the beginning of transcription and then reaches a plateau (reviewed in Hsin & Manley, 2012) (Figure 7). The CTD of RNA pol II plays an important role as a platform for recruitment of numerous elongation factors that allow efficient passage through the chromatin template. The PAF complex is associated with transcribing RNA pol II and mediates the binding of factors that have a preference for CTD Ser5 phosphorylation (reviewed in Jaehning, 2010). H3K4 methylation at transcribed genes is dependent on the PAF complex. Methylation of H3K4 can be mediated by the Set1 complex, which requires the PAF complex for recruitment to RNA pol II. Patterns of H3K4 methylation show a specific distribution along the transcribed gene: H3K4me3 peaks at the 5' end, H3K4me2 is enriched in the middle and H3K4me1 is highest towards the end of the gene. The PAF complex is only required for the higher methylation states, while H3K4me1 is PAF independent. The favored model is that the PAF complex travels along with the elongating polymerase and helps converting basal H3K4me1 levels into di- and trimethylation (reviewed in Li, Carey, *et al.*, 2007). Further, the PAF complex also mediates interaction between Rad6 and elongating RNA pol II, while Rad6 recruitment to promoters is independent of PAF. Rad6 together with Bre1 then mediate ubiquitylation of H2B, a histone mark that is found along the entire ORF of transcribed genes and also has a function at promoters, as described above (see chapter 1.2.1). H2Bub1 facilitates transcriptional elongation by stimulating the FACT complex, a histone chaperone that

binds to H2A and H2B. FACT is thought to be required for disassembly of H2A-H2B dimers in front of the transcribing polymerase and for reassembly after passage (Orphanides *et al.*, 1998; Belotserkovskaya *et al.*, 2003; Saunders *et al.*, 2003; Pavri *et al.*, 2006). A similar function for H3-H4 disassembly and assembly appears to play the histone chaperone Spt6, which is also dependent on the PAF complex (Bortvin & Winston, 1995; Saunders *et al.*, 2003). Another histone modification that is related to transcription elongation is H3K36me3. The corresponding histone methyltransferase for H3K36 is Set2, which binds the RNA pol II CTD when phosphorylated at Ser5 and Ser2. The distribution patterns of H3K36me3 and Ser2 phosphorylation are highly similar (reviewed in Buratowski, 2009). H3K36me3 is recognized by the chromo domain of Eaf3, a subunit of the Rpd3S histone deacetylase complex (Li, Gogol, *et al.*, 2007; Sun *et al.*, 2008). Recruitment of Rpd3S leads to hypoacetylation within the ORF and helps to avoid cryptic transcription (Carrozza *et al.*, 2005; Joshi & Struhl, 2005). Eaf3 is a subunit of both the histone deacetylase Rpd3S and the histone acetyltransferae NuA4. The action of NuA4 and other histone acetyltransferases such as p300 and SAGA are important to overcome the nucleosome barrier during transcription (Li, Carey, *et al.*, 2007).

1.2.4. Termination

With the notable exception of replication-dependent histone mRNAs, 3’ processing of eukaryotic mRNAs involves the addition of a poly(A) tail consisting of up to 250 adenosines (reviewed in Brown, 2002; Proudfoot, 2011). The poly(A) tail is not encoded by the gene, but is added by the specialized poly(A) polymerase to the new 3’ end that is generated by

cleavage of the mRNA. The mRNA cleavage is mediated by the protein complexes CPSF and CstF and associated factors. CPSF and CstF recognize conserved sequences within the mRNA. Interestingly, CPSF, and probably also CstF, are not newly recruited to the poly(A) signal sequence once this has been synthesized. Instead, CPSF is already recruited during transcription initiation via a contact with the GTF TFIID and then is loaded onto the CTD of RNA pol II. CPSF might then travel along with elongating RNA pol II and bind to the poly(A) signal once it has been transcribed. The interaction with the poly(A) signal might alter the contact to the CTD of RNA pol II and favor termination by destabilizing the RNA:DNA hybrid (Brown, 2002). Indeed, it is well established that 3' end cleavage and polyadenylation are tightly linked to termination (reviewed in Mischo & Proudfoot, 2013). As expected, the CTD is also required for termination through its interaction with CPSF, CstF and other proteins, such as the cleavage factor Pcf11. In addition, it has been proposed that 5'-to-3' exoribonuclease mediated degradation of the downstream nascent RNA after cleavage is involved in signaling termination. Again, the CTD of RNA pol II plays a role in recruitment of these nucleases, yeast Rat1 and human Xrn2 (reviewed in Hsin & Manley, 2012).

1.3. HP1 proteins

HP1 proteins were identified initially in *Drosophila* when in 1986 HP1a was described as a non-histone chromosomal protein. It was found that antibodies against HP1a specifically stain heterochromatic sites in polytene chromosomes (James & Elgin, 1986). A later study revealed that a mutation in the HP1a encoding gene *Su(var)205* acts as a dominant suppressor of position effect variegation (PEV), suggesting a function of HP1a in defining heterochromatin identity (Eissenberg *et al.*, 1990). The phenomena of PEV was first characterized in *Drosophila* in 1930 and describes the variegated inactivation of an euchromatic gene that is translocated into the vicinity of a heterochromatic region (Muller, 1930).

HP1 proteins are conserved throughout the eukaryotic kingdoms. The genomes of most eukaryotic organisms encode for one or often several HP1 homologs, with the notable exception of *Saccharomyces cerevisiae*, where no HP1 homolog has been found (reviewed in Hiragami & Festenstein, 2005; Lomberk *et al.*, 2006). In *Saccharomyces cerevisiae* an important role has been attributed to the silent information regulatory (SIR) proteins in mediating gene silencing (reviewed in Moazed, 2001). The other yeast model organism *Schizosaccharomyces pombe* however contains two HP1 homologs, Swi6 and Chp2. Other organisms in which HP1 homologs have been found include *Arabidopsis thaliana* (LHP1), *Xenopus laevis* (xHP1α and xHP1γ), *Caenorhabditis elegans* (HPL-1 and HPL-2), chicken (CHCB1, CHCB2 and CHCB3) and mammals (HP1α, HP1β and HP1γ) (reviewed in Hiragami & Festenstein, 2005; Libault *et al.*, 2005; Lomberk *et al.*, 2006; Zeng *et al.*, 2010). In the *Drosophila* genome five HP1 proteins (HP1a-e) are encoded (reviewed in Vermaak & Malik, 2009). Three of them, HP1a, HP1b and HP1c, are ubiquitously

expressed, while the other two, HP1d/Rhino and HP1e, are mainly expressed in the female and male germline, respectively (Figure 12A).

1.3.1. Domain organization

HP1 proteins are characterized by an N-terminal chromo domain and a C-terminal chromo shadow domain. These two conserved domains are separated by a flexible and less conserved linker sequence, the so-called hinge region (Figure 10A). The chromo domain and the chromo shadow domain are related and both form a similar globular structure (Ball *et al.*, 1997; Cowieson *et al.*, 2000). Despite their structural similarity the two domains contribute distinctly to HP1 function. The chromo domain can mediate binding to methylated H3K9 (Bannister *et al.*, 2001; Lachner *et al.*, 2001) (Figure 10B, C). The chromo shadow domain, but not the chromo domain, is involved in dimer formation (Brasher *et al.*, 2000) (Figure 10D). Dimerization of the chromo shadow domain generates a groove that is required for the recognition of a conserved motif in HP1 binding partners (Thiru *et al.*, 2004). Chromo domains have also been described in non-HP1 proteins, such as Polycomb and Chromator (Paro & Hogness, 1991; Eggert *et al.*, 2004). The chromo shadow domain in contrast is characteristic for the HP1 protein family. However, in *Drosophila* species several HP1 related genes have been described that only encode either a chromo or a chromo shadow domain, putatively having lost the other domain (reviewed in Levine *et al.*, 2012).

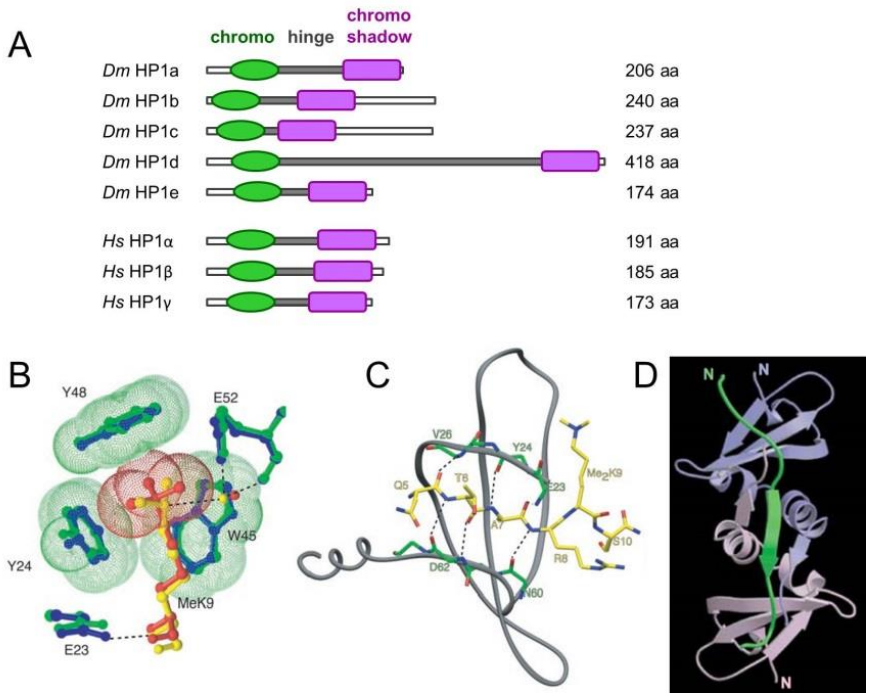

Figure 10. HP1 proteins are characterized by a chromo and a chromo shadow domain.
(A) The scheme shows the domain organization of the HP1 isoforms in *Drosophila melanogaster* (*Dm*) and in *Homo sapiens* (*Hs*). The representations are drawn to scale and for each isoform the total length in amino acids (aa) is indicated at the right. **(B)** Shown is the aromatic cage of the chromo domain (blue and green) of *Drosophila* HP1a in complex with H3K9me2 (yellow) and H3K9me3 (orange), respectively. The van der Waals representation is shown for the interaction with H3K9me3. **(C)** The illustration shows the HP1a chromo domain in complex with an H3K9me2 peptide and the backbone interactions that are involved. The peptide is inserted as a β-strand into a groove that is formed by the chromo domain. **(D)** The structural representation shows the dimerized chromo shadow domain (blue) of murine HP1β in complex with a PXVXL motif containing fragment of CAF-1 (green). The illustrations of the structures were extracted from (Jacobs & Khorasanizadeh, 2002; Thiru *et al.*, 2004).

1.3.1.1. The chromo domain

The chromo domain forms a globular structure of approximately 30 Å in diameter, consisting of an antiparallel three-stranded β-sheet flanked by one α-helix that folds against the sheet (Ball *et al.*, 1997). As mentioned above the chromo domain of HP1 binds to methylated H3K9 (Bannister *et al.*, 2001; Lachner *et al.*, 2001). Binding studies using the chromo domain of *Drosophila* HP1a showed that the domain binds the di- and trimethylated forms of the H3K9 peptide with similar affinities (Kd = 15 µM and 10 µM, respectively) (Hughes *et al.*, 2007). A much lower affinity was found towards the monomethylated peptide (Kd = 96 µM). This binding preference is in agreement with *in vivo* localization studies that showed extensive co-staining of heterochromatic HP1 proteins with H3K9me2/3 (Lachner *et al.*, 2001; Font-Burgada *et al.*, 2008). Su(var)3-9, the main methyltransferase for H3K9 in constitutive heterochromatin, is required for the correct localization of heterochromatic HP1 proteins at most sites (Lachner *et al.*, 2001; Nakayama *et al.*, 2001; Schotta *et al.*, 2002). However, HP1a recruitment to the heterochromatic fourth chromosome of *Drosophila* does not depend on Su(var)3-9, but on Setdb1, the methyltransferase that is responsible for H3K9 methylation on the fourth chromosome (Tzeng *et al.*, 2007).

The structure of the HP1 chromo domain bound to a methylated H3K9 peptide was solved and gave more insights into the mode of interaction (Jacobs & Khorasanizadeh, 2002; Nielsen *et al.*, 2002). The bound histone peptide adopts a β-strand conformation and the methylated lysine is recognized by a cage that is formed by three aromatic residues (Y24, W45 and Y48 in *Drosophila* HP1a). The context of the methyllysine is important, as mutations in adjacent residues affect binding. Chromo domains in non-HP1 proteins have been shown to bind a variety of other

histone methyllysines (reviewed in Eissenberg, 2012). For example, the chromo domain of Polycomb is a reader of di- and trimethylated H3K27 (Cao *et al.*, 2002). The binding of the HP1 and Polycomb chromo domains to their respective target is very specific, even though the bound methyllysines are occurring in a very similar context, within the ARKS motif. Domain swapping experiments suggest that the specificity is dictated by the chromo domain (Fischle *et al.*, 2003).

The interaction of HP1 proteins with methylated H3K9 is negatively regulated by phosphorylation of the adjacent serine (H3S10) (Fischle *et al.*, 2005; Hirota *et al.*, 2005). HP1 proteins are mostly lost from chromatin during mitosis, but levels of H3K9 methylation remain unchanged. Phosphorylation of H3S10 by the kinase Aurora B is thought to be involved in HP1 displacement during the cell cycle. The interaction of HP1 with methylated H3K9 is also regulated by phosphorylation within the chromo domain (Ayoub *et al.*, 2008). The casein kinase 2 (CK2) phosphorylates threonine 51 of mammalian HP1β upon DNA damage and leads to its release from chromatin and promotes phosphorylation of H2AX, an early marker of DNA breaks (for more details about HP1 function in DNA damage response, see chapter 1.3.2.3). All the three mammalian HP1 isoforms have been found to be highly modified (LeRoy *et al.*, 2009). Several of the amino acids that can be modified lie within the chromo domain, suggesting a complex regulation of HP1 function by post-translational modifications. However, the actual functional contribution of the majority of these modifications is unknown and needs further investigation.

The chromo domain of mammalian HP1 isoforms can also mediate binding to other methylated proteins. The mammalian linker histone variant H1.4 that is methylated at lysine 26 serves as a binding site for HP1 proteins (Daujat *et al.*, 2005). Further, mammalian HP1 proteins

were shown to interact with the methyltransferase G9a when automethylated at K239 (Chin *et al.*, 2007; Sampath *et al.*, 2007). G9a is responsible for H3K9 methylation in euchromatic regions (Rice *et al.*, 2003). HP1 interaction with methylated G9a is functionally required *in vivo*, as a G9a K239A mutant affects co-localization with HP1α and HP1γ (Sampath *et al.*, 2007). Structural studies of HP1γ bound to methylated peptides of G9a or histone H1.4 only showed subtle differences compared to the H3K9me3 interaction and binding affinities are very similar for all the three peptides (Ruan *et al.*, 2012). As in the case of binding to methylated H3K9, the interaction with methylated histone H1.4 and methylated G9a is blocked by adjacent phosphorylation (Daujat *et al.*, 2005; Sampath *et al.*, 2007).

Interestingly, the chromo domain of mammalian HP1β in addition can bind the histone fold domain of H3, an interaction that is independent of H3K9 methylation (Nielsen, Oulad-Abdelghani, *et al.*, 2001; Dialynas *et al.*, 2006). The interaction with the histone fold domain is thought to play a role in HP1β incorporation during S phase.

1.3.1.2. The chromo shadow domain

The chromo shadow domain forms a globular structure that is similar to the chromo domain (Brasher *et al.*, 2000; Cowieson *et al.*, 2000). Like the chromo domain it involves three β-strands that form an antiparallel sheet, but while the chromo domain has a single subsequent α-helix, the chromo shadow domain has two α-helices. The residues that form the aromatic cage in the chromo domain are not conserved. The chromo shadow domain dimerizes in solution, while the chromo domain is found as a monomer (Brasher *et al.*, 2000). Structural data, sequence conservation

and *in vitro* interaction data suggest that HP1 isoforms might also heterodimerize through the chromo shadow domain (Ye, 1997; Brasher *et al.*, 2000; Nielsen, Oulad-Abdelghani, *et al.*, 2001). Though, whether HP1 heterodimers play a functional role *in vivo* is currently unknown.

A large number of HP1 interacting partners have been described, of which many are binding via the chromo shadow domain (reviewed in Hiragami & Festenstein, 2005; Hediger & Gasser, 2006; Lomberk *et al.*, 2006; Kwon & Workman, 2011) (Figure 11). Most proteins bound by the chromo shadow domain contain the conserved motif PXVXL (Smothers & Henikoff, 2000). Dimerization of the chromo shadow domain is a prerequisite for the interaction with this pentapeptide, as the peptide binds to a hydrophobic pocket at the interface of the dimer (Thiru *et al.*, 2004). Studies using *Drosophila* HP1 proteins indicate that partner specificity of the chromo shadow domain and isoform specific interactions can be modulated by the C-terminal extension and phosphorylation of the binding surface within the chromo shadow domain (Mendez *et al.*, 2011, 2013). Interestingly, the chromo shadow domain of human HP1α was shown to have a binding activity for histone H3 (Dawson *et al.*, 2009). The region that is recognized by HP1α maps to amino acids 31-56 of histone H3 and binding is abolished by JAK2 mediated phosphorylation of tyrosine 41 of histone H3.

Direct HP1 interacting partners				
Partner	Organism	Variant	Domain	References
Histones				
H1	*Xl, Mm*	xHP1α, HP1α	Hinge	(Nielsen, Oulad-Abdelghani, *et al.*, 2001; Meehan *et al.*, 2003)
H3 (fold)	*Hs*	HP1β	CD	(Dialynas *et al.*, 2006)
H3 (aa31-56)	*Hs*	HP1α	CSD	(Dawson *et al.*, 2009)
H3K9me2/3	*Sp, Dm, Hs, Mm*	Swi6, HP1a, HP1α, HP1β, HP1γ	CD	(Bannister *et al.*, 2001; Jacobs *et al.*, 2001; Jacobs & Khorasanizadeh, 2002)
H1.4K26me2/3	*Mm, Hs*	HP1α, HP1β, HP1γ	CD	(Daujat *et al.*, 2005; Ruan *et al.*, 2012)
Chromatin remodelers and modifiers				
Su(var)3-9	*Dm, Mm, Hs*	HP1a, HP1α, HP1β	CSD	(Aagaard *et al.*, 1999; Schotta *et al.*, 2002; Yamamoto & Sonoda, 2003)
G9a (me2/3)	*Mm, Hs*	HP1α, HP1β, HP1γ	CD	(Sampath *et al.*, 2007)
dKDM4A	*Dm*	HP1a	CSD	(Lin *et al.*, 2008)
FACT	*Dm*	HP1a, HP1b, HP1c	CSD	(Kwon *et al.*, 2010)
Transcription				
Pol II CTD (ph)	*Dm*	HP1c	nd	(Kwon *et al.*, 2010)
ROW	*Dm*	HP1c	nd	(Abel *et al.*, 2009)
KAP-1	*Hs, Mm*	HP1α, HP1β, HP1γ	CSD	(Ryan *et al.*, 1999)
DNA replication and repair				
CAF-1 p150	*Hs,Mm*	HP1α, HP1β	CSD	(Murzina *et al.*, 1999; Brasher *et al.*, 2000; Lechner *et al.*, 2000)
Ku70	*Hs*	HP1α	CSD	(Song *et al.*, 2001)
Telomere associated proteins				
HOAP	*Dm*	HP1a	Hinge + CSD	(Badugu *et al.*, 2003)
TIN2	*Hs*	HP1γ	CSD	(Canudas *et al.*, 2011)
RNA / RNA pathways				
RNA	*Dm*	HP1a	CD	(Piacentini *et al.*, 2009)
RNA	*Mm, Sp*	HP1α, Swi6	Hinge	(Muchardt *et al.*, 2002; Keller *et al.*, 2012)
Piwi	*Dm*	HP1a	CSD	(Brower-Toland *et al.*, 2007)

Figure 11. Examples of direct HP1 interacting partners.
The table contains a non-exhaustive enumeration of direct HP1 interacting partners grouped according to their functions. Abbreviations: me2/3, di- or trimethylated; ph, phosphorylated; *Xl, Xenopus laevis; Mm, Mus musculus; Hs, Homo sapiens; Sp, Schizosaccharomyces pombe; Dm, Drosophila melanogaster*; CD, chromo domain; CSD, chromo shadow domain; nd, not defined. See references and main text for details.

1.3.1.3. The hinge region

The sequence that separates the two conserved globular domains is called hinge or linker region. This part of HP1 is much less conserved than the globular domains and can vary considerably in length between different isoforms. In mammals, all the HP1 isoforms have similar hinge lengths, which in humans range from 33 amino acids in HP1γ to 43 amino acids in HP1α. In *Drosophila* however, the variability in hinge lengths is much higher, ranging from 18 amino acids in HP1c to 279 amino acids in HP1d/Rhino (Figure 10A). It has been suggested that the hinge region is flexible and exposed to the surface (reviewed in Lomberk *et al.*, 2006). Even though it is poorly conserved, several functions have been attributed to the hinge regions of various HP1 proteins.

The hinge regions of several HP1 isoforms have been described to be directly involved in binding to chromatin. In 1996, Sugimoto et al. detected that the hinge region of human HP1α contains a DNA binding activity (Sugimoto *et al.*, 1996). This activity is conserved in the hinge region of *Xenopus* xHP1α, whose binding to chromatin also involves recognition of histone H1, in addition to unspecific DNA binding (Meehan *et al.*, 2003). A hinge region dependent interaction with histone H1 has also been detected in murine HP1α (Nielsen, Oulad-Abdelghani, *et*

al., 2001). In addition, nuclear localization motifs in the hinge region have been described in the yeast HP1 homolog Swi6 and in *Drosophila* HP1a (Wang *et al.*, 2000; Smothers & Henikoff, 2001). Interestingly, this nuclear localization motif is not conserved in the *Drosophila* HP1c isoform. Further, it was shown that the hinge region of *Drosophila* HP1a by its own possesses heterochromatin targeting activity (Smothers & Henikoff, 2001). The hinge region of murine HP1α binds RNA and is required for association with pericentromeric heterochromatin (Muchardt *et al.*, 2002). In a later study it was shown that a SUMO-1 modification in the hinge region plays a role in this process (Maison *et al.*, 2011). Sumoylated HP1α can bind to noncoding transcripts from the pericentromeric heterochromatin, an interaction that is important for targeting, but not for maintenance of HP1 domains. The hinge region of the yeast HP1 homolog Swi6 can also bind RNA, but in contrast to murine HP1α, RNA binding is not required for Swi6 recruitment to heterochromatin (Keller *et al.*, 2012). Binding of HP1 proteins to RNA and to factors of the RNAi machinery plays a role in heterochromatic gene silencing (see chapter 1.3.2.1 for more details). In *Drosophila* HP1a, the hinge region and the chromo shadow domain cooperate in order to enable interaction with HOAP, which is important for telomere protection (Badugu *et al.*, 2003). The interaction with HOAP can be affected by phosphorylation within the hinge region (Badugu *et al.*, 2005).

1.3.2. HP1 functions and recruitment

Intensive research during the last two decades revealed that HP1 functions are not limited to gene silencing and heterochromatin formation (reviewed in Hediger & Gasser, 2006; Fanti & Pimpinelli, 2008; Kwon & Workman,

2011). Different HP1 isoforms within species can have distinct functions. Localization studies indicate that the three mammalian HP1 proteins exhibit isoform specific patterns (Horsley *et al.*, 1996; Minc *et al.*, 1999). Likewise, the *Drosophila* HP1 isoforms have been shown to have specific localization patterns (Smothers & Henikoff, 2001; Font-Burgada *et al.*, 2008) (Figure 12B, C).

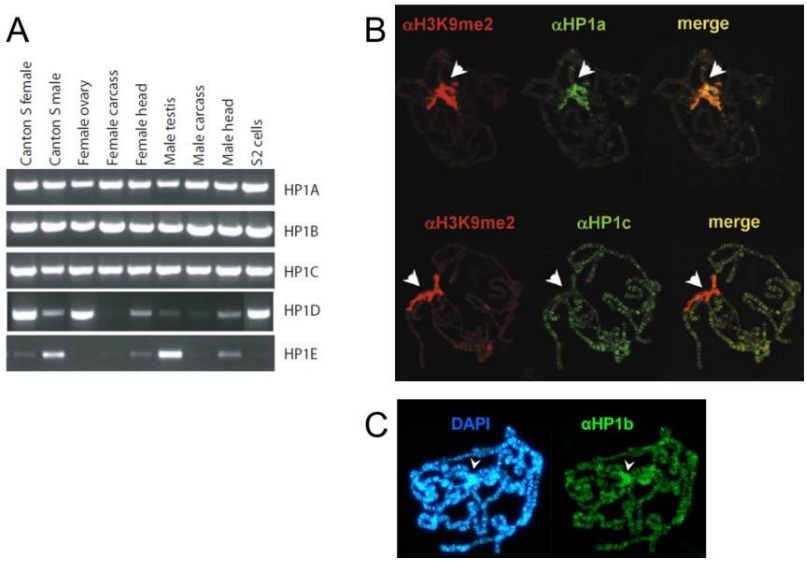

Figure 12. *Drosophila* HP1 isoforms.
(A) Expression levels of *Drosophila* HP1 isoforms in various tissues were determined by semi-quantitative RT-PCR. The analysis suggests that HP1a, HP1b and HP1c are ubiquitously expressed and that HP1d (Rhino) and HP1e are predominantly expressed in the female and male germline, respectively. Extracted from (Vermaak & Malik, 2009). **(B)** Co-immunostainings of polytene chromosomes with the heterochromatic marker H3K9me2 and the HP1 isoforms HP1a (top) and HP1c (bottom). A merge of the two stainings is shown at the right. The arrow head indicates the chromo center. **(C)** Polytene chromosomes stained for DNA with DAPI and for the HP1b isoform. The arrow head indicates the chromo center. Extracted from (Font-Burgada *et al.*, 2008).

HP1a is found mainly at heterochromatin, while HP1c is exclusively detected in euchromatin. HP1b localizes both to euchromatic and heterochromatic sites. The diverse roles of HP1 isoforms include regulation of euchromatic gene expression and functions in DNA damage pathways. In the following sections I review the insights that have been obtained from these studies on HP1 proteins and the molecular mechanisms contributing to these functions.

1.3.2.1. Heterochromatic functions

As its name indicates and as already mentioned above, HP1 proteins have been initially described in heterochromatin formation and gene silencing (James & Elgin, 1986; Eissenberg *et al.*, 1990). However, unlike reporter genes that typically are silenced in an HP1 dependent manner when ectopically placed into heterochromatin, most heterochromatic genes that are bound by HP1 are actually actively transcribed (de Wit *et al.*, 2007). In *Drosophila*, the expression of the two heterochromatic genes *rolled* and *light* is reduced in HP1a mutants (Lu *et al.*, 2000). This might suggest that genes have adopted specific mechanisms to ensure their expression depending on their chromatin context. Indeed, it was described that rearrangements that move heterochromatic genes into an euchromatic environment can affect their expression negatively (Wakimoto & Hearn, 1990).

The fact that HP1 proteins both interact with methylated H3K9 and the responsible histone methyltransferase Su(var)3-9, led to the proposition of a reiterative mechanism of heterochromatin spreading (Bannister *et al.*, 2001; Lachner *et al.*, 2001; Schotta *et al.*, 2002) (Figure 13). Su(var)3-9 is the major heterochromatin specific histone methyltransferase for H3K9.

Su(var)3-9 and HP1a are interdependent for correct localization, supporting the reiterative model (Schotta *et al.*, 2002). A tethering study with all the three human HP1 proteins in a reporter assay in *Xenopus* oocytes supports a two interaction model (Stewart *et al.*, 2005).

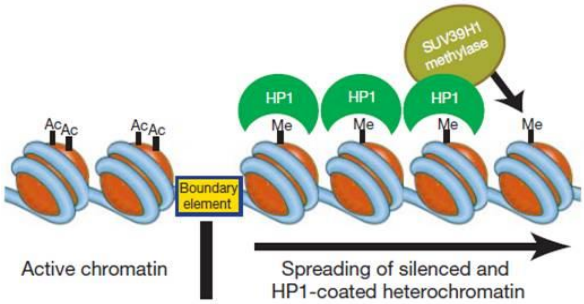

Figure 13. Model for HP1 spreading in heterochromatin.
The cartoon shows an active chromatin domain characterized by histone acetylation (Ac) and a silenced domain marked by methylation (Me) of H3K9. A boundary element separates the two chromatin domains. H3K9 methylation is recognized by HP1 proteins, which in turn recruit the histone methyltransferase Su(var)3-9/SUV39H1. In this model, the methyltransferase consecutively methylates neighboring nucleosomes and thereby leads to spreading of HP1 containing heterochromatic domains. Extracted from (Bannister *et al.*, 2001).

Both tethering SUV39H1, an human homolog of Su(var)3-9, and G9a induces H3K9 methylation and silencing, but only SUV39H1 is able to recruit HP1, suggesting that H3K9 methylation alone is not sufficient for HP1 recruitment. In contrast, localization studies using *Drosophila* HP1a suggest that the chromo domain and the chromo shadow domain can be recruited to heterochromatin independently of the other domain (Powers & Eissenberg, 1993; Platero *et al.*, 1995). In similar studies using GFP tagged human HP1 proteins, deletion of the chromo shadow domain does not affect heterochromatin binding neither, while deletion of the chromo domain does (Cheutin *et al.*, 2003). A possible explanation for the chromo

domain independent recruitment observed in *Drosophila* could be the dimerization via the chromo shadow domain with endogenous HP1 proteins. Subsequent tethering studies with *Drosophila* HP1a further supported the view that HP1 can induce silencing independently of Su(var)3-9 and H3K9 methylation (Li *et al.*, 2003; Danzer & Wallrath, 2004). All these divergent observations suggest that depending on the chromatin environment and the experimental system, different HP1 binding activities contribute distinctly to its recruitment and to its ability to induce silencing. This principle is well exemplified by the mode of recruitment of HP1a to the heterochromatic fourth chromosome of *Drosophila*, which is different from recruitment to the other chromosomes. The chromosome 4 specific protein POF and HP1a are interdependent for recruitment to this chromosome. POF and HP1a bind to the gene body of active genes with a preference for exons and affect gene expression differently, HP1a is repressing and POF is activating (Johansson, Stenberg, Bernhardsson, *et al.*, 2007; Johansson, Stenberg, Pettersson, *et al.*, 2007). HP1a, but not POF, has an additional peak at the promoter region of these genes. Methylation of H3K9 on the fourth chromosome is mediated by Setdb1. Nevertheless, Su(var)3-9 binds also to the fourth chromosome, but is not required for HP1a recruitment (Figueiredo *et al.*, 2012). In the same study, HP1a recruitment to promoters of active genes on all chromosomes was found to be independent of methylated H3K9, which however is required for spreading and also for recruitment to pericentromeric heterochromatin.

HP1 mediated heterochromatic silencing depends also on the recruitment of chromatin remodelers and histone modifying enzymes. Studies with the yeast HP1 homolog Swi6 suggest a contribution of the chromatin remodelers INO80 and FACT in heterochromatin formation (Lejeune *et al.*, 2007; Motamedi *et al.*, 2008). The other yeast HP1 homolog Chp2

associates with the SHREC2 complex, which contains Clr3, a histone H3 lysine 14 deacetylase (Motamedi *et al.*, 2008). Chp2 and the Su(var)3-9 homolog Clr4 are required for Clr3 deacetylase activity. In *Drosophila*, the HP1a protein has been shown to interact with the histone H3 lysine 36 demethylase dKDM4A via the chromo shadow domain (Lin *et al.*, 2008). The HP1a – dKDM4A interaction and a functional chromo domain are crucial for the demethylation activity.

HP1 proteins are well known for their ability to dimerize through the chromo shadow domain (Brasher *et al.*, 2000) (see chapter 1.3.1.2) . A recent study with the yeast HP1 homolog Swi6 suggests that heterochromatin spreading might involve oligomerization of HP1 proteins (Canzio *et al.*, 2011).

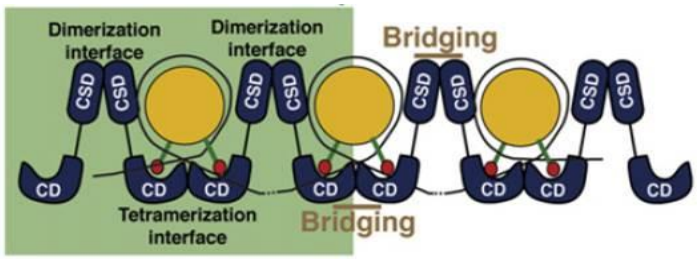

Figure 14. Model for HP1 (Swi6) oligomerization.
HP1 proteins form dimers through the chromo shadow domain (CSD). The yeast HP1 homolog Swi6 in addition has a weak self-interaction ability mediated by the chromo domain (CD). The model proposes that two chromo domains recognize methylated H3K9 (red dots) on the same nucleosome and induce tetramerization. The free chromo domains of the tetramers can function as sticky ends, by binding to methylated H3K9 of neighboring nucleosomes and to another free chromo domain, thereby leading to oligomerization of HP1 proteins. HP1 oligomerization might promote compaction of chromatin. Extracted from (Canzio *et al.*, 2011).

In this study Canzio et al. found that Swi6 assembles on the nucleosome as a tetramer involving a weak chromo domain self-interaction in addition

to the chromo shadow domain dimerization. They suggest a model in which the dimerized chromo domains of an HP1 tetramer recognize two methylated H3K9s of the same nucleosome and the two other chromo domains serve as sticky ends that can recruit neighboring nucleosome and induce heterochromatin spreading through HP1 oligomerization (Figure 14).

FRAP experiments with HP1 proteins challenged the view that heterochromatin is a very static structure, which would predict that HP1 proteins remain stably bound to heterochromatin. Contrary to this prediction, human HP1 proteins associate with heterochromatin in a highly dynamic manner (Cheutin *et al.*, 2003). Within only 2.5 seconds 50% of the heterochromatic HP1 fraction is exchanged. Similar dynamics of HP1 binding to heterochromatin was confirmed using the yeast Swi6 protein (Keller *et al.*, 2012). This binding behavior is in agreement with a model, in which the chromatin state is defined by a constant competition of activating and repressing factors for the same binding sites (Cheutin *et al.*, 2003).

In recent years, an important contribution to heterochromatic silencing has been attributed to the RNAi machinery, which has been most intensively studied in yeast (Motamedi *et al.*, 2004; Bühler *et al.*, 2006, 2007). The involvement of the RNAi machinery in heterochromatic silencing is conserved in flies and mammals (Pal-Bhadra *et al.*, 2004; Kanellopoulou *et al.*, 2005). Furthermore, in *Drosophila*, a direct interaction has been observed between HP1a and Piwi, an Argonaute protein that functions in the RNAi pathway (Brower-Toland *et al.*, 2007). The Piwi – HP1a interaction is required for silencing and Piwi is bound to chromatin in a RNA dependent manner (Figure 15A, B). In a more recent study, Piwi was found to be important for targeting HP1a during early embryogenesis and for establishment of heterochromatin, while it is dispensable for

maintenance of heterochromatin during later stages (Gu & Elgin, 2013). Another *Drosophila* HP1 isoform, HP1d/Rhino, has been implicated in the Piwi pathway and in transposon silencing in the female germline (Klattenhoff *et al.*, 2009). HP1d/Rhino binds to piRNA clusters and is required for piRNA production, which appears to involve an assisting function in shuttling the precursor RNA to the sites of processing (reviewed in Luteijn & Ketting, 2013) (Figure 15C).

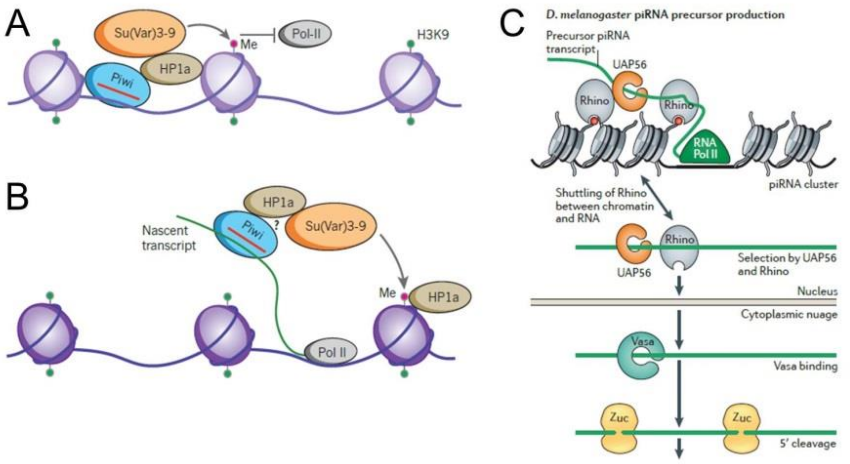

Figure 15. Models for *Drosophila* HP1 functions in the Piwi pathway. **(A)** In heterochromatin, Piwi bound piRNA (red) might complement with genomic DNA and thereby target Piwi to its target sequences. Piwi is required for binding of HP1a, which then recruits Su(var)3-9 that through methylation of H3K9 leads to efficient silencing. **(B)** In euchromatin, Piwi targets nascent RNA pol II transcripts (green) through piRNA complementarity. Piwi then recruits Su(var)3-9, either directly or through HP1a. Su(var)3-9 then methylates H3K9, resulting in binding of HP1a and silcening of transcription. Extracted from (Ross *et al.*, 2014). **(C)** HP1d/Rhino plays a role in piRNA production. HP1d/Rhino binds to many piRNA producing loci. Furthermore, HP1d/Rhino also can interact with the RNA helicase UAP56 and piRNA precursor transcripts. HP1d/Rhino appears to be important for selection and shuttling of piRNA precursors for further processing. Extracted from (Luteijn & Ketting, 2013).

In yeast, the HP1 homolog Swi6 associates with noncoding centromeric transcripts and is required for processing them into siRNAs (Motamedi *et al.*, 2008). The association of RNAi complexes with heterochromatic transcripts is dependent on Swi6. Keller et al. generated a Swi6 RNA binding mutant and showed that Swi6 recruitment and methylation of H3K9 is independent of RNA binding (Keller *et al.*, 2012). The RNA binding of Swi6 however is required for silencing, suggesting a posttranscriptional regulation involving RNA degradation. RNA and methylated H3K9 are competing for Swi6 binding, prompting a model where upon binding to a transcript, Swi6 is evicted from heterochromatin and is targeting the RNA for degradation (Keller *et al.*, 2012). Further, it was shown that long noncoding RNAs function in heterochromatin boundary formation in yeast (Keller *et al.*, 2013). A noncoding RNA that is transcribed from the boundary is bound by Swi6 independently of the underlying sequence and results in a conformational switch that evicts Swi6 from chromatin and prevents heterochromatin spreading. Unlike RNA from the centromeric repeats, the RNA transcribed from the boundary does not get incorporated into Ago1 and does not recruit Clr4, the yeast Su(var)3-9 homolog (Keller *et al.*, 2013). It is currently unknown, what is the basis for the different effects of centromeric repeat RNA and boundary RNA.

1.3.2.2. Euchromatic functions

HP1 proteins are not only found at the heterochromatic chromocenters and telomeres, but also localize to many sites on euchromatic arms, where they are involved in diverse aspects of gene regulation (reviewed in Hediger & Gasser, 2006; Fanti & Pimpinelli, 2008). For instance, the

Drosophila HP1a protein binds to approximately 200 euchromatic sites, which do not seem to be enriched in repetitive DNA (Fanti *et al.*, 2003). The euchromatic HP1a fraction only partially co-localizes with H3K9me3 and Su(var)3-9 (Cowell *et al.*, 2002; Greil *et al.*, 2003). This suggests that in euchromatin, H3K9me3 is neither sufficient nor necessary for HP1a recruitment.

Several studies showed that targeting HP1 proteins to euchromatin can induce a compact state of chromatin that correlates with gene silencing. Li et al. tested the effect of an lacI-HP1a fusion that was tethered to lac repeats 500 base pairs upstream of a mini-white reporter gene (Li *et al.*, 2003). Out of the 26 *Drosophila* stocks that had the reporter inserted at different euchromatic sites, in 25 cases targeting of HP1a led to silencing. The only not silenced stock had the reporter inserted at an active promoter, suggesting that the chromatin state present at active promoters opposes HP1 mediated gene silencing. The silenced transgenes were found to associate spatially with endogenous HP1a containing regions. Surprisingly, at the HP1a targeted sites, no increase of H3K9me2 was apparent and silencing of the reporter gene was not affected in Su(var)3-9 mutants. The authors concluded that tethering HP1a to euchromatic sites is sufficient to induce silent chromatin and that HP1a functions downstream of Su(var)3-9. A similar tethering study by Seum et al. used a GAL4 fusion of *Drosophila* HP1a to target it to a reporter transgene at six different euchromatic loci (Seum *et al.*, 2001). Only in one of the six lines silencing of the reporter gene could be observed. The silenced transgene was inserted into a repetitive DNA sequence, which seems to facilitate silencing by HP1. The distinct outcome of the two studies might be explained by the different fusions that were used. Indeed, while the lacI-HP1a can rescue a mutant for the endogenous protein, the GAL4-HP1a fusion is not able to rescue (Li *et al.*, 2003). In another study in a

mammalian cell line, the HP1α and HP1β proteins were used as EGFP-lacR-HP1 fusions for targeting them to an amplified genomic domain containing lac operators (Verschure *et al.*, 2005). This amplified region exhibits a euchromatin like structure that upon HP1α and HP1β tethering is transformed to a compact chromatin state. Tethered HP1 recruits the histone methyltransferase Setdb1 and leads to an increase in H3K9me3. HP1α and HP1β were also found to recruit each other to these sites, suggesting the formation of heterodimers. The ability to induce chromatin compaction in this system might also be attributed to the repetitive sequence effect. In a study performed in murine cells, the recruitment of HP1 proteins to a luciferase reporter upon hormone induced repression was addressed (Ayyanathan *et al.*, 2003). In this assay, hormone treatment leads to binding of a KRAB fusion protein to the promoter of the transgene and to recruitment of the co-repressor KAP1. Repression of the transgene further involves KAP1 mediated recruitment of HP1α, HP1γ and the histone methyltransferase Setdb1. Repression is accompanied by increased levels of H3K9me3 and relocation of the transgene to condensed chromatin regions. Induction of repression by a short exposure to the hormone is sufficient to maintain the silenced state and inherit it epigenetically over many generations.

While the above mentioned studies used exogenous transgenes to address HP1 mediated silencing in euchromatin, HP1 proteins have also been shown to be required for the repression of endogenous euchromatic genes. In *Drosophila*, four euchromatic genes have been described to be repressed by HP1a in a Su(var)3-9 dependent manner (Hwang *et al.*, 2001). That these four genes are probably representative for a larger number of genes is suggested by the fact that HP1a and Su(var)3-9 target genes on the chromosomes arms are preferentially low expressed (Greil *et al.*, 2003). Further, mammalian HP1 proteins have been shown to interact

with several repressor complexes and to be recruited to promoters of euchromatic genes to induce silencing (Nielsen, Schneider, *et al.*, 2001; Ogawa *et al.*, 2002; Yahi *et al.*, 2008).

Recently, several reports have linked HP1 proteins to active gene expression in euchromatin (reviewed in Kwon & Workman, 2011). *Drosophila* HP1a associates with heat-shock induced puffs on polytene chromosomes (Piacentini *et al.*, 2003). HP1a contributes positively to heat-shock induced expression of *Hsp70*. The formation of heat-shock induced puffs and RNA pol II binding however is not affected on polytene chromosomes of HP1a mutant larvae. Also the *Drosophila* HP1c isoform was shown to be recruited to heat-shock induced loci (Kwon *et al.*, 2010). The authors of this study showed that HP1c can interact both with subunits of the FACT complex and the CTD of RNA pol II when phosphorylated at Ser2 or Ser5. Upon HP1c depletion, heat-shock induced gene expression and FACT recruitment is affected. Thus, a model was proposed where HP1c mediates binding of FACT to RNA pol II. HP1c is also recruited to euchromatic sites in the absence of heat-shock and this localization is strictly dependent on the two zinc finger proteins WOC and ROW (Font-Burgada *et al.*, 2008) (see following paragraph for details). In this respect, it has been reported that WOC is not recruited to heat-shock induced puffs, suggesting that HP1c might function independently of WOC and ROW at these sites (Raffa *et al.*, 2005) *Drosophila* HP1a binds and positively regulates the three euchromatic genes *Pros35*, *CG5676* and *cdc2* (Cryderman *et al.*, 2005). Of these three genes only *cdc2* contains methylated H3K9 and none of them shows altered expression in Su(var)3-9 mutants. A microarray expression analysis in *Drosophila* Kc cells upon HP1a knockdown revealed approximately 400 down regulated genes (De Lucia *et al.*, 2005). Many of these down regulated genes are cell cycle regulators and were shown by ChIP to be direct HP1a targets. Indeed, it

was found that cell cycle progression is affected upon HP1a knockdown. The euchromatic fraction of *Drosophila* HP1a co-localizes with active RNA pol II and is recruited in a RNA dependent manner (Piacentini *et al.*, 2003, 2009). RIP-chip was performed and identified 105 HP1a bound transcripts (Piacentini *et al.*, 2009). The binding to RNA is dependent on the chromo domain and affects transcript levels positively. HP1a appears to regulate transcripts by its interaction with heterogeneous nuclear ribonucleoproteins (hnRNPs).

Also the two other ubiquitously expressed *Drosophila* HP1 isoforms HP1b and HP1c have been implicated in active gene expression (Font-Burgada *et al.*, 2008; Abel *et al.*, 2009; Zhang *et al.*, 2011). HP1c co-localizes with marks of active transcription and its targeting to a reporter gene resulted in increased transcription (Font-Burgada *et al.*, 2008). HP1c is found in a complex with the two zinc finger proteins WOC and ROW, which are required for HP1c recruitment to chromatin (Font-Burgada *et al.*, 2008; Abel *et al.*, 2009) (Figure 16C, D). While HP1c is not required for recruiting ROW and WOC, the recruitment of the latter two is interdependent (Figure 16A, B). ROW and HP1c can interact directly *in vitro* (Abel *et al.*, 2009). In absence of ROW or WOC, HP1c protein levels are strongly reduced. Font-Burgada et al. suggested that this effect on HP1c levels is due to destabilization of the protein when it cannot be bound to chromatin (Font-Burgada *et al.*, 2008). Abel et al. in contrast proposed an auto-regulatory mechanism of HP1c transcription that involves a WOC dependent activation, which is counteracted by high HP1c levels (Abel *et al.*, 2009). Expression profiling in larvae was performed in ROW, WOC and HP1c knockdown conditions (Font-Burgada *et al.*, 2008). In all the three conditions slightly more genes were found to be down regulated than up regulated. ROW and WOC co-regulate a very similar set of genes, while the correlation with HP1c

regulated genes is less extensive. Almost 80% of the genes that are mis-regulated both upon ROW and WOC depletion do not change in HP1c knockdown conditions. An explanation for this observation might be that ROW and WOC knockdowns displace the entire complex from its targets, in contrast to HP1c knockdown, and thus lead to stronger synergistic effects. The set of genes that are co-regulated by the three factors are enriched in developmental genes and many of them are involved in functions related to the nervous system. *Drosophila* HP1b also appears to be involved in transcriptional regulation (Zhang *et al.*, 2011). In euchromatin, HP1b seems to counteract repression by HP1a, as out of seven genes that are up regulated upon HP1a depletion, five are down regulated upon HP1b depletion.

In murine cells, HP1γ and H3K9me2/3 were shown to occur in the transcribed region of active genes (Vakoc *et al.*, 2005). Induction of differentiation of an arrested erythroid cell line led to rather surprising changes in euchromatic H3K9me3 levels: an increase at induced genes and a decrease at repressed genes was observed. H3K9me3 and HP1γ at active genes are dependent on elongating Polymerase. HP1γ co-immunoprecipitates with phosphorylated RNA pol II, suggesting a mechanism for recruitment to transcribed genes.

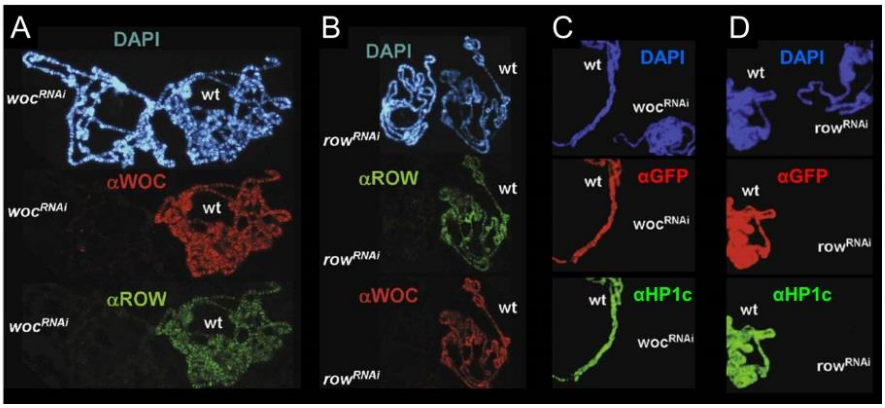

Figure 16. ROW and WOC are required for mutual and for HP1c recruitment.
(A, B) Wild-type (wt) polytene chromosomes were mixed with polytene chromosomes, in which WOC (A) or ROW (B) was depleted by RNAi (*woc*^{RNAi} or *row*^{RNAi}, respectively). DNA was stained with DAPI (blue) and co-immunostainings with αWOC (red) and αROW (green) antibodies were performed. **(C, D)** H2B-GFP labeled control (wt) polytene chromosomes were mixed with polytene chromosomes, in which WOC (C) or ROW (D) was depleted by RNAi (*woc*^{RNAi} or *row*^{RNAi}, respectively). DNA was stained with DAPI (blue) and co-immunostainings with αGFP (red) and αHP1c (green) antibodies were performed. Extracted from (Font-Burgada *et al.*, 2008).

1.3.2.3. DNA damage response

Seemingly opposing roles for HP1 proteins have been described in DNA repair pathways. A number of reports have found that the presence of HP1 appears to be inhibitory for efficient repair and that it is released upon induction of damage, while other studies described the recruitment of HP1 to sites of damage, implying an active role for HP1 in DNA repair (reviewed in Dinant & Luijsterburg, 2009; Cann & Dellaire, 2011).

It has been shown that double-strand breaks are in general repaired more slowly within heterochromatin than euchromatin and that repair of breaks within heterochromatin requires ATM kinase dependent relaxation of chromatin (Goodarzi *et al.*, 2008). This ATM dependent signaling involves phosphorylation of the co-repressor KAP-1, which is a known HP1 interacting partner (Ryan *et al.*, 1999). Goodarzi et al. showed that ATM becomes dispensable for efficient repair when either KAP-1, SUV39H1/H2 or all three HP1 isoforms are depleted (Goodarzi *et al.*, 2008). This can be explained by the fact that heterochromatin becomes more accessible in these depleted conditions and an ATM dependent chromatin relaxation is no longer necessary. No effects on repair efficiency could be detected when the HP1 isoforms were depleted in the presence of ATM. Another study, in line with an inhibitory function in damage repair, reported the release of mammalian HP1β upon damage induction by ionizing radiation (Ayoub *et al.*, 2008). By FRAP experiments, HP1β mobility was found to be increased in response to DNA breaks, both in eu- and heterochromatin. The release from chromatin is not induced by altered H3K9me3 levels, but instead by a phosphorylation event by the CK2 kinase. CK2 phosphorylates HP1β at threonine 51 within the chromo domain, which abolishes H3K9me3 binding and is sufficient for HP1β mobilization. Phosphorylated HP1β is appearing locally at damaged sites and the subsequent release from chromatin facilitates phosphorylation of H2AX, an early marker of double-strand breaks. Work by Sun et al. showed that CK2 dependent release of HP1β upon damage is required for Tip60 activation (Sun *et al.*, 2009). Tip60 is an acetyltransferase that acetylates both the ATM kinase and histones. ATM acetylation by Tip60 is important for ATM activation and for efficient double-strand break repair. Tip60 contains a chromo domain that interacts with H3K9me3, which triggers the activation of Tip60 and the acetylation of ATM. The interaction with H3K9me3

however is not required for recruitment. A model was suggested, where an inactive ATM-Tip60 complex is recruited to sites of damage. Then, Tip60 is activated by H3K9me3 that has been made available for binding by previous phosphorylation of HP1β and its release. The activated Tip60 then acetylates ATM and nearby histones, leading to a chromatin state that is favorable for DNA repair (Figure 17).

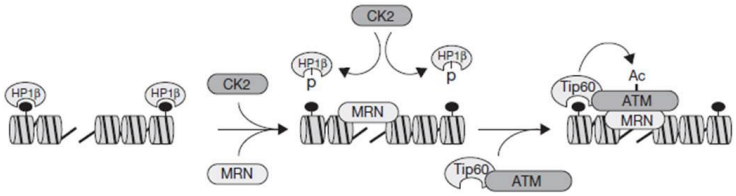

Figure 17. Model for the role of HP1β release in ATM activation.
In response to a double-strand break, MRN and CK2 are recruited to the damaged site. CK2 dependent phosphorylation of HP1β promotes its mobilization from chromatin. Subsequently, the Tip60-ATM complex is recruited. Methylated H3K9 that has been made available by HP1β release is bound by the chromo domain of Tip60. Binding to methylated H3K9 stimulates the acetyltransferase activity of Tip60. Acetylation of ATM by Tip60 is required to activate the ATM kinase and to induce the damage response pathway. Extracted from (Sun *et al.*, 2009).

In contrast to the results described above, several groups have found that HP1 proteins are recruited to sites of DNA damage. Zarebski et al. found that in human cells all the three HP1 isoforms are recruited to sites of oxidative damage, both in eu- and heterochromatin (Zarebski *et al.*, 2009). Recruitment of HP1 proteins becomes visible five minutes after damage induction and continues during 30 minutes, which is much slower than the mobilization of HP1β that has been observed within seconds (Ayoub *et al.*, 2008). Thus, it has been speculated that there are two different HP1 populations, a model that could explain both the mobilization and the recruitment of HP1 proteins after damage induction (Zarebski *et al.*,

2009). In this hypothesis, constitutively bound HP1 gets immediately phosphorylated and released upon DNA damage, while shortly afterwards HP1 gets recruited again by different factors and plays an active role in repair (Figure 18). Another study confirmed the recruitment of the three human HP1 isoforms both to sites of UV lesions and double-strand breaks (Luijsterburg *et al.*, 2009). The damage induced recruitment is independent of H3K9me3 and SUV39H1/H2 and instead requires the chromo shadow domain, supporting the two population model. HP1 recruitment appears to be an early event in repair signaling as it is independent of repair activity. Luijsterburg et al. used *C. elegans* to investigate how the worm HP1 homologs HPL-1 and HPL-2 affect damage repair (Luijsterburg *et al.*, 2009). The finding that worms deficient for both HPL-1 and HPL-2 have an increased UV sensitivity suggests that the two HP1 homologs play a partially redundant role in the response to UV lesions. A different phenotype was observed for X-ray induced damage, where the two HP1 homologs have opposing functions. While HPL-1 mutants are more resistant to this type of damage, HPL-2 mutants are more sensitive. Also the human HP1 isoforms have been shown to differentially contribute to damage repair (Soria & Almouzni, 2013). In homologous recombination repair, the recruitment of RAD51 is affected in HP1α and HP1β, but not HP1γ depleted cells. In agreement with this, efficiency of homologous repair is decreased upon HP1α and HP1β knockdown, while it is increased upon HP1γ knockdown. HP1α and HP1β seem to play a role in homologous recombination repair during DNA end resection. As mentioned above, the recruitment of HP1 to DNA damage was found to be dependent on the chromo shadow domain and does not require the chromo domain (Luijsterburg *et al.*, 2009). In murine cells it was shown that recruitment of HP1α and KAP-1 to double-strand breaks requires the p150 subunit of the CAF-1 complex (Baldeyron *et al.*, 2011). The recruitment is dependent on an intact PXVXL motif in p150,

but does not require the entire CAF-1 complex, as the p60 subunit is dispensable for recruitment.

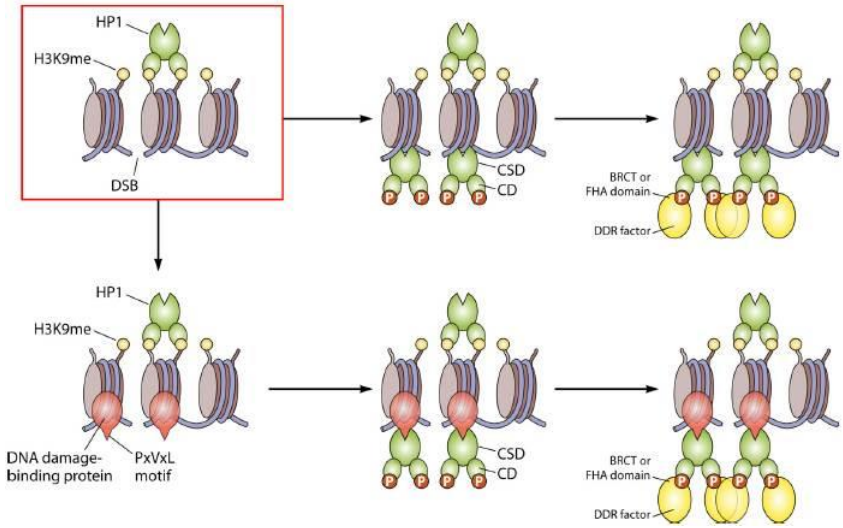

Figure 18. Model for the role of HP1 in recruitment of DNA damage response proteins.
Upon occurrence of a double-strand break (DSB) a fraction of HP1 gets phosphorylated within the chromo domain (CD) and is rapidly released from chromatin (not shown). The mobilized HP1 fraction gets re-recruited to the sites of damage by an alternative mechanism that involves the chromo shadow domain (CSD). Recruitment of HP1 proteins to double-strand breaks appears to promote the induction of the DNA damage response (DDR) pathway, possibly by recruiting repair factors through the phosphorylated chromo domain. Recruitment of HP1 to sites of DNA damage might either be mediated by direct binding to chromatin (upper pathway) or through another DNA damage binding protein (lower pathway). Extracted from (Dinant & Luijsterburg, 2009).

In summary, HP1 proteins have emerged as players that affect DNA repair in different ways. If damage is occurring within heterochromatin, the underlying DNA needs to be made accessible for the repair machinery. Therefore, it is plausible that HP1 proteins can hinder efficient repair as being components of heterochromatin. Apart from this passive inhibitory role, it has become evident that HP1 proteins can also play an active role in the DNA damage repair pathway. Importantly, it should be noted that

the above summarized studies have been performed in different systems and using different experimental settings, which might be a source for the partially contradictory observations.

1.3.2.4. Telomeres

Binding of HP1 proteins to telomeres has been observed both in mammals and *Drosophila* (Fanti *et al.*, 1998; Minc *et al.*, 1999; García-Cao *et al.*, 2004; Font-Burgada *et al.*, 2008). Despite the highly different mechanisms how telomeres are regulated in *Drosophila* and mammals, at least some telomeric HP1 functions seem to be conserved (reviewed in Raffa *et al.*, 2013).

At *Drosophila* telomeres, HP1a is required for stability, elongation and silencing (Fanti *et al.*, 1998; Savitsky *et al.*, 2002; Perrini *et al.*, 2004). HP1a recruitment to telomeres does not require a functional chromo domain, indicating that binding to H3K9me3 is dispensable for localization (Fanti *et al.*, 1998; Perrini *et al.*, 2004). While the chromo domain is not needed for targeting to telomeres, it is functionally required for correct H3K9me3 levels, telomere silencing and elongation (Perrini *et al.*, 2004). HP1a recruitment to telomeres seems to involve a DNA binding activity within the hinge region. However, HP1a is also recruited to the ends of terminally deleted chromosomes that lack the telomeric HeT-A and TART retrotransposons, which indicates that conserved telomeric DNA sequences are not absolutely required for recruitment (Fanti *et al.*, 1998). Flies that carry a heterozygous HP1a mutation over many generations accumulate long arrays of telomeric retrotransposons, suggesting that HP1a dominantly regulates telomere length (Savitsky *et al.*, 2002). HP1a function at telomeres involves an interaction with HOAP,

which is required for telomere capping (Cenci *et al.*, 2003). HOAP interacts specifically with HP1a, but not with the HP1b and HP1c isoforms (Badugu *et al.*, 2003). Further evidence that HP1a and HOAP function together at telomeres is provided by the fact that recruitment of both the proteins depend on ATM, which is another factor that is required for telomere stability and silencing (Oikemus *et al.*, 2004). *Drosophila* WOC, which at interbands is found in a complex with HP1c, is required to protect telomeres and when mutated leads to end-to-end fusions (Raffa *et al.*, 2005). WOC function at telomeres seems to act via a different pathway than HP1a and HOAP, as localization is not interdependent. Interestingly, WOC and HP1c not only co-localize at interbands, but also at telomeres (Font-Burgada *et al.*, 2008). However, it has not been addressed if and how HP1c contributes to WOC function at telomeres.

Also the mammalian HP1 isoforms have been implicated in telomere regulation. Overexpression of HP1α and HP1β affects association of a catalytic subunit of telomerase and leads to telomere instability (Sharma *et al.*, 2003). This overexpression phenotype is dependent on the chromo domain and is manifested by shortened telomeres. That the mammalian HP1 isoforms play a role in telomere length maintenance was also confirmed in a study using SUV39H1/H2 double null murine cells (García-Cao *et al.*, 2004). In these conditions, H3K9me2/3 at telomeres and binding of all three HP1 isoforms was reduced and telomere length increased. Additionally, it has been shown that the interaction of human HP1γ with the shelterin subunit TIN2 is important for sister telomere cohesion and telomere length maintenance (Canudas *et al.*, 2011).

1.4. Extra-proteasomal ubiquitin receptors

Ubiquitin receptors play an important role in proteasome function, recognizing ubiquitylated substrates and targeting them for degradation to the proteasome. Five evolutionarily conserved proteasome associated ubiquitin receptors have been characterized (reviewed in Finley, 2009; Su & Lau, 2009) (Figure 19). These ubiquitin receptors can be divided into two major groups: Rpn10/p54/S5a and Rpn13 are subunits of the proteasome, while Rad23, Dsk2/Ubiquilin and Ddi1/rings lost are extra-proteasomal ubiquitin receptors that can interact with proteasome subunits. These receptors recognize ubiquitin trough different domains: Rpn10/p54/S5a contains ubiquitin interacting motifs (UIM), Rpn13 binds via its pleckstrin-like receptor for ubiquitin (Pru) domain and the extra-proteasomal receptors contain one or two ubiquitin associated domains (UBA). The extra-proteasomal receptors all belong to the UbL/UBA family, which in addition to the UBA domain contain a single N-terminal ubiquitin-like (UbL) domain. The UbL domain mediates interaction with the proteasome (Schauber *et al.*, 1998; Hiyama, 1999; Elsasser *et al.*, 2002; Kaplun *et al.*, 2005). In addition to this, Dsk2 and Rad23 contain internal stress-inducible protein 1 (Sti1)-like domains. These domains have a similarity with domains found in the yeast Sti1 and the mammalian Hop protein, where they are known to mediate interaction with Hsp70 (Smith *et al.*, 1993; Höhfeld *et al.*, 1995).

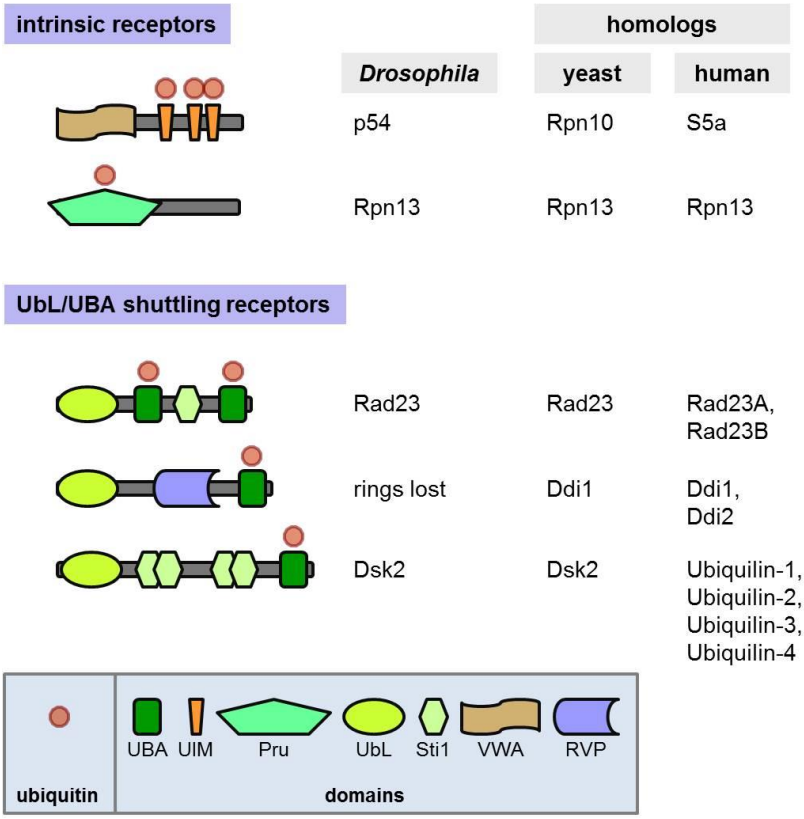

Figure 19. Proteasome associated ubiquitin receptors.
The scheme shows the domain organization of the two intrinsic ubiquitin receptors of the proteasome and the three shuttling receptors of the UbL/UBA family. The illustrations correspond to the *Drosophila* proteins. The homologous proteins in yeast and human are indicated. Domains that have the ability to bind ubiquitin are indicated with a red circle. Domains: UBA, ubiquitin associated; UIM, ubiquitin interacting motif; Pru, pleckstrin-like receptor for ubiquitin; UbL, ubiquitin-like; Sti1, stress-inducible protein 1-like; VWA, von Willebrand factor A; RVP, retroviral aspartyl-protease.

1.4.1. Proteasomal functions

Extra-proteasomal ubiquitin receptors have been shown to interact with proteasome subunits such as Rpn1 and Rpn10/p54/S5a via the UbL domain and with ubiquitylated substrates via the UBA domain (Hiyama, 1999; Lambertson *et al.*, 1999; Wilkinson *et al.*, 2001; Chen & Madura, 2002; Elsasser *et al.*, 2002; Funakoshi *et al.*, 2002). Due to these interactions, members of the UbL/UBA ubiquitin receptor family have been proposed to function as shuttling factors that deliver ubiquitylated proteins for degradation to the proteasome (Figure 20A). Experimental evidence, mainly obtained in budding yeast, is supporting such a model. It was described that both the UbL and UBA domains of Rad23 are functionally important and that overexpression of the UbL interferes with the delivery of substrates to the proteasome (Chen & Madura, 2002; Verma *et al.*, 2004). Both Rpn10 and Rad23 were found to be involved in the degradation of ubiquitylated substrates. It was further observed that Rpn10 and Rad23 exhibit some specific contributions in the degradation of different substrates. However, synthetic effects in Rpn10 and Rad23 mutants suggest that the two receptors also function partially redundant (Chen & Madura, 2002; Elsasser *et al.*, 2004; Verma *et al.*, 2004). Some data is contradicting a shuttling function of UbL/UBA proteins. It was described that human Rad23A can inhibit the degradation of substrates marked by K48-linked ubiquitin chains (Raasi, 2003). This inhibitory effect is dependent on the two UBA domains, but independent of the UbL domain. Therefore, it was suggested that the UBA domains of Rad23 can compete with the proteasome for binding to ubiquitin chains. An alternative mechanism might be that UBA binding to ubiquitylated substrates can affect both the assembly and disassembly of ubiquitin chains, probably by hindering the access of ubiquitin modifying enzymes

(Chen *et al.*, 2001; Raasi, 2003) (Figure 20B). A further possibility is that the observed stabilization of ubiquitylated substrates is a dominant negative overexpression effect. A study using another UbL/UBA protein, the yeast Dsk2, would be in agreement with this latter explanation (Funakoshi *et al.*, 2002). Upon Dsk2 overexpression an accumulation of poly-ubiquitylated substrates was observed, which might suggest that Dsk2 negatively affects degradation. In a Dsk2 mutant however, degradation of ubiquitylated substrates was affected. Taken together, these observations indicate that levels of UbL/UBA proteins are critical and when in excess can interfere with efficient targeting of substrates to the proteasome. That the ratio of different ubiquitin receptors is important for function has been demonstrated in the case of Rpn10/p54 and Dsk2, both in yeast and *Drosophila* (Matiuhin *et al.*, 2008; Lipinszki *et al.*, 2011). The toxicity resulting from Dsk2 overexpression can be rescued by concomitant overexpression of Rpn10. Interestingly, even though the lethality of increased Dsk2 levels in *Drosophila* was rescued by p54 expression, the accumulation of poly-ubiquitylation was not reduced (Lipinszki *et al.*, 2011). While in *Drosophila* the interaction of Dsk2 with the proteasome seems to depend strictly on p54, the situation in yeast was shown to be slightly different (Lipinszki *et al.*, 2011). In yeast, even though the interaction between $Dsk2^{UbL}$ and $Rpn10^{UIM}$ is conserved, Rpn10 negatively affects Dsk2 incorporation into the proteasome (Matiuhin *et al.*, 2008). This counterintuitive effect has been explained by a pool of extra-proteasomal Rpn10 that competes with the proteasome for Dsk2 binding. In *Drosophila*, it was found that extra-proteasomal p54 is enriched in a poly-ubiquitin modification that interferes with Dsk2 and Rad23 interaction (Lipinszki *et al.*, 2012). A structural study performed in yeast gave more insights into how Dsk2 and Rpn10 cooperate in the recognition of ubiquitin chains (Zhang *et al.*, 2009). Dsk2 and Rpn10 recognize ubiquitin as a ternary complex, which adapts a different

conformation depending on the chain length, providing an elegant mechanism for an ubiquitin chain sensor.

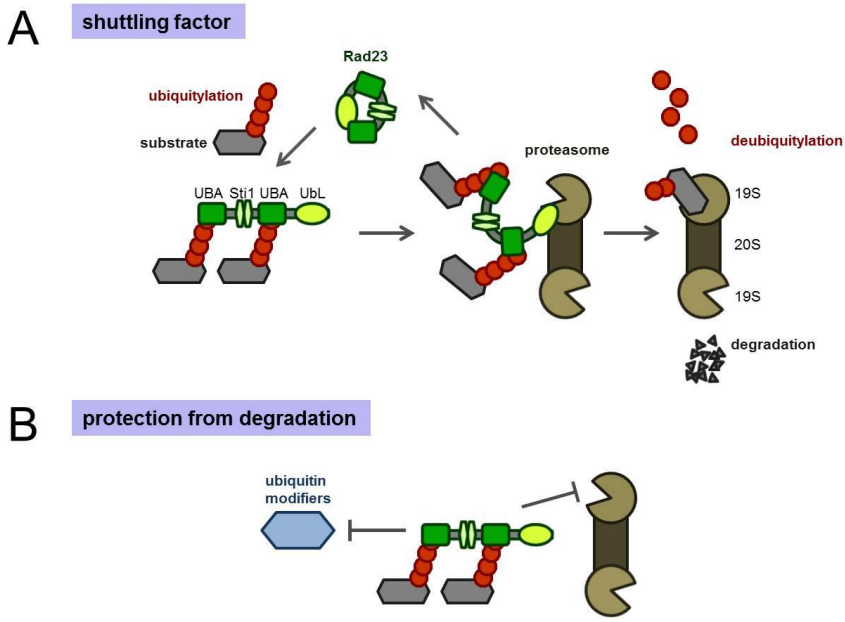

Figure 20. UbL/UBA proteins regulate proteasomal degradation.
(A) Rad23 and other UbL/UBA ubiquitin receptors can function as shuttling factors that target ubiquitylated substrates to the proteasome. The UBA domain interacts with the ubiquitylated substrate and the UbL domain with subunits of the proteasome. The substrate is handed over to the proteasome, where it gets deubiquitylated and degradaded. The free ubiquitin receptor is recycled for targeting further substrates. Intra- and intermolecular interactions between the UbL and the UBA domains might play a role. **(B)** Binding of UbL/UBA proteins to ubiquitylated proteins can also have a stabilizing effect, either by inhibiting ubiquitin modifying enyzmes or by hindering access to the proteasome.

A further layer of complexity is added by the fact that Dsk2 can be ubiquitylated in the UbL, which has been shown in yeast, and that this modification affects Dsk2 function in the proteasomal pathway (Sekiguchi *et al.*, 2011). Regulation of UbL/UBA protein function also involves intra-

and intermolecular interactions between these proteins (reviewed in Su & Lau, 2009).

1.4.2. Rad23 in DNA damage response

Beside its role as a shuttling ubiquitin receptor for the proteasome, Rad23 is also required for efficient nucleotide excision repair (NER). NER is the repair pathway that removes bulky DNA adducts, which includes lesions that are induced by UV light (reviewed in Kamileri *et al.*, 2012). The NER pathway comes in two flavors: transcription-coupled repair (TCR) that acts on the transcribed strand of active genes and global genome repair (GGR) that repairs lesions all over the genome. Rad23 together with Rad4 in yeast and XPC in mammals is involved in the recognition of the DNA lesions that are repaired by the GGR (Guzder, 1998; Jansen, 1998) (Figure 21A). The domain that is mediating interaction with Rad4/XPC lies in between the two UBAs of Rad23 and corresponds to the Sti1-like domain (Masutani *et al.*, 1997; Ortolan *et al.*, 2004). Rad23 function in NER is still not completely understood, but an important contribution appears to be the stabilization of Rad4/XPC. It has been observed that Rad4/XPC is degraded in the absence of Rad23 (Lommel *et al.*, 2002; Ng *et al.*, 2003). Defective NER in Rad23 mutant cells can be partially rescued by overexpression of Rad4/XPC, suggesting that Rad4/XPC stabilization might be the major function of Rad23 in NER (Ng *et al.*, 2003). The Rad4 binding domain of Rad23 is sufficient to stabilize Rad4, perhaps indicating that without this interaction Rad4 might not be able to fold correctly (Ortolan *et al.*, 2004). However, the model stating that Rad23 protects Rad4/XPC from proteolysis has been challenged. Gillette et al. obtained results that argue against a proteolytic regulation of Rad4 by

Rad23 and instead favor a regulation at the transcriptional level (Gillette *et al.*, 2006). In murine cells, more insights into the dynamics of Rad23 at DNA lesions have been obtained (Bergink *et al.*, 2012). While Rad23 is important for XPC to bind to lesions, upon recognition of the damaged DNA the Rad23-XPC complex is rapidly distorted and Rad23 dissociates from the damage bound XPC.

The function of Rad23 in NER appears not to be limited to Rad4 binding. It has been shown that the UbL domain of yeast Rad23 is required for its function in NER (Watkins *et al.*, 1993). A later study suggested that the Rad4 binding and the UbL domain of Rad23 fulfill two independent functions in NER (Ortolan *et al.*, 2004). The resistance to UV light in a Rad23 mutant strain is rescued by co-expressing two Rad23 constructs that lack the Rad4 binding and the UbL domain respectively. The UbL of Rad23 has been described to interact with proteasome subunits and it has been found that Rad4 and Rad23 co-fractionate with proteasome subunits (Schauber *et al.*, 1998). Similarly, Russell et al. showed that the UbL of Rad23 and the 19S regulatory complex of the proteasome are required for efficient NER (Russell *et al.*, 1999). Surprisingly however, they found that this proteasome function in NER does not involve protein degradation.

In summary, Rad23 plays a crucial role in GGR-NER in the recognition of distorted DNA by binding and stabilizing Rad4/XPC. The ability of Rad23 to interact with the proteasome via the UbL domain also seems to play a role for efficient NER. The involvement of the proteasome in NER however is not well understood and remains controversial. Both suppressive and enhancing functions of the proteasome in NER have been described (reviewed in Dantuma *et al.*, 2009).

1.4.3. Rad23 in transcriptional control

Rad23 at chromatin has not only been described to function in the recognition of damage within the NER pathway, but also in transcriptional regulation. Human Rad23B was found to act in concert with p53 in the response to DNA damage (Kaur *et al.*, 2007) (Figure 21B). The authors of this study suggested that Rad23B protects ubiquitylated p53, as its accumulation after DNA damage was found to depend on the presence of Rad23B. After DNA damage, Rad23B and ubiquitylated p53 localize to chromatin and are found at the promoter of the *p21* gene. Induction of *p21* requires Rad23B. In a yeast study, it was shown that Rad23 and the Snf1 kinase co-regulate transcription both in undamaged cells and in response to UV treatment (Wade *et al.*, 2009) (Figure 21C). Transcriptional regulation by Rad23 and Snf1 appears to be independent of Rad4, the cooperating factor in the NER pathway. Instead, the data suggests that it involves the proteasome, as the UbL domain, which is known to interact with proteasome subunits, is required for the transcriptional regulation. Furthermore, Rad23 co-regulates many genes with the 19S regulatory particle of the proteasome, but not with the 20S core particle. This suggests that it is a non-proteolytic function of the proteasome that is involved. Wade et al. further showed that upon UV induction, Snf1 and Rad23 seem to counteract transcriptional repression by Mig3. In mammals, Rad23 has been shown to function in transcription independent of DNA damage. In murine embryonic stem cells, it has been observed that the NER complex, involving XPC, Rad23B and CETN2, functions as a co-activator for Oct4 and Sox2 (Fong *et al.*, 2011) (Figure 21D). Furthermore, all these factors co-localize genome-wide and the NER co-activator complex is required for stem cell maintenance. Another study,

performed in HeLa cells, reported the recruitment of NER factors to active promoters in the absence of DNA damage (Le May *et al.*, 2010).

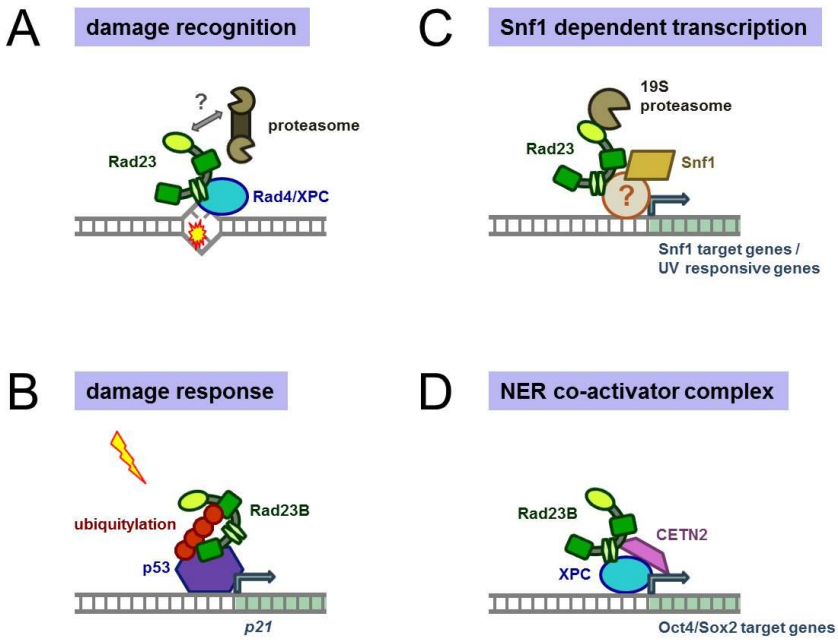

Figure 21. Functions of Rad23 at chromatin.
(A) Rad23 is required for recognition of DNA damage that is repaired by the global genome NER pathway. Rad23 directly binds to Rad4/XPC and thereby stabilizes it. The UbL domain of Rad23 is also required, possibly by recruiting the proteasome. **(B)** Human Rad23B is required for p53 mediated transcription in response to DNA damage. Rad23B appears to act through stabilization of ubiquitylated p53. **(C)** In yeast, the Snf1 kinase, Rad23 and the 19S proteasome co-regulate target genes both in absence and in response to damage. **(D)** In mammals, Rad23B functions as a co-activator together with other NER factors in the absence of damage. The complex binds promoters of Oct4/Sox2 activated genes, such as *Nanog*.

As described above, Rad23 has multiple functions in proteasomal degradation, DNA damage recognition and transcription regulation. Its role in transcription, at least in some cases, appears to involve other NER

factors and the proteasome. In this regard, it is interesting to note that both non-proteolytic and proteolytic contributions of the proteasome have been described to play a role in various transcriptional processes (reviewed in Collins & Tansey 2006). In yeast for example, it has been shown that the ATPases of the 19S proteasome particle are involved in the crosstalk between H2Bub1 and H3K4me3 (Ezhkova & Tansey, 2004). Furthermore, the 19S proteasomal subunit can stimulate the SAGA complex (Lee *et al.*, 2005). The 19S particle directly interacts with SAGA and enhances the targeting of the complex to promoters. On the other hand, proteolytic functions in transcriptional regulation involve degradation of RNA pol II and activators. In some cases, proteolysis was also shown to be required for efficient transcription (Collins & Tansey, 2006).

1.4.4. Dsk2 in neurodegenerative diseases

Dsk2 and two of its mammalian homologs, Ubiquilin-1 and Ubiquilin-2, have been associated with neurodegenerative diseases, most notably Alzheimer disease (AD) (reviewed in El Ayadi et al. 2013). Single nucleotide polymorphisms in the Ubiquilin-1 encoding gene have been described to be associated with an increased risk for late onset AD, however some studies failed to detect such an association in other populations (Bertram *et al.*, 2005; Arias-Vásquez *et al.*, 2007). Independently from the genetic background, decreased levels of Ubiquilin-1 protein in the brains of AD patients have been detected (Stieren *et al.*, 2011). Ubiquilin/Dsk2 has been shown to interact with Presenilin both in mammals and *Drosophila* (Mah *et al.*, 2000; Massey *et al.*, 2004; Ganguly *et al.*, 2008). Mutations in Presenilin are known to be

associated with an increased risk for early onset AD. Ubiquilins were shown to positively affect Presenilin protein levels (Mah *et al.*, 2000; Massey *et al.*, 2004). These studies suggest that both expression and turnover of Presenilin might be regulated by Ubiquilin. The effect on protein stability appears to involve binding of the Ubiquilin UBA domain to ubiquitylated Presenilin and thereby blocking ubiquitin chain elongation (Massey *et al.*, 2004). Mutation and overexpression experiments in *Drosophila* suggest an antagonistic relationship between Dsk2 and Presenilin (Ganguly *et al.*, 2008). Ubiquilin/Dsk2 further has been shown to regulate APP, another protein that is associated with AD (Hiltunen *et al.*, 2006; Gross *et al.*, 2008). Depletion of Ubiquilin-1 affects APP metabolism and leads to accelerated maturation of the protein and thereby modulates the secretion of the Aβ peptide, the main component of the plaques found in the brains of AD patients (Hiltunen *et al.*, 2006). In *Drosophila*, using transgenic APP, it was shown that Dsk2 interacts with APP and positively regulates its protein levels (Gross *et al.*, 2008). The Dsk2 UBA domain is required for the interaction with APP. Ubiquilin has been suggested to function as a chaperone that prevents aggregation of APP (Stieren *et al.*, 2011). Interestingly, a similar function for Ubiquilin-1 has been described in the suppression of aggregates of huntingtin polyQ repeats, which play a role in Huntington disease (Wang *et al.*, 2006).

2. OBJECTIVES

The main objectives of this thesis are to elucidate the molecular composition of the euchromatic HP1c complex in *Drosophila melanogaster* and to address its function at chromatin and in gene regulation.

In particular, we aim to characterize the HP1c complex by addressing the following objectives:

- Analyze the methyllysine binding activity of different HP1 isoforms *in vitro* and its functional relevance *in vivo*.
- Identify and characterize new interaction partners of the HP1c complex.
- Determine the genome-wide binding profile of the HP1c complex.
- Study the role of the HP1c complex in gene regulation.

3. RESULTS

3.1. Analysis of the HP1 – H3K9me3 interaction

The N-terminal chromo domain of HP1 proteins is best known for its ability to interact with H3K9me2/3, a modification marking heterochromatin (Bannister et al. 2001; Lachner et al. 2001). HP1 proteins have been described to interact with H3K9 methyltransferases such as Su(var)3-9 (Schotta *et al.*, 2002). A model for HP1 function in heterochromatin formation and gene silencing has been proposed that involves this dual interaction. Briefly, this reiterative model states that heterochromatin spreading requires H3K9me3 dependent targeting of HP1 proteins that consecutively recruit Su(var)3-9 in order to methylate neighboring nucleosomes (for more details see chapter 1.3.2.1). In the *Drosophila* model, most studies have used the HP1a isoform. Relatively little is known about the other four *Drosophila* HP1 isoforms and what is the importance of methylated H3K9 for their functions (Vermaak & Malik, 2009). It has been observed that the three ubiquitously expressed HP1 proteins show highly distinct chromatin binding patterns. HP1a is mainly found in heterochromatin, HP1c in contrast is apparently exclusively associated with euchromatin and HP1b is detected both in hetero- and euchromatin (Smothers & Henikoff, 2001; Font-Burgada *et al.*, 2008). Published data suggests that the euchromatic HP1c seems to be able to interact with methylated H3K9, even though the extent of co-localization in polytene chromosomes is low. In detail, it has been shown that both HP1a and HP1c bind to histones in a far-western experiment and that this binding can be competed with an H3K9me3 peptide, but not with the unmethylated control peptide. Complementary results were obtained in GST pull-downs with mononucleosomes, which suggest that both HP1a and HP1c preferentially bind to H3K9me2/3 (Font-Burgada *et al.*, 2008).

Here, we have further characterized the H3K9me3 interaction of HP1a, HP1b and HP1c using a histone peptide pull-down approach. In addition, we introduced single amino acid mutations in the chromo domain to abolish the interaction. Using these mutant HP1 variants we aimed to test, whether a functional methyl-binding motif is important for chromatin binding *in vivo*.

3.1.1. Conservation of the HP1 chromo domain

Methylated proteins and methylated histones in particular can be recognized by a large number of different domains (reviewed in Musselman et al. 2012). The methylated lysine is generally accommodated within an aromatic cage that is formed by two to four aromatic residues. The chromo domain is a member of the Royal superfamily, which also includes the chromo-barrel, the MBT, the PWWP, the Tudor and the TTD. The members of the Royal superfamily are characterized by a β-barrel conformation. The different domains that make up the Royal family were shown to bind to a variety of methylated lysines of histones and the Tudor domain in addition also can bind methylated arginines (Musselman *et al.*, 2012). The aromatic cage of the chromo domain consists of three aromatic residues (Figure 22A). Structural studies of chromo domains bound to methylated histone peptides showed that the methylated peptide inserts as a β-strand into a groove of the chromo domain and thereby completes an antiparallel β-barrel (Jacobs & Khorasanizadeh, 2002; Nielsen *et al.*, 2002; Fischle *et al.*, 2003; Min *et al.*, 2003). The chromo domains of Polycomb and HP1 bind specifically to H3K27me3 and H3K9me3, respectively. The specificity appears to be conferred by additional contacts between the

chromo domain and the neighboring residues of the methylated lysine (Fischle *et al.*, 2003; Musselman *et al.*, 2012).

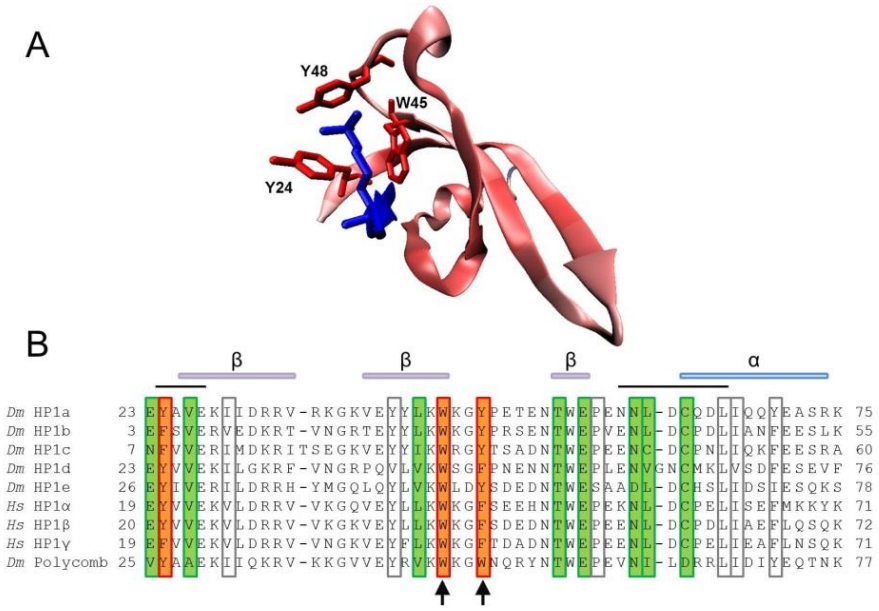

Figure 22. The HP1 chromo domain.
(A) Structure of the chromo domain (red) of *Drosophila* HP1a in complex with an H3K9me3 peptide (blue). The three side chains of the chromo domain that form the aromatic cage are shown and labeled. PDB ID: 1KNE (Jacobs & Khorasanizadeh, 2002). **(B)** Clustal omega alignment of the chromo domains of *Drosophila melanogaster* (*Dm*) and *Homo sapiens* (*Hs*) HP1s and *Drosophila* Polycomb. The β-strands and the α-helix are indicated on the top. The two black lines mark the residues that form the groove for peptide binding. The three aromatic residues forming the cage are highlighted in orange. The arrows point to the amino acids that were mutated to alanine in this study. Additional residues that are involved in peptide biding are highlighted in green. Hydrophobic amino acids boxed in grey are structurally important. Alignment based on (Jacobs & Khorasanizadeh, 2002; Nielsen *et al.*, 2002).

An alignment of the chromo domains of the three human HP1 proteins, the five *Drosophila* HP1 proteins and the *Drosophila* Polycomb protein shows that the aromatic residues forming the cage are conserved in all of

them (Figure 22B). However, different aromatic residues are used in some cases. Only the tryptophan 45 (W45; positions correspond to *Drosophila* HP1a) is invariable in all these chromo domains. Tyrosine 24 (Y24) on the other hand is changed to a phenylalanine in human HP1γ and *Drosophila* HP1b and HP1c. Interestingly, this variation (Y24F) correlates with HP1 proteins that appear to have a principal function in euchromatin (Minc *et al.*, 1999; Smothers & Henikoff, 2001; Vakoc *et al.*, 2005; Font-Burgada *et al.*, 2008). Furthermore, a Y24F mutation in *Drosophila* HP1a was shown to have functional consequences, as it affected its ability to induce silencing (Platero *et al.*, 1995). The third aromatic residue, tyrosine 48 (Y48), is a phenylalanine in all the mammalian HP1s and in *Drosophila* HP1d/Rhino, while the corresponding residue in *Drosophila* Polycomb is a tryptophan. Another difference is that among this set of chromo domains, only the *Drosophila* HP1c has an additional amino acid inserted between the two first β-strands of the domain. There are also differences in the amino acids that are known to contact the neighboring residues of the methylated lysine. One such example is the leucine 61 (L61), which interacts with the alanine (A) of the ARKS motif that is found both around H3K9 and H3K27. The L61 is altered to a cysteine (C) in *Drosophila* HP1c and to a valine (V) in *Drosophila* HP1d/Rhino, while it is conserved in most other HP1 proteins. The *S. pombe* HP1 homolog Swi6 however also has a cysteine at the corresponding position, suggesting that this change does not affect binding to methylated H3K9 (Bannister *et al.*, 2001). Another striking difference is the glutamate (E23) at the N-terminal end of the chromo domain, which is conserved in all human and *Drosophila* HP1 proteins, except in *Drosophila* HP1c, where it is an asparagine (N). Currently it is not known whether these differences in the chromo domain of HP1 proteins are functionally important. Alternatively, changes in the chromo shadow domain, the hinge or the

terminal extensions might be responsible for isoform specific interactions and functions.

3.1.2. Specific binding to methylated H3K9me3 peptides

We used a pull-down assay to test the binding of *Drosophila* HP1a, HP1b and HP1c to H3K9me3. Therefore N-terminal GST tagged HP1 proteins were induced and purified from *E. coli*. The bait in the pull-down was a biotinylated peptide that corresponds to amino acids 1-21 of histone H3 and that was either unmodified or trimethylated at K9. The H3 peptide was incubated with the GST-HP1 fusion and streptavidin sepharose. Binding was detected by western blotting against the GST tag.

The pull-down results suggest that HP1a, HP1b and HP1c all can bind to the N-terminal histone H3 tail when trimethylated at K9 (Figure 23A). Furthermore, this interaction is methylation specific, as it is not observed when using the unmodified control peptide as bait. We also used GST fusions of just the chromo domains of HP1a and HP1c and show that the chromo domain is sufficient for the interaction (Figure 23B).

Our results also reproducibly indicate that HP1c is less efficiently pulled down by H3K9me3, compared to HP1a and HP1b, suggesting that the binding affinity of HP1c for H3K9me3 might be lower than in the other isoforms (Figure 23). This difference between the HP1 isoforms can be observed both in context of the full-length protein and the chromo domain only. Though, it should be noted that this is a semi-quantitative assay and therefore this conclusion cannot be drawn unambiguously.

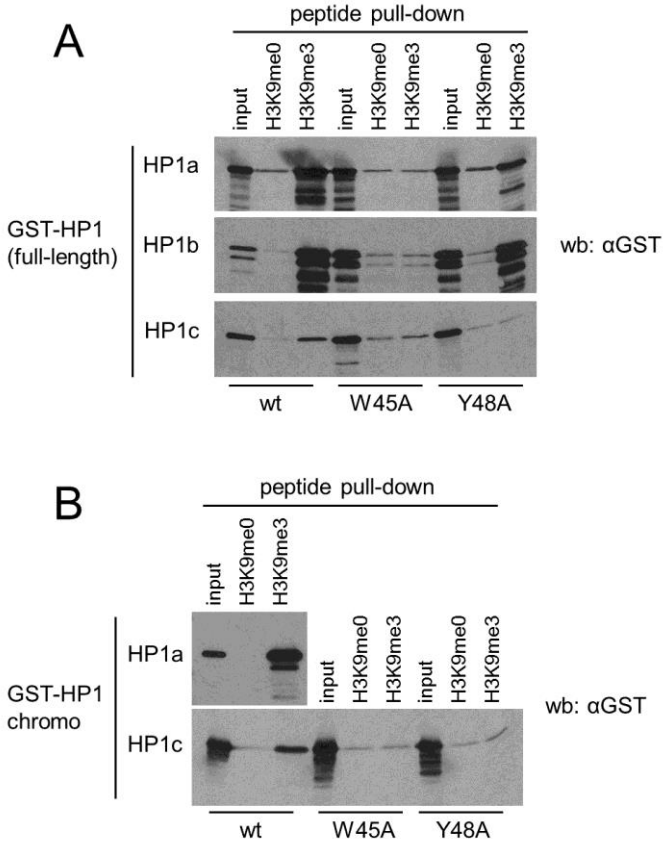

Figure 23. Histone peptide pull-down.
(A, B) Pull-down assay to study the interaction between H3K9me3 and GST fusions of full-length HP1 (A) or the HP1 chromo domain (B). A non-methylated peptide (H3K9me0) was used to show that the interaction is specific. Pull-downs were performed in the presence of wild-type (wt) or aromatic cage mutant (W45A and Y48A) HP1 variants. The GST fusion was detected by western using an αGST antibody. Input corresponds to 1% of the GST fusion used in the pull-down mix. Positions of the mutated aromatic residues are given for HP1a.

3.1.3. Abolishing H3K9me3 binding by point mutations

With the aim to establish mutants that specifically abolish interaction between HP1 and H3K9me3, we introduced single amino acid changes in conserved residues of the aromatic cage by site directed mutagenesis (Figure 22B). Of the three aromatic residues that make up the cage, two of them are invariable conserved in *Drosophila* HP1a, HP1b and HP1c. These two amino acids (W45 and Y48 in HP1a and corresponding residues in HP1b and HP1c) were mutated to alanine. Histone peptide pull-downs were performed as above with the mutant variants of the GST fusion proteins.

We found that the W45A mutation effectively abolishes binding to the methylated H3K9 peptide in all the three HP1 proteins (Figure 23A). The preference for the methylated peptide appears to be completely lost in this mutant, suggesting that W45 is absolutely required for the interaction with H3K9me3. The functional importance of W45 for binding to methylated lysines is also supported by the fact that this residue is highly conserved in chromo domain containing proteins (Figure 22B). For the Y48A mutation in contrast, the result is different. While the mutation in HP1c also results in efficient abolishment of the interaction with H3K9me3, the effects of the corresponding mutations in HP1a and HP1b are more subtle (Figure 23A). Y48A in HP1a and HP1b is slightly less efficient in H3K9me3 binding, but there is still clear preference for the methylated over the unmodified peptide. The histone peptide pull-down was also performed with a GST fusion of the HP1c chromo domain alone and the same mutations. Effects on H3K9me3 binding in this context are comparable to the full-length HP1c protein (Figure 23B).

3.1.4. HP1c localization is independent of a functional methyl-binding cage

For analyzing the requirement of the methyl-binding cage in flies, N-terminal FLAG-tagged versions of HP1a, HP1b and HP1c were generated. These constructs were inserted into a *pUASTattB* vector, which allows the generation of transgenic flies by site-directed integration. These transgenes are under the control of repeated *UAS* sites and thus can be induced by a GAL4 driver of choice. Apart from the wild-type versions of FLAG-HP1s, the same mutations in the aromatic cage as used in the peptide pull-down assay were introduced, W45A and Y48A (Figure 22B). For making transgenic flies, the HP1a and HP1b constructs were inserted into the *attP* landing site 86Fb on the third chromosome and the HP1c constructs were targeted to the 51C landing site on the second chromosome. Different landing sites were selected in order to facilitate the introduction of the constructs into a mutant background for the endogenous protein. Analysis in mutant background is desired, as HP1 proteins are known to dimerize through the chromo shadow domain (Brasher *et al.*, 2000). Thus, dimerization of the FLAG-HP1 protein with the endogenous counterpart could mask possible effects of the mutant variants.

For HP1a, the alleles *Su(var)2-5*^{04} and *Su(var)2-5*^{05} have been used, which have been characterized by others (Eissenberg *et al.*, 1992). *Su(var)2-5*^{04} contains a nonsense mutation that changes lysine 169 to a stop codon and leads to a truncated protein product that lacks part of the chromo shadow domain. The *Su(var)2-5*^{05} allele contains a frame-shift mutation at amino acid position ten. Both these alleles cause lethality during development and no adult flies are obtained neither in homozygotes nor in

transheterozygotes. Larvae however can be obtained and thus analysis of polytene chromosomes in these conditions is possible. The transgenic FLAG-HP1a constructs and a GAL4 driver were crossed either into homozygous *Su(var)2-5*^{04} or into transheterozyogous *Su(var)2-5*^{04}/*Su(var)2-5*^{05} background. However, using this strategy it was not possible to get larvae that were mutant for the endogenous protein and at the same time induced the transgene, neither the wild-type transgene nor the aromatic cage mutant transgenes. The ubiquitously expressed GAL4 drivers *armadillo*-GAL4 (*arm*-GAL4) and *daughterless*-GAL4 (*da*-GAL4) were used for these crosses. Inadequate induction of FLAG-HP1a protein levels by these drivers might be a possible explanation for the lethality. Alternatively, the FLAG tag might produce a non-functional protein and result in a dominant negative effect.

To obtain HP1c mutant conditions, a P-element insertion line was used that localizes to the 5'-UTR of the *HP1c* gene (Figure 24A). This insertion does not affect the coding sequence of the gene, however it is a strong hypomorphic allele, as in homozygous conditions no HP1c protein can be detected in immunostainings of polytene chromosomes (Figure 24C). In contrast to mutations in HP1a, flies carrying the HP1c allele homozygously develop normally and reach the adult stage without any obvious phenotypes, with the exception of sterility. The FLAG-HP1c transgene and the *arm*-GAL4 driver were brought into homozygous mutant HP1c conditions (Figure 24B, C). Such larvae are viable and were used for preparation of polytene chromosomes. Using an anti-FLAG antibody we could not detect any specific signal in these experiments. Nevertheless, with the antibody directed against the HP1c protein we were able to observe HP1c staining corresponding to the transgene in a mutant background for the endogenous protein (Figure 24B, C).

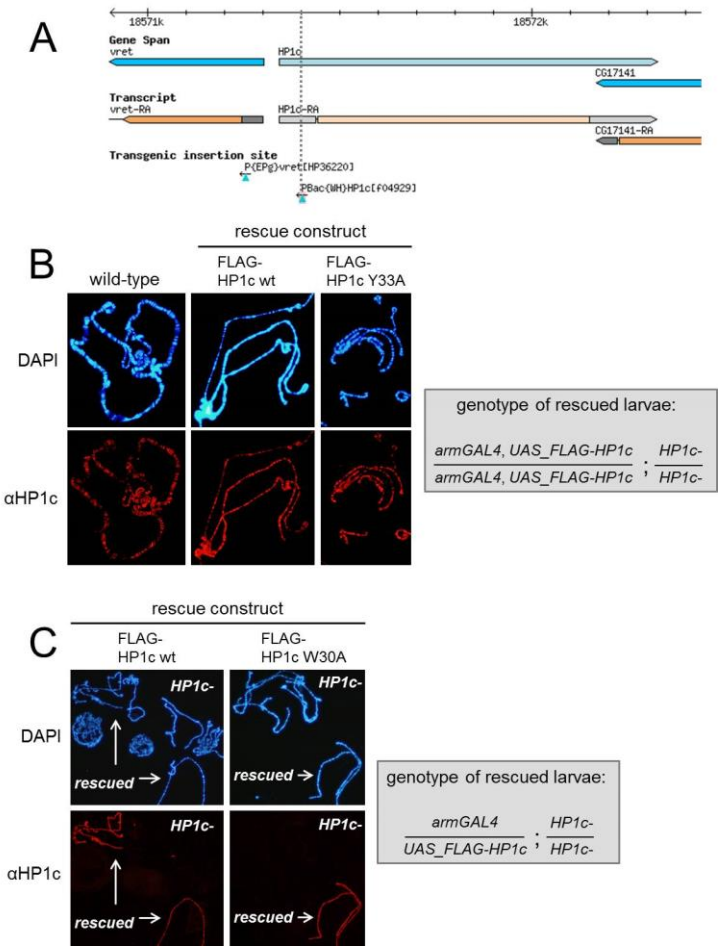

Figure 24. HP1c localization to polytene chromosomes is independent of a functional methyl-binding cage.
(A) Genome browser view of the *HP1c* gene region (FlyBase). The dotted line indicates the position of the *p-element* insertion (line f04929) that was used. **(B, C)** Polytene chromosomes were stained with DAPI (blue) and αHP1c (red). The first immunostaining on the left in (B) shows endogenous HP1c. In the other stainings, HP1c mutant (HP1c-) larvae were rescued by induction of either wild-type (wt) or mutant (W30A and Y33A) FLAG-HP1c rescue construct. The genetics of the rescued larvae are indicated on the right. In (C), polytene chromosomes from rescued larvae were mixed with such from non-rescued HP1c mutant larvae.

Staining patterns of the transgenes were highly similar to those of endogenous HP1c in wild-type flies, even for the FLAG-HP1c versions

bearing the mutations in the aromatic cage. The signal was observed at interbands all along the chromosome arms, as described in literature (Smothers & Henikoff, 2001; Font-Burgada *et al.*, 2008). The detected signal could origin from residual endogenous HP1c or from other HP1 isoforms, due to cross-reactivity. To exclude this possibility, we performed immunostainings of a mixture of polytene chromosomes obtained from HP1c mutant larvae, either inducing a FLAG-HP1c transgene or not. In these stainings, signal was only observed in a fraction of the chromosomes, suggesting that it exclusively originates from the FLAG-HP1c transgenes (Figure 24C). These results indicate that a functional methyl-binding cage is dispensable for correct HP1c targeting to chromatin.

We were not able to perform the analogous staining experiments for the FLAG-HP1b transgenes. Similar as in case of HP1a, the genetic combination of an HP1b allele, the GAL4-driver and the FLAG-HP1b transgene is not viable. The HP1b allele that was used, is a p-element insertion within the 5'-UTR of one of the annotated transcripts and upstream of the other two annotated transcripts (Figure 25A). Western analysis of brain extracts from larvae that are homozygous for the p-element, suggest that HP1b protein levels are significantly reduced, but still observable (Figure 25B). Thus, this HP1b allele can be considered a relatively weak hypomorphic mutant.

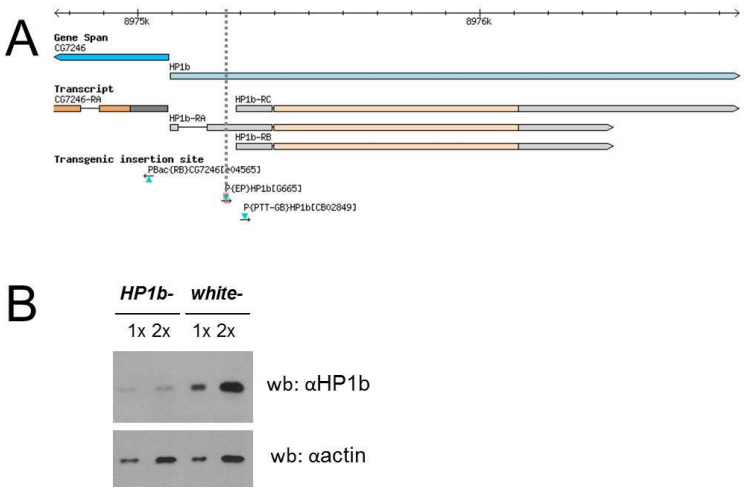

Figure 25. A hypomorphic *HP1b* allele.
(A) Genome browser view of the *HPb* gene region (FlyBase). The dotted line indicates the position of the *p-element* insertion (line G665) that was used. **(B)** Western blot showing reduced HP1b protein levels in larvae carrying the *HP1b-* allele homozygously compared to control (*white-*) larvae. Protein extracts were prepared from larval brains. Two different amounts were loaded for each condition. An αactin western was done as a loading control.

Instead of using HP1 mutant alleles, an alternative would be depletion by RNAi. However, to rescue such mutants, RNAi resistant HP1 rescue constructs would be required.

3.2. Purification of ROW and WOC complexes

HP1 function and recruitment to chromatin is commonly believed to depend on a dual interaction with methylated H3K9 and the H3K9 specific histone methyltransferase Su(var)3-9 (Schotta *et al.*, 2002) (see chapter 1.3.2.1). The fact however that HP1 proteins were shown to be able to interact with a large number of factors and that they possess isoform specific functions, suggests that HP1 targeting is by far more complex (reviewed in Hediger & Gasser, 2006; Kwon & Workman, 2011). The euchromatic *Drosophila* HP1c protein is such a case, where H3K9 methylation independent modes of recruitment exist. HP1c binding sites only partially co-localizes with methylated H3K9. Instead, as previous work from our lab and others showed, HP1c recruitment depends on the two proteins WOC and ROW (Font-Burgada *et al.*, 2008; Abel *et al.*, 2009). WOC and ROW are large proteins of 188 and 144 kDa that contain several zinc fingers and AT-hook domains and thus are potential DNA binding factors (Font-Burgada *et al.*, 2008). The types of zinc fingers (MYM) found in WOC however also have been described in mediating protein-protein interactions (Gocke & Yu, 2008). WOC and ROW were identified in purification experiments using HP1c as a bait (Font-Burgada *et al.*, 2008; Abel *et al.*, 2009). Here, we used a similar strategy to identify further factors that associate with the HP1c complex and to get more insights into HP1c function at its target sites. Therefore we generated tagged versions of ROW and WOC and used them to perform affinity purifications and subsequently to identify the associated proteins by mass spectrometry.

3.2.1. Establishing the system

We decided to use a tandem affinity purification (TAP) tag that consists of Protein A modules and a calmodulin binding peptide (CBP), which are separated by a TEV protease cleavage site. N-terminal TAP (NTAP) tagged and C-terminal TAP (CTAP) tagged versions of both full-length ROW and WOC were generated. These constructs were cloned into a *pMK33* based vector that has been described by Veraksa et al. (Veraksa *et al.*, 2005). The *pMK33* vector contains a hyromycin resistance and thus is suitable to establish stable lines of cultured *Drosophila* cells and the fusion construct is inducible by the addition of cooper, due to a metallothionein (Mt) promoter.

As a first step, the four constructs encoding tagged ROW and WOC were transiently transfected into S2 cells and induced overnight in the presence of 0.35 mM $CuSO_4$. The induction was then analyzed by western blotting using an anti-TAP antibody. In all the four cases a TAP tagged fusion was observed (Figure 26A, B). There are however marked differences depending on the position of the tag. In case of ROW the CTAP appears to give less degradation products than the NTAP version. For the WOC fusions it seems to be the opposite, as much less bands of lower molecular weights are found in the NTAP than in the CTAP variant. Based on these results we decided to use NTAP-WOC and ROW-CTAP stable cell lines for the induction and the purification experiments. Further, we aimed to find conditions that lead to induction of the TAP tagged bait in a range that is similar to the level of the endogenous protein. Vast overexpression might have the result that the majority of the tagged protein is not incorporated into the complex. To find these conditions, we checked

different concentrations of $CuSO_4$ and checked the induced levels with respect to endogenous protein (Figure 26C).

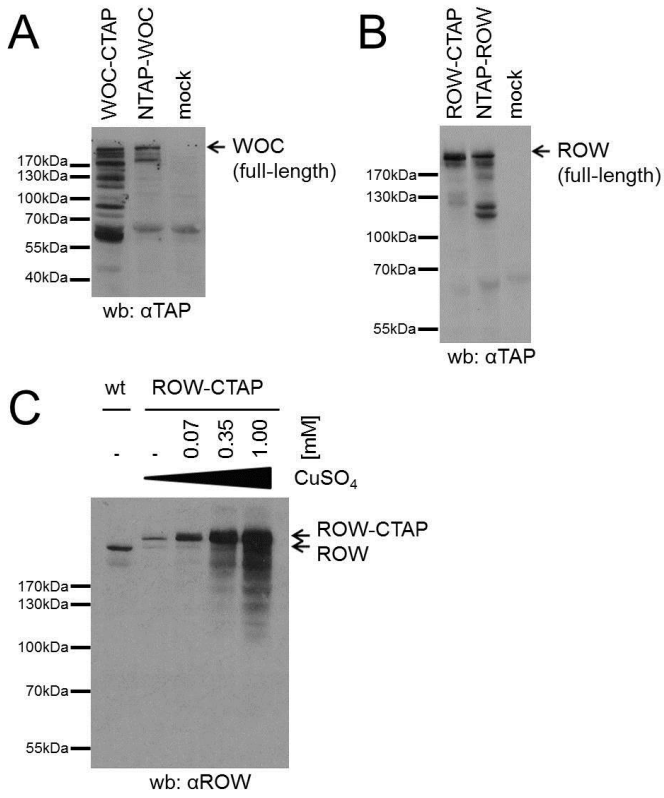

Figure 26. Induction of TAP tagged ROW and WOC in S2 cells.
(A, B) S2 cells were transiently transfected with C- or N-terminal tagged (CTAP or NTAP) WOC (A) and ROW (B) constructs. A mock transfection was done using an empty plasmid. Constructs were induced overnight with 0.35 mM $CuSO_4$. Induction was analyzed by western blotting using an αTAP antibody. **(C)** Stably transfected ROW-CTAP S2 cells were induced overnight with increasing concentrations of $CuSO_4$ or left uninduced (-). Non-transfected wild-type (wt) cells served as a control. Induction was analyzed by western blotting using an αROW antibody.

Some induction of the fusion protein can already be observed in the absence of $CuSO_4$. Addition of cooper however leads to a strong increase of the TAP tagged protein in a concentration-dependent manner. In case of ROW, the expression of the fusion protein appears to negatively regulate the endogenous protein and we found that using $CuSO_4$ at a concentration of 0.07mM leads to ROW-CTAP levels in the range of the endogenous protein. We could not compare the levels of NTAP-WOC with endogenous WOC by western due to the poor performance of the WOC antibody. For the complex purification experiments, we decided to induce the stable cell lines for both ROW and WOC with 0.15 mM $CuSO_4$, which is expected to result in a slight overexpression.

3.2.2. The purifications

For each of the purification experiments a total volume of two to three liters of confluent S2 cell culture of the NTAP-WOC and ROW-CTAP stable cell lines was induced. After overnight treatment with $CuSO_4$ the cells were collected and a nuclear extract was prepared. This extract was then used for purification of ROW and WOC associated factors. We performed a single step purification using IgG beads that interact with the Protein A modules within the TAP tag (Figure 27A). Even though the TAP tag is designed for tandem purifications, we did not do the subsequent purification involving the CBP tag. The single step purification was chosen, because previous experience in the lab suggested that the tandem strategy works inefficiently in S2 cells. After purification and washing, the bound protein complexes were eluted using an acid glycine buffer at pH3, which proved to be a good choice in order to avoid co-elution of large amounts of IgGs.

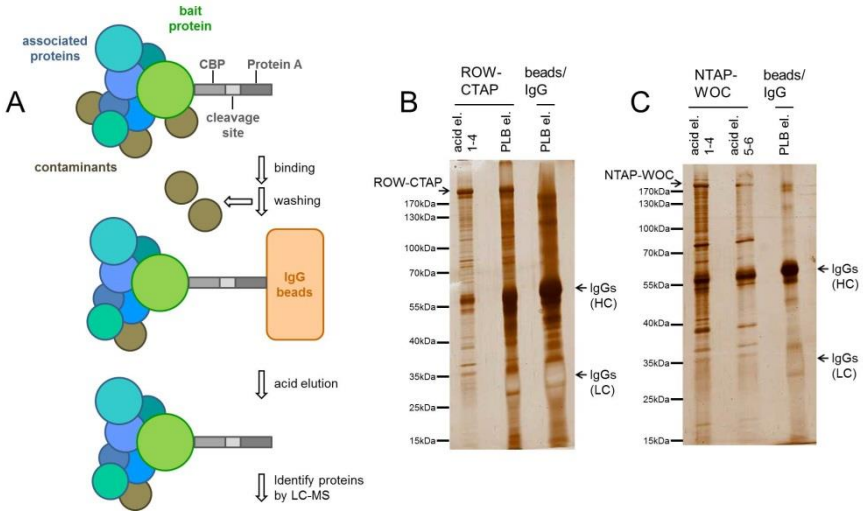

Figure 27. Purification of ROW and WOC protein complexes.
(A) The scheme illustrates the main steps of the protein complex purification experiments. The bait protein (green) is tagged with a calmodulin binding peptide (CBP) and a Protein A module. The bait protein, associated proteins (blue) and contaminants (brown) are immobilized on IgG beads and extensively washed to reduce unspecific binding of contaminants. The protein complex is eluted from the beads and associated proteins are identified by LC-MS. **(B)** Elutions of the ROW-CTAP complex were analyzed by silver staining. Four consecutive acid elutions were pooled (acid el. 1-4) and followed by an elution with SDS loading buffer (PLB el.). IgG beads (without bound material) were eluted with SDS loading buffer as a control. **(C)** Elutions of NTAP-WOC were analyzed as in (B). Six consecutive acid elutions were done. Elutions 1-4 (acid el. 1-4) and elutions 5-6 (acid el. 5-6) were pooled. In (B, C) the positions of the bait, the heavy chain (HC) and the light chain (LC) IgGs are indicated.

For visualization, aliquots of the eluted samples were analyzed by silver staining (Figure 27B, C). The rest of the samples were run into a SDS-PAGE stacking gel, without separating the proteins into single bands. The concentrated samples were then cut from the gel and analyzed by LC-MS in order to identify the purified proteins. In total, three purification experiments were performed using these conditions. Two replicates were done with the ROW-CTAP and one experiment with NTAP-WOC as bait.

3.2.3. Identification of ROW and WOC associated proteins

The proteins identified by MS in the three purification experiments were overall highly similar (Figure 28). Among the proteins with the highest MASCOT score we found in all the cases the bait and the already known subunits of the complex. Besides ROW, WOC and HP1c we also identified the HP1b isoform, further underpinning previous observations that the euchromatic fraction of HP1b forms part of a WOC and ROW containing complex (Font-Burgada *et al.*, 2008). Apart from these known subunits we also identified several proteins that have not been previously studied in relation to the HP1c complex. One such factor is Dsk2, an ubiquitin receptor of the UbL/UBA family, which is also known as Ubiquilin (see chapter 1.4 for details). Several peptides corresponding to Dsk2 were detected in each purification experiment and MASCOT scores were between 647 and 1133. Dsk2 is known to play a role in the regulation of ubiquitylated substrates and can interact with the proteasome (reviewed in Su & Lau, 2009). A function for Dsk2 in chromatin however has not been described before. Two other factors that were reproducibly identified are Z4 and Chromator, which are chromosomal proteins that bind to interbands of polytene chromosomes and that were shown to interact with each other (Eggert *et al.*, 2004; Gortchakov *et al.*, 2005). Z4 contains seven zinc fingers and a coiled-coil region and Chromator contains a single chromo domain, whose binding target is currently unknown (reviewed in Eissenberg, 2012). Z4 has also been described to be a subunit of the TRF2/DREF complex, which has a function in core promoter selection and gene regulation in *Drosophila* (Hochheimer *et al.*, 2002). More recent results suggest that Chromator is required for correct localization of Z4 to chromatin (Gan *et al.*, 2011). Z4 has also been

implicated in the regulation of Notch target genes (Kugler & Nagel, 2007, 2010). Further, both Z4 and Chromator have been co-purified with the nonspecific lethal (NSL) complex, which has a function at actively transcribed genes (Raja *et al.*, 2010). In addition, Z4 and Chromator have been shown to co-localize with the kinase Jil-1 and being required for its recruitment to polytene chromosomes (Rath *et al.*, 2006; Gan *et al.*, 2011). While Z4 was detected in both ROW and WOC purifications with relatively high scores (96-440), scores for Chromator were lower and no peptide at all was detected in the WOC complex. We also detected peptides corresponding to the BEAF-32 boundary factor in all the three experiments, although with relative low scores. Besides being involved in boundary functions, BEAF-32 has also been suggested to play a broader role related to transcription. In a genome-wide localization study it was found that most BEAF-32 sites are in close proximity to transcription start sites of actively transcribed genes (Jiang *et al.*, 2009). The dsRNA binding protein Blanks was also found in all the three complex purifications, with a high score of 360 in case of WOC and with much lower scores in the ROW purifications. Little is known about Blanks function, apart from a role in the male germline during spermiogenesis (Gerbasi *et al.*, 2011). In addition to the common factors, several proteins were just identified either in the WOC or ROW complex purifications. For example, coilin was identified with very high scores (652 and 1146) when using ROW as a bait, but not at all in the respective experiment using WOC. Coilin associates with Cajal bodies, which are nuclear organelles that function in the metabolism of ribonucleoproteins (Liu *et al.*, 2009). Interestingly, in one of the ROW experiments, we also co-purified WDR79, another protein that has a Cajal body related function (Tycowski *et al.*, 2009). Noteworthy, we also identified several peptides corresponding to chromatin modifiers or remodelers, namely the histone chaperone CAF-1, the histone deacetylase RPD3, the Brahma (SWI/SNF) complex subunits

Snr1, moira and Bap170 and the Brahma associated protein pontin (Rubertis *et al.*, 1996; Martens & Winston, 2003; Mohrmann *et al.*, 2004; Diop *et al.*, 2008; Avvakumov *et al.*, 2011). Several of the proteins identified, Chromator, pontin and cut up, have been reported to have a function at microtubule spindles during mitosis (Rath *et al.*, 2004; Ducat *et al.*, 2008; Wang *et al.*, 2011). Other peptides that got identified might be considered typical contaminants, such as actin, tubulin and heat-shock related proteins.

			ROW-CTAP I			ROW-CTAP II			NTAP-WOC		
	Protein	Function	Score	Pept.	Cov.	Score	Pept.	Cov.	Score	Pept.	Cov.
HP1c complex	ROW	HP1c complex	4376	73	55.7	2762.6	44	37.6	2111.3	34	32.5
	WOC	HP1c complex; telomeres	1295.6	24	37	836.1	14	17.7	2119.3	32	24.8
	HP1b	HP1c complex	555.1	10	47.5	250.4	5	27.9	204	4	27.9
	HP1c	HP1c complex; FACT	357.6	5	35.9	264	3	24.5	112.1	1	7.6
transcription	Z4	transcription; NSL; TRF2/Dref	440.2	7	12.3	229.4	3	4.5	96.1	2	4.8
	Chromator	NSL; mitotic spindles	264	5	10	42.2	1	1.9			
	BEAF-32	transcription; boundary	104	2	10.6	48	1	3.2	59.7	1	4.6
chromatin remodeling	WDS	NSL; ATAC complex (HAT)				102.8	1	7.2			
	RPD3	HDAC				61.6	1	4.4	63.7	1	4.4
	CAF-1	histone chaperone	69.5	2	8.4						
	pontin	Brahma; mitotic spindles				115.3	2	7.5	56.9	1	3.5
	moira	Brahma				100.9	1	1.3			
	Snr1	Brahma	41.3	1	3.5	79.6	1	3.5			
	Bap170	Brahma				38.7	1	1.3			
others	Dsk2	ubiquitin receptor	719	10	32.2	647.1	8	32.7	1133.4	15	40
	coilin	Cajal bodies	1146.1	18	46.7	651.9	10	20.5			
	WDR79	Cajal bodies; RNA binding	116.7	3	5.2						
	Blanks	RNA binding; spermiogenesis	63.9	1	4.1	89.6	1	10.8	360.1	6	23.9
	cut up	mitotic spindles							374.2	5	62.9

Figure 28. Proteins identified in ROW and WOC complex purifications.
The table lists proteins that were identified associated with ROW or WOC in complex purifications. Two experiments with ROW-CTAP and one experiment with NTAP-WOC were performed. The MASCOT score, the numbers of identified peptides (Pept.) and the coverage (Cov.) in percentage of each protein are indicated for the individual purification experiments. Known functions of the identified proteins are mentioned (see main text for details and references). Some proteins that were identified with very low scores and only in individual experiments were omitted. Typical contaminants such as actin, tubulin and heat-shock proteins are not shown.

3.2.4. Validation by co-immunoprecipitation

The above described complex purification experiments have been done with ectopically expressed TAP tagged ROW and WOC variants. In a first set of follow-up experiments we aimed to test whether the identified interactions can be reproduced in co-immunoprecipitation (CoIP) studies using antibodies recognizing the endogenous proteins. However, we made a preselection based on the number of experiments in which the protein had been identified and on the MASCOT scores. On this shortlist were Dsk2, coilin, Z4, Chromator, BEAF-32 and Blanks. Note that the CoIPs with Dsk2 and other experiments related to Dsk2 are described in a separate chapter (see chapter 3.3).

While coilin was identified by MS with high MASCOT scores in the ROW complexes, but not in the WOC complex, we were not able to detect a specific interaction by CoIP, neither with WOC nor with ROW (Figure 29D). Similarly, we could not confirm an interaction between Blanks and the HP1c complex (Figure 29E). Interestingly, the boundary factor BEAF-32 efficiently co-immunoprecipitates with WOC, but neither with ROW nor HP1c (Figure 29C). The significance of this finding is unclear, as in the complex purifications, BEAF-32 was detected in both WOC and ROW complexes (Figure 28). Further, we could also confirm the interaction with Z4 to some extent. Z4 co-immunoprecipitates with ROW, WOC and HP1c (Figure 29A). In the other direction however, when using Z4 as bait, we could not reproduce the interaction (Figure 29B). Z4 and Chromator have been described to function within the same complex (Eggert *et al.*, 2004; Gortchakov *et al.*, 2005; Gan *et al.*, 2011). While we identified both proteins in the ROW complex purifications, we

could not corroborate the interaction with Chromator in CoIP experiments (Figure 29B).

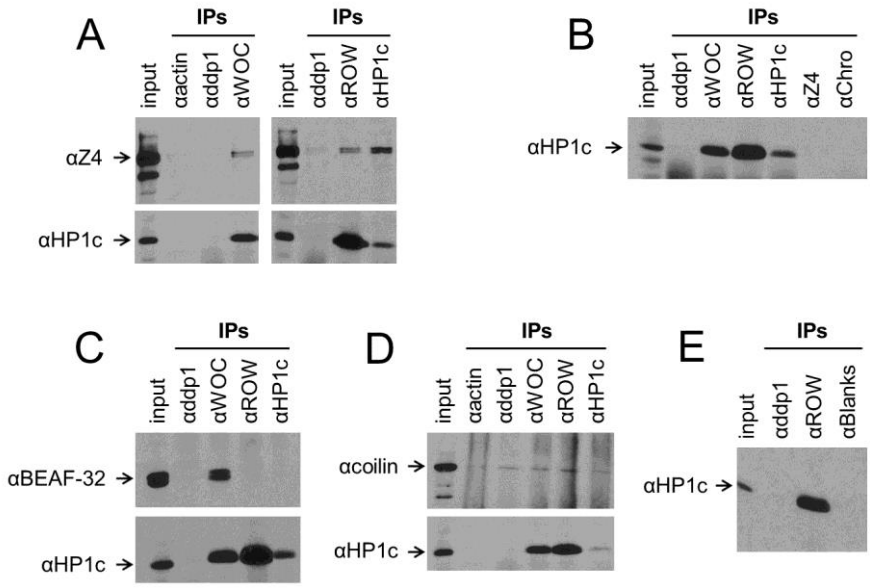

Figure 29. Validation of interactions by co-immunoprecipitation.
(A-E) Protein extracts were prepared from S2 cells and subjected to immunoprecipitation (IP) with the indicated antibodies, which were raised in rabbit, except for the guinea pig αZ4 antibody used in (B). IPs with αddp1 and αactin served as negative control. CoIPs were analyzed by western blotting using rat polyclonal αHP1, αZ4, guinea pig polyclonal αcoilin and mouse monoclonal αBEAF-32. Input corresponds to 2.5% of the extract used for immunoprecipitation. αChro, αChromator.

3.3. The interaction with Dsk2

In this chapter we describe the characterization of the novel HP1c complex subunit Dsk2, an ubiquitin receptor, which we have found by purifying ROW and WOC complexes (Figure 28). We reveal a non-proteolytic function of Dsk2 that is required for transcription of HP1c complex target genes. Our results further suggest that Dsk2 regulates transcription via its interaction with H2Bub1, thereby protecting it from preliminary deubiquitylation by Ubp8/Nonstop.

This chapter corresponds to a draft for an article that was submitted to Molecular Cell in February 2014. The major part of experimental work presented in this chapter has been performed by Roman Kessler. Joan Font-Burgada has done the microarray expression analysis (Figure 31D, E) and assisted in ROW and WOC complex purifications (Figure 30A). Johan Tisserand has performed a susbset of the ChIP-qPCR experiments (Figure 32B, Figure 33B, Figure 35A, Figure S 2 and Figure S 4) and the ROW/Dsk2 co-immunostaining in wing imaginal discs (Figure 32B). The ChIP-seq experiments have been done in collaboration with the IRB functional genomics facility led by Herbert Auer. Analysis of microarray and ChIP-seq data was done in collaboration with Camille Stephan-otto Attolini and Oscar Reina of the IRB Biostatistics/Bioinformatics unit.

The *Drosophila* ubiquitin receptor dDsk2 is a component of the dHP1c/WOC/ROW transcription complex that regulates H2B mono-ubiquitylation (H2Bub1)

Roman Kessler[1,2], Joan Font-Burgada[1,2,4,+], Johan Tisserand[1,2,4], Oscar Reina[2], Camille Stephan-otto Attolini[2], Ivan Garcia-Bassets[3] and Fernando Azorín[1,2,*]

[1]Institute of Molecular Biology of Barcelona, CSIC. 08028 Barcelona. Spain.

[2]Institute for Research in Biomedicine, IRB Barcelona. 08028 Barcelona. Spain

[3]Department of Medicine, School of Medicine. University of California, San Diego. La Jolla, CA 92093, USA

[4]these authors contribute equally to this work

Running title: dDsk2 regulates H2Bub1

[+]present address:

Laboratory of Gene Regulation and Signal Transduction, Departments of Pharmacology and Pathology, School of Medicine, University of California, San Diego, 9500 Gilman Drive, La Jolla, CA 92093, USA.

*Corresponding author:

Dr. F. Azorín
Institute of Molecular Biology of Barcelona, CSIC
Institute for Research in Biomedicine of Barcelona
Baldiri Reixac, 10. 08028 Barcelona. Spain
Phone#: 3493 4034958; Fax#: 3493 4034979
e-mail: fambmc@ibmb.csic.es

ABSTRACT

dDsk2 is a highly conserved extraproteasomal ubiquitin receptor that selectively binds ubiquitylated proteins and targets them to the proteasome. Here, we report that, in addition to regulating protein stability, dDsk2 is a chromosomal protein that regulates transcription. We show that dDsk2 is a component of the dHP1c/WOC/ROW transcription complex that localizes at promoters of active genes and is required for transcription. Through the ubiquitin-binding domain, dDsk2 specifically recognizes H2Bub1, a modification that occurs at promoters and regulates transcription. Decreased H2Bub1 does not impair binding of the dHP1c-complex. In contrast, dDsk2 depletion strongly reduces H2Bub1. Co-depletion of the main H2Bub1 deubiquitinase (dUbp8/Nonstop) suppresses this effect, indicating that dDsk2 regulates H2Bub1 deubiquitylation, a process that mediates release of active RNApol II from the promoter into elongation. These results unveil the essential function of dDsk2 in transcription regulation, suggesting a general role of ubiquitin receptors as epigenetic regulators of chromatin.

INTRODUCTION

Ubiquitin receptors bind ubiquitylated substrates by directly recognizing ubiquitin and play a central role in targeting proteins for degradation (reviewed in Hicke *et al.*, 2005; Raasi & Wolf, 2007; Finley, 2009; Clague & Urbé, 2010; Trempe, 2011). They stably associate with the proteasome as intrinsic subunits (Rpn10 and Rpn13) or only transiently as extraproteasomal receptors that act as shuttling factors that bring ubiquitylated proteins to the proteasome. Ubiquitin receptors also participate in autophagy and endolysosomal protein degradation. Dsk2 is a highly conserved extraproteasomal ubiquitin receptor that in yeast, *Drosophila* and mammals has been shown to selectively target ubiquitylated proteins to the proteasome for degradation (Li, Xie, *et al.*, 2007; Lipinszki *et al.*, 2009). Dsk2 belongs to a family of receptors that are characterized by the presence of ubiquitin-like (UbL) and ubiquitin-associated (UBA) domains (reviewed in Su & Lau, 2009; Wade & Auble, 2010), where the UBA domain mediates recognition of ubiquitylated substrates by directly binding the ubiquitin moiety (Wilkinson *et al.*, 2001; Funakoshi *et al.*, 2002; Nakayasu *et al.*, 2013), while the UbL domain mediates interaction with the proteasome (Hiyama, 1999; Wilkinson *et al.*, 2001; Elsasser *et al.*, 2002; Gomez *et al.*, 2011).

To date, apart from its role in regulating protein stability, no other functions had been attributed to Dsk2. Here, we report that *Drosophila* dDsk2 is also a chromosomal protein that plays an essential role in regulating expression of dHP1c target genes. HP1s constitute a diverse family of proteins that are widely conserved in eukaryotes, with most species containing several isoforms (reviewed in Hiragami & Festenstein, 2005; Lomberk *et al.*, 2006; Fanti & Pimpinelli, 2008; Vermaak & Malik,

2009; Kwon & Workman, 2011). In particular, *Drosophila* encodes three ubiquitously expressed isoforms (dHP1a, dHP1b and dHP1c) that have distinct localization patterns and functional properties. dHP1a preferentially associates with heterochromatin and contributes to gene silencing. In contrast, dHP1c localizes to euchromatin, forms a complex with the transcription factors WOC and ROW, and regulates gene expression (Smothers & Henikoff, 2001; Font-Burgada *et al.*, 2008; Abel *et al.*, 2009; Kwon *et al.*, 2010), whereas dHP1b is found both at heterochromatin and euchromatin (Smothers & Henikoff, 2001; Font-Burgada *et al.*, 2008). Results reported here identify dDsk2 as an intrinsic component of the dHP1c/WOC/ROW transcription complex that localizes at promoters of active genes and is required for transcription. We also show that, through the UBA-domain, dDsk2 recognizes mono-ubiquitylated H2B (H2Bub1), a histone modification that occurs at promoters of active genes and extends along the entire coding region (reviewed in Laribee *et al.*, 2007; Weake & Workman, 2008, 2010; Lee *et al.*, 2010). At promoters, H2Bub1 depends on an activator-mediated recruitment of the E2/E3 ubiquitin ligases Rad6/Bre1, stimulates H3K4me3 and is required for transcription. Later, Ubp8 dependent H2Bub1 deubiquitylation is required for Ser2 phosphorylation of the RNApol II CTD and, thus, for release of active RNApol II from the promoter into productive elongation. Our results show that dDsk2 prevents premature H2Bub1 deubiquitylation by dUbp8 and, thus, regulates an essential step in transcription. To our knowledge, this study provides the first evidence for a direct involvement of ubiquitin receptors in the epigenetic regulation of chromatin structure and function.

RESULTS

dDsk2 interacts with the dHP1c/WOC/ROW transcription complex

Biochemical analyses of proteins co-purifying with dHP1c showed that it forms a complex with the transcription factors WOC and ROW (Font-Burgada *et al.*, 2008; Abel *et al.*, 2009). Here, to identify additional components of this complex, we performed affinity purifications using stable S2 cell lines expressing ROW-TAP and TAP-WOC fused proteins. Co-purified proteins identified with high confidence are listed in Figure 30A. In addition to dHP1c, WOC and ROW, these experiments detected the following interacting proteins: the dHP1b isoform (Vermaak *et al.*, 2005); the boundary protein BEAF-32 (Gerasimova & Corces, 1996); the chromosomal proteins Chromator and Z4, which are known to form a complex (Eggert *et al.*, 2004; Gortchakov *et al.*, 2005); the RNA-binding protein Blanks (Gerbasi *et al.*, 2011); the ubiquitin receptor protein dDsk2 (Li, Xie, *et al.*, 2007), and coilin, a factor that marks Cajal bodies and associates to the histone *locus* (Liu *et al.*, 2009). Co-IP experiments directly confirmed several of these interactions. In particular, a strong interaction with dDsk2 was detected, as IPs performed with αdHP1c, αWOC and αROW antibodies bring down dDsk2 (Figure 30B) and, *vice versa*, αdDsk2 antibodies co-immunoprecipitate dHP1c and ROW (Figure 30C). Notice that the poor performance of αWOC antibodies in Western blot analyses prevented detection of WOC in these experiments (Figure S 7A). Furthermore, immunostaining experiments in polytene chromosomes detected a strong co-localization of dHP1c and dDsk2 (Figure 30D).

A

PROTEIN	SCORE	PEPTIDES	COVERAGE
ROW	2111	34	55.7%
WOC	1295	24	37%
coilin*	1146	18	46.7%
dDsk2	1133	15	40%
dHP1b	555	10	47.5%
Z4	440	7	12.3%
dHP1c	358	5	35.9%
Blanks	360	6	23.9%
Chromator*	264	5	10%
BEAF-32	104	2	10.6%

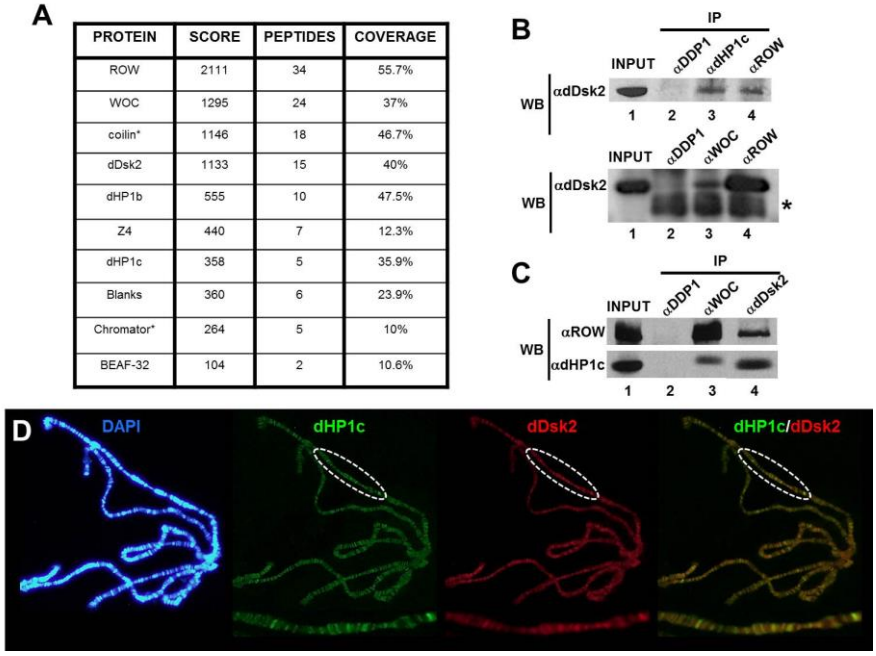

Figure 30. The dHP1c-complex interacts with dDsk2.
(A) Proteins co-purifying with ROW-TAP and/or TAP-WOC in at least two independent purification experiments are listed. The best scores are indicated. The asterisk (*) indicates proteins identified only in ROW-TAP purification experiments. **(B)** dDsk2 co-immunoprecipitates with components of the dHP1c-complex. On the top, IPs were performed with rat polyclonal αdHP1c (lane 3), αROW (lane 4) and control αDDP1 (lane 2) antibodies. On the bottom, IPs were performed with rabbit polyclonal αWOC (lane 3), αROW (lane 4) and control αDDP1 (lane 2). IP-materials were analyzed by western blot using rabbit polyclonal αdDsk2. Lanes 1 corresponds to 2.5% of the input material. At the bottom, the asterisk (*) indicates a band corresponding to IgGs. **(C)** Components of the dHP1c-complex co-immunoprecipitate with dDsk2. IPs were performed with rabbit αdDsk2 (lane 4), and control αWOC (lane 3) and αDDP1 (lane 2) antibodies, and analyzed by western blot using rat polyclonal αROW (top) and αdHP1c (bottom). Lane 1 corresponds to 2.5% of the input material. **(D)** dHP1c and dDsk2 strongly co-localize. Polytene chromosomes were immunostained with rat polyclonal αdHP1c (green) and rabbit polyclonal αdDsk2 (red) antibodies. Enlarged images of the indicated region are shown at the bottom. DNA was stained with DAPI (blue).

The dHP1c-complex localizes at promoters of active genes and is required for transcription

Immunostaining experiments in polytene chromosomes showed that the dHP1c-complex localizes at active chromatin domains, suggesting a role in gene expression regulation (Font-Burgada *et al.*, 2008; Abel *et al.*, 2009). However, the actual nature and molecular mechanism of this contribution remained largely unknown. To address these questions, we determined by ChIP-seq the actual localization of the complex at the genomic level and the extent of overlapping of its components. As shown in Figure 31A, dHP1c, WOC, ROW and dDsk2 predominantly localize at promoters with ~60% of peaks lying within ± 1 kb to a transcription-start-site (TSS). The distributions of dHP1c, WOC and dDsk2 are centered at TSS and largely overlap, whereas ROW shows a bimodal distribution with a major peak slightly displaced downstream from the TSS and a second peak localizing about 0.5 kb upstream (Figure 31B). The four factors strongly co-localize (Figure 31C), with more than 1500 common target genes being identified. Common genes account for a high proportion (~70%) of dHP1c targets but, on the other hand, they constitute a much lower proportion of WOC (~30%), ROW (~25%) and dDsk2 (~35%) targets. These differences are largely arising from the different performance of the antibodies used in ChIP-experiments, since dHP1c is actually enriched at WOC/ROW/dDsk2 target genes regardless of whether they are statistically identified as dHP1c targets or not. Indeed, dHP1c abundance at these genes is significantly higher than at non-WOC/ROW/dDsk2 target genes (Figure S 1A) and its distribution is similar to that observed in target genes (Figure S 1B). Furthermore, ChIP-chip data generated by the modENCODE project identify a higher number

of dHP1c target genes (Figure S 1C), a majority of which is also detected as WOC/ROW/dDsk2 target genes in our experiments (Figure S 1D).

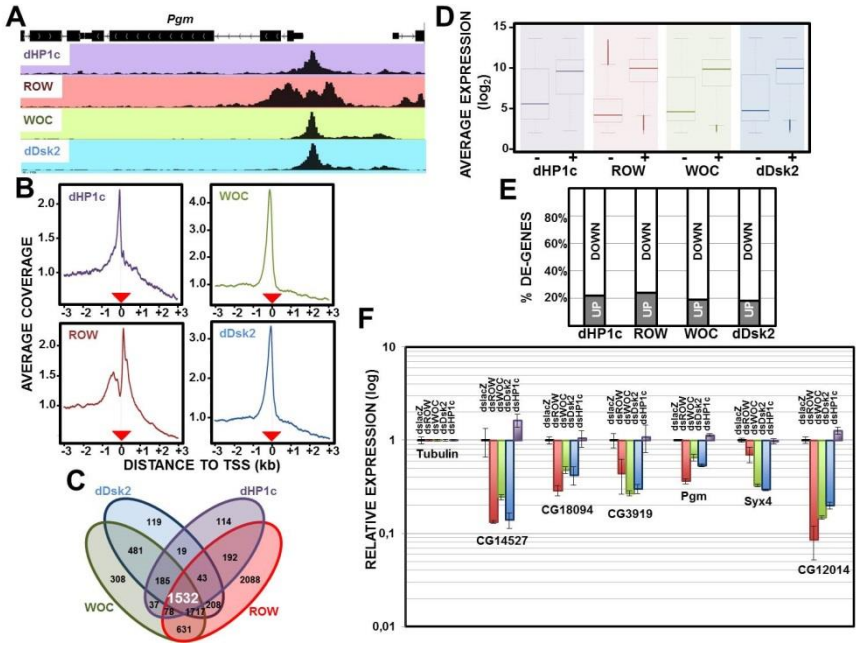

Figure 31. The dHP1c-complex localizes at TSS.
(A) ChIP-seq coverage profiles of dHP1c, ROW, WOC and dDsk2 across a representative region. Genomic organization of the region is indicated. Antibodies used were rabbit polyclonal αdHP1c, αROW, αWOC and αdDsk2. **(B)** The distribution around TSS is presented for dHP1c, ROW, WOC and dDsk2. For each gene, the coverage profile was normalized dividing by the average coverage in that gene. The position of the TSS is indicated. **(C)** Venn diagram showing the intersection between dHP1c, ROW, WOC and dDsk2 target genes. **(D)** Box plot showing the expression of dHP1c, ROW, WOC and dDsk2 target (+) and non-target (-) genes. **(E)** The percentage of dHP1c, ROW, WOC and dDsk2 target genes that are found differentially down- and up-regulated upon depletion of ROW in S2 cells is presented. **(F)** mRNA levels of six dHP1c-complex target genes are determined by RT-qPCR in S2 cells upon depletion of dHP1c (purple), ROW (red), WOC (green) and dDsk2 (blue). mRNA levels were determined in relation to cells treated with dsRNA against LacZ. Results were normalized with respect to Tubulin levels.

Expression profiling analyses indicate that the dHP1c-complex is required for transcription since target genes for any of its components are actively

transcribed (Figure 31D) and, upon RNAi-mediated depletion of ROW, ~80% of the target genes changing expression are found down regulated (Figure 31E). RT-qPCR experiments confirmed these results since several selected target genes were found significantly down regulated upon ROW depletion (Figure 31F). WOC and dDsk2 depletion led to a similar effect on expression. In contrast, dHP1c depletion showed no significant effect (Figure 31F). In this regard, it must be mentioned that dHP1b also interacts with WOC and ROW (Font-Burgada *et al.*, 2008) (Figure 30A), suggesting that its association with the complex could compensate for the absence of dHP1c (see Discussion).

dDsk2 is required for binding of the dHP1c-complex

The contribution of the proteasome to transcription regulation has been extensively documented (reviewed in Lipford & Deshaies, 2003; Collins & Tansey, 2006; Geng *et al.*, 2012). In particular, proteasome-mediated degradation has been shown to directly affect transcription by coupling transcription factor turnover to activation (Salghetti *et al.*, 2001; Lipford *et al.*, 2005). Thus, the interaction of dDsk2 with the dHP1c-complex could regulate proteolytic degradation of the complex. However, opposite to this hypothesis, dDsk2 depletion in S2 cells does not increase stability of the complex but it results on a slightly decrease in total dHP1c and ROW content (Figure 32A, lane 5). Immunostaining experiments in wing imaginal discs confirmed these results. In these experiments, we used *dsk2*^{RNAi} flies that carry a UAS_{GAL4} synthetic hairpin construct to generate siRNAs to silence *dDsk2* expression at the anterior/posterior (A/P)-border using a *ptc*-GAL4 driver that is specifically active at the A/P-border.

Under these conditions, dDsk2 depletion is strong and consistently reduces dHP1c, WOC and ROW (Figure 32B).

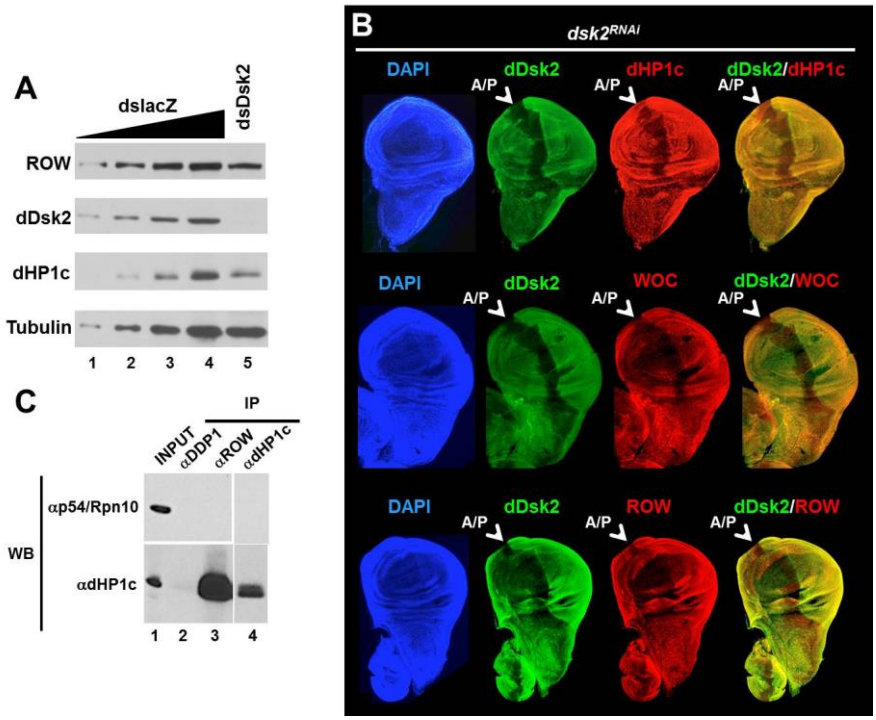

Figure 32. dDsk2 does not mediate proteolytic degradation of the dHP1c-complex.
(A) The levels of ROW, dHP1c and dDsk2 are determined by western blot in extracts prepared from control S2 cells treated with dsRNA against LacZ (lanes 1-4: increasing amounts of extract are analyzed) and upon depletion of dDsk2 (lane 5). Tubulin levels are also presented as loading control. Antibodies used were rabbit polyclonal αROW and αdDsk2, rat polyclonal αdHP1c and mouse αTubulin. **(B)** Wing imaginal discs obtained from *dsk2*^{RNAi}*; ptc*-GAL4 larvae were immunostained with rabbit polyclonal αdDsk2 (green) and rat polyclonal αHP1c (top), αWOC (center) and αROW (bottom) antibodies (red). DNA was stained with DAPI (blue). The arrows indicate the A/P-boundary where the *ptc*-promoter is specifically active. **(C)** p54/Rpn10 does not co-immunoprecipitate with the dHP1c-complex. IPs were performed with rabbit polyclonal αROW (lane 3), αdHP1c (lane 4) and control αDDP1 (lane 2) antibodies. IP-materials were analyzed by western blot using mouse polyclonal αp54/Rpn10 (top) and rat polyclonal αdHP1c (bottom). Lanes 1 correspond to 2.5% of the input material.

Moreover, co-IP experiments failed to detect an interaction with p54/Rpn10, the proteasome subunit that mediates dDsk2 binding (Su & Lau, 2009; Wade & Auble, 2010; Lipinszki *et al.*, 2011, 2012) (Figure 32C). Actually, it is unlikely that dDsk2 interacts with both the dHP1c-complex and the proteasome at the same time since, as shown below (Figure 34D), the interaction with the dHP1c-complex involves the UbL domain of dDsk2 that also mediates binding to the proteasome (Su & Lau, 2009; Wade & Auble, 2010). Altogether, these results indicate that dDsk2 does not regulate proteasome-mediated degradation of the dHP1c-complex.

Next, we analyzed whether dDsk2 is involved in binding of the dHP1c-complex to chromatin. Immunostaining experiments confirmed this hypothesis, as binding of dHP1c, WOC and ROW are strongly reduced in polytene chromosomes from *dsk2*^{RNAi} flies, where dDsk2 depletion was ubiquitously induced using an *actin5C*-GAL4 driver (Figure 33A). ChIP-qPCR analyses in S2 cells corroborated these results since depletion of dDsk2 reduces binding of WOC and ROW at promoters of several selected target genes (Figure 33B). Previous results showed that WOC and ROW are mutually required for binding to chromatin, as well as for binding of dHP1c (Font-Burgada *et al.*, 2008). Therefore, we also determined whether dDsk2 binding depends on the rest of components of the complex. As shown by immunostaining experiments in polytene chromosomes, dDsk2 binding is strongly reduced upon WOC and ROW depletion (Figure 33C, top and center panels). ChIP-qPCR analyses confirmed these results since dDsk2 binding at promoters of several target genes is strongly reduced upon ROW depletion (Figure 33D). In contrast, dHP1c depletion does not significantly affect dDsk2 binding (Figure 33C, bottom panel). Interestingly, it was also shown that dHP1c depletion does

not affect binding of WOC and ROW to chromatin (Font-Burgada *et al.*, 2008).

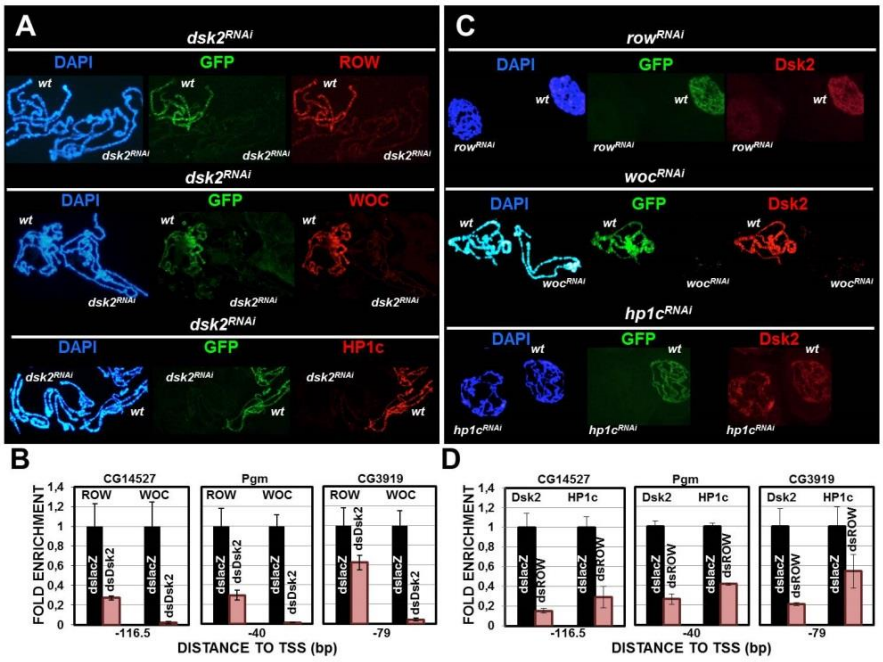

Figure 33. dDsk2 is required for binding of the dHP1c-complex and *vice versa*.

(A) The patterns of immunolocalization of ROW (top), WOC (center) and dHP1c (bottom) (in red) are presented in polytene chromosomes obtained from mutant *dsk2^{RNAi}; act5C-GAL4* larvae. Polytene chromosomes obtained from control *H2Av-GFP* wild-type larvae (*wt*) were mixed and squashed together with mutant *dsk2^{RNAi}* polytene chromosomes, which are identified by their lack of reactivity with αGFP antibodies (in green). DNA was stained with DAPI. **(B)** ROW and WOC levels at the indicated positions respect to the TSS of selected target genes are determined by ChIP-qPCR in control S2 cells treated with dsRNA against LacZ (black) and upon depletion of dDsk2 (red). Results are presented as fold enrichment with respect to the control (dsLacZ). **(C)** As in panel A but the patterns of immunolocalization of dDsk2 (in red) are presented in polytene chromosomes obtained from *row^{RNAi}; lio-GAL4* (top), *woc^{RNAi}; lio-GAL4* (center) and *hp1c^{RNAi}; act5C-GAL4* (bottom) mutant larvae. **(D)** As in panel B but for dDsk2 and dHP1c levels in control S2 cells treated with dsRNA against LacZ (black) and upon depletion of ROW (red). Antibodies used were rabbit polyclonal αROW, αWOC, αdDsk2 and αdHP1c.

dDsk2 regulates H2Bub1

Binding sites of the dHP1c-complex are decorated with H2Bub1 (Figure 34A), a histone modification that generally occurs at promoters of active genes (reviewed in Laribee *et al.*, 2007; Weake & Workman, 2008, 2010; Lee *et al.*, 2010), suggesting the possibility that, as a subunit of the dHP1c-complex, dDsk2 interacts with H2Bub1. Peptide pull-down assays confirmed this hypothesis since the UBA domain of dDsk2, which mediates binding to ubiquitylated substrates (Wilkinson *et al.*, 2001; Funakoshi *et al.*, 2002; Nakayasu *et al.*, 2013), specifically recognizes a biotinylated H2B-peptide encompassing the ubiquitylation-site, K118 in *Drosophila*, only when it is ubiquitylated (ubK118) (Figure 34B, row UBA). Full-length dDsk2, however, binds ubK118 very inefficiently (Figure 34B, row dDsk2). This is likely the consequence of the reported self-interaction between the UBA and UbL domains, which blocks recognition of ubiquitylated substrates (Lowe *et al.*, 2006). Consistent with this hypothesis, deleting the UbL domain restores specific binding to ubK118 (Figure 34B, row ΔUbL). Next, we analyzed the contribution of the UBA domain to binding of the dHP1-complex to chromatin. For this purpose, full-length V5-tagged dDsk2 and truncated forms missing the UBA and/or the UbL domain were transiently expressed in S2 cells and their relative abundance in cytosolic, nuclear soluble and chromatin-bound fractions determined. Full-length dDsk2 is detected in both the cytosolic and chromatin-bound fractions (Figure 34C, row dDsk2), while deleting the UBA domain largely abolishes binding to chromatin (Figure 34C, row ΔUBA). Chromatin binding is also abolished upon deletion of the UbL domain (Figure 34C, row ΔUbL).

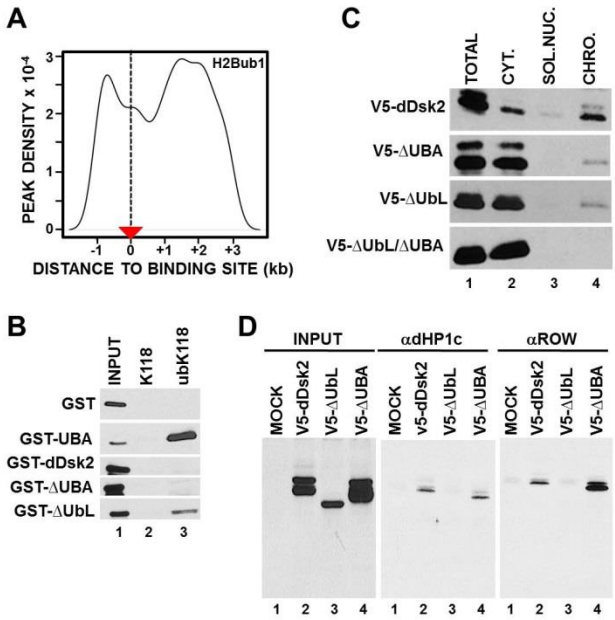

Figure 34. The UBA domain of dDsk2 binds H2Bub1.
(A) H2Bub1 distribution at binding sites of the dHP1c-complex as determined from ChIP-chip data generated by the modENCODE project (ID 290). Binding sites of the dHP1c-complex were oriented with respect to the direction of transcription of the closest gene. Peak density is presented as a function of the distance to the center of the binding site. **(B)** The indicated recombinant GST-tagged dDsk2 constructs were assayed for binding to a biotinylated H2B peptide (aa 104-123) carrying ubiquitylated K118 (lanes 3) or not (lanes 2). Binding was analyzed by peptide pull-down using streptavidin-sepharose beads and western blot of the bound material using αGST antibodies. Lanes 1 correspond to 1% of the GST-constructs used in the binding experiments. **(C)** Extracts prepared from S2 cells expressing the indicated V5-tagged dDsk2 constructs were fractionated into cytosolic (lanes 2), soluble nuclear (lanes 3) and chromatin-bound (lanes 4) fractions, and analyzed by western blot using mouse monoclonal αV5 antibodies. Lanes 1 correspond to a total extract prepared from S2 cells expressing the indicated V5-tagged constructs. Notice that full-length dDsk2 and the truncated dDsk2-ΔUBA give rise to a proteolytic product missing the first ~25 N-terminal residues. **(D)** Nuclear extracts obtained from S2 cells expressing the indicated V5-tagged dDsk2 constructs (lanes 2-4) were subjected to immunoprecipitation with rabbit polyclonal αHP1c (center) and αROW (right) antibodies, and analyzed by western blot using mouse monoclonal αV5 antibodies. The panel on the left corresponds to 1% of the input material used in each case for the immunoprecipitation. Lanes 1 correspond to a mock extract prepared from S2 cells expressing no V5-tagged construct.

Co-IP experiments provided an explanation for this effect since αHP1c and αROW antibodies efficiently precipitate full length dDsk2 and the truncated ΔUBA form, but failed to precipitate the truncated ΔUbL form (Figure 34D), indicating that the UbL domain is required for assembly into the dHP1c-complex that, in turn, requires WOC and ROW for binding to chromatin (Font-Burgada *et al.*, 2008) (Figure 33). Notice that ΔUbL shows residual binding to chromatin, which is fully abolished upon UBA-deletion (Figure 34C, row ΔUbL/ΔUBA).

Next, to analyze the contribution of the interaction of dDsk2 with H2Bub1 to binding of the complex, we performed depletion of the E2/E3-ligases that mediates H2Bub1, dRad6/dBre1. Under these conditions, H2Bub1 at promoters of dHP1c-complex target genes is strongly reduced (Figure 35A, top), resulting only in a weak effect on dDsk2 (Figure 35A, bottom), ROW (Figure S 2A, top) and WOC binding (Figure S 2A, bottom). In contrast, depletion of the dHP1c-complex causes a strong reduction on H2Bub1 levels (Figure 35B and Figure S 2B) and, concomitantly, of H3K4me3 (Figure 35C) and occupancy by Pol IIo^{ser5}, the promoter-proximal active RNApol II form phosphorylated at Ser5 in the CTD (Figure 35D). Depletion of the H2Bub1 deubiquitinase dUbp8/Nonstop suppresses this effect, as H2Bub1 levels are restored upon dDsk2 and dUbp8/Nonstop co-depletion (Figure 35B), indicating that dDsk2 prevents active H2Bub1 deubiquitylation by dUbp8/Nonstop.

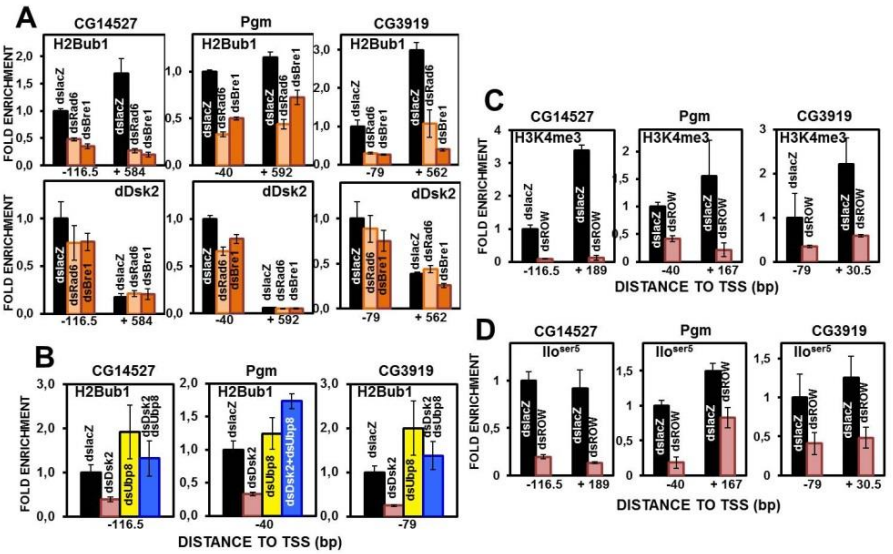

Figure 35. dDsk2 regulates H2Bub1.
(A) H2Bub1 (top) and dDsk2 (bottom) levels at the indicated positions with respect to TSS of selected target genes are determined by ChIP-qPCR in control S2 cells treated with dsRNA against LacZ (black), and upon depletion of dRad6 (light brown) and dBre1 (dark brown). **(B)** As in panel A but for H2Bub1 levels in control S2 cells treated with dsRNA against LacZ (black) and upon depletion of dDsk2 (red), dUbp8/Nonstop (yellow) and both (blue). **(C)** As in A but for H3K4me3 levels in control S2 cells treated with dsRNA against LacZ (black) and upon depletion of ROW (red). **(D)** As in C but for RNApol IIo^{ser5}. Results are presented as fold enrichment with respect to the control (dsLacZ) at the most upstream position. Antibodies used were mouse monoclonal αH2Bub1 and rabbit polyclonal αdDsk2, αH3K4me3 (Abcam, ab8580) and αIIoser5 (Abcam, ab5151).

DISCUSSION

Here, we report that the extraproteasomal ubiquitin receptor dDsk2 is an integral subunit of the dHP1c-complex. We also show that the complex localizes at promoters of active genes and is required for transcription. In the dHP1c-complex, dDsk2 does not mediate proteolysis but, instead, interacts with H2Bub1, a histone modification that is present at binding sites of the dHP1c-complex and is important for transcription regulation. This interaction, however, is not a main determinant of its recruitment to promoters since it only weakly stabilizes binding of the complex. Actually, dDsk2 contains a single ubiquitin-binding site of low affinity (K_d ~ 400 μM), which is in contrast to most ubiquitin receptors that contain several weak ubiquitin-binding sites that act synergistically to provide high-affinity binding (Hicke *et al.*, 2005; Finley, 2009; Trempe, 2011). On the other hand, binding of the dHP1c-complex depends on the zinc finger proteins WOC and ROW (Font-Burgada *et al.*, 2008), suggesting that it involves the recognition of specific DNA sequences. Noteworthy, binding sites of the dHP1c-complex are significantly enriched in a specific DNA sequence motif (Figure S 3). These observations favor a model by which binding of the dHP1c-complex at promoters involves first high-affinity recognition of specific DNA sequences by WOC and/or ROW and, then, stabilization through low-affinity binding of dDsk2 to H2Bub1 (Figure 36). It must also be pointed out that WOC, ROW and dDsk2 are fully interdependent for binding to chromatin, indicating that the three proteins constitute the actual binding module of the complex.

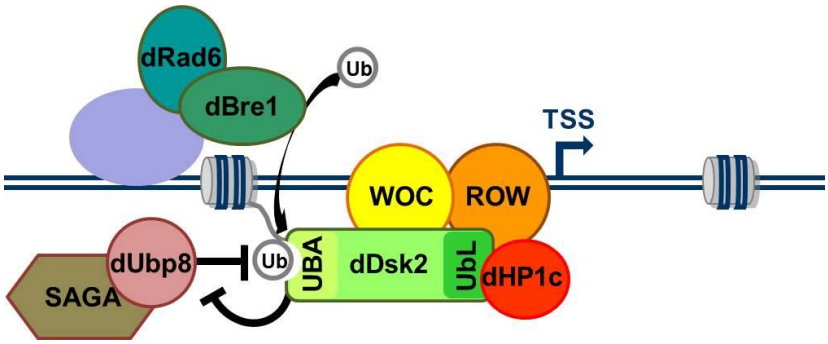

Figure 36. A model of the contribution of the dHP1c-complex to transcription regulation.
The dHP1c-complex is recruited to promoters through the recognition of specific DNA sequences by ROW and/or WOC, and is stabilized by the interaction of dDsk2 with H2Bub1. This interaction prevents H2Bub1 deubiquitylation by dUbp8/Nonstop (see the text for details).

Depletion of the dHP1c-complex strongly reduces H2Bub1. This reduction is dependent on active H2Bub1 deubiquitylation by dUbp8/Nonstop, suggesting that a main contribution of dDsk2 in the complex is to prevent H2Bub1 deubiquitylation. Actually, several ubiquitin receptors, including yeast Dsk2, have been shown to protect poly-ubiquitylated conjugates against deubiquitylation (Su & Lau, 2009; Wade & Auble, 2010). Work in yeast showed that, at promoters, H2Bub1 is an early event during transcription initiation that depends on the recruitment of Rad6/Bre1 by activators and stimulates additional epigenetic modifications required for transcription, such as H3K4me3 and H3K79me3 (reviewed in Laribee *et al.*, 2007; Weake & Workman, 2008; Lee *et al.*, 2010). On the other hand, H2Bub1 deubiquitylation by the SAGA subunit Ubp8 is required for phosphorylation of RNApol II at Ser2 in the CTD (Wyce *et al.*, 2007) and, thus, regulates its release from the promoter into productive elongation. In this regard, deregulated H2Bub1 deubiquitylation induced by depletion of the dHP1c-complex would lead to premature exit of RNApol II from the promoter and abortive

transcription. Consistent with this hypothesis, occupancy by the promoter-proximal Pol IIo^{ser5} form is highly reduced. Altogether, these results support a model by which, through the action of dDsk2, the dHP1c-complex prevents premature H2Bub1 deubiquitylation and regulates transcription (Figure 36). The high H2Bub1 levels observed upon dDsk2 and dUbp8/Nonstop co-depletion indicate that dDsk2 is not essential for H2Bub1. However, these levels appear to be lower than when only dUbp8/Nonstop is depleted, suggesting that dDsk2 depletion also affects H2Bub1. In fact, dRad6/dBre1 recruitment at promoters is decreased upon dDsk2 depletion (Figure S 4). Nevertheless, this effect is most likely indirect since co-IP experiments failed to detect any direct interaction between the dHP1c-complex and dRad6/dBre1 (not shown). Actually, the activities of elongator complexes, such as PAF and FACT, are known to reinforce H2Bub1 at promoters (reviewed in Laribee *et al.*, 2007; Weake & Workman, 2008), suggesting that the effects on dRad6/dBre1 recruitment are probably a consequence of the collapse of transcription in the absence of the dHP1c-complex. Also in this regard, it was shown that dHP1c contributes to recruitment of FACT, particularly at heat-shock induced genes (Kwon *et al.*, 2010).

What role dHP1c plays in the complex is not fully understood. Its depletion does not significantly affect expression of target genes, suggesting that it is not essential for transcriptional activity of the complex. In this regard, it must be mentioned that dHP1b also interacts with WOC and ROW, which are required for its association with euchromatin (Font-Burgada *et al.*, 2008; Abel *et al.*, 2009). Actually, dHP1b appears to be a component of the dHP1c-complex since, according to modENCODE ChIP-chip data, it co-localizes with dHP1c at promoters (Figure S 5A, B) and, furthermore, co-immunopreciates with dHP1c,

ROW and dDsk2 (Figure S 5C). Altogether, these observations suggest that dHP1b might compensate for the loss of dHP1c.

In summary, this study unveils a novel nonproteolytic function of dDsk2 in transcription regulation, where it interacts with and stabilizes H2Bub1. Nonproteolytic functions of ubiquitin receptors have been previously described in relation to various signaling kinase complexes and the DNA repair machinery (Chen & Sun, 2009; Finley, 2009). This work expands the catalogue of nonproteolytic functions of ubiquitin receptors to transcription regulation and chromatin dynamics. Several observations indicate that the contribution of ubiquitin receptors to the regulation of chromatin functions is likely to be more general. On one hand, it was shown that Rad23, another ubiquitin receptor of the same family, plays an important role in the transcriptional response to UV-irradiation in yeast, being required for proper regulation of about two-thirds of UV-regulated genes (Wade *et al.*, 2009). However, in this case, the role of Rad23 appears to depend on its association with the proteasome. On the other hand, in response to DNA damage, human Rad23B was found to interact with ubiquitylated p53, localize at chromatin and accumulate at the p21 promoter (Kaur *et al.*, 2007). In addition, in mouse embryonic stem cells, several components of the NER complex, including Rad23B, have been shown to act as an Oct4/Sox2 co-activator complex that associates with chromatin and is required for stem cell maintenance (Fong *et al.*, 2011). Recruitment of NER factors to active promoters has also been reported in HeLa cells in the absence of DNA damage (Le May *et al.*, 2010). However, in these cases, the precise function of Rad23 has not been elucidated. It must also be noted that ubiquitylation participates in the regulation of multiple genomic functions and the number of ubiquitin receptor proteins is large, ~100 in humans. From this point of view, the

role of ubiquitin receptors as general epigenetic regulators of chromatin structure and function emerges as a distinct possibility.

SUPPLEMENTARY DATA

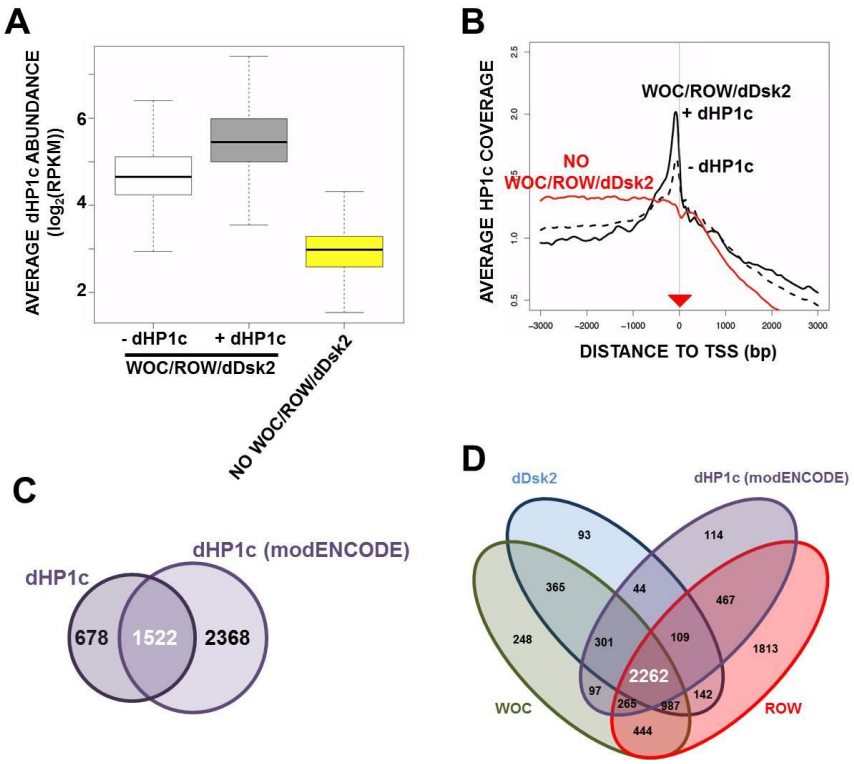

Figure S 1.
(A) dHP1c abundance is presented for WOC/ROW/dDsk2 target genes containing detectable dHP1c peaks (grey) or not (white), and for non-target genes (yellow). **(B)** dHP1c distribution around TSS is presented for WOC/ROW/dDsk2 target genes containing detectable dHP1c peaks (solid black line) or not (dotted black line), and for non-target genes (solid red line). For each gene, the coverage profile was normalized dividing by the average coverage in that gene. The position of the TSS is indicated. **(C)** Venn diagram showing the intersection between dHP1c target genes determined by ChIP-seq in this study (left) or by ChIP-chip data generated by the modENCODE project (right) (ID 3291). **(D)** Venn diagram showing the intersection between dHP1c target genes determined by ChIP-chip data generated by the modENCODE project, and ROW, WOC and dDsk2 target genes determined by ChIP-seq in this study.

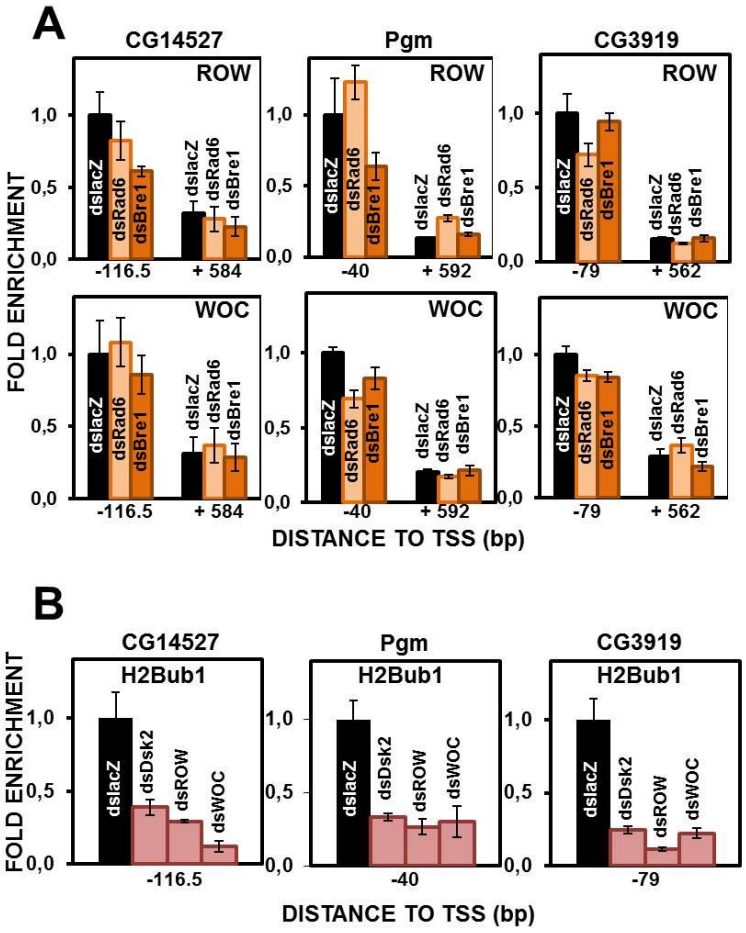

Figure S 2.
(A) ROW (top) and WOC (bottom) levels at the indicated positions with respect to TSS of selected target genes are determined by ChIP-qPCR in control S2 cells treated with dsRNA against LacZ (black) and upon depletion of dRad6 (light brown) and dBre1 (dark brown). Results are presented as fold enrichment with respect to the control (dsLacZ) at the most upstream position. **(B)** As in A but for H2Bub1 levels in control S2 cells treated with dsRNA against LacZ (black) and upon depletion of dDsk2, ROW and WOC (red). Results are presented as fold enrichment with respect to the control (dsLacZ). Antibodies used were mouse monoclonal αH2Bub1, and rabbit polyclonal αROW and αWOC.

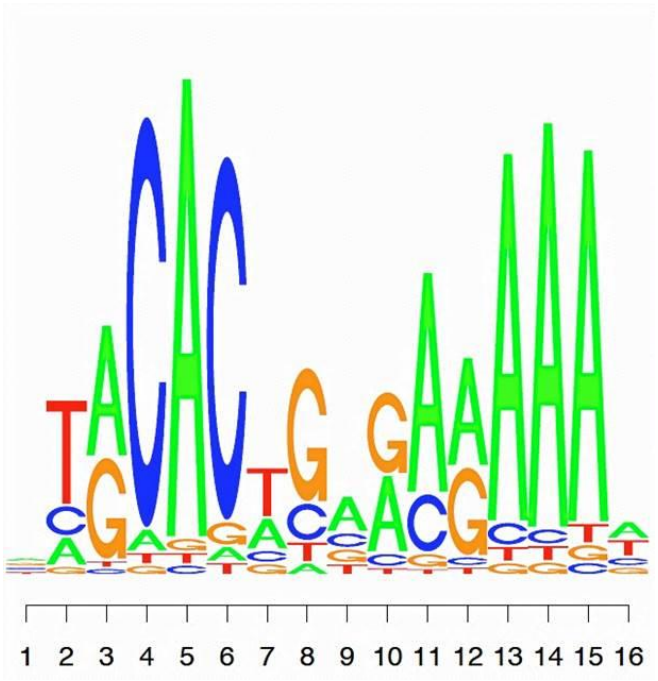

Figure S 3.
Logo representation of the DNA sequence motif highly enriched in dHP1c-complex target genes with respect to non-target genes (p-value<2.2e-16).

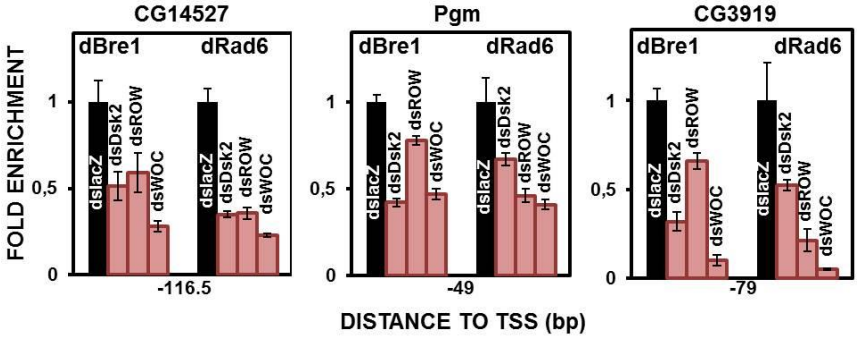

Figure S 4.
dBre1 and dRad6 levels at the indicated positions with respect to TSS of selected target genes are determined by ChIP-qPCR in control S2 cells treated with dsRNA against LacZ (black) and upon depletion of dDsk2, ROW and WOC (red). Results are presented as fold enrichment with respect to the control (dsLacZ). Antibodies used were rabbit polyclonal αdBre1 and αdRad6.

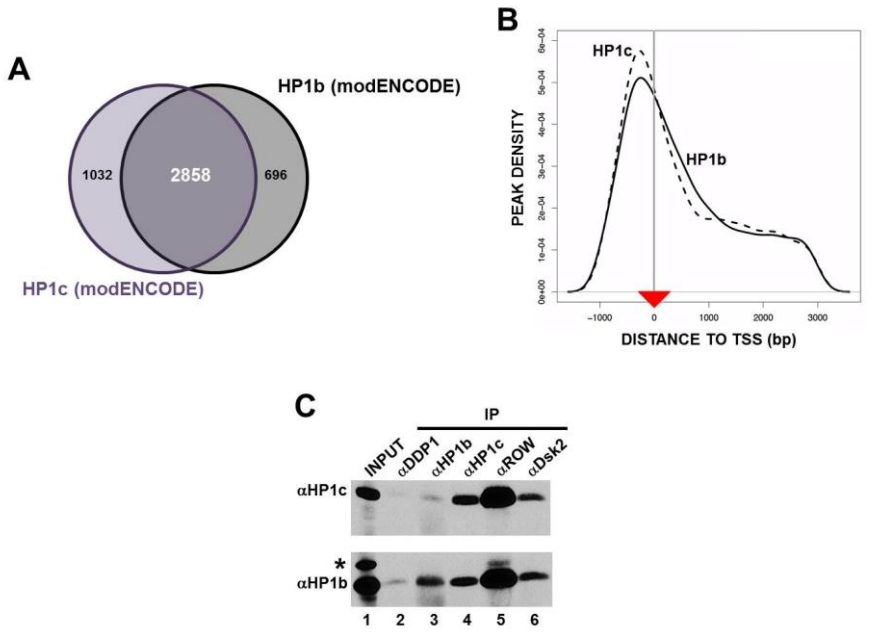

Figure S 5.
(A) Venn diagram showing the intersection between dHP1c (purple) and dHP1b (grey) target genes determined by ChIP-chip data generated by the modENCODE project (IDs 3291 and 941). **(B)** dHP1c (dotted line) and dHP1b (solid line) distribution around the TSS as determined from ChIP-chip data generated by the modENCODE project. Peak density is presented as a function of the distance to the TSS. **(C)** dHP1b co-immunoprecipates with the dHP1c-complex. IPs were performed with rabbit polyclonal αdHP1b (lane 3), αdHP1c (lane 4), αROW (lane 5) and αdDsk2 (lane 6) or with control αDDP1 (lane 2) antibodies. IP-materials were analyzed by western blot using rat polyclonal αdHP1c (top) and αdHP1b (bottom). At the bottom, a minor band of lower electrophoretic mobility is detected (indicated by the asterisk (*)) that, most likely, corresponds to a modified dHP1b form. Lane 1 corresponds to 2.5% of the input material used for immunoprecipitation.

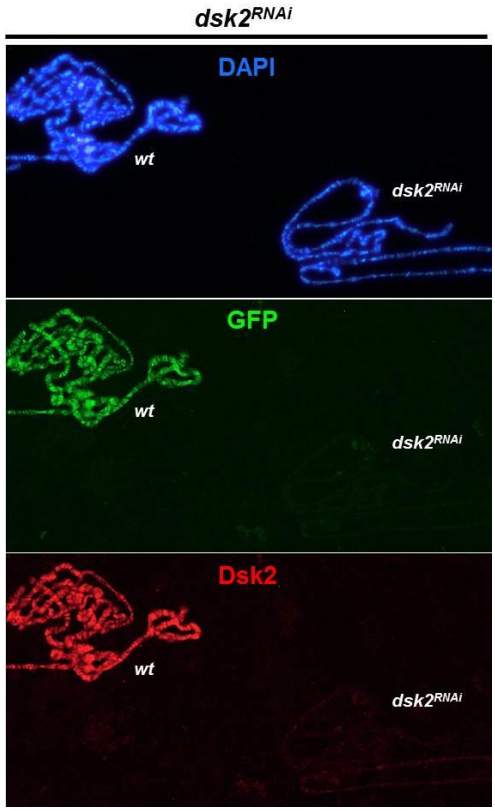

Figure S 6.
Polytene chromosomes obtained from mutant *dsk2*^{RNAi}*; act5C-GAL4* larvae are immunostained with rabbit polyclonal αdDsk2 (red) antibodies. Polytene chromosomes obtained from control *H2Av-GFP* wild-type larvae were mixed and squashed together with mutant polytene chromosomes. Control wild-type chromosomes (wt) are identified by their reactivity with αGFP antibodies (green). DNA was stained with DAPI.

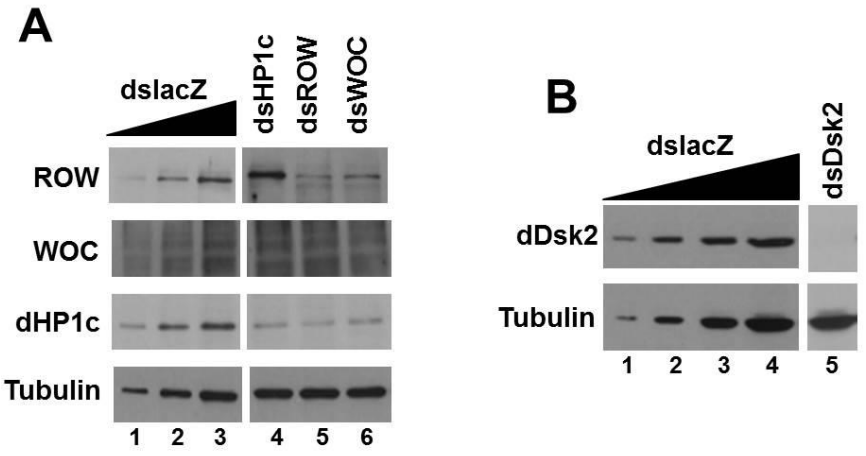

Figure S 7.
(A) The levels of dHP1c, ROW and WOC are determined by western blot in extracts prepared from control S2 cells treated with dsRNA against LacZ (lanes 1-3: increasing amounts of extract are analyzed) and upon depletion of dHP1c, ROW and WOC (lanes 4-6). Tubulin levels are also presented as loading controls. Antibodies used were rabbit polyclonal αROW and αWOC, rat polyclonal αdHP1c and mouse polyclonal αTubulin (Millipore, MAB3408). Notice that rabbit polyclonal αWOC does not give rise to any specific signal. Therefore, in this case, the extent of depletion was determined from the destabilization of dHP1c observed when its binding to chromatin is impaired in the absence of WOC or ROW (Font-Burgada *et al.*, 2008). **(B)** As in panel A but when the levels of dDsk2 are determined by western blot in extracts prepared from control S2 cells treated with dsRNA against LacZ (lanes 1-4: increasing amounts of extract are analyzed) and upon depletion of dDsk2 (lane 5).

ACKNOWLEDGEMENTS

We are thankful to Drs. A. Akhtar, J. G. Gall, M. Gatti, A. C. Nagel, E. J. Sontheimer and A. Udvardy for antibodies, and to Dr. B. Crosas for critical reading of the manuscript. We are also thankful to Dr. H. Auer of the Functional Genomics Core Facility (IRB Barcelona) for ChIP-seq library preparation and sequencing, and to Mrs E. Fuentes, E. Freire and A. Vera for technical assistance. This work was supported by grants from MICINN (CSD2006-49, BFU2009-07111 and BFU2012-30724) and the Generalitat de Catalunya (SGR2009-1023). This work was carried out within the framework of the “Centre de Referència en Biotecnologia” of the “Generalitat de Catalunya”. R.K. acknowledges receipt of a "La Caixa" PhD fellowship.

3.4. The interaction with Z4 and Chromator

The zinc finger protein Z4 and the chromo domain protein Chromator were identified in ROW and WOC complex purifications, suggesting that they may play a role for HP1c complex function (see chapter 3.2.3). Furthermore, an interaction with Z4 was confirmed in CoIP experiments (Figure 29A).

3.4.1. Localization to polytene chromosomes

The subunits of the HP1c complex as well as Z4 and Chromator have been previously described to bind to interbands of polytene chromosomes (Eggert *et al.*, 2004; Font-Burgada *et al.*, 2008). When DNA of polytene chromosomes is stained, it presents a characteristic pattern consisting of condensed bands and less condensed interbands. While bands are considered heterochromatic, interbands correlate with active transcription.

Given this preference for interbands, we first wanted to determine to what extent Z4 and the HP1c complex co-localize or if they bind to different subsets of interbands. Thus, we prepared polytene chromosomes from squashed salivary glands of wild-type *Drosophila* larvae and did a co-immunostaining. As expected Z4 and subunits of the HP1c complex stain a large number of interbands along the arms of each chromosome (Figure 37). Concerning the co-localization, Z4 coincides with ROW and WOC at many sites. However, the stainings suggest that co-localization is not complete. A subset of interbands is bound by Z4, but is negative for ROW and WOC. Also the opposite situation can be observed, sites that are exclusively stained by WOC and ROW antibodies.

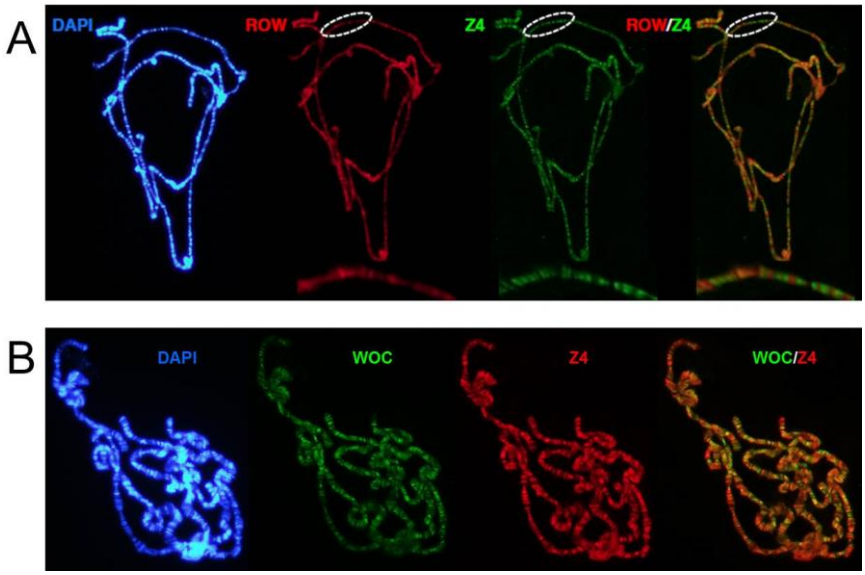

Figure 37. Co-localization of Z4 and the HP1c complex at polytene chromosomes.
(A) Polytene chromosomes were prepared from wild-type larvae and co-immunostained with DAPI (blue), rabbit polyclonal αROW (red) and rat polyclonal αZ4 (green). On the right, αROW and αZ4 stainings are merged. The enlarged region at the bottom corresponds to the region within the white oval. **(B)** Wild-type polytene chromosomes were co-immunostained with DAPI (blue), rabbit polyclonal αWOC (green) and rat polyclonal αZ4 (red). On the right, αWOC and αZ4 stainings are merged.

As a next step, we performed immunostainings at polytene chromosomes prepared from knockdown conditions. In this way we aimed to address the issue, whether Z4/Chromator and the HP1c complex affect chromatin binding of each other. We knocked down Z4 by RNAi, which led to a drastic reduction of Z4 staining (Figure 38A). In this condition we analyzed binding of HP1c. It was previously found in our lab that HP1c binding is dependent on both WOC and ROW (Font-Burgada *et al.*, 2008). Thus, if Z4 would be involved in ROW and WOC recruitment, we should also observe an effect in HP1c staining. Z4 knockdown appears to have an effect on the integrity of the overall chromosome structure. However, HP1c binding to chromatin appears to be largely independent of

Z4 (Figure 38A). This observation is supported in Chromator knockdown conditions, where HP1c binding to chromatin is retained as well (Figure 38B). As Chromator was shown to be required for Z4 recruitment, in a Chromator knockdown, Z4 is also depleted from chromatin (Gan *et al.*, 2011).

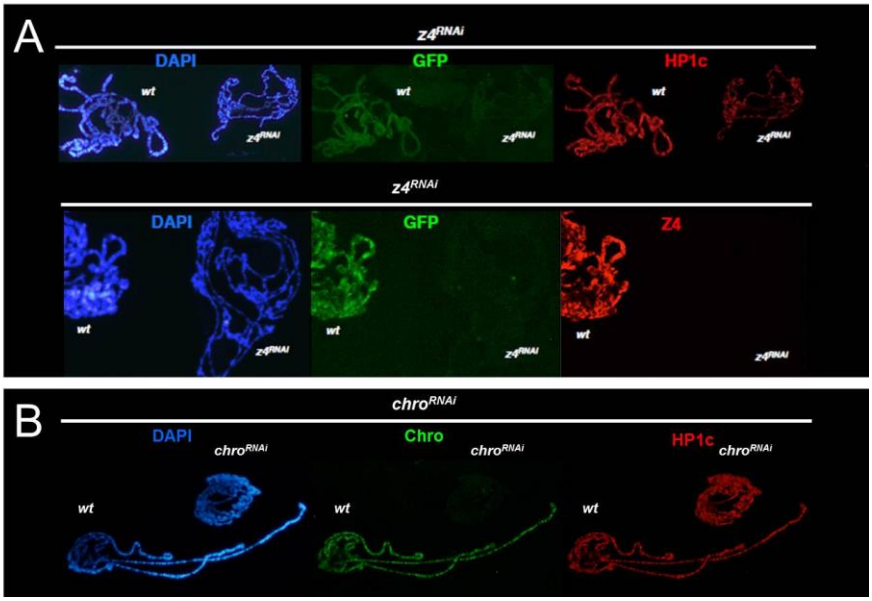

Figure 38. HP1c localization is independent of Z4 and Chromator.
(A) Polytene chromosomes from *H2Av-GFP wild-type* (*wt*) larvae were mixed and squashed together with polytene chromosomes from $z4^{RNAi}$; *lioGal4* larvae. At the top, chromosomes were co-immunostained with DAPI (blue), mouse monoclonal αGFP (green) and rat polyclonal αHP1c (red). At the bottom, chromosomes were co-immunostained with DAPI (blue), mouse monoclonal αGFP and rat polyclonal αZ4 (red). **(B)** Polytene chromosomes from *wild-type* (*wt*) larvae were mixed and squashed together with polytene chromosomes from $chromator^{RNAi}$; *lioGal4* ($chro^{RNAi}$) larvae. Chromosomes were co-immunostained with DAPI (blue), rabbit polyclonal αChromator (green) and rat polyclonal αHP1c (red).

We also tested if the HP1c complex contributes to recruitment of Z4. Therefore, WOC or ROW was depleted by RNAi and polytene chromosomes were stained against Z4. The Z4 staining patterns in these

mutant conditions suggest that ROW and WOC are not necessary for Z4 binding to chromatin (Figure 39A, B). Within this work we have described the new HP1c complex subunit Dsk2, which is required for recruitment of the entire complex (Figure 33A, B). In line with an independent recruitment of the HP1c complex and Z4/Chromator, we detected clear Z4 staining in the absence of Dsk2 (Figure 39C).

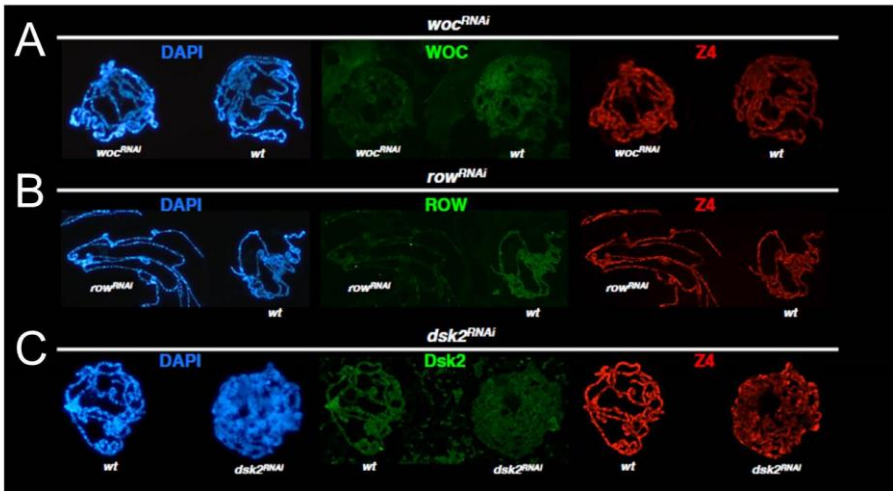

Figure 39. Z4 localization is independent of the HP1c complex.
(A) Polytene chromosomes from *wild-type* (*wt*) larvae were mixed and squashed together with polytene chromosomes from *woc*^{RNAi}*; act5cGal4* larvae. Chromosomes were co-immunostained with DAPI (blue), rabbit polyclonal αWOC (green) and rat polyclonal αZ4 (red). **(B)** Polytene chromosomes from *wild-type* (*wt*) larvae were mixed and squashed together with polytene chromosomes from *row*^{RNAi}*; act5cGal4* larvae. Chromosomes were co-immunostained with DAPI (blue), rabbit polyclonal αROW (green) and rat polyclonal αZ4 (red). **(C)** Polytene chromosomes from *wild-type* (*wt*) larvae were mixed and squashed together with polytene chromosomes from *dsk2*^{RNAi}*; act5cGal4* larvae. Chromosomes were co-immunostained with DAPI (blue), rabbit polyclonal αDsk2 (green) and rat polyclonal αZ4 (red).

Altogether, our data from polytene chromosomes suggest that Z4 and the HP1c complex share many target sites. The fact that there are also sites

that are exclusively stained by one of the two factors indicates that they do not always form part of the same protein complex. This is confirmed by the finding that Z4 and the HP1c complex can bind independently of each other to chromatin.

3.4.2. Genome-wide localization

Immunostainings of polytene chromosomes can give a broad idea on the localization of chromosomal proteins and whether the distribution pattern correlates with other factors. However, the resolution of this technique is very limited. Therefore, we decided to perform chromatin immunoprecipitation followed by high-throughput sequencing of the associated DNA (ChIP-seq). This method allows getting a much more accurate idea of the features and the exact sequences that are bound by the factor of interest. We performed a ChIP-seq experiment with a specific antibody recognizing Z4, using chromatin prepared from *Drosophila* S2 cells. Also an input sample was sequenced, in order to be able to define regions that are enriched in the ChIP experiment. As we have performed analogous ChIP-seq experiments with ROW, WOC, HP1c and Dsk2, we could easily compare the respective distribution patterns of the different proteins (see also chapter 3.3).

The numbers of peaks identified as significant in the ChIP-seq experiments vary from 2711 for HP1c and 8999 for ROW. For Z4 7491 peaks were identified (Figure 40). The large differences in the number of peaks that were found for the different factors might at least partially reflect the quality of the ChIP. HP1c and Dsk2 peaks were generally lower than for the other proteins, which might be an explanation why the

fewest peaks were identified for these two proteins. Similar as for the subunits of the HP1c complex, the vast majority of the Z4 peaks localize to genes (Figure 40). 95% of the total Z4 peaks are within or in close proximity (≤1kb) to genes. Another similarity between Z4 and the HP1c complex is that they target mainly TSS of genes (Figure 40). 70% of the genic peaks of Z4 are found within a range of 1kb of the TSS.

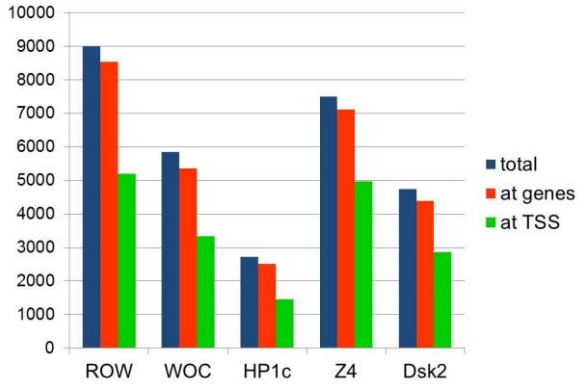

Figure 40. Number of peaks identified in ChIP-seq experiments.
The chart shows the number of peaks identified in the indicated ChIP-seq experiments. The blue bar represents the total number of peaks identified. Close peaks, within a distance of 300bp, are considered as single peak. The red bar corresponds to the number of peaks that overlap with genes or are up to 1kb up- or downstream. The green bar shows the number of peaks in the proximity (≤ 1kb) of TSS.

Despite the overall similarity between the HP1c complex and Z4 binding profiles, at individual genes some differences become evident. Such an example is *Pgm*, which is a target gene of the HP1c complex. Z4 in contrast is not highly enriched at *Pgm* and its profile looks different (Figure 41B). The opposite is true for the neighbouring gene *SsRbeta*, which has a clear Z4 peak at the TSS, but no strong enrichment for HP1c, ROW and WOC (Figure 41B). The normalized coverage at the average

target gene shows that Z4 has a sharp peak that is centered slightly upstream of the TSS, which resembles the distribution of WOC and HP1c, rather than the one found for ROW (Figure 41A).

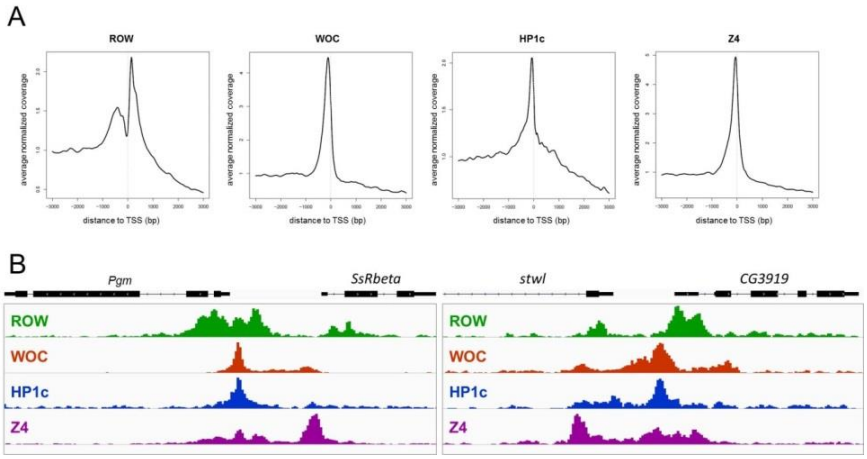

Figure 41. Enrichment of Z4 and the HP1c complex at TSS.
(A) ChIP-seq profiles for ROW, WOC, HP1c and Z4 at target genes are represented around the TSS. The coverage profile at each gene was normalized dividing by the average coverage at that gene. **(B)** ChIP-seq coverage profiles at two representative regions are shown for ROW (green), WOC (red), HP1c (blue) and Z4 (purple).

Genome-wide binding data in S2 cells for HP1c and Chromator are available from the modENCODE consortium. However, this data was generated by ChIP-chip. To compare the average peak location at target genes between ChIP-seq and ChIP-chip data, a representation showing the average peak density around the TSS was chosen, which takes just the midpoints of the peaks into account (Figure 42). The ChIP-chip data for HP1c and Chromator is in agreement with the notion that the complex is preferentially bound close to the TSS of its target genes (Figure 42B).

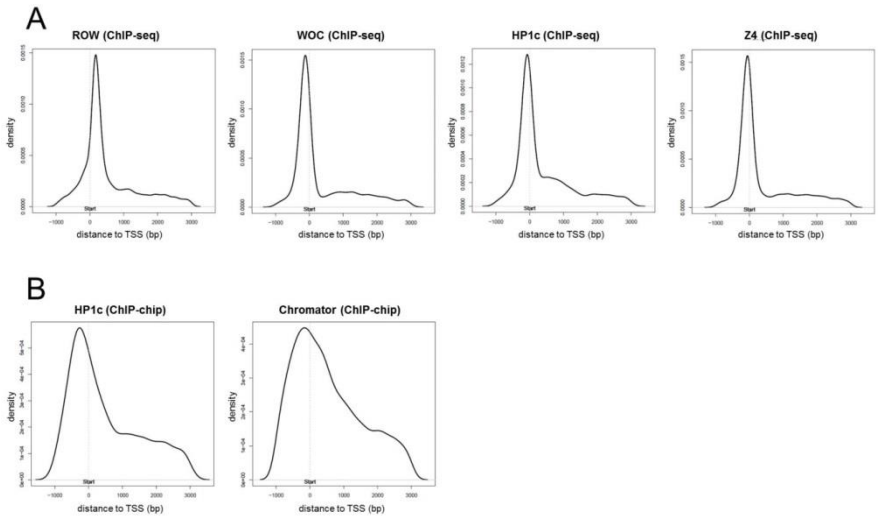

Figure 42. Comparison with ChIP-chip data for HP1c and Chromator.
(A) The peak density of the ChIP-seq data for ROW, WOC, HP1c and Z4 is represented in the proximity of the TSS at the average target genes. **(B)** The peak density at the average target gene using ChIP-chip data from modENCODE is shown for HP1c and Chromator. The position of the TSS is indicated.

Further, target genes were deduced by annotating the peaks to the overlapping or closest gene. 7187 and 8353 target genes were annotated to Z4 and Chromator (modENCODE), respectively. The number of target genes annotated to subunits of the HP1c complex range from 2200 for HP1c to 6489 for ROW. As mentioned above, the large differences might be due to experimental conditions, such as the antibody used. An overlap between Z4 and HP1c complex target genes shows that a large fraction of them are shared. 95% of the genes that are common targets of HP1c, ROW and WOC are also bound by Z4. Only 10% of all the Z4 target genes are exclusive and not found among ROW, WOC and HP1c target genes (Figure 43A). ROW, WOC, Z4 and Chromator share 3408 target genes. Further, the comparison of our Z4 ChIP-seq with the Chromator ChIP-chip data from modENCODE confirms the close relation between

these two proteins. Our analysis identified 6627 common Chromator and Z4 target genes (Figure 43B).

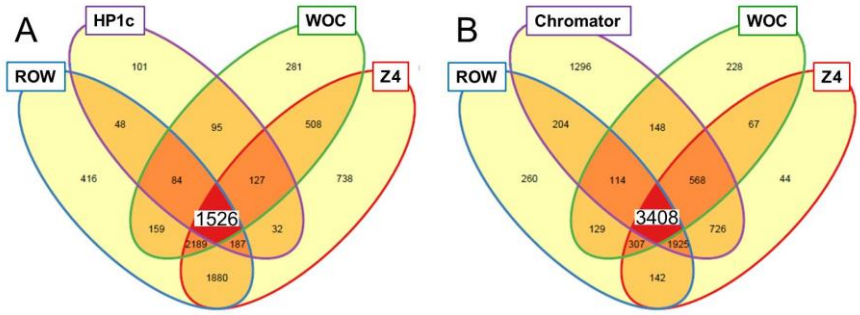

Figure 43. Target gene overlap between Z4, Chromator and the HP1c complex.
Venn diagrams showing the intersections between ROW, HP1c, WOC and Z4 target genes (A) and between ROW, Chromator, WOC and Z4 target genes (B), respectively. Target genes were defined by annotating significant ChIP-seq peaks (ROW, HP1c, WOC and Z4) or ChIP-chip peaks (Chromator) to their closest or overlapping gene.

3.4.3. Effects on target gene expression

Our results suggest that the HP1c complex has mainly a positive effect on the expression of its target genes (Figure 31D, E). The ChIP-seq data indicates that there is a large overlap between Z4 and HP1c complex target genes. Further, as it has been observed for the HP1c complex, Z4 has been described to be related to active gene expression (Hochheimer *et al.*, 2002; Kugler & Nagel, 2007, 2010; Raja *et al.*, 2010). This raised the possibility that Z4 and the HP1c complex might co-regulate a similar set of target genes. To address this question we chose a set of shared target

genes that are regulated by ROW and WOC to test whether their expression is also affected in Z4 mutant conditions. Z4 protein levels in S2 cells were efficiently depleted by treating the cells with long dsRNA to activate the RNAi machinery against Z4 (Figure 44A). From these Z4 depleted cells RNA was extracted and retro-transcribed into cDNA, which was then analyzed by real-time PCR to measure the mRNA levels of the selected target genes. The same selection of genes has also been analyzed in ROW and WOC depleted conditions. WOC and ROW depletion affects target gene expression to a very similar extent and leads to down regulation of all the six analyzed target genes. We also observed some changes in expression of these target genes in Z4 knockdown conditions, but only in the case of *CG18094*, down regulation to a similar extent is evident (Figure 44B). For the other target genes down regulation is less pronounced or not observed at all. The gene *CG12014* was even found to be up regulated.

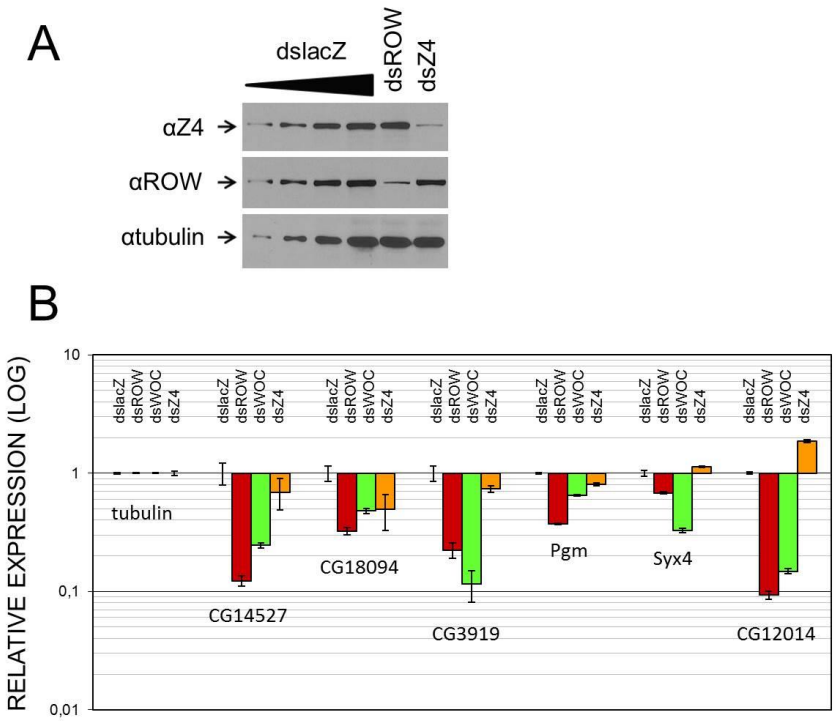

Figure 44. Z4 and the HP1c complex affect target gene expression differently.
(A) Knockdown against Z4 and ROW was done in S2 cells and analyzed by western blotting. As control, increasing amounts of dslacZ treated cells were loaded. An αtubulin western was done as loading control. **(B)** mRNA levels of six HP1c complex target genes were determined by RT-qPCR in S2 cells upon knockdown of ROW (red), WOC (green) and Z4 (orange). Relative expression is shown compared to levels in cells treated with dslacZ. Results were normalized with respect to tubulin.

The expression analysis of target genes suggests that Z4 and the HP1c complex are not strictly co-regulating the same target genes. Rather, it seems that they have at least partially independent roles in the activation of target genes.

3.5. Co-localization of BEAF-32 and the HP1c complex

Our interaction studies using ROW and WOC suggest that the boundary protein BEAF-32 might be an interaction partner of the HP1c complex. We detected BEAF-32 in both ROW and WOC complex purifications, however with relative low scores (Figure 28). Further, BEAF-32 co-purifies with WOC in CoIP experiments, but not with ROW and HP1c (Figure 29C). Based on this relative weak evidence, we decided to concentrate our effort on other candidates (described in chapters 3.3 and 3.4). However, we took advantage of the fact that genome-wide binding data for BEAF-32 is available from the modENCODE consortium. This data was generated by ChIP-chip and two different data sets are available that differ in the antibody used. Plotting the average peak density of the ChIP-chip data at their target genes suggests that BEAF-32 is localized preferentially in close proximity to the TSS (Figure 45A). This pattern is reminiscent of the distribution of the HP1c complex and is in agreement with published data (Figure 31A, B) (Jiang *et al.*, 2009). Further, BEAF-32 peaks were assigned to overlapping or the closest gene. Comparision of BEAF-32 target genes with that of the HP1c complex and Z4 shows that all these factors bind to a related set of genes (Figure 45B).

In addition, the BEAF-32 data is a good example to illustrate the effects that particular experimental conditions can have on the identified peaks and thus target genes. Using the two data sets, 2144 and 7276 target genes were identified, respectively (Figure 45B). Also the average peak density is slightly different in the two data sets (Figure 45A). Thus, the numbers of target genes and the binding profiles obtained from this kind of experiments should be taken with care, as they are very susceptible to

experimental settings. Nevertheless, it remains a valuable tool to get an idea about the overall similarity between different chromatin factors and their target sites.

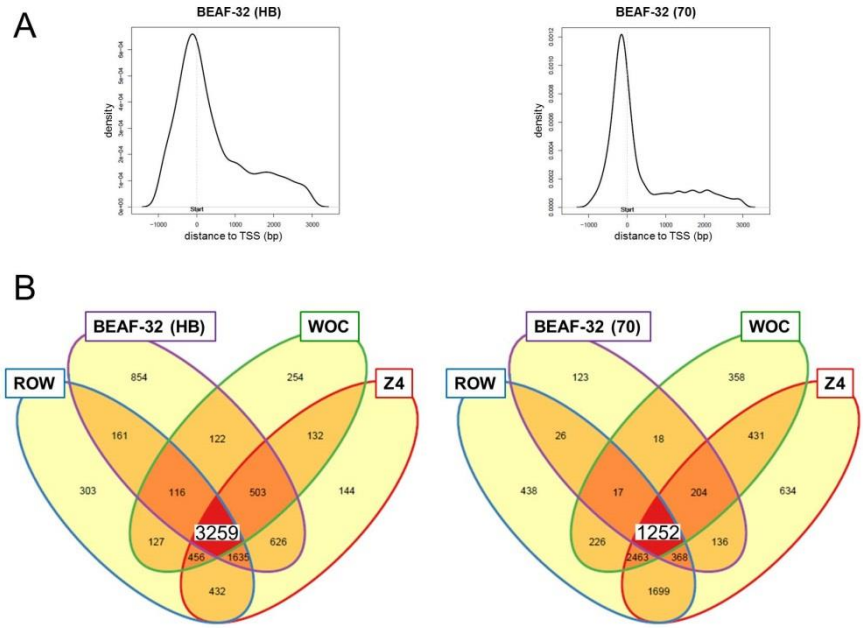

Figure 45. Comparison with BEAF-32 ChIP-chip data.
(A) The peak density at the average target gene using ChIP-chip data from modENCODE is shown for BEAF-32. The position of the TSS is indicated. BEAF-32 (HB) and BEAF-32 (70) are two different ChIP-chip data sets generated with distinct antibodies. **(B)** Venn diagrams showing the intersection between ROW, BEAF-32, WOC and Z4 target genes. Two diagrams are shown for each data set of BEAF-32.

4. DISCUSSION

4.1. The function of the HP1 chromo domain

HP1 proteins contain an N-terminal chromo domain that has been demonstrated to specifically bind to H3K9me2/3 (Bannister *et al.*, 2001; Lachner *et al.*, 2001). HP1 recruitment to chromatin has been shown to be dependent on methyltransferases that generate methylated H3K9 (Bannister *et al.*, 2001; Schotta *et al.*, 2002; Tzeng *et al.*, 2007). Thus, it was suggested that the interaction of the HP1 chromo domain with methylated H3K9 is important for its recruitment. However, also other functions of the histone methyltransferases might be required for HP1 recruitment. In this respect, it is important to note that HP1 and Su(var)3-9 proteins can physically interact (Schotta *et al.*, 2002; Yamamoto & Sonoda, 2003). This could provide a possible H3K9 methylation independent mechanism for Su(var)3-9 mediated HP1 recruitment. There is contradictory data in the literature, whether H3K9me2/3 binding is required, sufficient or dispensable for chromatin targeting of HP1 proteins (see chapter 1.3.2.1). Briefly, chromatin targeting activities have been attributed to both the chromo domain and the chromo shadow domain (Powers & Eissenberg, 1993; Platero *et al.*, 1995). Further, it has been shown that human HP1 proteins cannot be targeted to methylated H3K9 independently of SUV39H1, supporting a two-interaction model (Stewart *et al.*, 2005). In *Drosophila*, mutating the chromo domain of HP1a does not affect localization to heterochromatin and domain swapping experiments suggest that the chromo shadow domain and the hinge region are important for HP1 targeting (Platero *et al.*, 1995; Smothers & Henikoff, 2001). Contradictory to this, Cheutin et al. described that heterochromatin targeting of human HP1 proteins depends on the chromo domain, but not on the chromo shadow domain (Cheutin *et al.*, 2003).

More recent data from *Drosophila* suggests that HP1a targeting, but not spreading, is independent of methylated H3K9 (Figueiredo *et al.*, 2012).

While the exact contribution of the HP1 methyl-binding activity for its function at heterochromatin is still poorly understood, this is even more the case for euchromatic functions of HP1 proteins. H3K9me2/3 is generally considered to be a marker for heterochromatin where it is highly enriched, however a fraction of this methylation mark is also found at euchromatin (Czermin *et al.*, 2002; Ringrose *et al.*, 2004; Vakoc *et al.*, 2005; Font-Burgada *et al.*, 2008). Mammalin HP1γ co-localizes with H3K9me2/3 at transcribed genes in euchromatin (Vakoc *et al.*, 2005). Nevertheless, it has been proposed that HP1 proteins might be recruited to euchromatin by other mechanisms than binding to methylated H3K9. Studies in mammalian and *Drosophila* systems suggest that a physical interaction with phosphorylated RNA pol II might play a role in the recruitment of HP1γ and HP1c, respectively (Vakoc *et al.*, 2005; Kwon *et al.*, 2010). In case of *Drosophila* HP1c, the interaction with RNA pol II appears to play a role in the recruitment of the FACT complex to heat-shock induced genes (Kwon *et al.*, 2010). However, it remains unclear, whether this interaction also contributes to transcription of HP1c target genes in the absence of heat-shock. *Drosophila* HP1c also forms a stable complex with ROW, WOC and the ubiquitin receptor Dsk2, and each of these subunits is required for HP1c localization to chromatin (Font-Burgada *et al.*, 2008) (Figure 33A). WOC and ROW both contain multiple zinc fingers and AT-hook domains, which suggests that they might bind directly to DNA (Font-Burgada *et al.*, 2008) (see chapter 4.7). Despite these alternative modes of recruitment of euchromatic HP1 proteins, the degree of evolutionary conservation of the HP1 chromo domain suggests that methyl-binding might also play a role (see alignment of chromo domains in Figure 22B). The overall similarity between the chromo

domains is high and the three aromatic residues that accommodate the methylated lysine are conserved also in euchromatic HP1 isoforms. *In vitro* it has been demonstrated that *Drosophila* HP1c binds preferentially to nucleosomes and histone H3 when methylated at H3K9 (Font-Burgada *et al.*, 2008).

Here, we confirm that HP1c can bind directly and specifically to an H3K9me3 peptide. However, we obtained evidence that HP1c is less efficient in binding than the HP1 isoforms that have heterochromatic localization, HP1a and HP1b (Figure 23). This suggests that HP1c might have a lower affinity for H3K9me3. We did not test other methylation states of H3K9 for binding to HP1 isoforms. Though, it is unlikely that H3K9me2 plays a role for HP1c function, as H3K9me2 was shown to have very few euchromatic sites, compared to H3K9me3 (Czermin *et al.*, 2002; Ringrose *et al.*, 2004; Font-Burgada *et al.*, 2008). Also the co-localization of H3K9me3 with HP1c is only partial, as at least 50% of HP1c sites are negative for H3K9me3 staining in polytene chromosomes (Font-Burgada *et al.*, 2008). Possibly, HP1c and other euchromatic HP1 proteins might recognize a methylated substrate that is different from H3K9. There is actually data that HP1 chromo domains can bind to methylated lysines in other contexts than H3K9. Mammalian HP1 proteins were shown to bind methylated histone H1.4 and the methylated methyltransferase G9a (Daujat *et al.*, 2005; Chin *et al.*, 2007; Sampath *et al.*, 2007) (see chapter 1.3.1.1). Thus, it appears feasible that also *Drosophila* HP1c could recognize another methylated lysine than H3K9, either in a histone or another protein. The most evident candidates would be ROW, WOC and Dsk2. ROW however might be excluded, as *in vitro* translated ROW is able to interact with HP1c, suggesting that this interaction is independent of any post-translational modification (Abel *et al.*, 2009). Little is known about the molecular mechanism of the other

interactions within the complex, except that the UbL domain of Dsk2 is required to mediate interaction with the complex (Figure 34D). However, it is not known, whether Dsk2 UbL binds directly to any of the other known subunits of the complex.

We tested if the methyl-binding activity of the HP1c chromo domain is required for correct chromatin localization *in vivo*. Therefore, we generated transgenic flies to express HP1c with a defective aromatic cage in an HP1c mutant background. Our results from polytene chromosome stainings indicate that a functional aromatic cage is dispensable for HP1c localization (Figure 24). At this moment we do not know if the aromatic cage of HP1c has any functional contribution downstream of recruitment. In this respect, the results by Platero et al. are interesting to note, as they describe that mutations in the *Drosophila* HP1a chromo domain affect silencing but not heterochromatin localization (Platero *et al.*, 1995). However, one should also consider that HP1 proteins can form homo- and heterodimers (Ye, 1997; Brasher *et al.*, 2000; Nielsen, Oulad-Abdelghani, *et al.*, 2001). It is not known if heterodimers of HP1 proteins are important for *in vivo* function, but the heterodimerization of a chromo domain mutant HP1 protein with another wild-type HP1 isoform might occlude a possible function of the methyl-binding cage.

4.2. Genome-wide localization of the HP1c complex

The HP1c complex has been previously suggested to play a role in gene regulation (Font-Burgada *et al.*, 2008; Abel *et al.*, 2009). However, little was known about the genome-wide targets of this complex and by which mechanisms it is acting on its targets. Here, we have determined genome-wide binding profiles for HP1c, ROW and WOC by performing ChIP-seq experiments in S2 cells. The binding profiles suggest that these proteins associate with chromatin almost exclusively at genes, rather than in intergenic regions. Further, we showed that they bind their target genes preferentially in close proximity to the TSS (Figure 40). The numbers of target genes that we could identify are varying quite a lot for the different subunits of the complex. While for ROW and WOC we identified as many targets as 6489 and 4969, respectively, in case of HP1c we only obtained 2200 target genes. Nevertheless, an intersection of the target genes indicates that the three factors coincide at a large fraction of target genes (Figure 31C). Moreover, we reason that the differences in identified target genes might be explained to a large extent by technical reasons. The ChIP-seq experiments have been performed by using antibodies against the endogenous proteins. These antibodies differ in the efficiency of immunoprecipitating their target. Compared to the αROW and αWOC antibodies, the αHP1c antibody used for the ChIP-seq experiment immunoprecipitates much less efficiently (see CoIPs in Figure 29). Consequently, the enrichment of sequences at target sites varies depending on the antibody used. Thus, as peaks are generally lower in the HP1c data set, a smaller fraction of the target sites could be identified as significant. This explanation is supported by the fact that HP1c is still enriched at ROW and WOC target genes, even if they are not assigned as

HP1c targets (Figure S 1A, B). A further indication that we seem to miss many HP1c targets is the HP1c ChIP-chip experiment that is provided by the modENCODE consortium (Figure S 1C, D). Using this ChIP-chip data, we found 3890 HP1c target genes and 2527 of them are shared both with WOC and ROW. Another factor that may play a role is the mechanism of how these proteins contact chromatin. ROW and WOC might bind to DNA more directly than HP1c and thus it would be easier to co-immunoprecipitate associated DNA. A further possibility might be that ROW and WOC are associated with the target sites firmer and HP1c in contrast is exchanged more dynamically.

When we compare the ChIP-seq data with expression profiles from S2 cells we see a strong correlation with transcription. Target genes tend to be actively expressed (Figure 31D). This observation is not unexpected, as it has been reported before that at polytene chromosomes the HP1c complex co-localizes with marks of active transcription (Font-Burgada *et al.*, 2008). A gene ontology analysis revealed that the target genes of the HP1c complex are enriched in developmental functions. Our localization studies by ChIP-seq have been limited to S2 cells, so that it is currently not known whether a similar set of target genes would be bound in another type of cell line or tissue. Alternatively, the complex might be redistributed to genes that would be active in that particular cell type. A possible approach to test these two options could be to determine the binding patterns of the complex both in an undifferentiated cell line and upon induction of differentiation.

Even though our data indicates that ROW, WOC and HP1c are all found at the TSS of a largely overlapping set of target genes, we detected some differences in the binding profiles. Especially in case of ROW the distribution at TSS appears to be different. While WOC and HP1c show a single peak slightly upstream of the TSS at the average target gene, the

ROW profile is broader and shows a bimodal peak flanking both sites of the TSS (Figure 31A, B). The reason for this difference is not clear and could possibly be a technical artefact due to the antibody used for the ChIP-seq experiment. However, it might also reflect an actual difference in binding to chromatin. The bimodal peak could indicate that ROW makes an additional contact with DNA downstream of the TSS. An alternative explanation is that ROW might occur in two subcomplexes. In this model ROW, WOC and HP1c would associate together with the TSS and subsequently ROW might travel along with the RNA pol II during early elongation, while HP1c and WOC would get released from chromatin. More experimental data would be necessary to distinguish between these different options.

4.3. Dsk2 is an intrinsic component of the HP1c complex

Our complex purifications in S2 cells revealed solid evidence that the ubiquitin receptor Dsk2 is found in a protein complex together with the two zinc finger proteins ROW and WOC. In particular, two ROW complexes and one WOC complex were purified and Dsk2 was identified in every experiment with a very high score and with a protein coverage that reaches between 32% and 40% (Figure 28). We note that Dsk2 has been purified independently in other labs together with ROW and HP1c, by using slightly different purification strategies (Abel *et al.*, 2009; Kwon *et al.*, 2010; Guruharsha *et al.*, 2011). Dsk2 belongs to the UbL/UBA family of extra-proteasomal ubiquitin receptors that have been described to function in shuttling ubiquitylated substrates to the proteasome for degradation (Chen & Madura, 2002; Elsasser *et al.*, 2004; Verma *et al.*, 2004) (Figure 20A). Due to this function in protein degradation, it would be a possibility that the co-purification of Dsk2 is a result of overexpressing the bait protein that might get targeted for degradation when in excess. The fact however that Dsk2 does not appear to be commonly co-purified with overexpressed bait proteins argues against this explanation (Guruharsha *et al.*, 2011). Further evidence that Dsk2 is a stable subunit of the HP1c complex was obtained by performing CoIP experiments with the endogenous proteins using protein extracts from S2 cells (Figure 30B, C). Furthermore, Dsk2 localizes to chromatin together with the HP1c complex. At polytene chromosomes, Dsk2 binds to euchromatic interbands and appears to co-localize perfectly with other subunits of the HP1c complex (Figure 30D). In addition, exhaustive genome-wide Dsk2 binding profiles were generated by ChIP-seq in S2 cells. This data set confirms that the target sites of Dsk2 are highly similar

to other factors of the HP1c complex. Dsk2 co-localizes with subunits of the HP1c complex at most target genes and also generally binds its targets at the TSS (Figure 31A-C, Figure 40). We identified 4304 Dsk2 target genes and 77.3% of them are also targets for both ROW and WOC.

CoIP experiments with Dsk2 deletion constructs suggest that for incorporation into the HP1c complex, the UbL domain is required, while the UBA domain is dispensable (Figure 34D). We currently do not know whether the UbL domain is binding directly to one of the known HP1c complex subunits, as the CoIP experiments were performed using total protein extracts. The Dsk2 UbL domain has also been shown to interact with a UIM motif of the proteasome subunit p54/Rpn10 (Lipinszki *et al.*, 2011). We could not detect an UIM motif or any other conserved ubiquitin binding domain within the HP1c complex that would be a candidate for Dsk2 binding.

Proteolytic and non-proteolytic roles of the proteasome have been described at chromatin and in gene regulation (reviewed in Collins & Tansey, 2006). For several reasons we think that the function of Dsk2 within the HP1c complex does not involve the recruitment of proteasome subunits. We did not find any proteasome component in our ROW and WOC complex purifications, nor could we detect an association of p54/Rpn10 with the HP1c complex in CoIP experiments (Figure 32C). The UbL domain is mediating interaction with both the HP1c complex and the p54/Rpn10 proteasome subunit, which might suggest that the two binding activities are exclusive. Further, it is rather unlikely that Dsk2 functions as a proteasome shuttling factor for the HP1c complex, as we do not observe any evidence for Dsk2 mediated degradation of the subunits. On the contrary, Dsk2 actually has a positive effect on the protein levels of the HP1c complex subunits (Figure 32A, B). Another member of the UbL/UBA family, Rad23, has been described to stabilize substrates in

some cases (Chen *et al.*, 2001; Raasi, 2003). Rad23 was suggested to stabilize substrates by binding ubiquitylated lysines through its UBA domains and by competing with the proteasome or blocking the access of ubiquitin modifying enzymes. It appears that the mechanism by which Dsk2 can stabilize its interacting partners is different from how Rad23 can protect substrates from degradation. In case of Dsk2, the protection does not seem to involve ubiquitylation, as the interaction is not dependent on the UBA and as we do not have indications for ubiquitylation of any subunit of the HP1c complex in western blots. In the absence of Dsk2, the other subunits of the HP1c complex are unable to bind chromatin and perhaps might be misfolded and thus be more prone to degradation.

In the central part of the protein, between the UbL and the UBA, Dsk2 contains four Sti1-like domains (Figure 19). Also another member of the UbL/UBA family, Rad23, contains a Sti1-like domain, however just a single one. In Rad23 this domain is important for the function in the NER pathway, as it is required to mediate interaction with Rad4/XPC (Masutani *et al.*, 1997; Ortolan *et al.*, 2004). In other proteins, the Sti1-like domain has been described to interact with Hsp70 proteins (Smith *et al.*, 1993; Höhfeld *et al.*, 1995). In humans, the Dsk2 homolog Ubiquilin-2 has also been described to interact with Stch, an Hsp70-like protein (Kaye *et al.*, 2000). We currently do not know whether the Sti1-like domains in Dsk2 play a functional role in the context of the HP1c complex. Interestingly, we identified the Hsp70 family protein Hsc70-4 in all the purified WOC and ROW complexes with very high scores (978-1363) and coverages (31.5-37%). However, we discarded this protein and did not further analyze it, as it appears to be a common contaminant in protein complex purifications (Guruharsha *et al.*, 2011). Nevertheless, a potential function of Hsc70-4 in association with the HP1c complex

should not be excluded, as heatshock proteins are actually known to play a role in chromatin and transcription (reviewed in Sawarkar & Paro, 2013).

The Dsk2 protein and its proteasome related function has been described to be evolutionary conserved (reviewed in Su & Lau, 2009). Here we describe a novel chromosomal function for Dsk2 in *Drosophila* that seems to be independent from the proteasome. Interestingly, Rad23, another UbL/UBA protein, has also been described to function at chromatin, suggesting that Dsk2 is not a singular case. Rad23 at chromatin appears to have various functions, some of them being related to DNA damage (Figure 21). Rad23 is best known for being involved in damage recognition in the NER pathway (reviewed in Dantuma *et al.*, 2009). In addition, gene induction by p53 upon DNA damage has been described to involve an interaction with Rad23 (Kaur *et al.*, 2007). Rad23 and other NER factors have been described to be recruited to active promoters and function as co-activators (Le May *et al.*, 2010; Fong *et al.*, 2011). In contrast to this apparently multi-functional role of Rad23 at chromatin, our data indicates that Dsk2 function at chromatin is tightly linked to the HP1c complex. Currently it is not known to what extent the role of UbL/UBA proteins in gene regulation is evolutionarily conserved and whether it is a general function of members of this protein family. In *Drosophila* it has not been addressed whether Rad23, like in mammals and yeast, also plays a role in gene regulation. Likewise, it is unknown if the function of Dsk2 at chromatin is evolutionarily conserved in other species than *Drosophila*.

4.4. Interaction partners of the HP1c complex

Results from this and previous studies suggest that the core HP1c complex consists of HP1c, HP1b, ROW, WOC and Dsk2 (Font-Burgada *et al.*, 2008; Abel *et al.*, 2009) (Figure 28). Apart from this stable complex, subunits of the HP1c complex might interact with further proteins in a more transient manner or only in a subset of the complex. Indeed, we reproducibly identified several proteins in WOC and ROW complex purification experiments that appear to be related to the function of the HP1c complex to some extent.

We have co-purified the chromosomal proteins Z4 and Chromator with WOC and ROW complexes. Evidence for an interaction with Z4 is more evident, as we found this protein both associated with WOC and ROW (Figure 28). Further, we could confirm an interaction between Z4 and subunits of the HP1c complex in CoIP experiments using the endogenous proteins (Figure 29). Chromator in contrast was only identified in the ROW complexes but not in the WOC complex. Further, we were not able to confirm an interaction between Chromator and any of the HP1 complex subunits. Z4 and Chromator are known to interact with each other and to co-localize at interbands of polytene chromosomes (Eggert *et al.*, 2004). Z4 contains several zinc finger domains and Chromator contains a single chromo domain. Interestingly, the zinc finger domains and the chromo domain are not required for the direct physical interaction between the two proteins and for the recruitment to chromatin. Chromator depletion affects Z4 protein stability and localization to polytene chromosomes (Gan *et al.*, 2011). We addressed whether recruitment of Z4/Chromator to chromatin depends on the HP1c complex, or vice versa. Therefore, we performed immunostainings of polytene chromosomes in knockdown

conditions. Our results suggest that the HPc complex and Z4/Chromator can bind to chromatin independently of each other (Figure 38, Figure 39). Co-immunostainings at polytene chromosomes and ChIP-seq experiments using S2 cells further suggest that the genome-wide localization of Z4/Chromator and the HP1c complex is similar but not identical (Figure 37, Figure 41). Like the HP1c complex, Z4/Chromator binds preferentially to the promoter region of actively transcribed genes. Several studies have characterized Z4 as a factor related to active transcription. Z4 was co-purified with the TRF2/DREF complex, which has a role in core promoter selection and transcription initiation of its target genes (Hochheimer *et al.*, 2002). A TRF2/DREF independent role for Z4 has been described in the positive regulation of Notch target genes (Kugler & Nagel, 2007). Z4 function at Notch targets depends on the NURF nucleosome remodeling complex (Kugler & Nagel, 2010). Z4 and Chromator have also been described to be associated with the nonspecific lethal (NSL) complex (Raja *et al.*, 2010). The NSL complex is a transcriptional regulator that binds to the promoter region of more than 4000 actively transcribed genes. We identified also the WDS protein, which is a subunit of the NSL complex, in one of the two ROW purification experiments (Figure 28). However, a possible contribution of WDS to the function of the HP1c complex was not further addressed.

In this work we show that the HP1c complex localizes to promoters of a large fraction of actively transcribed genes. Studies by others have revealed that there are striking similarities between active promoters and chromatin boundaries (Raab & Kamakaka, 2010). In purifications of ROW and WOC complexes we identified the protein BEAF-32, which was initially described to function at a subset of chromatin boundaries (Zhao *et al.*, 1995) (Figure 28). Genome-wide mapping of BEAF-32 suggests a function in active transcription (Jiang *et al.*, 2009). By doing

ChIP-chip, Jiang et al. detected almost 2000 BEAF-32 peaks and 85% of them are in close proximity to a TSS. The presence of BEAF-32 correlates with active transcription and the protein tends to positively affect the activity of its target genes. BEAF-32 ChIP-chip data is also available from the modENCODE consortium. Analysis of this data confirms the preferential localization of BEAF-32 to promoter regions and suggests that it binds a similar set of target genes as the HP1c complex (Figure 45). Curiously, in CoIP experiments we could detect a firm interaction between BEAF-32 and WOC, but not with other subunits of the HP1c complex (Figure 29). In purifications using TAP-tagged baits however, we co-purified BEAF-32 both in ROW and WOC complexes (Figure 28). With the available data we are not able to conclude what is the significance of this interaction between BEAF-32 and WOC. Additional experiments would be necessary to address the role of BEAF-32 in this context. The absence of interaction between BEAF-32 and ROW or HP1c in CoIP experiments might be explained by technical reasons. Alternatively, BEAF-32 might interact with WOC independently of the HP1c complex. Noteworthy, BEAF-32 has also been described to co-immunoprecipitate with Z4 (Gan *et al.*, 2011).

In the ROW and WOC complexes we identified several chromatin modifying and remodeling factors (Figure 28). In particular we found several subunits of the Brahma complex, the *Drosophila* homolog of the SWI/SNF remodeler. Further, we also identified peptides corresponding to the chromatin assembly factor CAF-1 and the histone deacetylase RPD3. These suggestive interaction partners have not been further characterized in relation with the HP1c complex and it has to be mentioned that most of these factors were identified with relatively low scores and not in every single experiment. However, we envision that the HP1c complex might interact with proteins that act on chromatin in order to establish an

environment that is predisposed for its function. Interestingly, in mammals a direct interaction between the p150 subunit of the CAF-1 complex and the chromo shadow domain of HP1α and HP1β has been described (Murzina *et al.*, 1999; Brasher *et al.*, 2000; Lechner *et al.*, 2000).

In both the ROW purifications, but not in the WOC purification, we identified coilin with high MASCOT scores (Figure 28). Coilin is known as a marker protein for Cajal bodies, which are nuclear organelles that are involved in RNA metabolism (Liu *et al.*, 2006, 2009). In one of the ROW purification experiments we further detected the WD40 protein WDR79, which is a RNA binding protein that has been functionally related to Cajal bodies (Tycowski *et al.*, 2009). In CoIP experiments however we could not confirm binding between coilin and ROW (Figure 29). Thus, the significance of such an interaction remains doubtful. Nevertheless, a possibility might be that ROW plays a second role in Cajal body function. Interestingly, the coilin homolog in mammals has been described to be recruited to damaged centromeres, where it appears to contribute to a kind of safeguard mechanism (Morency *et al.*, 2007).

Worth mentioning, several of the putative interaction partners found in ROW and WOC complexes have been related to mitotic spindles (Figure 28). One of these proteins is Chromator that binds to interbands during interphase, as also does the HP1c complex. During mitosis however, Chromator detaches from chromatin and localizes to a spindle-like structure (Rath *et al.*, 2004). Little is known about the behavior of the HP1c complex during mitosis. It might be a feasible scenario that subunits of the HP1c complex follow a similar pattern during the cell cycle such as Chromator.

4.5. The role in transcription

Localization studies of subunits of the HP1c complex suggest a role in transcription. HP1c at polytene chromosomes binds to active chromatin domains and is co-localizing with RNA pol II and histone modifications related to active transcription (Font-Burgada *et al.*, 2008). We have determined genome-wide binding profiles of subunits of the HP1c complex by ChIP-seq, which confirms the correlation with active transcription (Figure 31). The HP1c complex binds a large number of target genes at the promoter region, suggesting that the presence of the complex might be a relatively common feature of actively transcribed genes. One question that arises from these observations is whether the complex actively regulates transcription or if the presence of the complex at active genes is rather a consequence of transcription. In respect to this, in the lab we have performed a microarray expression analysis in S2 cells upon depletion of ROW. Removal of ROW is expected to release the entire complex from chromatin, as experiments using polytene chromosomes suggest (Font-Burgada *et al.*, 2008) (Figure 33C, D). The microarray results suggest that the HP1c complex is involved in transcriptional regulation. More than 200 genes were found to be significantly ($p>0.95$) misregulated. Approximately two thirds of the genes that significantly alter expression upon ROW depletion are down regulated. Observed transcriptional changes in the microarray experiment might also include genes that are not direct targets of the HP1c complex, but rather change expression due to secondary effects. However, the fact that the misregulated genes are enriched in HP1c complex targets suggests that many of the effects are direct. The complex mainly appears to promote transcription as approximately 80% of the target genes that change expression are down regulated in the ROW depleted cells (Figure

31E). RT-qPCR experiments at selected target genes indicate that effects on gene expression are very similar in ROW, WOC or Dsk2 depleted cells. Surprisingly however, in HP1c depleted cells no general effect on transcription of this selection of target genes is evident (Figure 31F). Possibly, the depletion of HP1c protein levels might not be efficient enough to observe clear effects on transcription. However, as judged by western, HP1c protein levels upon knockdown were strongly diminished. Therefore, the absence of expression effects upon HP1c depletion might indicate that a ROW, WOC and Dsk2 containing complex can activate transcription without requiring HP1c. This could be due to replacement of HP1c functions by other HP1 isoforms (see chapter 4.6 for more details about HP1 isoforms). Further, it should be noted that only a relatively small fraction of HP1c complex target genes, as determined by ChIP-seq, were found to significantly alter expression upon ROW depletion. These limited effects might be explained by the experimental conditions used. ROW was depleted by RNAi, which reduced protein levels strongly but might have been insufficient in order to observe strong expression effects at many target genes. Alternatively, the HP1c complex might have a role in fine-tuning the expression of its target genes, which would be in agreement with the rather subtle expression changes of most target genes. It also has to be considered that the depletion experiment takes place over several days and that negative feedback loops or redundant functions might overcome possible effects of the HP1c complex on transcription.

Another issue that we addressed is how the HP1c complex can affect expression of its target genes. Given that the complex preferentially binds its targets in the proximity of the TSS, the function might involve recruitment of transcription factors, stimulation of initiating RNA pol II or regulation of release of RNA pol II into elongation. We have performed ChIP-qPCR experiments to get further insights into the function of the

HP1c complex at target genes. Therefore, we prepared chromatin from ROW, WOC or Dsk2 depleted cells and did ChIP with antibodies recognizing factors related to active transcription. These experiments suggest that levels of RNA pol II ser5 phosphorylation, H3K4me3 and H2Bub1 at target genes are reduced upon depletion of the complex (Figure 35C, D and Figure S 2B). H2Bub1 at promoters has been described to mediate a crosstalk with H3K4me3 (Lee *et al.*, 2007). These effects indicate that the HP1c complex appears to have an effect on an early step during transcription initiation. The reduced levels of H2Bub1 and H3K4me3 might suggest a role of the HP1c complex in establishment of a chromatin environment that is permissive for transcription. The various chromatin modifying proteins that were purified together with ROW and WOC complexes are supporting such a role. On the other hand, the HP1c complex might regulate transcription more directly and the observed changes in transcription related marks could be an indirect effect of reduced transcription. Our experimental data does not allow us to clearly distinguish these two possibilities, which are not mutually exclusive.

Another aspect that called our attention is the ability of the UBA domain of Dsk2 to mediate interaction with ubiquitylated proteins (reviewed in Su & Lau, 2009). Our interaction studies suggest that incorporation of Dsk2 into the HP1c complex is independent of the UBA domain and involves the UbL domain (Figure 34D). However, the UBA does not seem to be dispensable for Dsk2 function at chromatin. Cellular fractionation experiments with Dsk2 deletion variants indicate that Dsk2 association with chromatin is partially dependent on the UBA domain (Figure 34C). This observation raises the possibility that Dsk2 might bind an ubiquitylated chromatin component. Several histones and other chromosomal proteins have been described to be ubiquitylated (reviewed

in Braun & Madhani, 2012). For several reasons H2B monoubiquitylated at lysine 118 (H2Bub1) seems to be a likely substrate for the Dsk2 UBA domain. As is the case for Dsk2, H2Bub1 is enriched at active genes and has also been suggested to play a role at promoters during gene activation (reviewed in Weake & Workman, 2008) (Figure 8). H2Bub1 is mediated by the E2 and E3 ubiquitin enzymes Rad6 and Bre1, which are recruited to promoters in an activator dependent manner. Establishment of H2Bub1 is also dependent on the PAF complex (reviewed in Laribee *et al.*, 2007). Further, as mentioned above, H2Bub1 at target genes is affected upon depletion of Dsk2, WOC or ROW. Thus, the Dsk2 UBA domain might be directly involved in regulation of correct H2Bub1 levels at HP1c complex target genes. Using a pull-down assay, we have demonstrated that the UBA domain of Dsk2 can indeed bind to a monoubiquitylated H2B peptide, but not to a non-modified H2B peptide (Figure 34B). Recognition of H2Bub1 by Dsk2 might be required for recruitment of the HP1c complex to chromatin. However, we have evidence that this does not seem to be the case. If H2Bub1 levels are reduced by knocking down Rad6 or Bre1, recruitment of the HP1c complex to chromatin appears to be largely unaffected (Figure S 2A). This and the fact that the HP1c complex positively regulates H2Bub1 levels at target genes might rather point to a function of the complex in establishment or stabilization of the H2Bub1 mark. Interestingly, even though H2Bub1 is related to active transcription, the removal of the mark is also required for optimal transcription (reviewed in Frappier & Verrijzer, 2011). H2Bub1 is erased by the deubiquitylase Ubp8, a SAGA complex subunit, and deubiquitylation is a requisite for Ctk1 dependent phosphorylation of Ser2 of the RNA pol II CTD and for transition into elongation (Wyce *et al.*, 2007) (Figure 8). While the latter study was performed in yeast, Ubp8 is conserved in *Drosophila*, where it is called Nonstop and also deubiquitylates H2Bub1 (Frappier & Verrijzer, 2011). A tentative model

assigns Dsk2 a role in the control of H2B deubiquitylation by Ubp8/Nonstop. It has been shown that UBA domains can protect ubiquitylated substrates from being accessed by ubiquitin modifying enzymes (Chen *et al.*, 2001; Raasi, 2003). In this way, Dsk2 bound H2Bub1 might be protected from preliminary deubiquitylation by Ubp8/Nonstop (Figure 36). In the absence of Dsk2, initiating RNA pol II might be released prematurely and lead to abortive or inefficient transcription. Our data supports such a model, as reduction of H2Bub1 at target genes upon Dsk2 depletion is dependent on the deubiquitylase Ubp8/Nonstop, (Figure 35B). This indicates that Dsk2 regulates H2Bub1 by protecting it from deubiquitylation and that this mechanism becomes dispensable in the absence of Ubp8/Nonstop.

Transcription is a very dynamic process that involves continuous remodeling of the chromatin template and perpetual association and dissociation events of a plethora of transcription factors. Experimentally however it is very challenging to capture these dynamic events. For example, by doing ChIP-seq experiments an average distribution profile of the factor of interest can be obtained. However, it cannot be distinguished whether the protein is bound to these sites in a very transient or in a more stable manner. Hence, we currently do not know if the HP1c complex is associated constantly with the promoters of its target genes or if it is recruited transiently to fulfill a specific function during the transcription cycle.

4.6. HP1 isoforms

In most species where HP1 proteins have been described, several HP1 isoforms are encoded in the genome (reviewed in Hiragami & Festenstein, 2005; Lomberk *et al.*, 2006). This is also true for *Drosophila melanogaster*, where five HP1 proteins are found. Three of them, HP1a, HP1b and HP1c, are ubiquitously expressed, while the other two, HP1d/Rhino and HP1e, are mainly expressed in the germline (reviewed in Vermaak & Malik, 2009) (Figure 12A). In addition to this, in *Drosophila*, several uncharacterized HP1-like genes are found that lack either the chromo domain or the chromo shadow domain (Levine *et al.*, 2012). HP1 proteins can have isoform specific localization patterns and functions. The ubiquitous *Drosophila* HP1 proteins are known to have distinct binding patterns along the genome. HP1a is highly enriched in heterochromatin, while HP1c is exclusively associated with euchromatic sites. HP1b has a hybrid distribution pattern, being found both at heterochromatic and euchromatic loci (Smothers & Henikoff, 2001; Font-Burgada *et al.*, 2008) (Figure 12B, C). Interestingly, ROW and WOC not only affect HP1c binding, but also euchromatic HP1b localization to some extent. However, HP1b and HP1c functions at euchromatin might not be redundant, as targeting experiments had silencing and activating effects on a reporter gene, respectively (Font-Burgada *et al.*, 2008)

Complex purification and CoIP experiments suggest that ROW and WOC are associated with HP1b and HP1c, but not with HP1a (Font-Burgada *et al.*, 2008) (Figure 28). HP1 proteins dimerize through the chromo shadow domain and thereby generate a binding motif for protein-protein interactions (Brasher *et al.*, 2000; Thiru *et al.*, 2004). Notably, also heterodimers of different HP1 isoforms have been reported (Ye, 1997;

Brasher *et al.*, 2000; Nielsen, Oulad-Abdelghani, *et al.*, 2001). Based on this, several scenarios are conceivable. One possibility would be that euchromatic HP1b and HP1c are functionally redundant and that they might associate with ROW, WOC and Dsk2 either as homo- or heterodimers. In another model, different subcomplexes characterized by association of either HP1 homo- or heterodimers could have specific functions. Further, the HP1c complex might require a heterodimer of HP1b and HP1c to be functional. Alternatively, HP1b and HP1c might only form homodimers that either would compete for being incorporated into the complex or that might bind to the complex simultaneously through distinct motifs. There is some experimental data available that favors some of these models over the others. CoIP experiments using cellular protein extracts suggest that HP1b and HP1c can form part of the same complex (Figure S 5C). Thus, the existence of two subcomplexes that are characterized by having either homodimers of HP1b or HP1c as a subunit is unlikely. Furthermore, ChIP-chip data of HP1b and HP1c from the modENCODE consortium suggest that the distribution of euchromatic HP1b and HP1c is basically identical. These observations and the fact that HP1c depletion has no strong effect on target gene expression indicate that HP1b and HP1c might be redundant. This hypothesis might be tested in double null mutants for HP1b and HP1c. However, it is not trivial to generate such mutants.

The detailed mechanisms of the molecular interactions between the subunits would also reveal more information about the respective role of HP1b and HP1c within the complex. However, currently we know very little about direct protein interactions within the complex and the stoichiometry of the subunits. *In vitro* binding experiments suggest that HP1c can directly bind to ROW (Abel *et al.*, 2009). The interaction between ROW and HP1c is isoform specific, as no binding to ROW was

detected when using the HP1a isoform. It has not been addressed whether this interaction is conserved in HP1b. Many of the known interaction partners of HP1 proteins contain the pentapeptide PXVXL, which is recognized by the dimerized chromo shadow domain (Brasher *et al.*, 2000; Smothers & Henikoff, 2000). It is not known if the chromo shadow domain is required for binding to ROW, yet the consensus PXVXL motif is not present in ROW. The interaction neither appears to require a binding event between the chromo domain and a methylated lysine, as ROW was translated *in vitro* and thus unmodified. Possibly, the long C-terminal extension of HP1c, which is absent in HP1a, might provide isoform specificity. In *Drosophila*, it has actually been described that the C-terminal extensions of HP1 proteins are important for isoform specificity (Mendez *et al.*, 2011, 2013). *In vitro*, no direct interaction was detected between HP1c and WOC, not even when ROW was co-expressed (Abel *et al.*, 2009). This possibly indicates that the proteins might not be properly folded, that the interaction is dependent on a modification or that it requires the presence of Dsk2 or further proteins. Interestingly, WOC contains the pentapeptide motif PHVLL in the C-terminal part of the protein, which would be a possible candidate for interaction with HP1 proteins.

It has been reported that *Drosophila* HP1 proteins, HP1c in particular, can contribute to heat-shock induced gene expression by mediating the recruitment of the FACT complex to RNA pol II (Kwon *et al.*, 2010). Thus, recruitment of the FACT complex might also play a role in regulation of the HP1c complex target genes. Our results however are rather in disagreement with such a role. Firstly, we did not observe important transcriptional effects upon depletion of HP1c (Figure 31F). Secondly and more important, in the ROW and WOC complex purification experiments we did not detect a single peptide corresponding

to FACT complex subunits (Figure 28). Therefore, it seems likely that HP1c forms part of at least two distinct complexes that regulate transcription by different mechanisms. In this regard, WOC was reported not to be recruited to heat-shock induced puffs, which is supporting that HP1c might function independently of WOC, ROW and Dsk2 at these sites. Furthermore, upon heat-shock HP1c binds all along the transcribed region of *Hsp70* (Kwon *et al.*, 2010). In the absence of heat-shock however, we found that the HP1c complex is highly enriched at the TSS but not along the transcribed region of its target genes, supporting a functionally different contribution of HP1c in these two situations (Figure 31A, B). Apart from HP1c, also HP1a and HP1b can interact with the FACT complex, but with apparently lower affinities (Kwon *et al.*, 2010). Indeed, in another study HP1a was also shown to be recruited to *Hsp70* upon heat-shock treatment (Piacentini *et al.*, 2003). It seems feasible that a similar process of HP1 redistribution could take place upon heat-shock treatment as it has been suggested in response to DNA damage induction (see chapter 1.3.2.3 for more details about HP1 in relation to DNA damage). Briefly, HP1 proteins were found to be released from chromatin shortly after damage induction and subsequently recruited again through a distinct mode (Dinant & Luijsterburg, 2009; Zarebski *et al.*, 2009) (Figure 17, Figure 18). In case of mammalian HP1β, it was shown that initial release from damaged sites involves a phosphorylation event that disrupts the interaction with methylated H3K9 (Ayoub *et al.*, 2008). Similarly, HP1 proteins might be modified and mobilized from chromatin upon heat-shock treatment. In case of HP1b and HP1c such a modification might disrupt the interaction with ROW, WOC and Dsk2 and thereby promote an alternative recruitment mechanism. HP1 proteins have been described to be heavily decorated by post-translational modifications (LeRoy *et al.*, 2009). The functions of the vast majority of these modifications still need to be investigated. However, phosphorylation in the chromo shadow

domain of *Drosophila* HP1a is known to alter the affinity for some of its interaction partners (Mendez *et al.*, 2011).

In addition to ubiquitously expressed HP1a, HP1b and HP1c, other HP1 and HP1-like proteins have been described that are mainly expressed in either the male or female germline (Vermaak *et al.*, 2005; Levine *et al.*, 2012). These HP1 and HP1-like proteins are not well characterized and it is not known whether they interfere or cooperate with the functions of the ubiquitously expressed HP1 isoforms. A GFP fusion of HP1d/Rhino localizes to heterochromatic regions in cultured cells and does not co-localize with HP1a, HP1b or HP1c, suggesting an isoform specific function (Vermaak *et al.*, 2005). In the *Drosophila* genome, several HP1-like proteins are encoded that are derived from HP1 proteins but that only have retained either the chromo domain or the chromo shadow domain (Levine *et al.*, 2012). Umbrea, which is also known as HP6, is such an HP1-like protein and contains just a chromo shadow domain. Umbrea is found in a complex with HP1a and Hip and co-localizes with these proteins at heterochromatin (Greil *et al.*, 2007; Joppich *et al.*, 2009). *In vitro* binding experiments suggest that HP1a and Umbrea can interact directly through their chromo shadow domains. In Umbrea mutants, chromosome end-to-end fusions were observed, suggesting a role in telomere protection in wild type conditions (Joppich *et al.*, 2009). This role of Umbrea indicates that HP1-like proteins have the potential to form heterodimers with HP1 proteins and can influence their function. The functions of HP1b and HP1c might be similarly modified by the action of other HP1 isoforms or HP1-like proteins. However, we did not identify additional HP1 isoforms or derived proteins in our ROW and WOC complexes apart from HP1b and HP1c (Figure 28). Nevertheless, HP1a, along with Su(var)3-9, was co-purified in HP1c purification experiments,

suggesting that HP1c might form part of distinct complexes (Kwon *et al.*, 2010).

4.7. Recruitment to chromatin

HP1 proteins are known to interact with a stunning number of partners that involve histones, other chromosomal proteins and RNA components (reviewed in Hiragami & Festenstein, 2005; Hediger & Gasser, 2006; Lomberk *et al.*, 2006) (Figure 11). Several of these interaction partners have been suggested to contribute to correct HP1 localization to chromatin. Special interest has been attracted by the direct interactions of HP1 proteins with both methylated H3K9 and the corresponding histone methyltransferase Su(var)3-9 (see chapter 1.3.2.1 for details). Based on this dual interaction, an elegant model for heterochromatin spreading has been proposed (Schotta *et al.*, 2002) (Figure 13). However, the numerous HP1 interaction partners and isoform specific functions and localizations suggest that HP1 recruitment can occur via different mechanisms depending on the context. This is well exemplified by *Drosophila* HP1c, which co-localizes poorly with methylated H3K9 (Font-Burgada *et al.*, 2008). Furthermore, a functional methyl-binding cage does not appear to be required for HP1c localization to chromatin (Figure 24). Instead, previous work from our lab demonstrated that the two zinc finger proteins ROW and WOC are essential for HP1c targeting to chromatin (Font-Burgada *et al.*, 2008). Here, we characterized the ubiquitin receptor Dsk2 as a new subunit of the HP1c complex and show that it plays a crucial role for recruitment (see chapter 3.3). Furthermore, Dsk2, ROW and WOC are not only required for HP1c targeting, but also for mutual recruitment to chromatin (Font-Burgada *et al.*, 2008) (Figure 33). In contrast, HP1c is not necessary for chromatin binding of Dsk2, ROW and WOC, suggesting that HP1c is recruited downstream of the other subunits of the complex. The mutual requirement of Dsk2, ROW and WOC might have different explanations. These three proteins might make several contacts with

chromatin that alone are not sufficient, but which may be required in combination to stably recruit the complex. Another possibility is that some component of this tripartite complex induces a conformational switch or facilitates a modification in one of its partners and thereby promotes binding to the target sites. The mutual requirement could also be explained by a more indirect effect, as a subunit might have a function in connecting the complex to a downstream function, such as a chromatin remodeling activity. In the absence of this bridging function, the chromatin environment may be altered in a way that hinders efficient binding of the other subunits to their targets.

Both ROW and WOC contain multiple zinc finger and AT-hook domains and thus are potential candidates for mediating interaction with DNA (Font-Burgada *et al.*, 2008). The zinc fingers found in WOC belong to the MYM family and are conserved in the mammalian WOC homologs ZNF198, ZNF261 and ZNF262. Interestingly, the MYM zinc fingers of ZNF198 have been described to mediate a protein-protein interaction (Gocke & Yu, 2008). ZNF198 associates with the LSD1-CoREST-HDAC1 complex through its zinc finger domains and competes with REST for binding to the complex. In contrast, the zinc fingers in ROW are of the C2H2 family. Many examples of protein-protein interactions, in addition to DNA binding, have also been described for C2H2 zinc finger containing proteins. Furthermore, several cases of C2H2 zinc finger proteins are known that interact with various partners, both proteins and DNA (reviewed in Brayer & Segal, 2008). Noteworthy, we identified a conserved DNA motif at binding sites of the HP1c complex, which is a possible target for the zinc fingers found in WOC or ROW (Figure S 3). Interestingly, several ubiquitin interacting proteins mediate binding to ubiquitin through a zinc finger domain (reviewed in Randles & Walters, 2012). We have found that the ubiquitin receptor Dsk2 is incorporated

into the HP1c complex through its ubiquitin-like (UbL) domain (Figure 34D). Therefore, it might be possible that a zinc finger domain in ROW or WOC could mediate binding to Dsk2. However, the zinc fingers that have been described to be ubiquitin binders are of different classes than the zinc fingers found in ROW and WOC. Likely, recruitment of the HP1c complex to chromatin or its stabilization involves interactions with additional chromatin components in addition to DNA. Binding of the complex to chromatin is expected to be regulated by chromatin remodelers and modifying enzymes that affect the accessibility of the binding sites. Furthermore, direct physical interactions with various chromosomal factors might play a role. In this regard, HP1 proteins have been described to interact with a large variety of chromatin components. HP1 isoforms in humans and in *Xenopus* can bind directly to DNA through their hinge domain (Sugimoto *et al.*, 1996; Meehan *et al.*, 2003). Apart from the well characterized interaction between the HP1 chromo domain and methylated H3K9, HP1 proteins have also been shown to interact with histone proteins through other mechanisms. For example, mammalian HP1α and HP1β have been described to interact with the fold domain of histone H3 (Nielsen, Oulad-Abdelghani, *et al.*, 2001; Dialynas *et al.*, 2006). Furthermore, binding to the linker histone H1 has been observed. The hinge regions of both mammalian HP1α and *Xenopus* xHP1α have a binding activity towards histone H1 (Nielsen, Oulad-Abdelghani, *et al.*, 2001; Meehan *et al.*, 2003). In mammals, the chromo domain of HP1 isoforms has also been shown to interact with the histone H1.4 variant when methylated at lysine 26 (Daujat *et al.*, 2005). Further, also the methylated histone methyltransferase G9a has been described to be a target for the chromo domain of mammalian HP1 isoforms (Chin *et al.*, 2007; Sampath *et al.*, 2007). This illustrates that the chromo domain can interact with various methylated substrates depending on the context. It appears likely that in *Drosophila*, euchromatic HP1b and HP1c can also

interact with a methylated partner, given the conservation of the chromo domains and their ability to bind to methylated H3K9 *in vitro* (Figure 22B, Figure 23). *Drosophila* and mammalian HP1 isoforms involved in active transcription can interact with the phosphorylated CTD of RNA pol II (Vakoc *et al.*, 2005; Kwon *et al.*, 2010). Such an interaction might also play a role for the HP1c complex at active genes. The interaction with RNA pol II was studied at induced genes where HP1 is recruited to the entire transcribed region, suggesting an association with elongating RNA pol II. In wild-type S2 cells however, the HP1c complex binds its target genes at the TSS, suggesting that the mechanism is different in this system. Further, several reports described the association of HP1 proteins with RNA. In *Drosophila*, the binding of the euchromatic fraction of HP1a was shown to be RNA dependent (Piacentini *et al.*, 2003). HP1a was found to associate with more than 100 transcripts through the chromo domain and this interaction was shown to affect transcription positively (Piacentini *et al.*, 2009). In mammals and yeast in contrast, RNA binding by HP1 proteins was shown to occur through the hinge region and play a role in defining heterochromatin identity (Muchardt *et al.*, 2002; Motamedi *et al.*, 2008; Keller *et al.*, 2012). It is tempting to speculate that the role of the HP1c complex in active transcription also involves an interaction with the corresponding transcripts. However, it has not been addressed whether HP1b and HP1c possess RNA binding activity. Interestingly, in ROW and WOC purification experiments we identified the proteins Blanks and WDR79, which both are known to interact with RNA (Tycowski *et al.*, 2009; Gerbasi *et al.*, 2011).

Based on the available literature and the multitude of described HP1 interaction partners, it can be concluded that HP1 proteins and associated complexes are not recruited by a common and unique mechanism. Rather, several binding activities appear to function cooperatively in the

recruitment of HP1 protein complexes to chromatin. Furthermore, HP1 proteins involved in active transcription, such as HP1c, might be dynamically regulated and contribute to several steps during the transcription cycle. Further, we envision that reinforcing mechanisms might play an important role in this process. The HP1c complex is involved in promoting active transcription of its target genes. However, transcription by itself and the chromatin state associated with it might also regulate the HP1c complex through a kind of feedback mechanism.

5. CONCLUSIONS

- *In vitro*, the chromo domain of HP1c binds less efficiently to H3K9me3 than the chromo domains of HP1a and HP1b.
- The H3K9me3 binding activity of HP1c is not required for targeting to polytene chromosomes.
- The target genes of the HP1c complex are predominantly bound at the TSS and are actively expressed
- The HP1c complex contributes positively to target gene expression and levels of H3K4me3 and RNA pol II Ser5 phosphorylation.
- In contrast to ROW and WOC, HP1c has very minor effects on target gene expression in S2 cells.
- The ubiquitin receptor Dsk2 is a core component of the HP1c complex and is required for target gene expression.
- Dsk2, ROW and WOC are mutually required for recruitment to chromatin.
- Dsk2 does not mediate proteolytic degradation of the HP1c complex, but positively affects protein levels of ROW, WOC and HP1c.
- Both the UbL and the UBA domain of Dsk2 contribute to chromatin binding, but only the UbL domain is required for incorporation into the HP1c complex.
- Dsk2 positively affects H2Bub1 at target genes and *in vitro* binding studies suggest that Dsk2 can bind directly to H2Bub1.
- Binding of Dsk2 to H2Bub1 prevents deubiquitylation by Ubp8/Nonstop.
- BEAF-32 and Z4 are associated with the HP1c complex and co-localize at the TSS of many target genes.
- Recruitment of Z4 and the HP1c complex to chromatin is independent.
- Z4 and the HP1c complex regulate target gene expression differently.

6. MATERIALS AND METHODS

6.1. Materials

6.1.1. Oligos

Abbreviations and explanations	
fw	forward; indicates that the oligo has the same orientation as the sense strand of its target gene
rv	reverse; indicates that the oligo has the same orientation as the antisense strand of its target gene
T7	T7 promoter; is added to the oligos in order to transcribe the PCR product and to generate dsRNA
seq	sequencing primer
qPCR	quantitative PCR; qPCR genomic indicates that the oligo pair cannot be used for amplifying cDNA; RT-qPCR indicates that the oligo pair cannot be used for amplifying genomic DNA
target	the gene or another feature that is targeted by the oligo is indicated
mut	mutagenesis; oligo for introducing a mutation using the QuikChange Site-Directed Mutagenesis Kit (Stratagene); the mutated amino acid is indicated (e.g. Y48A)
TSS	transcription start site; for oligos used in ChIP-qPCR the distance of the center of the amplicon to the TSS of the target is indicated in nucleotides; TSS+, downstream; TSS-, upstream
(230-X)	indicates that a forward oligo is binding to the CDS corresponding to amino acid 230
(X-626)	indicates that a reverse oligo is binding to the CDS corresponding to amino acid 626
ATG	indicates that a start codon is introduced with the oligo
STOP	indicates that a stop codon is introduced with the oligo

6.1.1.1. Designed oligos

Label	5'-3' sequence	Description
oRK001	AAAAACATATGAGCTTAGAGGAGCAGGAAAATGG	fw; NdeI; woc(230-X)
oRK002	AAAGAATTCGCTTTCGATCCTGTCCAGG	rv; woc(X-626); EcoRI

Label	5'-3' sequence	Description
oRK003	AAAGGATCCATGACGCGCGTAACGAGAAGTG	fw; BamHI; row
oRK004	AAAACTAGTTTGCGGATGGTGATGGTGCTGG	rv; row; SpeI
oRK005	AAAACTAGTTCATTGCGGATGGTGATGGTGC	rv; row; STOP; SpeI
oRK006	AAAGAATTCGATGACGCGCGTAACGAGAAG	fw; EcoRI; row
oRK007	AAATCTAGATTGCGGATGGTGATGGTGC	rv; row; XbaI
oRK008	AAATCTAGATCATTGCGGATGGTGATGGTGC	rv; row; STOP; XbaI
oRK009	AAAACTAGTATGGAGGAGATATCCAGTTTGG	fw; SpeI; woc
oRK010	AAAACTAGTCGTTAGTAGCGCTATGTTG	rv; woc; SpeI
oRK011	AAAACTAGTTTAAGTCGTTAGTAGCGCTATG	rv; woc; STOP; SpeI
oRK012	AAAGGTACCATGGAGGAGATATCCAGTTTGG	fw; Asp718; woc
oRK013	AAAGGTACCAGTCGTTAGTAGCGCTATGTTG	rv; woc; Asp718
oRK014	AAAGGTACCTTAAGTCGTTAGTAGCGCTATG	rv; woc; STOP; Asp718
oRK015	AAAAACATATGAAGGAGACACCTGCCAATGC	fw; NdeI; row(588-X)
oRK016	AAAGAATTCCTTTGGCGGTGGTATCAACATCG	rv; row(X-956); EcoRI
oRK017	TCCAGGCCATTCTTGAGC	fw; row; seq
oRK018	AGTGCAGCATCATGTGAGC	fw; row; seq
oRK019	TCAGTTGTGGTCAGCAGC	fw; pMK33 seq
oRK020	AGCAACACCATCAACAGG	fw; row; seq
oRK021	ACGAGGAAGATGCATTGG	rv; row; seq
oRK022	TTCCGCATCTCCTTCTGC	rv; woc; seq
oRK023	AACATTGGCGCCACAACG	fw; woc; seq
oRK024	AACAGCAGTCACCGAAGG	fw; woc; seq
oRK025	ATGTCAGGTGGCAGCTCC	fw; woc; seq
oRK026	ACGATCAGCAGCCAGTCG	fw; woc seq
oRK027	ATCTGACGACCGTGGAGG	fw; woc; seq
oRK028	AAAAACATATGGGCAAGAAAATCGACAACC	fw; NdeI; HP1a
oRK029	AAATCTAGATTAATCTTCATTATCAGAGTAC	rv; HP1a; XbaI
oRK030	AAAAACATATGGACTTCTGCAATGAGGTGTGC	fw; NdeI; woc(651-X)

Label	5'-3' sequence	Description
oRK031	AAAGAATTCGTGGTAGTATTTCGCCTGAC	rv; woc(X-1088); EcoRI
oRK032	AAACTCGAGATGGATTACAAGGATGACGACGATAAGCATATGGTTAAAAACGAGCCCAACTTCG	fw; XhoI; FLAG; NdeI; HP1c
oRK033	AAATCTAGATTATTGATTTTCCGCCATG	rv; HP1c; XbaI
oRK034	AAAAACATATGGCCGAATTCTCAGTGGAACG	fw; NdeI; HP1b
oRK035	AAATCTAGACTAGTCATCCGCATCCGGCTG	rv; HP1b; XbaI
oRK036	TTTTCTAGATTTAATCTTCATTATCAGAGTACCAG	rv; HP1a; XbaI
oRK037	AAAAACATATGGTTAAAAACGAGCCCAACTTC	fw; NdeI; HP1c
oRK038	TTTTCTAGACTTATTGATTTTCCGCCATG	rv; HP1c; XbaI
oRK039	TCGAGGATTACAAGGATGACGACGATAAGCATATGA	fw; XhoI; FLAG; NdeI; HindIII
oRK040	AGCTTCATATGCTTATCGTCGTCATCCTTGTAATCC	rv; XhoI; FLAG; NdeI; HindIII
oRK041	GAGTACTATCTGAAAGCGAAGGGCTATCC	fw; mut; HP1a W45A
oRK042	GGATAGCCCTTCGCTTTCAGATAGTACTC	rv; mut; HP1a W45A
oRK043	GAAATGGAAGGGCGCTCCCGAAACTGAG	fw; mut; HP1a Y48A
oRK044	CTCAGTTTCGGGAGCGCCCTTCCATTTC	rv; mut; HP1a Y48A
oRK045	GAATACTATCTAAAGGCGAAGGGCTATCC	fw; mut; HP1b W25A
oRK046	GGATAGCCCTTCGCCTTTAGATAGTATTC	rv; mut; HP1b W25A
oRK047	CTAAAGTGGAAGGGTGCTCCGCGCAGC	fw; mut; HP1b Y28A
oRK048	GCTGCGCGGAGCACCCTTCCACTTTAG	rv; mut; HP1b Y28A
oRK049	GTACTACATCAAGGCGCGTGGCTACAC	fw; mut; HP1c W30A
oRK050	GTGTAGCCACGCGCCTTGATGTAGTAC	rv; mut; HP1c W30A
oRK051	CAAGTGGCGTGGCGCTACGTCGGCGGAC	fw; mut; HP1c Y33A
oRK052	GTCCGCCGACGTAGCGCCACGCCACTTG	rv; mut; HP1c Y33A
oRK053	AAATCTAGACGACAACCATCCAACATCGCCTAC	fw; XbaI; row
oRK054	AAATCTAGAGCCATCCTTGCCGTCTTTGCT	rv; row; XbaI
oRK055	AAATCTAGACCAGAAGCCAGTGAGGGTGGA	fw; XbaI; woc
oRK056	AAATCTAGAGGCAGTTGATGGAGCAGGTGAG	rv; woc; XbaI
oRK057	AAATCTAGACCACCGACTCATCCGGGCACCT	fw; XbaI; HP1b

Label	5'-3' sequence	Description
oRK058	AAAAAGCTTATCCTCCTCGTCACCGCCATCT	rv; HP1b; HindIII
oRK059	AAAAAGCTTCGAGAAGAAACCCAAGTGCGAAG	fw; HindIII; HP1c
oRK060	AAACTCGAGTCTAGATTCCACCAAGATGTCCAGCCAAC	rv; HP1c; XbaI, XhoI
oRK061	AAAGGATCCATGGCCGAATTCTCAGTGGAAC	fw; BamHI; HP1b(1-X)
oRK062	AAAGGATCCTTACTCCTTCTTGTTGTTCTTCAGC	rv; HP1b(X-60); BamHI
oRK063	TAATACGACTCACTATAGGGAAGTCAGCAAACGGTCACA	fw; T7; HP1c (1)
oRK064	TAATACGACTCACTATAGGGCTTCTGGATCTCTTCGCAC	rv; HP1c (1); T7
oRK065	TAATACGACTCACTATAGGGAAGAGAGCGATAGTTGCCGA	fw; T7; HP1b (1)
oRK066	TAATACGACTCACTATAGGGTTTTCGCTGCGCGGATAG	rv; HP1b (1); T7
oRK067	TAATACGACTCACTATAGGGTCCAGCGTGAGGGGAGC	fw; T7; woc
oRK068	TAATACGACTCACTATAGGGCTGGAGGACAGAGAGCACT	rv; woc; T7
oRK069	TAATACGACTCACTATAGGGATGACCATGATTACGCCAAGC	fw; T7; lacZ
oRK070	TAATACGACTCACTATAGGGCAATTTCCATTCGCCATTCAG	rv; lacZ; T7
oRK071	TAATACGACTCACTATAGGGTGATACAGACGCTGAGTGATTG	fw; T7; row
oRK072	TAATACGACTCACTATAGGGAGGAACCACATCCCAAGATG	rv; row; T7
oRK073	TAATACGACTCACTATAGGGATGCCATTCACATTCTTGCC	fw; T7; NELF-e
oRK074	TAATACGACTCACTATAGGGTGAAGTGGCCAGGAAACTAA	rv; NELF-e; T7
oRK075	TAATACGACTCACTATAGGGCAAAAACTTGGTGACC	fw; T7; NELF-b
oRK076	TAATACGACTCACTATAGGGATGATTGGCACCAGTGTCAA	rv; NELF-b; T7
oRK077	TAATACGACTCACTATAGGGCGACTGTCCAGACCTGATAGC	fw; T7; HP1b (2)
oRK078	TAATACGACTCACTATAGGGACTCAACTAGTCATCCGCATCC	rv; HP1b (2); T7
oRK079	TAATACGACTCACTATAGGGCATCATGGACAAGCGCATTACCAG	fw; T7; HP1c (2)

Label	5'-3' sequence	Description
oRK080	TAATACGACTCACTATAGGGTCCACCAAGATG TCCAGCCAACTCA	rv; HP1c (2); T7
oRK081	TGCGAGGAGAAACCCACA	fw; qPCR; CG15526
oRK082	CTGGCACTCGAAAGATAAC	rv; qPCR; CG15526
oRK083	GAACGCCTGGAGCTACT	fw; RT-qPCR; CG8398
oRK084	TCGGTGAGGTTCTTTAGCTT	rv; RT-qPCR; CG8398
oRK085	ATCAATTCGCACGGCAA	fw; RT-qPCR; pyr
oRK086	AAATCCAGGCTGAACACA	rv; RT-qPCR; pyr
oRK087	ATTTCTACCACGACGACTC	fw; RT-qPCR; CG14253
oRK088	CGATGGACATTGTGCTC	rv; RT-qPCR; CG14253
oRK089	AAGTATCTGGGATGTGTCG	fw; RT-qPCR; numb
oRK090	GGATTGCCTCAAGACCTT	rv; RT-qPCR; numb
oRK091	GCGTAATAGGAGCTGGAACA	fw; RT-qPCR; Fmo-2
oRK092	TCCGATTTCGGTGCCTC	rv; RT-qPCR; Fmo-2
oRK093	TATTCCTGGGCGTGCTC	fw; RT-qPCR; mnd
oRK094	GCCTCCACGTAGCTGAC	rv; RT-qPCR; mnd
oRK095	GCCCGTCCTAATCTTGG	fw; RT-qPCR; CG32521
oRK096	TGCGTTATGGCTCACCT	rv; RT-qPCR; CG32521
oRK097	TCCAGCAGCAACTTCCTAA	fw; qPCR; CG14527
oRK098	GTCCGCAATGTTCTCCGA	rv; qPCR; CG14527
oRK099	ACTTTAGCAGAGATTGGCAC	fw; RT-qPCR; CG12014
oRK100	GGGCATCAGGTTCAATTCC	rv; RT-qPCR; CG12014
oRK101	AGTATGGCTCGAATGTGG	fw; RT-qPCR; Syx4
oRK102	GCTATCTGTGCGAGTTGT	rv; RT-qPCR; Syx4
oRK103	GCTCACCGTCAGTATTCC	fw; qPCR; Hsp26
oRK104	CCTCGCTTTCATTTGCCTTA	rv; qPCR; Hsp26
oRK105	ACTCTGTCTGGATCGGT	fw; qPCR; Act5c
oRK106	TCGTCGTACTCCTGCTTG	rv; qPCR; Act5c
oRK107	CGCTGCTTCTTGGAGAC	fw; RT-qPCR; CG14325

Label	5'-3' sequence	Description
oRK108	CCCTTCTTCAGTGATCTTGT	rv; RT-qPCR; CG14325
oRK109	TACCTTAATCCCTGGACCC	fw; RT-qPCR; Ac78C
oRK110	AGCATATTGGATCGGAACAT	rv; RT-qPCR; Ac78C
oRK111	TCACCTCTATCCTGCTCG	fw; RT-qPCR, CG1358
oRK112	CTGACTTGCTCCGCTTC	rv; RT-qPCR; CG1358
oRK113	TACGACAGACTACGACCG	fw; RT-qPCR; rho
oRK114	AAGTGTTTGACCTCTGGG	rv; RT-qPCR; rho
oRK115	CCATGTATCCAGGTATCGC	fw; RT-qPCR, Act79B
oRK116	TCTTGATGGTGGACGGG	rv; RT-qPCR, Act79B
oRK117	AAAAACATATGGAAGCAAAGCAATTGTTG	fw; NdeI; CG10630
oRK118	AAAGAATTCGGTTTTTGTGGATAGTCGGTT	rv; CG10630; EcoRI
oRK119	AAACTCGAGGCCATGGATAACACGTGTGC	fw; XhoI; Z4(292-X)
oRK120	AAACTCGAGTCACATGGCAACATGCTCGCCA	rv; Z4(X-779); STOP; XhoI
oRK121	AAAAACATATGTCGGACTCCGATTCGGACAAC	fw; NdeI; woc(1230-X)
oRK122	AAAGAATTCTGTGATGAGCGCTT	rv; woc(X-1578); EcoRI
oRK123	AAAAACATATGTCCTGCCAGTGGTGCAAGGTG	fw; NdeI, woc(849-X)
oRK124	AAAGGATCCTCTGGCATCTTGTC	rv; woc(X-1211); BamHI
oRK125	AAAAACATATGTTGGCACAGGAGATTTCAC	fw; NdeI; chro(1-X)
oRK126	AAAGAATTCACGGTTTCATTGACCCACTG	rv; chro(X-341); EcoRI
oRK127	TAATACGACTCACTATAGGGAAATGCGTTAGC CGAAAAC	fw; T7; Dsk2 (UTR)
oRK128	TAATACGACTCACTATAGGGCGCTTGTGTGCA ACAACTTT	rv; Dsk2 (UTR); T7
oRK129	TAATACGACTCACTATAGGGCATGCGTCAGCT TATCACGTCCAA	fw; T7; Dsk2 (CDS)
oRK130	TAATACGACTCACTATAGGGCAGGGGATTGCG GTTCTC	rv; Dsk2 (CDS); T7
oRK131	AAAGAATTCATGGCGGAAGGCGGCAGCAAG	fw; EcoRI; Dsk2
oRK132	AAACTCGAGACTCAAGGACAACTGGTTGAG	rv; Dsk2; XhoI
oRK133	AAAGAATTCATGCCGACGCGCAACAACGAGCA G	fw; EcoRI; Dsk2(81-X)
oRK134	AAACTCGAGTGTGTTGTCCGCGTTGTTCG	rv; Dsk2(X-495); XhoI

Label	5'-3' sequence	Description
oRK135	AAAGATATCAAGCTTATTGTTGAGCAGCTCGTTC	rv; Dsk2(X-135); HindIII; EcoRV
oRK136	AAAAAGCTTCAGGGCATGGAGCAGCTGC	fw; HindIII; Dsk2(403-X)
oRK137	AAAGATATCAAGCTTGTCGTGCGAACGCATCAGC	rv; Dsk2(X-209); HindIII; EcoRV
oRK138	AAAAAGCTTGCCAATTCGGGAACCAATGG	fw; HindIII, Dsk2(281-X)
oRK139	GGTTTCCCTTCTTTGCATGA	fw; qPCR genomic; CG14527; TSS-116.5
oRK140	TAAGCTGCCGAAAATGGAAT	rv; qPCR genomic; CG14527; TSS-116.5
oRK141	GCTGCTGAGATCGAGAGCTT	fw; qPCR; CG14527; TSS+189
oRK142	TCAATACCCGCATGTTCAAA	rv; qPCR; CG14527; TSS+189
oRK143	CCCACCGATACGGAATAATG	fw; qPCR; CG14527; TSS+584
oRK144	GGTAGATGGCCGTTTCGTTA	rv; qPCR; CG14527; TSS+584
oRK145	ATCCGAGGGTCGAGTCTTTT	fw; qPCR genomic; CG18094; TSS-73.5
oRK146	TCCAAATCCACTTTTTCAAACC	rv; qPCR genomic; CG18094; TSS-73.5
oRK147	TTCAAATCCTTTGGGGTGAC	fw; qPCR; CG18094; TSS+301.5
oRK148	CCACCGGATAGAAACTCAGG	rv; qPCR; CG18094; TSS+301.5
oRK151	TATTGTAGCCGCCAAAGAGG	fw; RT-qPCR; CG18094
oRK152	GTCACCCCAAAGGATTTGAA	rv; RT-qPCR; CG18094
oRK153	GGGTTGTATGCTGCTCGAAT	fw; qPCR genomic; CG3919; TSS-79
oRK154	ATCTTTAACGGGCGGAGAAT	rv; qPCR genomic; CG3919; TSS-79
oRK155	ATTCTCCGCCCGTTAAAGAT	fw; qPCR genomic; CG3919; TSS+30.5
oRK156	CTGCCAACAAGTGATGCAGT	rv; qPCR genomic; CG3919; TSS+30.5
oRK157	CGAACGTTTACGCCATCAAT	fw; qPCR; CG3919; TSS+562.5
oRK158	TTTCCTTCCACGCATTTTTC	rv; qPCR; CG3919; TSS+562.5
oRK159	GAAAAATGCGTGGAAGGAAA	fw; RT-qPCR; CG3919
oRK160	CTTTATTGAGCGGGCATAGC	rv; RT-qPCR; CG3919
oRK161	GACGCACCCCCAATACTAGA	fw; qPCR genomic; Pgm; TSS-40

Label	5'-3' sequence	Description
oRK162	CCTCCCACTGATAAGCCAAA	rv; qPCR genomic; Pgm; TSS-40
oRK163	CGCTAACGGTGGAAATTGTT	fw; qPCR genomic; Pgm; TSS+167
oRK164	AAAATGCAAGTGCGAGCTTT	rv; qPCR genomic; Pgm; TSS+167
oRK165	CAGCCTTCACTGTGCTCGTA	fw; qPCR genomic; Pgm; TSS+591.5
oRK166	TTGCCCGAGTAACGAACTCT	rv; qPCR genomic; Pgm; TSS+591.5
oRK167	AGTTGCTGGTGGGTCAAAAC	fw; RT-qPCR; Pgm
oRK168	GCCGAAATCATTCTCTGGAC	rv; RT-qPCR; Pgm
oRK169	CGGTCGAAGTTGACGAAGAT	fw; RT-qPCR; Dsk2
oRK170	ATCTGAAGGGTGTCCGTGTC	rv; RT-qPCR; Dsk2
oRK171	CTGGAGGGTAAGACCTGTGC	fw; RT-qPCR; row
oRK172	CATTACATTCCACGCCATGA	rv; RT-qPCR; row
oRK173	TCGAGTACCCATACGATGTTCCAGATTACGCTT GAAT	fw; XhoI, HA; STOP; XbaI
oRK174	CTAGATTCAAGCGTAATCTGGAACATCGTATG GGTAC	rv; XhoI, HA; STOP; XbaI
oRK175	GTACCATGTACCCATACGATGTTCCAGATTAC GCTGAATTCAAACTCGAGTGAAT	fw; ATG; HA; EcoRI; XhoI, STOP, XbaI
oRK176	CTAGATTCACTCGAGTTTGAATTCAGCGTAATC TGGAACATCGTATGGGTACATG	rv; ATG; HA; EcoRI; XhoI, STOP, XbaI
oRK177	TAATACGACTCACTATAGGGTTTTACGTCCTTA CCACTGGC	fw; T7, Bre1
oRK178	TAATACGACTCACTATAGGGCGACAAATCGAA GTGATGGA	rv; Bre1; T7
oRK179	TAATACGACTCACTATAGGGTGGATGTTAATA TGGCTGACACA	fw; T7; UbcD6 (Rad6)
oRK180	TAATACGACTCACTATAGGGTCAAGAGGATCC ACCTACGG	rv; UbcD6 (Rad6); T7
oRK181	TAATACGACTCACTATAGGGCCAAAAACAATC GACAGAAAA	fw; T7; Ash2
oRK182	TAATACGACTCACTATAGGGCTCGGACCATGC AGTAAC	rv; Ash2; T7
oRK183	CCCCTGTTTCAGTTCCAAGC	fw; qPCR genomic; tsh; TSS-65
oRK184	ACTGACTGACTCTTGGCGAA	rv; qPCR genomic; tsh; TSS-65
oRK185	AGGCTAGTGACGAAGGAACC	fw; qPCR; tsh; TSS+476

Label	5'-3' sequence	Description
oRK186	TGCGTCTTCTCATCCGGATT	rv; qPCR; tsh; TSS+476
oRK187	GAATCACTTTGTTCTTGTATCGCA	fw; qPCR genomic; CG14100; TSS-64.5
oRK188	CGTAAGCAAACACATTTAAGGGG	rv; qPCR genomic; CG14100; TSS-64.5
oRK189	AGGACGCACTGGACATAGAG	fw; qPCR; CG14100; TSS+186.5
oRK190	CTCGTGTTCATCGGCTCATG	rv; qPCR; CG14100; TSS+186.5
oRK191	ACGAGACATTTTAACGGTAAATCAA	fw; qPCR genomic; CG5846; TSS-64.5
oRK192	TACCCTGTATTGGAAGCCCC	rv; qPCR genomic; CG5846; TSS-64.5
oRK193	CCTCCTACGGTCAACTGGTT	fw; qPCR; CG5846; TSS+398
oRK194	GGCAGCTAGGAGTAGAGGAC	rv; qPCR; CG5846; TSS+398
oRK195	CCCCAGTTTTCGTCCAACAG	fw; qPCR genomic; CG5367; TSS-89.5
oRK196	TTCCAGTCGTTCCCACAGAA	rv; qPCR genomic; CG5367; TSS-89.5
oRK197	AGTTACAAGGCGTTCGAGGA	fw; qPCR; CG5367; TSS+582.5
oRK198	ACCTGAAGCTCGTTTGACCT	rv; qPCR; CG5367; TSS+582.5
oRK199	GATCCGAATTCACATCTAGA	fw; BamHI, EcoRI, XbaI, EcoRI
oRK200	AATTTCTAGATGTGAATTCG	rv; BamHI, EcoRI, XbaI, EcoRI
oRK201	TAATACGACTCACTATAGGGAACCACCACAATCATCAGCA	fw; T7; scrawny
oRK202	TAATACGACTCACTATAGGGCGTAATGGACACATGGTTGC	rv; scrawny; T7
oRK203	TAATACGACTCACTATAGGGCTGAACTGTTTGGTGGAC	fw; T7; nonstop (Ubp8)
oRK204	TAATACGACTCACTATAGGGTCTATTCCGGCTCCCGTT	rv; nonstop (Ubp8); T7

6.1.1.2. Other oligos used

Name	5'-3' sequence	Description
M13 fw	GTAAAACGACGGCCAGT	fw; seq

Name	5'-3' sequence	Description
M13 rev	AACAGCTATGACCATG	fw; seq
HP1c forwa	CATATGGTTAAAAACGAGCCCAACTTC	fw; HP1c(1-X); NdeI; Joan Font
pGEX 5'	GGGCTGGCAAGCCACGTTTGGTG	fw; GST; seq
Tub 2 for	ACCTGAACCGTCTGATTGGC	fw; αtubulin84B; qPCR; Sergi Cuartero
Tub 2 rev	GCAGAGAGGCGGTAATCGAG	rv; αtubulin84B; qPCR; Sergi Cuartero
HP1c 3 for	GCATTACCAGCGAAGGCAA	fw; HP1c; qPCR; Joan Font
HP1c 3 rev	TGTAGCCACGCCACTTGATG	rv; HP1c; qPCR; Joan Font
Z4 R1 LOWER	TAATACGACTCACTATAGGGTGCTGCTTG CAGGTTTCATA	fw; Z4; T7; Sergi Cuartero
Z4 R1 UPPER	TAATACGACTCACTATAGGGATCGCTCGT TGGAGGAGAGT	rv; Z4; T7; Sergi Cuartero
Ac5 fw	ACACAAAGCCGCTCCATCAG	fw; seq; actin 5C promoter
BGH rv	TAGAAGGCACAGTCGAGG	rv; seq; poly(A) signal

6.1.2. Plasmids

Explanations of cloning procedures	
PCR(cDNA, oRK1,2) x RE1, RE2 in pRK1	A PCR product is generated using cDNA as a template and the oligo pair oRK1, oRK2. The PCR product is digested with the restriction enzymes RE1 and RE2 and inserted into the plasmid pRK1 that was opened with the same restriction enzymes.
pRK1 x RE1, RE2 in pRK2	An insert from the plasmid pRK1 is cut using the restriction enzymes RE1 and RE2 and is inserted into the plasmid pRK2 that was opened using the same restriction enzymes.
pRK1_ΔRE1-RE2 (blunted)	The plasmid pRK1 is digested with the restriction enzymes RE1 and RE2. Then the sticky ends are filled in (blunted) with T4 DNA polymerase and the plasmid is re-ligated.
oligo(oRK1,2) x RE1, RE2 in pRK1	the oligos oRK1 and oRK2 are hybridized, which generates sticky ends compatible with the restriction sites RE1 and RE2, and inserted into the plasmid pRK1 that was opened with the restriction enzymes RE1 and RE2.
QC(pRK1, oRK1,2)	Using the QuikChange Site-Directed Mutagenesis Kit (Stratagene), the plasmid pRK1 is mutated, using the oligos oRK1 and oRK1.

6.1.2.1. Generated plasmids

Label	Description	Cloning Info	Comments
pRK001	pET_woc(230-626)	PCR(cDNA, oRK1,2) x NdeI, EcoRI in pET29a	His tag not in frame
pRK002	pMK33_row-TAP	PCR(cDNA, oRK3,4) x BamHI, SpeI in pMK33-CTAP	C-term. TAP tag
pRK003	pMK33_TAP-row	PCR(cDNA, oRK3,5) x BamHI, SpeI in pMK33-NTAP	N-term. TAP tag
pRK004	pUAST_row-TAP	PCR(cDNA, oRK6,7) x EcoRI, XbaI in pUAST-CTAP	C-term. TAP tag
pRK005	pUAST_TAP-row	PCR(cDNA, oRK6,8) x EcoRI, XbaI in pUAST-NTAP	N-term. TAP tag
pRK006	pMK33_woc-TAP	PCR(cDNA, oRK9,10) x SpeI in pMK33-CTAP	C-term. TAP tag
pRK007	pMK33_TAP-woc	PCR(cDNA, oRK9,11) x SpeI in pMK33-NTAP	N-term. TAP tag
pRK008	pUAST_woc-TAP	PCR(cDNA, oRK12,13) x Asp718 in pUAST-CTAP	C-term. TAP tag
pRK009	pUAST_TAP-woc	PCR(cDNA, oRK12,14) x Asp718 in pUAST-NTAP	N-term. TAP tag
pRK010	pET_row(588-956)	PCR(cDNA, oRK15,16) x NdeI, EcoRI in pET29a	His tag not in frame
pRK011	pET_ΔSacI-SalI	pET29a_ΔSacI-SalI (blunted)	correcting frame, Kanamycin
pRK012	pET_row(588-956)_ΔSacI-SalI	pRK10_ΔSacI-SalI(blunted)	for raising rabbit ab's; Kanamycin; C-term. His
pRK013	pET_woc(230-626)_ΔSacI-SalI	pRK1 x NdeI, EcoRI in pRK12	Kanamycin; C-term. His
pRK014	pMAL_woc(230-626)	cDNA x HindIII in pMAL-p2	for raising rat ab's; N-term. MBP
pRK015	pET_woc(651-1088)	PCR(cDNA, oRK30,31) x NdeI, EcoRI in pET29a	Kanamycin
pRK016	pUASTattB_FLAG-HP1c	pRK21 x XhoI, XbaI in pUASTattB	for transgenic flies (sites 22A & 51C)
pRK017	pUASTattB_FLAG-HP1a	pRK22 x XhoI, XbaI in pUASTattB	for transgenic flies (site 86Fb)
pRK018	pUASTattB_FLAG-HP1b	pRK23 x XhoI, XbaI in pUASTattB	for transgenic flies (site 86Fb)
pRK019	pGEX-2TK_HP1c_FL	cDNA x AvaI, ClaI in pGEX-2TK_HP1c_FL(I100F)	exchange I100F with wt

Label	Description	Cloning Info	Comments
pRK020	pBS-FLAG	oligo(oRK39,40) x XhoI, HindIII in pBS-SK(-)	no ATG
pRK021	pBS_FLAG-HP1c	PCR(cDNA, oRK32,38) x XhoI, XbaI in pBS-SK(-)	precursor for pRK16
pRK022	pBS_FLAG-HP1a	PCR(cDNA, oRK28,36) x NdeI, XbaI in pRK21	precursor for pRK17
pRK023	pBS_FLAG-HP1b	PCR(cDNA, oRK34,35) x NdeI, XbaI in pRK21	precursor for pRK18
pRK024	pGEX-2TK_HP1a_W45A	pRK32 x BglII, SacI in pGEX-2TK_HP1a_FL	GST-HP1a(FL)_W45A
pRK025	pGEX-2TK_HP1a_Y48A	pRK33 x BglII, SacI in pGEX-2TK_HP1a_FL	GST-HP1a(FL)_Y48A
pRK026	pGEX-2TK_HP1b_W25A	QC(pGEX_HP1b, oRK45,46)	GST-HP1b(FL)_W25A
pRK027	pGEX-2TK_HP1b_Y28A	QC(pGEX_HP1b, oRK47,48)	GST-HP1b(FL)_Y28A
pRK028	pGEX-2TK_HP1c_W30A	QC(pRK19, oRK49,50)	GST-HP1c(FL)_W30A
pRK029	pGEX-2TK_HP1c_Y33A	QC(pRK19, oRK51,52)	GST-HP1c(FL)_Y33A
pRK030	pGEX-2TK_HP1c_N_W30A	pRK28 x AvaI, BalI in pGEX-2TK_HP1c_N	GST-HP1c(chromo)_W30A
pRK031	pGEX-2TK_HP1c_N_Y33A	pRK29 x AvaI, BalI in pGEX-2TK_HP1c_N	GST-HP1c(chromo)_Y33A
pRK032	pBS_FLAG-HP1a_W45A	QC(pRK22, oRK41,42)	precursor for pRK24 & 38
pRK033	pBS_FLAG-HP1a_Y48A	QC(pRK22, oRK43,44)	precursor for pRK25 & 39
pRK034	pBS_FLAG-HP1b_W25A	pRK26 x EheI, MluI in pRK23	precursor for pRK40
pRK035	pBS_FLAG-HP1b_Y28A	pRK27 x EheI, MluI in pRK23	precursor for pRK41
pRK036	pBS_FLAG-HP1c_W30A	QC(pRK21, oRK49,50)	precursor for pRK42
pRK037	pBS_FLAG-HP1c_Y33A	OC(pRK21, oRK51,52)	precursor for pRK43
pRK038	pUASTattB_FLAG-HP1a_W45A	pRK32 x XbaI, XhoI in pUASTattB	for transgenic flies (site 86Fb)
pRK039	pUASTattB_FLAG-HP1a_Y48A	pRK33 x XbaI, XhoI in pUASTattB	for transgenic flies (site 86Fb)
pRK040	pUASTattB_FLAG-HP1b_W25A	pRK34 x XbaI, XhoI in pUASTattB	for transgenic flies (site 86Fb)
pRK041	pUASTattB_FLAG-HP1b_Y28A	pRK35 x XbaI, XhoI in pUASTattB	for transgenic flies (site 86Fb)

Label	Description	Cloning Info	Comments
pRK042	pUASTattB_FLAG-HP1c_W30A	pRK36 x XbaI, XhoI in pUASTattB	for transgenic flies (site 51C)
pRK043	pUASTattB_FLAG-HP1c_Y33A	pRK37 x XbaI, XhoI in pUASTattB	for transgenic flies (site 51C)
pRK044	pGEX-2TK_HP1c(59-237)	pRK19 x PauI, EcoRI (blunted) in pGEX-2TK x EcoRI (blunted)	EcoRI destroyed; correct frame
pRK045	pGEX-2TK_HP1a(1-76)	pGEX-2TK_HP1a(1-76)_C2* x SacI, EcoRI in pGEX-2TK_HP1a-FL	correcting frame of C2*; GST-HP1(chromo)
pRK046	pMK33_WIZΔEco32I-SacI	pMK33-WIZ_ΔEco32I, SacI (blunted)	removing NheI site
pRK047	pRK46_row	PCR(cDNA, oRK53,54) x XbaI in pRK46 x AvrII	precursor for pRK54
pRK048	pRK46_woc	PCR(cDNA, oRK55,56) x XbaI in pRK46 x AvrII	precursor for pRK51
pRK049	pBS_HP1b-HP1c	PCR(cDNA, oRK57,58) x XbaI, HindIII & PCR(cDNA, oRK59,60) x XhoI, HindIII in pBS-SK- x XhoI, XbaI	precursor for pRK52 & 53
pRK051	pRK46_woc-hairpin	PCR(cDNA, oRK55,56) x XbaI in pRK48 x NheI	for RNA hairpin expr. in cells
pRK052	pRK46_HP1b-HP1c	pRK49 x XbaI in pRK46 x AvrII	precursor for pRK53
pRK053	pRK46_HP1b/c-hairpin	pRK49 x XbaI in pRK52 x NheI	for RNA hairpin expr. in cells
pRK054	pRK46_row-hairpin_antisense	PCR(cDNA, oRK53,54) x XbaI in pRK47_AS x NheI	for RNA hairpin expr. in cells; not clear if correct
pRK055	pGEX-2TK_HP1b(1-60)	PCR(cDNA, oRK61,62) x BamHI in pGEX-2TK	GST-HP1b(chromo)_wt
pRK056	pGEX-2TK_HP1a_N_W45A	pRK45 x Eco72I, AatII in pRK24	GST-HP1a(chromo)_W45A
pRK057	pGEX-2TK_HP1a_N_Y48A	pRK45 x Eco72I, AatII in pRK25	GST-HP1a(chromo)_Y48A
pRK058	pGEX-2TK_HP1b_N_W25A	QC(pRK55, oRK45,46)	GST-HP1b(chromo)_W25A
pRK059	pGEX-2TK_HP1b_N_Y28A	QC(pRK55, oRK47,48)	GST-HP1b(chromo)_Y28A
pRK060	pET_CG10630(FL)	PCR(cDNA, oRK117,118) x NdeI, EcoRI in pET29a	C-term. His; Kanamycin
pRK061	pET_Z4(292-779)	PCR(cDNA, oRK119,120) x XhoI in pET14b	N-term. His; Ampicillin
pRK062	pET_woc(1230-1578)	PCR(cDNA, oRK121,122) x NdeI, EcoRI in pET29a	C-term. His; Kanamycin

Label	Description	Cloning Info	Comments
pRK063	pET_woc(849-1211)	PCR(cDNA, oRK123,124) x NdeI, BamHI in pET29a	C-term. His; Kanamycin
pRK064	pET_chro(1-341)	PCR(cDNA, oRK125,126) x NdeI, EcoRI in pET29a	C-term. His; Kanamycin
pRK065	pET_woc(849-1578)	PCR(cDNA, oRK123,122) x NdeI, EcoRI in pET29a	C-term. His; Kanamycin
pRK066	pET_woc(651-1211)	PCR(cDNA, oRK30,124) x NdeI, BamHI in pET29a	C-term. His; Kanamycin
pRK067	pAc5.1_Dsk2(FL)-V5-His	PCR(cDNA, oRK131,132) x EcoRI, XhoI in pAc5.1_V5-His_A	Dsk2-V5-His
pRK068	pAc5.1_Dsk2(81-547)-V5-His	PCR(cDNA, oRK133,132) x EcoRI, XhoI in pAc5.1_V5-His_A	Dsk2(ΔUbL)-V5-His
pRK069	pAc5.1_Dsk2(1-495)-V5-His	PCR(cDNA, oRK131,134) x EcoRI, XhoI in pAc5.1_V5-His_A	Dsk2(ΔUBA)-V5-His
pRK071	pAc5.1_Dsk2(Δ136-402)-V5-His	PCR(cDNA, oRK131,135) x EcoRI, HindIII & PCR(cDNA, oRK136,132) x HindIII, XhoI in pAc5.1 x EcoRI, XhoI	Dsk2(ΔSTI1s)-V5-His
pRK072	pAc5.1_Dsk2(81-495)-V5-His	PCR(cDNA, oRK133,134) x EcoRI, XhoI in pAc5.1_V5-His_A	Dsk2(ΔUbL,ΔUBA)-V5-His
pRK074	pAc5.1_Dsk2(Δ210-280)-V5-His	PCR(cDNA, oRK131,137) x EcoRI, HindIII & PCR(cDNA, oRK138,132) x HindIII, XhoI in pAc5.1 x EcoRI, XhoI	Dsk2(Δ210-280)-V5-His
pRK075	pAc5.1_N-HA	oligo(oRK175,176) x Asp718, XbaI in pAc5.1_V5-His_A	precursor for pRK77-82
pRK076	pAc5.1_C-HA	oligo(oRK173,174) x XhoI, XbaI in pAc5.1_V5-His_A	precursor for pRK83-88
pRK077	pAc5.1_HA-Dsk2(FL)	pRK67 x EcoRI, XhoI in pRK75	HA-Dsk2
pRK078	pAc5.1_HA-Dsk2(81-547)	pRK68 x EcoRI, XhoI in pRK75	HA-Dsk2(ΔUbL)
pRK079	pAc5.1_HA-Dsk2(1-495)	pRK69 x EcoRI, XhoI in pRK75	HA-Dsk2(ΔUBA)
pRK080	pAc5.1_HA-Dsk2(Δ136-402)	pRK71 x EcoRI, XhoI in pRK75	HA-Dsk2(ΔSTI1s)
pRK081	pAc5.1_HA-Dsk2(81-495)	pRK72 x EcoRI, XhoI in pRK75	HA-Dsk2(ΔUbL,ΔUBA)
pRK082	pAc5.1_HA-Dsk2(Δ210-280)	pRK74 x EcoRI, XhoI in pRK75	HA-Dsk2(Δ210-280)
pRK083	pAc5.1_Dsk2(FL)-HA	pRK67 x EcoRI, XhoI in pRK76	Dsk2-HA
pRK084	pAc5.1_Dsk2(81-547)-HA	pRK68 x EcoRI, XhoI in pRK76	Dsk2(ΔUbL)-HA
pRK085	pAc5.1_Dsk2(1-495)-HA	pRK69 x EcoRI, XhoI in pRK76	Dsk2(ΔUBA)-HA

Label	Description	Cloning Info	Comments
pRK086	pAc5.1_Dsk2(Δ136-402)-HA	pRK71 x EcoRI, XhoI in pRK76	Dsk2(ΔSTI1s)-HA
pRK087	pAc5.1_Dsk2(81-495)-HA	pRK72 x EcoRI, XhoI in pRK76	Dsk2(ΔUbL,ΔUBA)-HA
pRK088	pAc5.1_Dsk2(Δ210-280)-HA	pRK74 x EcoRI, XhoI in pRK76	Dsk2(Δ210-280)-HA
pRK089	pGEX-2TK_EcoRI-XbaI	oligo(oRK199,200) x BamHI, EcoRI into pGEX-2TK	inserting RE sites
pRK090	pGEX_Dsk2(FL)	pRK77 x EcoRI, XbaI in pRK89	GST-Dsk2
pRK091	pGEX_Dsk2(81-547)	pRK78 x EcoRI, XbaI in pRK89	GST-Dsk2(ΔUbL)
pRK092	pGEX_Dsk2(1-495)	pRK79 x EcoRI, XbaI in pRK89	GST-Dsk2(ΔUBA)
pRK093	pGEX_Dsk2(Δ136-402)	pRK80 x EcoRI, XbaI in pRK89	GST-Dsk2(ΔSTI1s)
pRK094	pGEX_Dsk2(81-495)	pRK81 x EcoRI, XbaI in pRK89	GST-Dsk2(ΔUbL,ΔUBA)
pRK095	pAc5.1_Dsk2(FL)	pRK77 x EcoRI, XbaI in pAc5.1_V5-His_A	untagged Dsk2
pRK096	pAc5.1_Dsk2(81-547)	pRK78 x EcoRI, XbaI in pAc5.1_V5-His_A	untagged Dsk2(ΔUbL)
pRK097	pAc5.1_Dsk2(1-495)	pRK79 x EcoRI, XbaI in pAc5.1_V5-His_A	untagged Dsk2(ΔUBA)
pRK098	pAc5.1_Dsk2(Δ136-402)	pRK80 x EcoRI, XbaI in pAc5.1_V5-His_A	untagged Dsk2(ΔSTI1s)
pRK099	pAc5.1_Dsk2(81-495)	pRK81 x EcoRI, XbaI in pAc5.1_V5-His_A	untagged Dsk2(ΔUbL,ΔUBA)
pRK100	pGEX_Dsk2(469-547)	pRK90_ΔSmaI-EcoRI (blunted)	GST-Dsk2(UBA)

6.1.2.2. Other plasmids used

Name	Comments
cDNA clones	
pFLC-I_woc-cDNA	cDNA; clone RE05635; DGRC
pFLC-I_row-cDNA	cDNA; clone RE01954 (GOLD); DGRC
pBS-SK(-)_HP1a-cDNA	cDNA; clone LD10408; DGRC
pBS-SK(-)_HP1b-cDNA	cDNA; clone GM01918; DGRC

Name	Comments
pOT2_HP1c-cDNA	cDNA; clone LD23881; chloramphenicol; DGRC
pOT2_Blanks-cDNA	cDNA; clone GH28067 (GOLD); chloramphenicol; DGRC
pBS-SK(-)_Z4-cDNA	cDNA; clone LD15904 (GOLD); DGRC
pOT2_Chromator-cDNA	cDNA; clone SD06626; contains S91N & A304S; chloramphenicol; DGRC
pOT2_Dsk2-cDNA	cDNA; clone LD38919 (GOLD); chloramphenicol; DGRC
pMK33_Blanks-FLAG-HA	tagged ORF; C-term. FLAG-HA; clone FMO04837; DGRC
pMK33_Z4-FLAG-HA	tagged ORF; C-term. FLAG-HA; clone FMO07451; DGRC
lab plasmids	
pGEX-2TK_HP1c_FL	Joan Font; contains I100F; use pRK19
pGEX-2TK_HP1c_N	Joan Font; GST-HP1c(chromo); aa1-60
pGEX-2TK_HP1c_Δchromo	Joan Font; contains I100F; use pRK44
pGEX-2TK_HP1a_FL	Joan Font; GST-HP1a(FL)
pGEX-2TK_HP1b_FL	Joan Font; contains A211V; GST-HP1b
pGEX-2TK_HP1a(1-76)_C2*	Carles Bonet; frame shift after first aa; use pRK45
pMK33-WIZ	Joan Font; pMK33 based vector for generating hairpin for RNAi in cell culture; pWIZ x XhoI, BamHI & pWIZ x SpeI, XbaI in pMK33-CTAP
pMK33-WIZ_HP1b-hairpin	Joan Font; hairpin spans entire HP1b CDS
pMK33-WIZ_HP1c-hairpin	Joan Font; hairpin spans entire HP1c CDS
pMK33-WIZ_GFP-hairpin	Joan Font; control hairpin
general vectors	
pUASTattB	for generating constructs for site-directed fly transgenesis
pET14b	N-term. His tag; for induction in E. coli; Novagen
pET29a	C-term. His tag; for induction in E. coli; Kanamycin; Novagen
pGEX-2TK	N-term. GST tag; for induction in E. coli; Amersham
pAc5.1/V5-His A	for generating C-term. V5-His tagged fusions; for expression in cell culture; consitutive actin 5C promoter; Invitrogen
pUAST_C-TAP	for generating C-term. TAP tagged fusion; for fly transgenesis; GAL4/UAS inducible; (Veraksa *et al.*, 2005)
pUAST_N-TAP	for generating N-term. TAP tagged fusions; for fly transgenesis; GAL4/UAS inducible; (Veraksa *et al.*, 2005)

Name	Comments
pMK33_C-TAP	for generating C-term. TAP tagged fusions; for cell culture; inducible Mt promoter; (Veraksa *et al.*, 2005)
pMK33_N-TAP	for generating N-term. TAP tagged fusions; for cell culture; inducible Mt promoter; (Veraksa *et al.*, 2005)
pBluescript II SK(-)	pBS-SK(-); cloning vector; Stratagene
pMAL-p2	N-term. MBP tag; for induction in E. coli; NEB

6.1.3. Antibodies

Name	Species	Description or source
αHP1b	rabbit	custom-made by ABGENT; antigen HP1b(aa219-233) peptide; #133 and #134; #133 was generally used
αHP1c	rabbit	custom-made by ABGENT; antigen HP1c(aa143-157) peptide; #135 and #136; #135 was generally used
αWOC	rat	antigen WOC(aa230-626); induced from pRK14 as an N-term. tagged MBP fusion; tag removed by specific protease cleavage; #1 and #2; #1 is in use
αROW	rabbit	antigen ROW(aa588-956); induced from pRK12 as a C-term. tagged His fusion; #1 and #2; both are in use
αHP1c	rat	(Font-Burgada *et al.*, 2008); #1 is in use
αHP1b	rat	(Font-Burgada *et al.*, 2008); #2 is in use
αROW	rat	(Font-Burgada *et al.*, 2008); #1 is in use
αWOC	rabbit	(Raffa *et al.*, 2005)
αDDP1	rabbit	(Batlle *et al.*, 2011)
αDDP1	rat	(Batlle *et al.*, 2011)
αDsk2	rabbit	(Lipinszki *et al.*, 2009)
αp54	mouse	(Kurucz *et al.*, 2002)
αZ4	rat	(Raja *et al.*, 2010)
αChromator	rabbit	(Raja *et al.*, 2010)
αZ4	guinea pig	(Kugler & Nagel, 2007)
αcoilin	rabbit	(Liu *et al.*, 2009)
αcoilin	guinea pig	(Liu *et al.*, 2009)

Name	Species	Description or source
αBlanks	rabbit	(Gerbasi *et al.*, 2011)
αH3K4me3	rabbit	Abcam ab8580
αIIoser5	rabbit	Abcam ab5151
αGFP	mouse	Roche 1814460
αH2Bub1	mouse	Millipore 05-1312
αtubulin	mouse	Millipore MAB3408
αactin	rabbit	Sigma A2066
αV5	mouse	Invitrogen 460705
αBEAF-32	mouse	Hybridoma Bank
αGST	mouse	Novagen 71097-3
αHA	rat	Roche clone3F10

6.1.4. Fly lines

Stock ID	X chr.	2nd chr.	3rd chr.	Comments
RK024	w-	If/Cyo	T[4]/TM6b*	UAST_row-CTAP; pRK4; line 43.1; *no tubby marker
RK025	w-	If/Cyo	T[5]/TM6b*	UAST_NTAP-row; pRK5; line 62.4; *no tubby marker
RK026	w-	If/Cyo	T[8]/TM6b*	UAST_woc-CTAP; pRK8; line 49.1; *no tubby marker
RK027	w-	If/Cyo	T[9]/TM6b*	UAST_NTAP-woc; pRK9; line 151.1; *no tubby marker
RK029	w-	T[9]/Cyo	TM6b*/Mkrs	UAST_NTAP-woc; pRK9; line 144.1; *no tubby marker
RK036	w-	T[16]22A/Cyo	TM2/TM6b	attB-UAST_FLAG-HP1c wt; pRK16; line 11; landing site 22A
RK037	w-	T[16]22A/Cyo	TM2/TM6b	attB-UAST_FLAG-HP1c wt; pRK16; line 24; landing site 22A
RK038	w-	T[16]51C/Cyo	TM2/TM6b	attB-UAST_FLAG-HP1c wt; pRK16; line 1; landing site 51C
RK039	w-	T[16]51C/Cyo	TM2/TM6b	attB-UAST_FLAG-HP1c wt; pRK16; line 2; landing site 51C

Stock ID	X chr.	2nd chr.	3rd chr.	Comments
RK041	w-	T[42]51C/Cyo	TM2/TM6b	attB-UAST_FLAG-HP1c W30A; pRK42; line 1; landing site 51C
RK042	w-	T[42]51C/Cyo	TM2/TM6b	attB-UAST_FLAG-HP1c W30A; pRK42; line 2; landing site 51C
RK044	w-	T[43]51C/Cyo	TM2/TM6b	attB-UAST_FLAG-HP1c Y33A; pRK43; line 1; landing site 51C
RK045	w-	T[43]51C/Cyo	TM2/TM6b	attB-UAST_FLAG-HP1c Y33A; pRK43; line 2; landing site 51C
RK047	w-	Sp/Cyo	T[17]86Fb/TM6b	attB-UAST_FLAG-HP1a wt; pRK17; line 1; landing site 86Fb
RK048	w-	Sp/Cyo	T[38]86Fb/TM6b	attB-UAST_FLAG-HP1a W45A; pRK38; line 1; landing site 86Fb
RK049	w-	Sp/Cyo	T[39]86Fb/TM6b	attB-UAST_FLAG-HP1a Y48A; pRK39; line 1; landing site 86Fb
RK050	w-	Sp/Cyo	T[18]86Fb/TM6b	attB-UAST_FLAG-HP1b wt; pRK18; line 1; landing site 86Fb
RK051	w-	Sp/Cyo	T[40]86Fb/TM6b	attB-UAST_FLAG-HP1b W25A; pRK40; line 1; landing site 86Fb
RK052	w-	Sp/Cyo	T[41]86Fb/TM6b	attB-UAST_FLAG-HP1b Y28A; pRK41; line 1; landing site 86Fb
RK055	w-		daGAL4	daughterless-GAL4; bloomington
RK056	w-		armGAL4	armadillo-GAL4; bloomington; 2 copies
RK058	w-	HP1a-04/Cyo		HP1a allele; nonsense mut: Lys169 to STOP (ref: Eissenberg et al. 1992)
RK059	w-	HP1a-05/Cyo		HP1a allele; frameshift mut. at pos. aa10; (ref: Eissenberg et al. 1992)
RK060	w-		HP1c-/TM6b	P-element (f04929) insertion in 5'UTR of HP1c; strong hypomorph; bloomington 18819
RK061	w-	Sp/Cyo	HP1c-/TM6b	RK60 balanced
RK062	w-	armGAL4,T[16]22A/Cyo	TM2/TM6b	RK36 recombined with armGAL4
RK063	w-	armGAL4,T[16]22A/Cyo	TM2/TM6b	RK37 recombined with armGAL4
RK064	w-	armGAL4,T[16]51C/Cyo	TM2/TM6b	RK38 recombined with armGAL4
RK065	w-	armGAL4,T[42]51C/Cyo	TM2/TM6b	RK41 recombined with armGAL4
RK066	w-	armGAL4,T[43]51C/Cyo	TM2/TM6b	RK44 recombined with armGAL4

Stock ID	X chr.	2nd chr.	3rd chr.	Comments
RK072	w-	HP1a-04/Cyo	TM2/TM6b	RK58 balanced; stock was lost
RK073	w-	If/Cyo^	Mkrs/TM6b^	CyO^TM6b balancer chromosomes are a genetic linkage group
RK075	w-	ptcGAL4		patched-GAL4; bloomington
RK076	w-	armGAL4/Cyo	TM2/TM6b	armadillo-GAL4 balanced; bloomington
RK077	w-	armGAL4	HP1c-/TM6b	derived from RK76 and RK61
RK078	w-	Sp/Cyo	daGALl4/TM6b	RK55 balanced
RK079	HP1b-, w-			P-element (G665) insertion in HP1b gene; does not affect CDS; weak hypomorph; bloomington 33261
RK080	w-		actGAL4/TM6b	actin-GAL4; bloomington
RK081	w-	actGAL4/Cyo		actin-GAL4; bloomington
RK082	w-	Sp/Cyo	armGAL4/TM6b	RK56 balanced
RK084	HP1b-, w-		TM2/TM6b	RK79 balanced
RK086	w-	HP1a-04/Cyo^	daGAL4/TM6b^	derived from RK73, RK72 and RK78
RK089	w-	HP1a-04/Cyo^	T[38]86Fb/TM6b^	derived from RK48, RK72 and RK73
RK090	w-	HP1a-04/Cyo^	T[39]86Fb/TM6b^	derived from RK49, RK72 and RK73
RK091	w-	HP1a-04/Cyo^	T[17]86Fb/TM6b^	derived from RK47, RK72 and RK73
RK092	HP1b-, w-		armGAL4/TM6b	derived from RK84 and RK56
RK093	w-	HP1a-05/Cyo^	armGAL4/TM6b^	derived from RK82, RK73 and RK59
RK094	w-	HP1a-04/Cyo^	armGAL4/TM6b^	derived from RK82, RK73 and RK58
RK095	HP1b-, w-		T[18]86Fb	derived from RK50 and RK84; stock was lost
RK096	HP1b-, w-		T[40]86Fb	derived from RK51 and RK84; TM6b is floating
RK097	HP1b-, w-		T[41]86Fb	derived from RK52 and RK84
RK098	w-	T[16]51C	HP1c-/TM6b	derived from RK61 and RK38
RK099	w-	T[42]51C	HP1c-/TM6b	derived from RK61 and RK41
RK100	w-	T[43]51C	HP1c-/TM6b	derived from RK61 and RK44

Stock ID	X chr.	2nd chr.	3rd chr.	Comments
RK101	w-	Z4.RNAi_41		VDRC GD25541; no efficient Z4 kd?; use RK102
RK102	w-		Z4.RNAi_42	VDRC GD25542; Z4 knock-down
RK104	w-		Chro.RNAi_63	VDRC KK101663; Chromator knock-down
RK105	w-		Dsk2.RNAi_47	VDRC GD47447; Dsk2 kd; other line (RK106) was used
RK106	w-	Dsk2.RNAi_48		VDRC GD47448; Dsk2 knock-down
RK107	w-	coilin. RNAi_09		VDRC GD36009; coilin knock-down
RK109	w-		row.RNAi_96	VDRC GD28196; ROW knock-down
RK112	w-		HP1c.RNAi_pWIZ	HP1c hairpin/RNAi; line10-1; Joan Font
RK113	w-		WOC.RNAi_95	VDRC GD20995; WOC knock-down
RK114	w-		P{SUPor-P}blanks[KG00804]/TM3, Sb, Ser	P-element (KG00804) in 5'UTR of Blanks; bloomington 13914; not characterized
RK115	w-		P{GawB}AB1	GAL4 driver for salivary glands; bloomington 1824
RK116	w-		P{Sgs3-GAL4.PD}TP1	GAL4 driver for salivary glands; bloomington 6870
RK117	w-	row'/CyO^	wt/TM6b^	row allele; P-element insertion (SH2172); derived from stock 122119 (bloomington)
RK118	w-	lioGAL4/CyO	TM2/TM6b	RK120 balanced
RK119	w-, Blanks. RNAi_46			VDRC GD22846; Blanks knock-down
RK120	w-	lioGAL4		lioGAL4; bloomington 4669
RK121	w-	HP1a-04/Cyo^	wt/TM6b^	derived from RK72 and RK73
RK123	w-	lioGal4	HP1c-/TM6b	derived from RK118 and RK61
RK124	w-		Jil-1^{Z2}/TM6	Jil-1 null allele; (Wang *et al.*, 2001)
RK125	w-	Sp/Cyo	hhGAL4/TM6b	hedgehogGAL4 balanced
RK126	w-, P{EPgy2}EY22614			P-element (EY22614) insertion next to Dsk2 gene; bloomington 22572

Stock ID	X chr.	2nd chr.	3rd chr.	Comments
RK127	w-	Bre1.RNAi_06/ CyO		VDRC KK108206; Bre1 knock-down
RK128	w-	Bre1.RNAi_06/ CyO^	wt/TM6b^	derived from RK127 and RK73; to distinguish homozygous larvae
RK129	w-		UbcD6.RNAi_29	VDRC GD23229; UbcD6 (=Rad6) knock-down
RK130	w-	H2Av-GFP (Chr?)		GFP tagged histone H2Av; Chromosome unknown; (Clarkson & Saint, 1999)

6.1.5. Stable S2 cell lines

Aliquots of stable *Drosophila* S2 cell lines are frozen in FBS/10% DMSO in liquid nitrogen (box FAM5). All the transfected constructs are based on the *pMK33* vector and thus contain an inducible Mt promoter and a Hygromycin B resistance. See the plasmid lists in chapter 6.1.2 for more details about the transfected constructs.

Name	Transfected construct	Comments
RK2	pRK2 (pMK33_row-TAP)	2 lines a & b; line a used for ROW complex purification
RK3	pRK3 (pMK33_TAP-row)	
RK6	pRK6 (pMK33_woc-TAP)	
RK7	pRK7 (pMK33_TAP-woc)	used for WOC complex purification
RK51	pRK51 (pMK33-WIZ_woc-hairpin)	2 lines a & b
RK53	pRK53 (pMK33-WIZ_HP1b&HP1c-hairpin)	2 lines a & b
RK54	pRK54 (pMK33-WIZ_row-hairpin)	transfected construct might be erroneous
HP1b.RNAi	pMK-WIZ_HP1b-hairpin	2 lines A & B
HP1c.RNAi	pMK-WIZ_HP1c-hairpin	2 lines A & B
GFP.RNAi	pMK-WIZ_GFP-hairpin	2 lines A & B

6.2. Methods

6.2.1. Induction and purification of His-tagged proteins

1. Prepare 4 ml LB cultures of BL21 transformed with the plasmid for expression of the His-tagged protein and add antibiotics (Kanamycin for pET constructs).
2. Inoculate the starter cultures o/n at 37ºC.
3. Dilute the small o/n cultures in 500 ml LB containing antibiotics and inoculate at 37ºC until reaching approximately an OD_{600nm} of 0.7.
4. Take a 1 ml sample of the culture before induction (spin down, dissolve pellet in 100 µl PLB, β-mercaptoethanol).
5. Induce with 0.5-1mM IPTG for 3 hours at 37ºC.
6. Take a sample of the induced culture (analogous to the non-induced sample).
7. Spin down the culture at 8000rpm at 4ºC for 5min (if using 1 liter bottles: at 4000rpm for 20min).
8. Resuspend the bacterial pellet in in 200 ml STE buffer.

   STE buffer:

0.1	M	NaCl
10	mM	Tris-HCl pH8
1	mM	EDTA

9. Distribute the suspension to four 50 ml Falcon tubes and spin down at 4000rpm at 4ºC for 10min. (After this step, the protocol can be interrupted and the pellets be stored at -80ºC)

10. Resuspend each pellet in 25 ml lysis buffer.

Lysis buffer:

0.5	M	NaCl
20	%	Glycerol
20	mM	HEPES pH 7.9
1	mM	EDTA pH 8
0.1	%	NP-40 (Igepal)
20	mM	β-mercaptoethanol (add fresh; 1.4 µl/ml)
1	mM	PMSF (add fresh; 10 µl/ml)
		Leupeptina (add fresh; 1 µl/ml)
		Aprotina (add fresh; 1 µl/ml)

11. Perform sonication at 30% amplitude and do 10 cycles consisting of 20sec ON and 40sec OFF. Keep the samples cold and use an ice-water bath during sonication. Take a sample of the lysate before centrifugation.
12. Spin down at 10000rpm (JA25.50) at 4ºC for 30min. Transfer supernatant into a Falcon and take a sample for analysis. Keep also the pellet. Freeze pellet and supernatant at -80ºC.
13. Analyze the aliquots by coomassie and/or western blotting to determine, whether the His-tagged protein is soluble or insoluble.

Purifaction of insoluble proteins form the pellet

1. Resuspend the pellet in 10 ml guanidium chloride buffer. Resuspend by stirring with a magnet in order to completely dissolve the pellet (can be done o/n at 4ºC).

Guanidium chloride buffer:

6	M	guanidium chloride
20	mM	HEPES pH7,9
100	mM	NaCl
10	mM	β-mercaptoethanol (add fresh; 0,7 µl/ml)

2. Centrifuge at 10000rpm (JA25.50) at 4ºC for 1 hour and recover the supernatant.
3. Prepare a column (Biorad) with 0.5 ml Ni-NTA agarose (Qiagen).
4. Equilibrate the Ni-NTA agarose column with 10 ml guanidium chloride buffer.
5. Add the sample (supernatant) onto the column.
6. Wash with 10 ml guanidium chloride buffer.
7. Wash with 10 ml urea buffer.

Urea buffer:

8	M	Urea
100	mM	KCl
20	mM	HEPES pH7,9
10	mM	β-mercaptoethanol (add fresh; 0,7 µl/ml)

8. Pre-elute with 3 ml urea buffer containing 20mM Imidazol (68.08 g/mol).
9. Elute 5-10 fractions of 1 ml using urea buffer containing 100mM Imidazol.
10. Check aliquots of the elution fractions by SDS-PAGE and coomassie staining.

Purification of soluble proteins from the supernatant

1. Pack a column (Biorad) with 0.5 ml Ni-NTA agarose beads (Qiagen).
2. Equilibrate the Ni-NTA agarose column with 10 ml Lysis Buffer.

3. Load the sample onto the column. (Optionally, the flow-through can be re-loaded a second time, which might increase purification efficiency.)
4. Wash with 10 ml Lysis Buffer.
5. Wash with 5 ml Buffer D.

Buffer D:

20	%	Glycerol
20	mM	Hepes pH 7.9
0.1	M	KCl
0.2	mM	EDTA
0.1	mM	PMSF (add fresh)
0.5	mM	DTT (add fresh)

6. Pre-elute with 3 ml Buffer D + 20mM Imidazol (collect 1 ml fractions PE1-3).
7. Elute with 5 ml Buffer D + 100mM Imidazol (collect 1 ml fractions E1-5).
8. Elute with 5 ml Buffer D + 500mM Imidazol (collect 1 ml fractions E6-10).
9. Check aliquots of the elution fractions by SDS-PAGE and coomassie staining.

6.2.2. Induction and purification of GST-tagged proteins

1. Inoculate 4 ml LB cultures of BL21 transformed with the GST fusion encoding plasmid o/n at 37ºC in the presence of antibiotics.

2. Dilute the o/n cultures in 500 ml LB containing antibiotics and grow at 37ºC to an OD_{600nm} of 0.7.
3. Induce with 0.5 mM IPTG and incubate at 30ºC for 3-5 hours
4. Spin down the cells at 4000rpm at 4ºC for 30min.
5. Dissolve the pellet in 40 ml PBS and transfer it to a 50 ml Falcon tube and spin down at 4000rpm at 4ºC for 10min. (The pellet resulting from this step can be frozen at -80ºC until going on with the next step.)
6. Resuspend the pellet in 10 ml ice-cold NETN, 1mM PMSF, 10 µg/ml Leupeptin.

   NETN buffer:

20	mM	Tris-HCl pH8
100	mM	NaCl
1	mM	EDTA
0.5	%	NP-40 (Igepal)

7. Sonicate in an ice-water bath at 30% amplitude doing 6 cylces of 30sec ON / 30sec OFF.
8. Centrifuge at 10000rpm at 4ºC for 15min. Keep both the supernatant and the pellet.
9. Reextract the pellet with 10 ml ice-cold NETN, 2% N-Lauroyl-Sarcosine, 1mM PMSF, 10 µg/ml Leupeptin. Sonicate with the same settings as before, but only doing 4 cycles.
10. Centrifuge at 10000rpm at 4ºC for 10min. Take the supernatant and pool it with the previous one. This extract might be stored at -80ºC.
11. Transfer the extract to a column (Binding and washing steps can also be done in a Falcon, as columns tend to get clogged.) with 0.5 ml Glutathione sepharose, which was previously equilibrated with NETN.
12. Rotate on the wheel at 4ºC for 30min.

13. Wash 2 times with 10 ml NETN, 0.7M NaCl and 2 times with 10 ml NETN.
14. Wash once with 10 ml ice-cold TST, 5 mM DTT.

TST buffer:

50	mM	Tris-HCl pH8
150	mM	NaCl
0.1	%	Triton X-100

15. Resuspend the sepharose with 1 bed volume TST, 1mM DTT, 20mM GSH reduced and vortex shortly.
16. Leave 2min on ice, then vortex. Repeat this procedure once more.
17. Elute the column and keep the elution (E1).
18. Resuspend the sepharose with 1 bed volume TST, 1mM DTT, 20mM GSH reduced and repeat the elution steps in total 4-5 times (E2-E5). Freeze the eluted fractions.
19. Check eluted samples by SDS-PAGE and coomassie staining. (Load 5 µl of each elution sample.)
20. Pool the highly concentrated elution samples and dialyze against dialysis buffer at 4ºC while stirring. Use 2 liters of dialysis buffer and replace it 2 times. The first two dialysis steps are done for 1 hour the last one o/n.

Dialysis buffer:

20	mM	HEPES pH 7.9
20	%	Glycerol
0.2	mM	EDTA
0.1	M	NaCl
0.1	mM	PMSF (add fresh)
0.5	mM	DTT (add fresh)

6.2.3. Immunostainings of polytene chromosomes

Preparation of polytene chromosomes

1. Dissect salivary glands from third instar larvae in Cohen Buffer. The larvae should stay in Cohen Buffer during 8-10min. Prepare glands from approximately 5 larvae per preparation.

   Cohen buffer:

10	mM	$MgCl_2$
25	mM	Sodium Glycerol 3P (pH7)
3	mM	$CaCl_2$
10	mM	KH_2PO_4
0.5	%	NP-40 (Igepal)
30	mM	KCl
160	mM	Saccharose

2. Remove the buffer and add 100 µl Fixing Solution 1 to the glands, incubate them during 2min.

   Fixing solution 1:

250	µl	10xPBS
50	µl	Formaldehyde 37%
2.2	ml	H_2O

3. Exchange solution with 100 µl Fixing solution 2. Also put a drop of 14 µl Fixing solution 2 onto a silanized coverslip, where the glands are transferred to during the incubation time of 2-3min.

Fixing solution 2:

1.125	ml	Acetic acid
50	µl	Formaldehyde 37%
1.325	ml	H_2O

4. Collect the coverslip containing the glands with a slide.
5. Knock repeatedly onto the coverslip using a stick, while holding the coverslip on one side to avoid moving.
6. Put a Kleenex onto the top of the inversed slide (coverslip downwards) and press relatively strong using the thumb (taking care not to move around the coverslip).
7. Hold the preparation into liquid nitrogen until it is frozen (noise stops).
8. Carefully remove the coverslip using a razorblade.
9. Store the preparation in a slide container containing PBS at 4ºC up to 4 hours before starting the immunostaining.
10. For longer storage (up to 3 weeks), the preparations might be kept in Methanol at 4ºC (seal with parafilm). However, storage in Methanol should be avoided, as it can affect the performance of some antibodies.

Immunostainings

1. Wash the slides 3 times for 5min with PBS, 0.05% Tween, incubating on the shaker.
2. Block 2 times 20min in PBS, 0.05% Tween, 2% BSA.
3. Prepare box with wet paper (to keep it humid) and the dilutions of the primary antibodies (25 µl per slide) in the blocking solution (PBS, 0.05% Tween, 2% BSA).
4. Put the antibody dilution onto the polytene preparation and put a coverslip avoiding bubbles.

5. Incubate in the humid box, first 1 hour at room temperature and then o/n at 4ºC.
6. Wash 3 times for 5min with PBS, 0.05% Tween.
7. Dilute the secondary antibodies 400 times in PBS, 0.05% Tween.
8. Put 25 µl of the dilution containing the secondary antibodies, put a coverslip and incubate it in the humid box for 1 hour at RT.
9. Wash 3 times for 10min with PBS, 0.05% Tween.
10. Wash once for 5min with PBS.
11. Mount with 20 µl DAPI-MOWIOL. Add DAPI-MOWIOL with a cut tip and put a coverslip that was cleaned with ethanol.

    DAPI-MOWIOL (keep at -20ºC):

100	µl	DAPI (using a 2ng/µl dilution)
1	ml	MOWIOL

12. Let the slides dry in the dark for 15min (e.g. in the drawer).
13. After drying put them into a slide storage box and keep them at 4ºC.
14. Analyze the staining by fluorescence microscopy.

6.2.4. Histone peptide pull-down

This *in vitro* binding assay was used to study the interactions with H3K9me3 and H2Bub1. The H3 peptides were purchased from Millipore, correspond to amino acids 1-21 of histone H3 and are C-terminally biotinylated. H3K9 was either tri-methylated (Millipore, 12-568) or unmodified (Millipore, 12-403). The H2B peptides were custom-made by UbiQ (www.ubiqbio.com), correspond to amino acids 104-124 of *Drosophila* histone H2B and are N-terminally

biotinylated. H2B was either biotinylated at K118 (UbiQ-PEP2006) or unmodified (UbiQ-PEP2007).

1. Set up the following pull-down mix in eppendorf tubes and incubate o/n on the wheel at 4ºC.

   Peptide pull-down mix:

2	µg	GST fusion
2.5	µl	Biotinylated Histone peptide (using a 100 µM stock)
50	µl	Streptavidin sepharose (as 50% slurry in binding buffer)
500	µl	Peptide pull-down buffer

   Peptide pull-down buffer:

   (100mM and 300mM NaCl was used for H2Bub1 and H3K9me3 binding studies, respectively.)

100/300	mM	NaCl
50	mM	Tris-HCl pH8
0.1	%	NP-40 (Igepal)
1	mM	DTT (add fresh)
		Protease Inhibitor cocktail (add fresh)

2. Keep the samples always on ice/4ºC until the elution step.
3. Spin down the pull-down samples at 2000rpm at 4ºC for 2min and remove the supernatant.
4. Add 1 ml Peptide binding buffer and invert the tubes 10 times before spinning down as above.
5. Repeat the previous washing step 3 times in total.
6. Elute the beads by adding 2xPLB, β-mercaptoethanol (e.g. with 50 µl), then vortex and boil the samples.

7. Spin down at 13000rpm for 1min and load the supernatant onto an acrylamide gel together with a 1% (20ng) input sample of the GST fusion used.
8. Analyze the results by western using an anti-GST antibody.

6.2.5. Cellular fractionation

This protocol is derived and slightly modified from Wysocka et al. (Wysocka *et al.*, 2001).

1. Collect S2 cells (from 1-5 ml culture) and spin them down at 1000g for 5min.
2. Wash the pellet 2 times with PBS and spin down at 1000g at 4ºC for 5min.
3. Resuspend the pellet in 200 µl Buffer A.

   Buffer A:

10	mM	HEPES pH7,9
10	mM	KCl
1.5	mM	$MgCl_2$
0.34	M	Saccharose
10	%	Glycerol
1	mM	DTT (add fresh)
		Protease Inhibitor cocktail (add fresh)

4. Add TritonX-100 to a final concentration of 0.1% and mix gently.
5. Incubate on ice for 8min.
6. Centrifuge at 1300g at 4ºC for 5min and then separate the supernatant (S1) from the pellet (P1).

7. Clarify the supernatant S1 by centrifugation at full-speed (16100g) at 4ºC for 10min. The resulting supernatant **(S2)** is the **soluble cytosolic fraction**. Discard the pellet (P2).
8. Wash the pellet P1 once with Buffer A.
9. Resuspend the washed pellet in 200 µl Buffer B and lyse it on the wheel at 4ºC for 30min.

   Buffer B:

10	mM	HEPES pH7,9
3	mM	EDTA
0.2	mM	EGTA
1	mM	DTT (add fresh)
		Protease Inhibitor cocktail (add fresh)

10. Centrifuge at 1700g at 4ºC for 5min and then separate the supernatant **(S3)**, which is the **soluble nuclear fraction**, from the pellet (P3).
11. Wash the pellet P3 once with Buffer B and resuspend the washed pellet **(P4)**, the **chromatin fraction**, in loading buffer and boil it.
12. Analyze the different fractions by western blotting.

6.2.6. Histone acid extraction

1. Collect 5 ml of S2 cells and spin down at 300g at 4ºC for 5min.
2. Wash the pellet two times with PBS and spin down as before.
3. Resuspend the pellet in 1 ml Buffer A.

Buffer A:

0.23	M	Saccharose
60	mM	KCl
15	mM	NaCl
0.25	mM	$MgCl_2$
0.15	mM	Spermine
0.5	mM	Spermidine
15	mM	Tris pH 7.4
14	mM	β-mercaptoethanol (0.95 µl/ml; add fresh)
0.2	mM	PMSF (add fresh)

4. Lyse the cells using the dounce (loose=A pestle) by doing 40 strokes.
5. Pass the lysate into an eppendorf tube and centrifuge at 3300g at 4ºC for 15min.
6. Resuspend the pellet in 500 µl Buffer A and centrifuge at 13000rpm at 4ºC for 5min.
7. Resuspend the pellet in 500 µl 0.25N HCl (25% HCl solution is 7.68N) and incubate it o/n on the wheel at 4ºC.
8. Centrifuge at 13000rpm at 4ºC for 10min.
9. Take the supernatant (containing the histones) and split it into two aliquots of 250 µl.
10. Add 1.250 ml ice-cold (stored at -20ºC) Acetone-0.1N HCl to each aliquot.
11. Slightly shake the tubes and leave them on dry ice for 30min.
12. Centrifuge at 13000rpm at 4ºC for 10min.
13. Remove the supernatant using the pipette to avoid losing the pellet.
14. Add 1 ml ice-cold Acetone-0.1N HCl to the pellet, shake slightly and leave the tubes another 30min on dry ice.
15. Centrifuge at 13000rpm at 4ºC for 10min.
16. Remove the supernatant with a pipette and add 1 ml Acetone.

17. Slightly shake the tubes and centrifuge them at 13000rpm at 4ºC for 10min.
18. Remove the supernatant with a pipette and add 1 ml Acetone.
19. Slightly shake the tubes and centrifuge them at 13000rpm at 4ºC for 10min.
20. Remove as much of the supernatant as possible and let the pellet dry at RT for up to 30min.
21. Resuspend the pellet with 100 µl PLB, β-mercaptoethanol and vortex well and boil the sample (the pellet does not resuspend easily).
22. Analyze the extract by western blotting or store at -20ºC until it will be used.

6.2.7. RNAi in S2 cells by long double-stranded RNA

Preparation of double-stranded RNA

Use the MEGAscript T7 Transcription Kit (ambion) and RNeasy Mini Kit (QIAGEN) for RNA production and purification, respectively.

1. Set up the MEGAscript reaction mix.

   Reaction mix (total 20 µl):

8	µl	NTP's (2 µl of each)
2	µl	10X Buffer
2	µl	Enzyme mix
4	µl	PCR product flanked with T7
4	µl	H_2O (RNAse free)

2. Incubate at 37ºC overnight (incubation time can be reduced, according to handbook 2-4 hours).

3. DNase treatment is optional, as the amount of DNA will be very low compared to RNA. Add 1 µl TURBO DNase and incubate 15min at 37ºC.
4. Increase the volume to 100 µl with RNase free H_2O.
5. Add 350 µl Buffer RLT and mix well.
6. Add 250 µl 100% ethanol and mix by pipetting.
7. Transfer the sample (700 µl) to an RNeasy mini column and spin down for 15sec at full-speed. Discard the flow-through.
8. Add 500 µl Buffer RPE to the column and spin down 15sec at full-speed. Discard the flow-through.
9. Add another 500 µl Buffer RPE and spin down as before and discard the flow-through.
10. Spin down 1min at full-speed without any buffer to eliminate possible carryover of buffer RPE.
11. Place the column into a fresh collection tube and add 60 µl RNase free H_2O to the column membrane. Spin down 1min at full-speed to elute the RNA.
12. Do a second elution with 60 µl RNAse free H_2O, resulting in 120 µl total elution sample.
13. Quantify the RNA concentration by nanodrop. In addition, an aliquot might also be checked on an agarose gel.
14. Store the dsRNA samples at -20ºC.

dsRNA treatment of S2 cells

- Day 0: Dilute S2 cells to 10^6/ml (in complete media) and add 4 µg dsRNA per 10^6 cells. Gently shake the flasks and then incubate for 3 days.
- Day 3: Count the cells and dilute again to 10^6/ml and add 4 µg dsRNA per 10^6 cells. Gently shake the flask and then incubate for another 3 days.

- Day 6: Collect the cells and continue with the downstream experiment.

6.2.8. Transfection of S2 cells

The amounts given are for transfection of 3x10^6 cells in a 5 ml dish. Scale up if replicates or more cells are required.

1. Dilute S2 cells to 0.6x10^6 in complete medium and distribute to a 5 ml culture dish. Incubate overnight before starting the transfection.
2. Prepare 24 µg of the plasmid DNA (use maxi prep) to be transfected as a 0.4 µg/µl dilution in 60 µl H_20.
3. Add 480 µl 0.25M $CaCl_2$ to the DNA dilution.
4. Prepare a 480 µl aliquot of 2x HEBS in a 15 ml Falcon tube.
5. Mix DNA/$CaCl_2$ with pipette/vortex and add dropwise (using the 200 µl tips) to the HEBS aliquot in the Falcon, while vortexing at low intensity (level 1-2).
6. Leave 35min at RT (25ºC)
7. Mix the precipitates with the pipette and add 850 µl dropwise onto the cells. Gently shake the flask to distribute evenly. Follow with the previous step for transient transfection or skip to step 10 for Hygromycin B selection of stably transfected cells.
8. Incubate the cells for 2 days.
9. Collect the cells and continue with the downstream experiment.

Selection of stably transfected cell lines (continuation of step 7):

10. Incubate the transfected cells for 1 day.
11. Remove the calcium phosphate solution. Therefore, wash 2 times with 5 ml complete medium and spin down at 100g for 5min.

12. Resuspend the cells in 5 ml complete medium (in the absence of selective agent), distribute them to a fresh flask and incubate for 2 days.
13. Pellet the cells by centrifugation at 100g for 5min and resuspend in Hygromycin B containing medium (in the absence of Pen/Strep). Use 300 µg Hygromycin B per 1 ml medium.
14. Exchange with fresh Hygromycin B containing medium in intervals of 4-5 days until resistant colonies appear.
15. Maintain cell lines under enduring Hygromycin B selection, in order to avoid loss of the construct.

6.2.9. RNA extraction from S2 cells

This is a combined protocol for RNA extraction using Trizol and the RNeasy Mini Kit (QIAGEN).

1. Pellet the cells by centrifuging at 2000g for 5min. (use S2 cells from 1-5 ml medium per sample).
2. Dissolve the pellet (do not wash with PBS) in 500 µl Trizol by pipetting and transfer to a 2 ml tube.
3. Incubate 5min at RT.
4. Add 100 µl chloroform, vortex well and incubate for 5min at RT.
5. Centrifuge at full-speed at 4ºC for 15min and transfer 250 µl of the aqueous (upper) phase to a 2 ml tube (avoid touching the interphase).
6. Add 875 µl RLT buffer and briefly vortex.
7. Add 625 µl 100% ethanol and briefly vortex.

8. Load 700 µl onto an RNeasy column, centrifuge at full-speed at RT for 30sec. Discard the flow-through and repeat the loading step until the entire sample is loaded.
9. Add 350 µl RW1 buffer and spin the column at full-speed for 30sec to wash the column.
10. Prepare DNase mix consisting of 10 µl DNase I stock solution and 70 µl RDD buffer (QIAGEN).
11. Add the DNase mix (80 µl) onto the membrane of the column and incubate at RT for 15min.
12. Add 350 µl RW1 buffer and spin down at full-speed for 30sec.
13. Add 500 µl RPE buffer and spin down at full-speed for 30sec. Repeat this washing step once more.
14. Do an additional spin down step without buffer to remove possible carry-over of RPE buffer.
15. Place the column into a new collection tube and add 30 µl of RNase-free water.
16. Do a second elution with another 30 µl of RNase-free water.
17. Aliquot the eluted RNA (to avoid later thawing and freezing cycles) and freeze them at -20ºC. Also take a small aliquot for measuring RNA concentration at nanodrop.

6.2.10. RT-qPCR

Retro-transcription of mRNA into cDNA:

Use Transcriptor First Strand cDNA Synthesis Kit (Roche).

Use PCR tubes and PCR machine for incubating the reactions.

1. Dilute the RNA extract to 0.1 µg/µl in RNase-free water (see chapter 6.2.9 for the RNA extraction protocol).
2. Set up the following mix:
   (The amounts in parentheses are for a 10 µl genomic control reaction.)

10 (5)	µl	RNA [0.1 µg/µl]
1 (0.5)	µl	oligo $(dT)_{18}$
2 (1.25)	µl	RNAse-free H_2O

3. Incubate at 65ºC for 10min.
4. Add the following components in this order:

4 (2)	µl	5x Reaction Buffer
0.5 (0.25)	µl	Protector RNase Inhibitor
2 (1)	µl	dNTPs
0.5 (0)	µl	Transcriptor RT

5. Mix gently (do not vortex) and incubate using the following programme:
   - 50ºC for 1 hour
   - 85ºC for 5min
   - pause at 4ºC

6. Dilute the products of the retro-transcription and the genomic control 11x in H_2O (This corresponds to a 4.55 ng/µl dilution with respect to the RNA used for retro-transcription).
7. Store the samples at -20ºC or continue directly with qPCR.

qPCR

The qPCR is performed using 96 well plates and a Light Cycler 480 machine (Roche). Relative expression levels are calculated using the

standard curve method and normalization is done relative to *alphaTubulin84B* levels.

1. Prepare oligo/SYBR Green master mixes (given are the amounts required per 10 µl reaction.

0.3	µl	fw primer [10 µM]
0.3	µl	rv primer [10 µM]
5	µl	2X SYBR Green I Master (Roche)

2. Set up 10 µl PCR reactions in a 96 well plate. Apart from the cDNA include genomic DNA and non-template (H_2O) controls. Use the 11X dilutions of the RT products. The amount per well corresponds to 20 ng of initial RNA starting material.

5.6	µl	oligo/SYBR Green master mix
4.4	µl	template (cDNA or controls)

3. The following standard PCR program is used:

   5min at 95ºC

   45 cycles:

   10sec at 95ºC

   10sec at 60ºC

   10sec at 72ºC

6.2.11. Co-immunoprecipitation

Two different variations for performing CoIP experiments with material from S2 cells are described, either using a total protein extract or a soluble nuclear extract.

Preparation of total extract

1. Collect confluent S2 cells from 500 ml of medium and wash the pellet once with PBS.
2. Dissolve the washed pellet in 10 ml Lysis Buffer.

   Lysis Buffer:

50	mM	Tris-HCl pH8
250	mM	NaCl
5	mM	EDTA
0.5	%	NP-40 (Igepal)
		Protease Inhibitor cocktail (add fresh)

3. Incubate on the wheel at 4ºC for 30min.
4. Spin down at 15'000rpm (rotor JA25.50) at 4ºC for 20min.
5. Make aliquots (e.g. 500 µl) of the supernatant (soluble extract) and store them at -80ºC.

Preparation of nuclear extract

1. Collect confluent S2 cells from 500 ml of medium and wash the pellet once with PBS.
2. Dissolve the pellet in Buffer A, using 3 times the pellet volume. Prepare Buffer A as 2x concentrated and take the volume of the pellet into account, in order to reach a final Buffer concentration of 1x.

2xBuffer A:

0.46	M	Sacarose
120	mM	KCl
30	mM	NaCl
0.5	mM	MgCl2
1	mM	Spermine
0.3	mM	Spermidine
30	mM	Tris pH7.4
28	mM	β-mercaptoethanol (0.95 µl/ml; add fresh)
		Protease Inhibitor cocktail (add fresh)

3. Lyse the cells doing 40 strokes using the L (=A) pestle.
4. Spin down at 5500 rpm (rotor JA25.50) at 4ºC for 15min. Then, discard the supernatant.
5. Wash the pellet once with 1x Buffer A.
6. Resuspend the pellet in 2 pellet volumes 1x Buffer B.

1xBuffer B:

20	mM	Hepes-KOH pH7.9
20	%	Glycerol
300	mM	NaCl
1.5	mM	MgCl2
0.5	mM	EDTA
0.5	mM	DTT (add fresh)
		Protease Inhibitor cocktail (add fresh)

7. Do 35-40 strokes with the S (=B) pestle.
8. Add 0.1% NP-40 to the extract and incubate it on the wheel at 4ºC for 15min.
9. Spin down at 15’000rpm at 4ºC for 30min.

10. Make aliquots of the supernatant (soluble nuclear extract) and store them at -80ºC.

Immunoprecipitation

1. Set up the IP samples containing the protein extract, the antibody and binding buffer in Eppendorf tubes. Use the same buffer for binding as the extract is in: Lysis Buffer for total extract and 1x Buffer B for nuclear extract, respectively. Depending on the proteins studied, the amount of extract used might be in- or decreased. Larger quantities of antibody might be used, if it is of low IP efficiency. Include a negative (unrelated antibody) and a positive (whenever possible) IP sample.

   IP mix:

100	µl	protein extract
1	µl	antibody
400	µl	binding buffer

2. Incubate the IP samples on the wheel at 4ºC for 2 hours or up to o/n.
3. Add 50 µl Protein A sepharose or Protein G agarose (depending on the species and the Ig subclass of the antibody used) as a suspension in binding buffer. (Perform spin downs of Protein A/G beads at low speed 2000-3000rpm).
4. Incubate on the wheel at 4ºC for 2 hours.
5. Wash the beads 3 times with 1 ml binding buffer. Wash by inverting the tubes 10 times and then spin down at 2000rpm for 2min at 4ºC.
6. Add the desired elution volume of 2xPLB, β-mercaptoethanol to the washed beads. Vortex and boil the samples, then spin down and analyze the supernatant by western blotting for the interaction of interest. Also load a 1-5% input sample of the extract used for the IP samples.

6.2.12. Chromatin-immunoprecipitation in S2 cells

Preparation of chromatin

1. Use confluent S2 cells from 2 or 4 large (25 ml) flasks. (Depending on the antibody that will be used, more/less starting material might be used.)
2. Combine the cells from two flasks in one and crosslink by adding 1.8% Formaldehyde directly to the media. Crosslink during 10min at RT on the shaker.
3. Stop the reaction by adding glycine to a final concentration of 0.125M using a stock solution of 1.25M in 1xPBS.
4. Transfer the cross-linked cells into 50 ml tubes and centrifuge at 1500g at 4ºC for 3min.
5. Resuspend each pellet with 5 ml PBS and pool the suspensions in one tube (independently from using 2 or 4 flasks as starting material; if using more than 4 flasks, scale up), spin down as before.
6. Resuspend the pellet in 10 ml ChIP wash A buffer and transfer the suspension into a 15 ml tube.

   ChIP wash A buffer:

10	mM	Hepes pH7.9
10	mM	EDTA
0.5	mM	EGTA
0.25	%	Triton X100

7. Incubate 10min on the wheel at 4ºC, then spin down at 1500g at 4ºC for 3min.
8. Resuspend in 10 ml ChIP wash B buffer and incubate 10min on the wheel at 4ºC, then spin down as before.

ChIP wash B buffer:

10	mM	Hepes pH7.9
100	mM	NaCl
1	mM	EDTA
0.5	mM	EGTA
0.01	%	Triton X100

9. Add 4.5 ml TE and resuspend using the pipette.
10. Add 0.5 ml 10% SDS, invert the tube 5 times and spin down at 1500g at 4ºC for 3min.
11. Carefully remove the upper phase with a pipette (The 2 phases might not be easily distinguishable). Add 5 ml TE and invert 5 times, spin down.
12. Remove the upper phase and add another 5 ml TE, invert 5 times, spin down at 1500g at 4ºC for 3min.
13. After removing the upper phase, add TE, 1mM PMSF to obtain a final volume of 4 ml. Add 40 µl 10% SDS.
14. Aliquot into two 2 ml aliquots in 15 ml Falcons that will be used for doing the sonication (Bioruptor).
15. Do sonication cycles of 30sec ON / 30sec OFF. Do 2 sessions of 10min and then 1 session of 5min (the times include the OFF state). Before and in between the sessions cool down the water bath. Therefore remove water until 0.5-1.0 cm below the optimal level and replace with ice.
16. Combine the lysates in one tube and add the following solutions in this order and between each addition incubate it on the wheel at 4ºC for 2min.
    - 10% Triton X100, finally at 1% (add 0.42 ml)
    - 10% DOC (Deoxycholate), finally 0.1% (add 42 µl)
    - 4M NaCl, finally 140mM (add 150 µl)

17. Incubate it on the wheel at 4ºC for 10min, then aliquot into 4 Eppendorf tubes.
18. Spin down at full-speed at 4ºC for 5min. Pool the supernatants and then make 0.5 ml aliquots in eppendorf tubes and freeze them at -80ºC (Smaller aliquots might be used for ChIP-qPCR, if the antibody immunoprecipitates efficiently). To check the size of the sonicated DNA a 100 µl sample should be spared.

Checking DNA fragment size of the sonicated chromatin

1. Add 1% SDS (final conc.) and 0.1M $NaHCO_3$ (final conc.) to the 100 µl chromatin aliquot in a total volume of 300 µl.
2. Leave it o/n at 65ºC in order to de-crosslink.
3. Add 300 µl Phenol/Chloroform, vortex and spin down at full-speed for 3min.
4. Take 270 µl of the upper phase, add 30 µl 3M Na-Acetate and 700 µl ice-cold 100% ethanol.
5. Put to -80ºC for 10min.
6. Spin down at full-speed at 4ºC for 10min.
7. Wash with 70% ice-cold ethanol and spin down at full-speed at 4ºC for 5min.
8. Remove the supernatant, let the pellet dry and dissolve it in 10 µl milliQ.
9. Add 0.5 µl RNAse A and incubate at 37ºC for 20-30min.
10. Analyze the DNA on a 1% agarose gel.

Chromatin IP

1. Add 30 µl Protein A sepharose (PAS) as a 50% suspension in RIPA to 500 µl of cross-linked chromatin (if smaller aliquots were done, increase volume to 500 µl by adding RIPA).

RIPA buffer (-PMSF):

140	mM	NaCl
10	mM	Tris-HCl pH8
1	mM	EDTA
1	%	Triton X100
0.1	%	SDS
0.1	%	DOC (Deoxycholate)

2. Incubate on the wheel at 4ºC for 1h.
3. Spin down at 3000rpm at 4ºC for 2min. Transfer the supernatant (pre-cleared chromatin) to a fresh tube.
4. Add the antibody (use a similar amount as for standard CoIP; for most antibodies 1-5 µl) and incubate it o/n at 4ºC on the wheel.
5. Add 40 µl of PAS suspension and incubate it on the wheel at 4ºC for 3h.
6. Perform washing steps of 5min on the wheel at 4ºC using 1 ml (in between washes spin down at 3000rpm at 4ºC for 2min):
    - 5 times with RIPA.
    - 1 time with LiCl ChIP buffer.
    - 2 times with TE buffer.

LiCl ChIP buffer:

250	mM	LiCl
10	mM	Tris-HCl pH8
1	mM	EDTA
0.5	%	NP-40
0.5	%	DOC (Deoxycholate)

Elution

1. Do not forget to prepare an input sample (using 50 µl cross-linked chromatin) together with the elution of the ChIP samples and treating it the same way.
2. Add 40 µl TE and 0.5 µl RNAse A to the washed beads.
3. Incubate it at 37ºC for 30min.
4. Add 50 µl 0.2M $NaHCO_3$ and 10 µl 10% SDS and vortex for 30sec.
5. Spin down at full-speed for 30sec.
6. Collect the supernatant (100 µl).
7. Add 100 µl elution buffer (1% SDS, 0.1M $NaHCO_3$) and vortex for 30sec.
8. Spin down at full-speed for 30sec.
9. Collect the supernatant and repeat the previous elution step to have a final volume of 300 µl (pool the 3 elutions).
10. Incubate it o/n at 65ºC in order to de-crosslink.
11. Add 3 µl Proteinase K and incubate at 55ºC for 3h.
12. Add 300 µl phenol-chloroform, vortex for 30sec and spin down at full-speed at RT for 5min.
13. Collect 270 µl of the supernatant into a fresh tube, add 2 µl pellet paint, 30 µl 3M Na-acetate and 700 µl 100% ethanol. Precipitate o/n at -20ºC.
14. Spin down at full-speed at 4ºC for 15min.
15. Wash the pellet with 500 µl ice-cold 70% ethanol and spin down at full-speed at 4ºC for 10min.
16. Remove the supernatant and dry the pellet and dissolve it in 25-50 µl milliQ.
17. If the samples are analyzed by qPCR use 1% of the total elution per PCR reaction. The enrichment in ChIP is calculated with respect to an input sample. qPCR is performed as described in protocol 6.2.10.

18. For ChIP-seq, 10 ng of DNA, quantified by Qubit dsDNA HS Assay Kit (Invitrogen) are used for library preparation. End-repair, adenylation, ligation of adapters and PCR enrichment for 18 cycles is performed using TruSeqRNA Sample Prep Kit (Illumina) according to manufacturer's recommendations. Purified libraries are quantified by Qubit dsDNA HS Assay Kit (Invitrogen) and size distribution is evaluated using Bioanalyzer DNA 1000 assay (Agilent). Single-end sequencing of 50 nucleotides is performed on the Genome Analyzer IIx.

6.2.13. Protein complex purification

Preparation of the BSA/dynabeads and IgG/dynabeads

1. Resuspend 40 mg Dynabeads M-270 Epoxy (Invitrogen) in 3 ml 0.1M Na-Phosphate pH7.4 Buffer in a 15 ml Falcon.
2. Vortex for 30sec and distribute into two Eppendorf tubes.
3. Put onto the wheel for 10min, then 2min on the magnet. Discard the buffer.
4. Wash the beads with 0.1M Na-phosphate pH7.4 buffer, vortex, put 2min on the magnet and discard the buffer.
5. Repeat the previous washing step.
6. Incubate one of the tubes containing the washed beads with whole rabbit IgG (Pierce) and the other tube with BSA. Add the components in the following order:

IgG/dynabeads and BSA/dynabeads mixes:

20	mg	washed dynabeads
567	µl	0.2M Na-phosphate pH7.4
100	µl	IgGs (10 µg/µl) OR BSA (10 mg/ml)
333	µl	3M $NH_3(SO_4)_2$

7. Vortex and incubate on the wheel for 1-3 days.
8. Wash 3 times with PBS, 0.5% BSA.
9. Wash once with PBS.
10. Wash once with PBS, 0.5% Triton X-100, 0.5% Tween-20.
11. Wash once with PBS.
12. Store at for 4ºC in PBS containing 0.02% sodium azide (NaN_3) until starting the purification.

Extraction & Purification

1. For one purification experiment, a stable S2 cell line for expression of the bait protein (TAP-tagged) is expanded to 2-3 liters of medium.
2. Induce the metallothionein (Mt) promoter with 0.15 mM $CuSO_4$.
3. After o/n induction, collect the cells, wash the pellet once with PBS and transfer it to 50 ml tube. Store the pellet at -80ºC, while checking a small aliquot for efficient induction of the bait protein by western.
4. Dissolve the pellet in Buffer A, using 3 times the pellet volume. Prepare Buffer A as 2x concentrated and take the volume of the pellet into account, in order to reach a final Buffer concentration of 1x.

2x Buffer A:

0.46	M	Sacarose
120	mM	KCl
30	mM	NaCl
0.5	mM	MgCl2
1	mM	Spermine
0.3	mM	Spermidine
30	mM	Tris-HCl pH7.4
28	mM	β-mercaptoethanol (0.95 µl/ml; add fresh)
		Protease Inhibitor cocktail (add fresh)

5. Lyse the cells doing 40 strokes using the L (=A) pestle.
6. Spin down at 5500rpm (rotor JA25.50) at 4ºC for 15min. Then, discard the supernatant.
7. Wash the pellet once with 1x Buffer A.
8. Resuspend the pellet in 2 pellet volumes 1x Buffer B.
   (important: The TAP tag contains a CBP (calmodulin binding peptide) that, in this protocol, is not used for the purification. Therefore, EGTA (instead of EDTA), a calcium chelator, is used in all the buffers to avoid binding of contaminants to the CBP.)

   1x Buffer B:

20	mM	Hepes-KOH pH7.9
20	%	Glycerol
300	mM	NaCl
1.5	mM	MgCl2
0.5	mM	EGTA
0.5	mM	DTT (add fresh)
		Protease Inhibitor cocktail (add fresh)

9. Do 35-40 strokes with the S (=B) pestle.

10. Add 0.1% NP-40 to the extract and incubate it on the wheel at 4ºC for 15min.
11. Spin down at 15'000rpm at 4ºC for 30min. The resulting supernatant is the soluble nuclear extract.
12. Add the soluble nuclear extract to the BSA/dynabeads that were washed previously with 1x Buffer B.
13. Incubate for 1 hour on the wheel at 4ºC.
14. Remove the pre-cleared extract from the beads and add it to equilibrated (with 1x Buffer B) IgG/dynabeads.
15. Incubate on the wheel at 4ºC for 4 hours.
16. Use a 15 ml Falcon tube for performing the washing steps.
17. Wash the beads with 13 ml Wash Buffer and do totally 8 cycles of washing. After each washing step leave it on the wheel for 5min. (Note: If the complex will be sent to mass spec in solution, include wash steps to remove NP-40. For doing elution by TEV protease, modify the wash buffer for the last few washing steps, using 0.5 mM EDTA (instead of EGTA) and 1mM DTT.)

    1x Wash Buffer:

20	mM	HEPES pH7.9
20	%	Glycerol
0.3	M	NaCl
0.1	%	NP-40
0.5	mM	EGTA
0.5	mM	DTT (add fresh)
		Protease Inhibitor cocktail (add fresh)

18. Transfer the washed beads to an Eppendorf tube.
19. Elute with 50mM glycine, HCl pH3. Therefore, add 30 µl elution buffer to the beads, vortex, leave 2min, put on magnet and collect the elution.

20. Repeat the previous step totally 4 times and pool all the elutions. Take a 12 µl aliquot (10% of total elution) for analysis.
21. Subsequently, perform SDS (2x PLB, β-mercaptoethanol) elution steps to analyze the proteins that remained bound during the acid elution steps. Do 3 elution steps of 40 µl and take a 10% aliquot for analysis.
22. Freeze the samples at -80ºC.

Analysis of the elution samples by silver staining

1. Prepare a large acrylamide gradient gel (9-13%), 0.75 mm thick.
2. Load the 10% aliquots of both elutions. If the PLB buffer turns yellow in the acid elution sample add phosphate buffer pH8 to adjust the pH.
3. Load also an IgG only control sample. Therefore take 5% (of the amount used for the purification) of IgG/dynabeads and elute them with 30 µl PLB, β-mercaptoethanol.
4. Perform a silver staining, as described below.
5. Shake the gel in 50% methanol for at least one hour at RT (can also be done o/n).
6. Remove the methanol, add the staining solution and shake for 15min.

   Staining solution:

   Basic solution

40	ml	milliQ
1.4	ml	ammoniac
190	ul	10M NaOH

   Silver solution

4	ml	milliQ
0.8	g	silver nitrate

- Prepare the two solutions separately and stir with a magnet. Then add the silver solution drop-wise to the other basic solution. The solution can be diluted with milliQ (e.g. 100 ml) if a larger volume is required.

7. Wash the gel with deionized water for 5min with constant exchange of the water.
8. Add the developing solution to the gel and wait until the staining reaches the desired intensity (will take approximately 1min).
9. Remove the developing solution and stop the reaction by adding the stop solution.

Developing solution:

150	ml	milliQ
75	µl	formaldehyde
750	µl	1% citric acid

Stop solution:

80	ml	milliQ
20	ml	acetic acid
100	ml	methanol

Sample preparation for mass spectrometry analysis

1. Prepare an acrylamide gel for running the acid elution sample. Make sure that the entire elution can be loaded into one well. The elution sample might be concentrated by lyophilization.
2. Add PLB, β-mercaptoethanol to the sample. Add also 2 µl 1M phosphate buffer pH8 to adjust the pH and boil.
3. Load the sample and into the neighboring wells load glycine/PLB. Also load a protein ladder, but not right next to the elution sample.

4. Run the sample into the stacking gel, where it gets concentrated. Stop the gel, when the entire sample has just entered (1-2 mm) the main gel (observe the protein ladder).
5. Prepare coomassie staining solution.

   Coomassie staining solution:

   (First dissolve coomassie blue in methanol, before adding the rest.)

0.4	g	C.B. R250
160	ml	methanol
40	ml	acetic acid
200	ml	milliQ

6. Filter the coomassie solution with whatman paper before use.
7. Shake the gel in coomassie solution for 2 hours up to o/n.
8. Destain the gel with 30% ethanol, 10% acetic acid on the shaker.
9. Exchange the destaining solution several times until to remove background staining.
10. The gel is now ready for cutting the concentrated elution of the protein complex and for analysis by mass spectrometry. Meanwhile, the gel can be stored in millQ at 4ºC.

The samples were analyzed with LC/MS by the Proteomics Unit of the Institut de Recerca Vall d'Hebron (Barcelona)

6.2.14. Bioinformatics and Biostatistics analysis

Except where otherwise indicated, all analyses were performed with the Bioconductor software. For analysis of ChIP-seq data, Solexa/Illumina sequencing data for WOC, ROW, dHP1c and dDsk2 were pre-processed

with the standard Illumina pipeline version 1.5.1. Sequence alignment to the *Drosophila melanogaster* genome (UCSC dm3 version) and binding site determination were performed essentially as described in (Lloret-Llinares *et al.*, 2012) setting the coverage difference between IP and the corresponding input sample to 30 reads for WOC and ROW, and 20 reads for dHP1c and dDsk2. ChIP-Seq profiles and binding sites were deposited in the NCBI Gene Expression Omnibus repository (GSE49102). Binding sites were assigned to overlapping and closest genes using the UCSC refflat gene annotations (http://hgdownload.cse.ucsc.edu/goldenPath/dm3/database/refFlat.txt.gz) considering the longest possible transcript for each gene and using the annotatePeakInBatch from the ChIPpeakAnno Bioconductor package for annotation. Distance to overlapping and closest genes was measured from the midpoint of the peak to the gene TSS.

To determine the distribution of ChIP-seq reads around the TSS we plotted the average read coverage using the function plotMeanCoverage in the Bioconductor package htSeqTools (Planet *et al.*, 2012). Peak density around loci of interest was plotted using the PeakLocation function from the htSeqTools package.

When dHP1c abundance at WOC/ROW/dHP1c target genes was compared to abundance at WOC/ROW target and non-target genes, we computed the reads per kilobase per million (RPKM) as $10^6 R/(ML)$, where R is the number of reads mapped to a given gene, M is the total number of reads and L is the distance between TSS and TES in kb.

ChIP-on-chip binding site data for dHP1b, dHP1c and H2Bub1 in S2 cells (modENCODE IDs 941, 3291, 290) was annotated to the *Drosophila melanogaster* reference genome in the same way as ChIP-seq peaks to

assess gene-level overlap. Peak density plots were also produced for the downloaded modENCODE data.

For DNA motif search, summit for the reported peaks were identified with the NucleR package (Flores & Orozco, 2011), and genomic regions 250bp up and downstream of the summit were used to search for overrepresented motifs using the rGADEM package (Li, 2009) and the software default options. Logos for the reported motif sequences were produced with the seqLogo R package version 1.18.0.

7. BIBLIOGRAPHY

Aagaard, L., Laible, G., Selenko, P., Schmid, M., Dorn, R., Schotta, G., Kuhfittig, S., Wolf, a, Lebersorger, a, Singh, P.B., Reuter, G., & Jenuwein, T. (1999) Functional mammalian homologues of the Drosophila PEV-modifier Su(var)3-9 encode centromere-associated proteins which complex with the heterochromatin component M31. *EMBO J.*, **18**, 1923–1938.

Abel, J., Eskeland, R., Raffa, G.D., Kremmer, E., & Imhof, A. (2009) Drosophila HP1c is regulated by an auto-regulatory feedback loop through its binding partner Woc. *PLoS One*, **4**, e5089.

Adam, M., Robert, F., & Larochelle, M. (2001) H2A . Z Is Required for Global Chromatin Integrity and for Recruitment of RNA Polymerase II under Specific Conditions. *Mol. Cell. Biol.*, **21**, 6270–6279.

Adelman, K. & Lis, J.T. (2012) Promoter-proximal pausing of RNA polymerase II: emerging roles in metazoans. *Nat. Rev. Genet.*, **13**, 720–731.

Allis, C.D., Jenuwein, T., Reinberg, D., & Caparros, M.-L. (2007) *Epigenetics*. Cold Spring Harbor Laboratory Press New York.

Arias-Vásquez, A., de Lau, L., Pardo, L., Liu, F., Feng, B.-J., Bertoli-Avella, A., Isaacs, A., Aulchenko, Y., Hofman, A., Oostra, B., Breteler, M., & van Duijn, C. (2007) Relationship of the Ubiquilin 1 gene with Alzheimer's and Parkinson's disease and cognitive function. *Neurosci. Lett.*, **424**, 1–5.

Avvakumov, N., Nourani, A., & Côté, J. (2011) Histone chaperones: modulators of chromatin marks. *Mol. Cell*, **41**, 502–514.

Ayoub, N., Jeyasekharan, A.D., Bernal, J. a, & Venkitaraman, A.R. (2008) HP1-beta mobilization promotes chromatin changes that initiate the DNA damage response. *Nature*, **453**, 682–686.

Ayyanathan, K., Lechner, M.S., Bell, P., Maul, G.G., Schultz, D.C., Yamada, Y., Tanaka, K., Torigoe, K., & Iii, F.J.R. (2003) Regulated recruitment of HP1 to a euchromatic gene induces mitotically heritable , epigenetic gene silencing : a mammalian cell culture model of gene variegation. *Genes Dev.*, **17**, 1855–1869.

Badugu, R., Shareef, M.M., & Kellum, R. (2003) Novel Drosophila heterochromatin protein 1 (HP1)/origin recognition complex-

associated protein (HOAP) repeat motif in HP1/HOAP interactions and chromocenter associations. *J. Biol. Chem.*, **278**, 34491–34498.

Badugu, R., Yoo, Y., Singh, P.B., & Kellum, R. (2005) Mutations in the heterochromatin protein 1 (HP1) hinge domain affect HP1 protein interactions and chromosomal distribution. *Chromosoma*, **113**, 370–384.

Baldeyron, C., Soria, G., Roche, D., Cook, A.J.L., & Almouzni, G. (2011) HP1alpha recruitment to DNA damage by p150CAF-1 promotes homologous recombination repair. *J. Cell Biol.*, **193**, 81–95.

Ball, L.J., Murzina, N. V, Broadhurst, R.W., Raine, a R., Archer, S.J., Stott, F.J., Murzin, a G., Singh, P.B., Domaille, P.J., & Laue, E.D. (1997) Structure of the chromatin binding (chromo) domain from mouse modifier protein 1. *EMBO J.*, **16**, 2473–2481.

Bannister, a J., Zegerman, P., Partridge, J.F., Miska, E. a, Thomas, J.O., Allshire, R.C., & Kouzarides, T. (2001) Selective recognition of methylated lysine 9 on histone H3 by the HP1 chromo domain. *Nature*, **410**, 120–124.

Bannister, A.J. & Kouzarides, T. (2011) Regulation of chromatin by histone modifications. *Cell Res.*, **21**, 381–395.

Batlle, M., Marsellach, F.-X., Huertas, D., & Azorín, F. (2011) Drosophila vigilin, DDP1, localises to the cytoplasm and associates to the rough endoplasmic reticulum. *Biochim. Biophys. Acta*, **1809**, 46–55.

Beisel, C. & Paro, R. (2011) Silencing chromatin: comparing modes and mechanisms. *Nat. Rev. Genet.*, **12**, 123–135.

Belotserkovskaya, R., Oh, S., Bondarenko, V. a, Orphanides, G., Studitsky, V.M., & Reinberg, D. (2003) FACT facilitates transcription-dependent nucleosome alteration. *Science*, **301**, 1090–1093.

Bergink, S., Toussaint, W., Luijsterburg, M.S., Dinant, C., Alekseev, S., Hoeijmakers, J.H.J., Dantuma, N.P., Houtsmuller, A.B., & Vermeulen, W. (2012) Recognition of DNA damage by XPC coincides with disruption of the XPC-RAD23 complex. *J. Cell Biol.*, **196**, 681–688.

Bertram, L., Hiltunen, M., Ph, D., Parkinson, M., Ingelsson, M., Lange, C., Ramasamy, K., Mullin, K., Menon, R., Sampson, A.J., Hsiao, M.Y., Elliott, K.J., Velicelebi, G., Moscarillo, T., Hyman, B.T., Wagner, S.L., Becker, K.D., Blacker, D., Sc, D., & Tanzi, R.E. (2005) Family-Based Association between Alzheimer's Disease and Variants in UBQLN1. *N. Engl. J. Med.*, **352**, 884–894.

Black, J.C., Van Rechem, C., & Whetstine, J.R. (2012) Histone lysine methylation dynamics: establishment, regulation, and biological impact. *Mol. Cell*, **48**, 491–507.

Bortvin, A. & Winston, F. (1995) Evidence That Spt6p Controls Chromatin Structure by a Direct Interaction with Histones. *Science*, **765**, 1473–1476.

Brasher, S. V, Smith, B.O., Fogh, R.H., Nietlispach, D., Thiru, a, Nielsen, P.R., Broadhurst, R.W., Ball, L.J., Murzina, N. V, & Laue, E.D. (2000) The structure of mouse HP1 suggests a unique mode of single peptide recognition by the shadow chromo domain dimer. *EMBO J.*, **19**, 1587–1597.

Braun, S. & Madhani, H.D. (2012) Shaping the landscape: mechanistic consequences of ubiquitin modification of chromatin. *EMBO Rep.*, **13**, 619–630.

Brayer, K.J. & Segal, D.J. (2008) Keep your fingers off my DNA: protein-protein interactions mediated by C2H2 zinc finger domains. *Cell Biochem. Biophys.*, **50**, 111–131.

Brookes, E. & Pombo, A. (2009) Modifications of RNA polymerase II are pivotal in regulating gene expression states. *EMBO Rep.*, **10**, 1213–1219.

Brower-Toland, B., Findley, S.D., Jiang, L., Liu, L., Yin, H., Dus, M., Zhou, P., Elgin, S.C.R., & Lin, H. (2007) Drosophila PIWI associates with chromatin and interacts directly with HP1a. *Genes Dev.*, **21**, 2300–2311.

Brown, T.A. (2002) *Genomes. 2nd*, UK: Wiley-Liss Manchester. Wiley-Liss Manchester.

Bühler, M., Haas, W., Gygi, S.P., & Moazed, D. (2007) RNAi-dependent and -independent RNA turnover mechanisms contribute to heterochromatic gene silencing. *Cell*, **129**, 707–721.

Bühler, M., Verdel, A., & Moazed, D. (2006) Tethering RITS to a nascent transcript initiates RNAi- and heterochromatin-dependent gene silencing. *Cell*, **125**, 873–886.

Buratowski, S. (2009) Progression through the RNA polymerase II CTD cycle. *Mol. Cell*, **36**, 541–546.

Burgess, R.J. & Zhang, Z. (2013) Histone chaperones in nucleosome assembly and human disease. *Nat. Struct. Mol. Biol.*, **20**, 14–22.

Bushey, A.M., Dorman, E.R., & Corces, V.G. (2008) Chromatin insulators: regulatory mechanisms and epigenetic inheritance. *Mol. Cell*, **32**, 1–9.

Bycroft, M. (2011) Recognition of non-methyl histone marks. *Curr. Opin. Struct. Biol.*, **21**, 761–766.

Campos, E.I. & Reinberg, D. (2009) Histones: annotating chromatin. *Annu. Rev. Genet.*, **43**, 559–599.

Cann, K.L. & Dellaire, G. (2011) Heterochromatin and the DNA damage response: the need to relax. *Biochem. Cell Biol.*, **89**, 45–60.

Canudas, S., Houghtaling, B.R., Bhanot, M., Sasa, G., Savage, S. a, Bertuch, A. a, & Smith, S. (2011) A role for heterochromatin protein 1γ at human telomeres. *Genes Dev.*, **25**, 1807–1819.

Canzio, D., Chang, E.Y., Shankar, S., Kuchenbecker, K.M., Simon, M.D., Madhani, H.D., Narlikar, G.J., & Al-Sady, B. (2011) Chromodomain-mediated oligomerization of HP1 suggests a nucleosome-bridging mechanism for heterochromatin assembly. *Mol. Cell*, **41**, 67–81.

Cao, R., Wang, L., Wang, H., Xia, L., Erdjument-Bromage, H., Tempst, P., Jones, R.S., & Zhang, Y. (2002) Role of histone H3 lysine 27 methylation in Polycomb-group silencing. *Science*, **298**, 1039–1043.

Carrozza, M.J., Li, B., Florens, L., Suganuma, T., Swanson, S.K., Lee, K.K., Shia, W.-J., Anderson, S., Yates, J., Washburn, M.P., &

Workman, J.L. (2005) Histone H3 methylation by Set2 directs deacetylation of coding regions by Rpd3S to suppress spurious intragenic transcription. *Cell*, **123**, 581–592.

Castel, S.E. & Martienssen, R. a (2013) RNA interference in the nucleus: roles for small RNAs in transcription, epigenetics and beyond. *Nat. Rev. Genet.*, **14**, 100–112.

Cenci, G., Siriaco, G., Raffa, G.D., Kellum, R., & Gatti, M. (2003) The Drosophila HOAP protein is required for telomere capping. *Nat. Cell Biol.*, **5**, 82–84.

Chen, L. & Madura, K. (2002) Rad23 Promotes the Targeting of Proteolytic Substrates to the Proteasome. *Mol. Cell. Biol.*, **22**, 4902–4913.

Chen, L., Shinde, U., Ortolan, T.G., & Madura, K. (2001) Ubiquitin-associated (UBA) domains in Rad23 bind ubiquitin and promote inhibition of multi-ubiquitin chain assembly. *EMBO Rep.*, **2**, 933–938.

Chen, Z.J. & Sun, L.J. (2009) Nonproteolytic functions of ubiquitin in cell signaling. *Mol. Cell*, **33**, 275–286.

Cheutin, T., McNairn, A.J., Jenuwein, T., Gilbert, D.M., Singh, P.B., & Misteli, T. (2003) Maintenance of stable heterochromatin domains by dynamic HP1 binding. *Science*, **299**, 721–725.

Chin, H.G., Estève, P.-O., Pradhan, M., Benner, J., Patnaik, D., Carey, M.F., & Pradhan, S. (2007) Automethylation of G9a and its implication in wider substrate specificity and HP1 binding. *Nucleic Acids Res.*, **35**, 7313–7323.

Clague, M.J. & Urbé, S. (2010) Ubiquitin: same molecule, different degradation pathways. *Cell*, **143**, 682–685.

Clark, R.J. & Felsenfeld, G. (1974) Chemical probes of chromatin structure. *Biochemistry*, **13**, 3622–3628.

Clarkson, M. & Saint, R. (1999) A His2AvDGFP fusion gene complements a lethal His2AvD mutant allele and provides an in vivo marker for Drosophila chromosome behavior. *DNA Cell Biol.*, **18**, 457–462.

Collins, G. a & Tansey, W.P. (2006) The proteasome: a utility tool for transcription? *Curr. Opin. Genet. Dev.*, **16**, 197–202.

Comings, D.E. (1967) The Rationale for an Ordered Arrangement of Chromatin in the Interphase Nucleus. *Am J Hum Genet.*, **20**, 440–460.

Cowell, I., Aucott, R., Mahadevaiah, S., Huskisson, N., Bongiorni, S., Prantera, G., Fanti, L., Pimpinelli, S., Wu, R., Gilbert, D., Shi, W., Fundele, R., Morrison, H., Jeppesen, P., Singh, P., & Burgoyne, P. (2002) Heterochromatin, HP1 and methylation at lysine 9 of histone H3 in animals. *Chromosoma*, **111**, 22–36.

Cowieson, N.P., Partridge, J.F., Allshire, R.C., & McLaughlin, P.J. (2000) Dimerisation of a chromo shadow domain and distinctions from the chromodomain as revealed by structural analysis. *Curr. Biol.*, **10**, 517–525.

Craig, J.M. (2005) Heterochromatin--many flavours, common themes. *Bioessays*, **27**, 17–28.

Cryderman, D.E., Grade, S.K., Li, Y., Fanti, L., Pimpinelli, S., & Wallrath, L.L. (2005) Role of Drosophila HP1 in euchromatic gene expression. *Dev. Dyn.*, **232**, 767–774.

Czermin, B., Melfi, R., McCabe, D., Seitz, V., Imhof, A., & Pirrotta, V. (2002) Drosophila enhancer of Zeste/ESC complexes have a histone H3 methyltransferase activity that marks chromosomal Polycomb sites. *Cell*, **111**, 185–196.

Dalal, Y., Wang, H., Lindsay, S., & Henikoff, S. (2007) Tetrameric structure of centromeric nucleosomes in interphase Drosophila cells. *PLoS Biol.*, **5**, e218.

Dantuma, N.P., Heinen, C., & Hoogstraten, D. (2009) The ubiquitin receptor Rad23: at the crossroads of nucleotide excision repair and proteasomal degradation. *DNA Repair (Amst).*, **8**, 449–460.

Danzer, J.R. & Wallrath, L.L. (2004) Mechanisms of HP1-mediated gene silencing in Drosophila. *Development*, **131**, 3571–3580.

Daujat, S., Zeissler, U., Waldmann, T., Happel, N., & Schneider, R. (2005) HP1 binds specifically to Lys26-methylated histone H1.4,

whereas simultaneous Ser27 phosphorylation blocks HP1 binding. *J. Biol. Chem.*, **280**, 38090–38095.

Dawson, M. a, Bannister, A.J., Göttgens, B., Foster, S.D., Bartke, T., Green, A.R., & Kouzarides, T. (2009) JAK2 phosphorylates histone H3Y41 and excludes HP1alpha from chromatin. *Nature*, **461**, 819–822.

De Lucia, F., Ni, J.-Q., Vaillant, C., & Sun, F.-L. (2005) HP1 modulates the transcription of cell-cycle regulators in Drosophila melanogaster. *Nucleic Acids Res.*, **33**, 2852–2858.

De Wit, E., Greil, F., & van Steensel, B. (2007) High-resolution mapping reveals links of HP1 with active and inactive chromatin components. *PLoS Genet.*, **3**, e38.

Dialynas, G.K., Makatsori, D., Kourmouli, N., Theodoropoulos, P. a, McLean, K., Terjung, S., Singh, P.B., & Georgatos, S.D. (2006) Methylation-independent binding to histone H3 and cell cycle-dependent incorporation of HP1beta into heterochromatin. *J. Biol. Chem.*, **281**, 14350–14360.

Dinant, C. & Luijsterburg, M.S. (2009) The emerging role of HP1 in the DNA damage response. *Mol. Cell. Biol.*, **29**, 6335–6340.

Diop, S.B., Bertaux, K., Vasanthi, D., Sarkeshik, A., Goirand, B., Aragnol, D., Tolwinski, N.S., Cole, M.D., Pradel, J., Yates, J.R., Mishra, R.K., Graba, Y., Saurin, A.J., & Yates Iii, J.R. (2008) Reptin and Pontin function antagonistically with PcG and TrxG complexes to mediate Hox gene control. *EMBO Rep.*, **9**, 260–266.

Ducat, D., Kawaguchi, S., Liu, H., Yates, J.R., & Zheng, Y. (2008) Regulation of Microtubule Assembly and Organization in Mitosis by the AAA+ ATPase Pontin. *Mol. Biol. Cell*, **19**, 3097–3110.

Eggert, H., Gortchakov, A., & Saumweber, H. (2004) Identification of the Drosophila interband-specific protein Z4 as a DNA-binding zinc-finger protein determining chromosomal structure. *J. Cell Sci.*, **117**, 4253–4264.

Ehrensberger, A.H., Kelly, G.P., & Svejstrup, J.Q. (2013) Mechanistic Interpretation of Promoter-Proximal Peaks and RNAPII Density Maps. *Cell*, **154**, 713–715.

Eissenberg, J.C. (2012) Structural biology of the chromodomain: form and function. *Gene*, **496**, 69–78.

Eissenberg, J.C., James, T.C., Foster-Hartnett, D.M., Hartnett, T., Ngan, V., & Elgin, S.C. (1990) Mutation in a heterochromatin-specific chromosomal protein is associated with suppression of position-effect variegation in Drosophila melanogaster. *Proc. Natl. Acad. Sci. U. S. A.*, **87**, 9923–9927.

Eissenberg, J.C., Morris, G.D., Reuter, G., & Hartnett, T. (1992) The heterochromatin-associated protein HP-1 is an essential protein in Drosophila with dosage-dependent effects on position-effect variegation. *Genetics*, **131**, 345–352.

El Ayadi, A., Stieren, E.S., Barral, J.M., & Boehning, D. (2013) Ubiquilin-1 and protein quality control in Alzheimer disease. *Prion*, **7**, 164–169.

Elgin, S.C. (1996) Heterochromatin and gene regulation in Drosophila. *Curr. Opin. Genet. Dev.*, **6**, 193–202.

Elgin, S.C.R. & Grewal, S.I.S. (2003) Heterochromatin: silence is golden. *Curr. Biol.*, **13**, R895–8.

Elsaesser, S.J., Goldberg, A.D., & Allis, C.D. (2010) New functions for an old variant: no substitute for histone H3.3. *Curr. Opin. Genet. Dev.*, **20**, 110–117.

Elsasser, S., Chandler-Militello, D., Müller, B., Hanna, J., & Finley, D. (2004) Rad23 and Rpn10 serve as alternative ubiquitin receptors for the proteasome. *J. Biol. Chem.*, **279**, 26817–26822.

Elsasser, S., Gali, R.R., Schwickart, M., Larsen, C.N., Leggett, D.S., Müller, B., Feng, M.T., Tübing, F., Dittmar, G. a G., & Finley, D. (2002) Proteasome subunit Rpn1 binds ubiquitin-like protein domains. *Nat. Cell Biol.*, **4**, 725–730.

Ezhkova, E. & Tansey, W.P. (2004) Proteasomal ATPases link ubiquitylation of histone H2B to methylation of histone H3. *Mol. Cell*, **13**, 435–442.

Fanti, L., Berloco, M., Piacentini, L., & Pimpinelli, S. (2003) Chromosomal distribution of heterochromatin protein 1 (HP1) in

Drosophila: a cytological map of euchromatic HP1 binding sites. *Genetica*, **117**, 135–147.

Fanti, L., Giovinazzo, G., Berloco, M., & Pimpinelli, S. (1998) The heterochromatin protein 1 prevents telomere fusions in Drosophila. *Mol. Cell*, **2**, 527–538.

Fanti, L. & Pimpinelli, S. (2008) HP1: a functionally multifaceted protein. *Curr. Opin. Genet. Dev.*, **18**, 169–174.

Figueiredo, M.L. a, Philip, P., Stenberg, P., & Larsson, J. (2012) HP1a recruitment to promoters is independent of H3K9 methylation in Drosophila melanogaster. *PLoS Genet.*, **8**, e1003061.

Filion, G.J., van Bemmel, J.G., Braunschweig, U., Talhout, W., Kind, J., Ward, L.D., Brugman, W., de Castro, I.J., Kerkhoven, R.M., Bussemaker, H.J., & van Steensel, B. (2010) Systematic protein location mapping reveals five principal chromatin types in Drosophila cells. *Cell*, **143**, 212–224.

Finley, D. (2009) Recognition and processing of ubiquitin-protein conjugates by the proteasome. *Annu. Rev. Biochem.*, **78**, 477–513.

Fischle, W., Tseng, B.S., Dormann, H.L., Ueberheide, B.M., Garcia, B. a, Shabanowitz, J., Hunt, D.F., Funabiki, H., & Allis, C.D. (2005) Regulation of HP1-chromatin binding by histone H3 methylation and phosphorylation. *Nature*, **438**, 1116–1122.

Fischle, W., Wang, Y., Jacobs, S.A., Kim, Y., & Allis, C.D. (2003) Molecular basis for the discrimination of repressive methyl-lysine marks in histone H3 by Polycomb and HP1 chromodomains. *Genes Dev.*, **17**, 1870–1881.

Flores, O. & Orozco, M. (2011) nucleR: a package for non-parametric nucleosome positioning. *Bioinformatics*, **27**, 2149–2150.

Fong, Y.W., Inouye, C., Yamaguchi, T., Cattoglio, C., Grubisic, I., & Tjian, R. (2011) A DNA repair complex functions as an Oct4/Sox2 coactivator in embryonic stem cells. *Cell*, **147**, 120–131.

Font-Burgada, J., Rossell, D., Auer, H., & Azorín, F. (2008) Drosophila HP1c isoform interacts with the zinc-finger proteins WOC and

Relative-of-WOC to regulate gene expression. *Genes Dev.*, **22**, 3007–3023.

Frappier, L. & Verrijzer, C.P. (2011) Gene expression control by protein deubiquitinases. *Curr. Opin. Genet. Dev.*, **21**, 207–213.

Funakoshi, M., Sasaki, T., Nishimoto, T., & Kobayashi, H. (2002) Budding yeast Dsk2p is a polyubiquitin-binding protein that can interact with the proteasome. *Proc. Natl. Acad. Sci. U. S. A.*, **99**, 745–750.

Furuyama, T. & Henikoff, S. (2009) Centromeric nucleosomes induce positive DNA supercoils. *Cell*, **138**, 104–113.

Fussner, E., Ching, R.W., & Bazett-Jones, D.P. (2011) Living without 30nm chromatin fibers. *Trends Biochem. Sci.*, **36**, 1–6.

Gan, M., Moebus, S., Eggert, H., & Saumweber, H. (2011) The Chriz–Z4 complex recruits JIL-1 to polytene chromosomes,a requirement for interband-specific phosphorylation of H3S10. *J. Biosci.*, **36**, 425–438.

Ganguly, A., Feldman, R.M.R., & Guo, M. (2008) ubiquilin antagonizes presenilin and promotes neurodegeneration in Drosophila. *Hum. Mol. Genet.*, **17**, 293–302.

García-Cao, M., O'Sullivan, R., Peters, A.H.F.M., Jenuwein, T., & Blasco, M. a (2004) Epigenetic regulation of telomere length in mammalian cells by the Suv39h1 and Suv39h2 histone methyltransferases. *Nat. Genet.*, **36**, 94–99.

Geng, F., Wenzel, S., & Tansey, W.P. (2012) Ubiquitin and proteasomes in transcription. *Annu. Rev. Biochem.*, **81**, 177–201.

Gerasimova, T.I. & Corces, V.G. (1996) Boundary and insulator elements in chromosomes. *Curr. Opin. Genet. Dev.*, **6**, 185–192.

Gerbasi, V.R., Preall, J.B., Golden, D.E., Powell, D.W., Cummins, T.D., & Sontheimer, E.J. (2011) Blanks, a nuclear siRNA/dsRNA-binding complex component, is required for Drosophila spermiogenesis. *Proc. Natl. Acad. Sci. U. S. A.*, **108**, 3204–3209.

Gillette, T.G., Yu, S., Zhou, Z., Waters, R., Johnston, S.A., & Reed, S.H. (2006) Distinct functions of the ubiquitin-proteasome pathway influence nucleotide excision repair. *EMBO J.*, **25**, 2529–2538.

Gocke, C.B. & Yu, H. (2008) ZNF198 stabilizes the LSD1-CoREST-HDAC1 complex on chromatin through its MYM-type zinc fingers. *PLoS One*, **3**, e3255.

Gomez, T. a, Kolawa, N., Gee, M., Sweredoski, M.J., & Deshaies, R.J. (2011) Identification of a functional docking site in the Rpn1 LRR domain for the UBA-UBL domain protein Ddi1. *BMC Biol.*, **9**, 33.

Goodarzi, A. a, Noon, A.T., Deckbar, D., Ziv, Y., Shiloh, Y., Löbrich, M., & Jeggo, P. a (2008) ATM signaling facilitates repair of DNA double-strand breaks associated with heterochromatin. *Mol. Cell*, **31**, 167–177.

Gortchakov, A.A., Eggert, H., Gan, M., Mattow, J., Zhimulev, I.F., & Saumweber, H. (2005) Chriz, a chromodomain protein specific for the interbands of Drosophila melanogaster polytene chromosomes. *Chromosoma*, **114**, 54–66.

Greil, F., de Wit, E., Bussemaker, H.J., & van Steensel, B. (2007) HP1 controls genomic targeting of four novel heterochromatin proteins in Drosophila. *EMBO J.*, **26**, 741–751.

Greil, F., van der Kraan, I., Delrow, J., Smothers, J.F., de Wit, E., Bussemaker, H.J., van Driel, R., Henikoff, S., & van Steensel, B. (2003) Distinct HP1 and Su(var)3-9 complexes bind to sets of developmentally coexpressed genes depending on chromosomal location. *Genes Dev.*, **17**, 2825–2838.

Grigoryev, S. a, Arya, G., Correll, S., Woodcock, C.L., & Schlick, T. (2009) Evidence for heteromorphic chromatin fibers from analysis of nucleosome interactions. *Proc. Natl. Acad. Sci. U. S. A.*, **106**, 13317–13322.

Gross, G.G., Feldman, R.M.R., Ganguly, A., Wang, J., Yu, H., & Guo, M. (2008) Role of X11 and ubiquilin as in vivo regulators of the amyloid precursor protein in Drosophila. *PLoS One*, **3**, e2495.

Gu, T. & Elgin, S.C.R. (2013) Maternal Depletion of Piwi, a Component of the RNAi System, Impacts Heterochromatin Formation in Drosophila. *PLoS Genet.*, **9**, e1003780.

Guibert, S. & Weber, M. (2013) Functions of DNA methylation and hydroxymethylation in mammalian development. *Curr. Top. Dev. Biol.*, **104**, 47–83.

Guruharsha, K.G., Rual, J.-F., Zhai, B., Mintseris, J., Vaidya, P., Vaidya, N., Beekman, C., Wong, C., Rhee, D.Y., Cenaj, O., McKillip, E., Shah, S., Stapleton, M., Wan, K.H., Yu, C., Parsa, B., Carlson, J.W., Chen, X., Kapadia, B., VijayRaghavan, K., Gygi, S.P., Celniker, S.E., Obar, R. a, & Artavanis-Tsakonas, S. (2011) A protein complex network of Drosophila melanogaster. *Cell*, **147**, 690–703.

Guzder, S.N. (1998) Affinity of Yeast Nucleotide Excision Repair Factor 2, Consisting of the Rad4 and Rad23 Proteins, for Ultraviolet Damaged DNA. *J. Biol. Chem.*, **273**, 31541–31546.

Hammond-Martel, I., Yu, H., & Affar, E.B. (2012) Roles of ubiquitin signaling in transcription regulation. *Cell. Signal.*, **24**, 410–421.

Hardy, S., Jacques, P.-E., Gévry, N., Forest, A., Fortin, M.-E., Laflamme, L., Gaudreau, L., & Robert, F. (2009) The euchromatic and heterochromatic landscapes are shaped by antagonizing effects of transcription on H2A.Z deposition. *PLoS Genet.*, **5**, e1000687.

Hediger, F. & Gasser, S.M. (2006) Heterochromatin protein 1: don't judge the book by its cover! *Curr. Opin. Genet. Dev.*, **16**, 143–150.

Heidemann, M., Hintermair, C., Voß, K., & Eick, D. (2013) Dynamic phosphorylation patterns of RNA polymerase II CTD during transcription. *Biochim. Biophys. Acta*, **1829**, 55–62.

Heitz, E. (1928) Das Heterochromatin der Moose. *I Jahrb Wiss Bot.*, **69**, 762–818.

Hellman, A. & Chess, A. (2007) Gene body-specific methylation on the active X chromosome. *Science*, **315**, 1141–1143.

Henikoff, S. & Shilatifard, A. (2011) Histone modification: cause or cog? *Trends Genet.*, **27**, 389–396.

Hicke, L., Schubert, H.L., & Hill, C.P. (2005) Ubiquitin-binding domains. *Nat. Rev. Mol. Cell Biol.*, **6**, 610–621.

Hiltunen, M., Lu, A., Thomas, A. V, Romano, D.M., Kim, M., Jones, P.B., Xie, Z., Kounnas, M.Z., Wagner, S.L., Berezovska, O., Hyman, B.T., Tesco, G., Bertram, L., & Tanzi, R.E. (2006) Ubiquilin 1 modulates amyloid precursor protein trafficking and Abeta secretion. *J. Biol. Chem.*, **281**, 32240–32253.

Hiragami, K. & Festenstein, R. (2005) Heterochromatin protein 1: a pervasive controlling influence. *Cell. Mol. Life Sci.*, **62**, 2711–2726.

Hirota, T., Lipp, J.J., Toh, B.-H., & Peters, J.-M. (2005) Histone H3 serine 10 phosphorylation by Aurora B causes HP1 dissociation from heterochromatin. *Nature*, **438**, 1176–1180.

Hiyama, H. (1999) Interaction of hHR23 with S5a. THE UBIQUITIN-LIKE DOMAIN OF hHR23 MEDIATES INTERACTION WITH S5a SUBUNIT OF 26 S PROTEASOME. *J. Biol. Chem.*, **274**, 28019–28025.

Hochheimer, A., Zhou, S., Zheng, S., & Holmes, M.C. (2002) TRF2 associates with DREF and directs promoter-selective gene expression in Drosophila. *Nature*, **420**, 1–7.

Höhfeld, J., Minami, Y., & Hartl, F.U. (1995) Hip, a novel cochaperone involved in the eukaryotic Hsc70/Hsp40 reaction cycle. *Cell*, **83**, 589–598.

Horsley, D., Hutchings, A., Butcher, G., & Singh, P. (1996) M32, a murine homologue of Drosophila heterochromatin protein 1 (HP1), localises to euchromatin within interphase nuclei and is largely excluded from constitutive heterochromatin. *Cytogenet. Cell Genet.*, **73**, 308–311.

Hsin, J.-P. & Manley, J.L. (2012) The RNA polymerase II CTD coordinates transcription and RNA processing. *Genes Dev.*, **26**, 2119–2137.

Hughes, R.M., Wiggins, K.R., Khorasanizadeh, S., & Waters, M.L. (2007) Recognition of trimethyllysine by a chromodomain is not driven by the hydrophobic effect. *Proc. Natl. Acad. Sci. U. S. A.*, **104**, 11184–11188.

Hwang, K.K., Eissenberg, J.C., & Worman, H.J. (2001) Transcriptional repression of euchromatic genes by Drosophila heterochromatin protein 1 and histone modifiers. *Proc. Natl. Acad. Sci. U. S. A.*, **98**, 11423–11427.

Jacobs, S. a & Khorasanizadeh, S. (2002) Structure of HP1 chromodomain bound to a lysine 9-methylated histone H3 tail. *Science*, **295**, 2080–2083.

Jacobs, S.A., Taverna, S.D., Zhang, Y., Briggs, S.D., Li, J., Eissenberg, J.C., & Allis, C.D. (2001) Specificity of the HP1 chromo domain for the methylated N-terminus of histone H3. *EMBO J.*, **20**, 5232–5241.

Jaehning, J. a (2010) The Paf1 complex: platform or player in RNA polymerase II transcription? *Biochim. Biophys. Acta*, **1799**, 379–388.

James, T.C. & Elgin, S.C.R. (1986) Identification of a nonhistone chromosomal protein associated with heterochromatin in Drosophila melanogaster and its gene. *Mol. Cell. Biol.*, **6**, 3862–3872.

Jansen, L.E.T. (1998) Preferential Binding of Yeast Rad4 Rad23 Complex to Damaged DNA. *J. Biol. Chem.*, **273**, 33111–33114.

Jiang, N., Emberly, E., Cuvier, O., & Hart, C.M. (2009) Genome-wide mapping of boundary element-associated factor (BEAF) binding sites in Drosophila melanogaster links BEAF to transcription. *Mol. Cell. Biol.*, **29**, 3556–3568.

Johansson, A.-M., Stenberg, P., Bernhardsson, C., & Larsson, J. (2007) Painting of fourth and chromosome-wide regulation of the 4th chromosome in Drosophila melanogaster. *EMBO J.*, **26**, 2307–2316.

Johansson, A.-M., Stenberg, P., Pettersson, F., & Larsson, J. (2007) POF and HP1 bind expressed exons, suggesting a balancing mechanism for gene regulation. *PLoS Genet.*, **3**, 2235–2246.

Joppich, C., Scholz, S., Korge, G., & Schwendemann, A. (2009) Umbrea, a chromo shadow domain protein in Drosophila melanogaster heterochromatin, interacts with Hip, HP1 and HOAP. *Chromosome Res.*, **17**, 19–36.

Joshi, A. a & Struhl, K. (2005) Eaf3 chromodomain interaction with methylated H3-K36 links histone deacetylation to Pol II elongation. *Mol. Cell*, **20**, 971–978.

Kamileri, I., Karakasilioti, I., & Garinis, G. a (2012) Nucleotide excision repair: new tricks with old bricks. *Trends Genet.*, **28**, 566–573.

Kanellopoulou, C., Muljo, S. a, Kung, A.L., Ganesan, S., Drapkin, R., Jenuwein, T., Livingston, D.M., & Rajewsky, K. (2005) Dicer-deficient mouse embryonic stem cells are defective in differentiation and centromeric silencing. *Genes Dev.*, **19**, 489–501.

Kao, C.-F., Hillyer, C., Tsukuda, T., Henry, K., Berger, S., & Osley, M.A. (2004) Rad6 plays a role in transcriptional activation through ubiquitylation of histone H2B. *Genes Dev.*, **18**, 184–195.

Kaplun, L., Tzirkin, R., Bakhrat, A., Ivantsiv, Y., Raveh, D., & Shabek, N. (2005) The DNA Damage-Inducible UbL-UbA Protein Ddi1 Participates in Mec1-Mediated Degradation of Ho Endonuclease. *Mol. Cell. Biol.*, **25**, 5355–5362.

Kaur, M., Pop, M., Shi, D., Brignone, C., & Grossman, S.R. (2007) hHR23B is required for genotoxic-specific activation of p53 and apoptosis. *Oncogene*, **26**, 1231–1237.

Kaye, F.J., Modi, S., Ivanovska, I., Koonin, E. V, Thress, K., Kubo, A., Kornbluth, S., & Rose, M.D. (2000) A family of ubiquitin-like proteins binds the ATPase domain of Hsp70-like Stch. *FEBS Lett.*, **467**, 348–352.

Keller, C., Adaixo, R., Stunnenberg, R., Woolcock, K.J., Hiller, S., & Bühler, M. (2012) HP1(Swi6) mediates the recognition and destruction of heterochromatic RNA transcripts. *Mol. Cell*, **47**, 215–227.

Keller, C., Kulasegaran-Shylini, R., Shimada, Y., Hotz, H.-R., & Bühler, M. (2013) Noncoding RNAs prevent spreading of a repressive histone mark. *Nat. Struct. Mol. Biol.*,.

Kellum, R. & Schedl, P. (1991) A position-effect assay for boundaries of higher order chromosomal domains. *Cell*, **64**, 941–950.

Kim, J., Hake, S.B., & Roeder, R.G. (2005) The human homolog of yeast BRE1 functions as a transcriptional coactivator through direct activator interactions. *Mol. Cell*, **20**, 759–770.

Kim, T.H., Barrera, L.O., Zheng, M., Qu, C., Singer, M. a, Richmond, T. a, Wu, Y., Green, R.D., & Ren, B. (2005) A high-resolution map of active promoters in the human genome. *Nature*, **436**, 876–880.

Klattenhoff, C., Xi, H., Li, C., Lee, S., Xu, J., Khurana, J.S., Zhang, F., Schultz, N., Koppetsch, B.S., Nowosielska, A., Seitz, H., Zamore, P.D., Weng, Z., & Theurkauf, W.E. (2009) The Drosophila HP1 homolog Rhino is required for transposon silencing and piRNA production by dual-strand clusters. *Cell*, **138**, 1137–1149.

Kornberg, R.D. (1974) Chromatin Structure : A Repeating Unit of Histones and DNA. *Science*, **184**, 868–871.

Kornberg, R.D. (1977) Structure of chromatin. *Annu. Rev. Biochem.*, **46**, 931–954.

Kouzarides, T. (2007) Chromatin modifications and their function. *Cell*, **128**, 693–705.

Kugler, S.J. & Nagel, A.C. (2007) putzig Is Required for Cell Proliferation and Regulates Notch Activity in Drosophila. *Mol. Biol. Cell*, **18**, 3733–3740.

Kugler, S.J. & Nagel, A.C. (2010) A Novel Pzg-NURF Complex Regulates Notch Target Gene Activity. *Mol. Cell. Biol.*, **21**, 3443–3448.

Kurucz, E., Ando, I., Sumegi, M., Holzl, H., Kapelari, B., Baumeister, W., & Udvardy, A. (2002) Assembly of the Drosophila 26 S proteasome is accompanied by extensive subunit rearrangements. *Biochem. J.*, **365**, 527–536.

Kwon, S.H., Florens, L., Swanson, S.K., Washburn, M.P., Abmayr, S.M., & Workman, J.L. (2010) Heterochromatin protein 1 (HP1) connects the FACT histone chaperone complex to the phosphorylated CTD of RNA polymerase II. *Genes Dev.*, **24**, 2133–2145.

Kwon, S.H. & Workman, J.L. (2011) The changing faces of HP1: From heterochromatin formation and gene silencing to euchromatic gene

expression: HP1 acts as a positive regulator of transcription. *Bioessays*, **33**, 280–289.

Lachner, M., O'Carroll, D., Rea, S., Mechtler, K., & Jenuwein, T. (2001) Methylation of histone H3 lysine 9 creates a binding site for HP1 proteins. *Nature*, **410**, 116–120.

Lambertson, D., Chen, L., & Madura, K. (1999) Pleiotropic defects caused by loss of the proteasome-interacting factors Rad23 and Rpn10 of Saccharomyces cerevisiae. *Genetics*, **153**, 69–79.

Laribee, R.N., Fuchs, S.M., & Strahl, B.D. (2007) H2B ubiquitylation in transcriptional control: a FACT-finding mission. *Genes Dev.*, **21**, 737–743.

Laribee, R.N., Krogan, N.J., Xiao, T., Shibata, Y., Hughes, T.R., Greenblatt, J.F., & Strahl, B.D. (2005) BUR kinase selectively regulates H3 K4 trimethylation and H2B ubiquitylation through recruitment of the PAF elongation complex. *Curr. Biol.*, **15**, 1487–1493.

Lavelle, C., Recouvreux, P., Wong, H., Bancaud, A., Viovy, J.-L., Prunell, A., & Victor, J.-M. (2009) Right-handed nucleosome: myth or reality? *Cell*, **139**, 1216–7; author reply 1217–8.

Le May, N., Mota-Fernandes, D., Vélez-Cruz, R., Iltis, I., Biard, D., & Egly, J.M. (2010) NER factors are recruited to active promoters and facilitate chromatin modification for transcription in the absence of exogenous genotoxic attack. *Mol. Cell*, **38**, 54–66.

Lechner, M.S., Begg, G.E., Speicher, D.W., & Iii, F.J.R. (2000) Molecular Determinants for Targeting Heterochromatin Protein 1-Mediated Gene Silencing : Direct Chromoshadow Domain − KAP-1 Corepressor Interaction Is Essential Molecular Determinants for Targeting Heterochromatin Protein 1-Mediated Gene Silencing : Direc.

Lee, D., Ezhkova, E., Li, B., Pattenden, S.G., Tansey, W.P., & Workman, J.L. (2005) The proteasome regulatory particle alters the SAGA coactivator to enhance its interactions with transcriptional activators. *Cell*, **123**, 423–436.

Lee, J.-S., Shukla, A., Schneider, J., Swanson, S.K., Washburn, M.P., Florens, L., Bhaumik, S.R., & Shilatifard, A. (2007) Histone crosstalk between H2B monoubiquitination and H3 methylation mediated by COMPASS. *Cell*, **131**, 1084–1096.

Lee, J.-S., Smith, E., & Shilatifard, A. (2010) The language of histone crosstalk. *Cell*, **142**, 682–685.

Lejeune, E., Bortfeld, M., White, S. a, Pidoux, A.L., Ekwall, K., Allshire, R.C., & Ladurner, A.G. (2007) The chromatin-remodeling factor FACT contributes to centromeric heterochromatin independently of RNAi. *Curr. Biol.*, **17**, 1219–1224.

Lenhard, B., Sandelin, A., & Carninci, P. (2012) Metazoan promoters: emerging characteristics and insights into transcriptional regulation. *Nat. Rev. Genet.*, **13**, 233–245.

LeRoy, G., Weston, J.T., Zee, B.M., Young, N.L., Plazas-Mayorca, M.D., & Garcia, B. a (2009) Heterochromatin protein 1 is extensively decorated with histone code-like post-translational modifications. *Mol. Cell. Proteomics*, **8**, 2432–2442.

Levine, M.T., McCoy, C., Vermaak, D., Lee, Y.C.G., Hiatt, M.A., Matsen, F. a, & Malik, H.S. (2012) Phylogenomic analysis reveals dynamic evolutionary history of the Drosophila heterochromatin protein 1 (HP1) gene family. *PLoS Genet.*, **8**, e1002729.

Li, A., Xie, Z., Dong, Y., McKay, K.M., McKee, M.L., & Tanzi, R.E. (2007) Isolation and characterization of the Drosophila ubiquilin ortholog dUbqln: in vivo interaction with early-onset Alzheimer disease genes. *Hum. Mol. Genet.*, **16**, 2626–2639.

Li, B., Carey, M., & Workman, J.L. (2007) The role of chromatin during transcription. *Cell*, **128**, 707–719.

Li, B., Gogol, M., Carey, M., Lee, D., Seidel, C., & Workman, J.L. (2007) Combined action of PHD and chromo domains directs the Rpd3S HDAC to transcribed chromatin. *Science*, **316**, 1050–1054.

Li, L. (2009) GADEM: a genetic algorithm guided formation of spaced dyads coupled with an EM algorithm for motif discovery. *J. Comput. Biol.*, **16**, 317–329.

Li, Y., Danzer, J.R., Alvarez, P., Belmont, A. s, & Wallrath, L.L. (2003) Effects of tethering HP1 to euchromatic regions of the Drosophila genome. *Development*, **130**, 1817–1824.

Libault, M., Tessadori, F., Germann, S., Snijder, B., Fransz, P., & Gaudin, V. (2005) The Arabidopsis LHP1 protein is a component of euchromatin. *Planta*, **222**, 910–925.

Lin, C.-H., Li, B., Swanson, S., Zhang, Y., Florens, L., Washburn, M.P., Abmayr, S.M., & Workman, J.L. (2008) Heterochromatin protein 1a stimulates histone H3 lysine 36 demethylation by the Drosophila KDM4A demethylase. *Mol. Cell*, **32**, 696–706.

Lipford, J.R. & Deshaies, R.J. (2003) Diverse roles for ubiquitin-dependent proteolysis in transcriptional activation. *Nat. Cell Biol.*, **5**, 845–850.

Lipford, J.R., Smith, G.T., Chi, Y., & Deshaies, R.J. (2005) A putative stimulatory role for activator turnover in gene expression. *Nature*, **438**, 113–116.

Lipinszki, Z., Kiss, P., Pál, M., Deák, P., Szabó, A., Hunyadi-Gulyas, E., Klement, E., Medzihradszky, K.F., & Udvardy, A. (2009) Developmental-stage-specific regulation of the polyubiquitin receptors in Drosophila melanogaster. *J. Cell Sci.*, **122**, 3083–3092.

Lipinszki, Z., Kovács, L., Deák, P., & Udvardy, A. (2012) Ubiquitylation of Drosophila p54/Rpn10/S5a regulates its interaction with the UBA-UBL polyubiquitin receptors. *Biochemistry*, **51**, 2461–2470.

Lipinszki, Z., Pál, M., Nagy, O., Deák, P., Hunyadi-Gulyas, E., & Udvardy, A. (2011) Overexpression of Dsk2/dUbqln results in severe developmental defects and lethality in Drosophila melanogaster that can be rescued by overexpression of the p54/Rpn10/S5a proteasomal subunit. *FEBS J.*, **278**, 4833–4844.

Liu, J., Wu, Z., Nizami, Z., Deryusheva, S., Rajendra, T.K., Beumer, K.J., Gao, H., Matera, A.G., Carroll, D., & Gall, J.G. (2009) Coilin Is Essential for Cajal Body Organization in Drosophila melanogaster. *Mol. Biol. Cell*, **20**, 1661–1670.

Liu, J.-L., Murphy, C., Buszczak, M., Clatterbuck, S., Goodman, R., & Gall, J.G. (2006) The Drosophila melanogaster Cajal body. *J. Cell Biol.*, **172**, 875–884.

Lloret-Llinares, M., Pérez-Lluch, S., Rossell, D., Morán, T., Ponsa-Cobas, J., Auer, H., Corominas, M., & Azorín, F. (2012) dKDM5/LID regulates H3K4me3 dynamics at the transcription-start site (TSS) of actively transcribed developmental genes. *Nucleic Acids Res.*, **40**, 9493–9505.

Lomberk, G., Wallrath, L., & Urrutia, R. (2006) The Heterochromatin Protein 1 family. *Genome Biol.*, **7**, 228.

Lommel, L., Ortolan, T., Chen, L., Madura, K., & Sweder, K.S. (2002) Proteolysis of a nucleotide excision repair protein by the 26 S proteasome. *Curr. Genet.*, **42**, 9–20.

Lowe, E.D., Hasan, N., Trempe, J.F., Fonso, L., Noble, M.E.M., Endicott, J. a, Johnson, L.N., & Brown, N.R. (2006) Structures of the Dsk2 UBL and UBA domains and their complex. *Acta Crystallogr. D. Biol. Crystallogr.*, **62**, 177–188.

Lu, B.Y., Emtage, P.C., Duyf, B.J., Hilliker, a J., & Eissenberg, J.C. (2000) Heterochromatin protein 1 is required for the normal expression of two heterochromatin genes in Drosophila. *Genetics*, **155**, 699–708.

Luger, K., Dechassa, M.L., & Tremethick, D.J. (2012) New insights into nucleosome and chromatin structure: an ordered state or a disordered affair? *Nat. Rev. Mol. Cell Biol.*, **13**, 436–447.

Luger, K., Ma, A.W., Richmond, R.K., Sargent, D.F., & Richmond, T.J. (1997) Crystal structure of the nucleosome core particle at 2.8 A resolution. *Nature*, **389**, 251–260.

Luijsterburg, M.S., Dinant, C., Lans, H., Stap, J., Wiernasz, E., Lagerwerf, S., Warmerdam, D.O., Lindh, M., Brink, M.C., Dobrucki, J.W., Aten, J. a, Fousteri, M.I., Jansen, G., Dantuma, N.P., Vermeulen, W., Mullenders, L.H.F., Houtsmuller, A.B., Verschure, P.J., & van Driel, R. (2009) Heterochromatin protein 1 is recruited to various types of DNA damage. *J. Cell Biol.*, **185**, 577–586.

Luteijn, M.J. & Ketting, R.F. (2013) PIWI-interacting RNAs: from generation to transgenerational epigenetics. *Nat. Rev. Genet.*, **14**, 523–534.

Mah, a L., Perry, G., Smith, M. a, & Monteiro, M.J. (2000) Identification of ubiquilin, a novel presenilin interactor that increases presenilin protein accumulation. *J. Cell Biol.*, **151**, 847–862.

Maison, C., Bailly, D., Roche, D., Montes de Oca, R., Probst, A. V, Vassias, I., Dingli, F., Lombard, B., Loew, D., Quivy, J.-P., & Almouzni, G. (2011) SUMOylation promotes de novo targeting of HP1α to pericentric heterochromatin. *Nat. Genet.*, **43**, 220–227.

Mandrioli, M. & Borsatti, F. (2006) DNA methylation of fly genes and transposons. *Cell. Mol. Life Sci.*, **63**, 1933–1936.

Marshall, N.F., Peng, J., Xie, Z., & Price, D.H. (1996) Control of RNA Polymerase II Elongation Potential by a Novel Carboxyl-terminal Domain Kinase. *J. Biol. Chem.*, **271**, 27176–27183.

Martens, J. a & Winston, F. (2003) Recent advances in understanding chromatin remodeling by Swi/Snf complexes. *Curr. Opin. Genet. Dev.*, **13**, 136–142.

Massey, L.K., Mah, A.L., Ford, D.L., Miller, J., Liang, J., Doong, H., & Monteiro, M.J. (2004) Overexpression of ubiquilin decreases ubiquitination and degradation of presenilin proteins. *J. Alzheimer's Dis.*, **6**, 79–92.

Masutani, C., Araki, M., Sugasawa, K., Spek, P.J. Van Der, Yamada, A., Uchida, A., Maekawa, T., Bootsma, D., Hoeijmakers, J.H., Masutani, C., Araki, M., Sugasawa, K., & Spek, P.J.V.A.N.D.E.R. (1997) Identification and characterization of XPC-binding domain of hHR23B. *Mol. Cell. Biol.*, **17**, 6915–6923.

Matiuhin, Y., Kirkpatrick, D.S., Ziv, I., Kim, W., Dakshinamurthy, A., Kleifeld, O., Gygi, S.P., Reis, N., & Glickman, M.H. (2008) Extraproteasomal Rpn10 restricts access of the polyubiquitin-binding protein Dsk2 to proteasome. *Mol. Cell*, **32**, 415–425.

McGhee, J.D. & Felsenfeld, G. (1980) Nucleosome structure. *Annu. Rev. Biochem.*, **49**, 1115–1156.

Meehan, R.R., Kao, C.-F., & Pennings, S. (2003) HP1 binding to native chromatin in vitro is determined by the hinge region and not by the chromodomain. *EMBO J.*, **22**, 3164–3174.

Mendez, D.L., Kim, D., Chruszcz, M., Stephens, G.E., Minor, W., Khorasanizadeh, S., & Elgin, S.C.R. (2011) The HP1a disordered C terminus and chromo shadow domain cooperate to select target peptide partners. *CHEMBIOCHEM*, **12**, 1084–1096.

Mendez, D.L., Mandt, R.E., & Elgin, S.C.R. (2013) Heterochromatin Protein 1a (HP1a) Partner Specificity is Determined by Critical Amino Acids in the Chromo Shadow Domain and C-terminal Extension. *J. Biol. Chem.*,.

Min, J., Zhang, Y., & Xu, R.-M. (2003) Structural basis for specific binding of Polycomb chromodomain to histone H3 methylated at Lys 27. *Genes Dev.*, **17**, 1823–1828.

Minc, E., Allory, Y., Worman, H.J., Courvalin, J., & Buendia, B. (1999) Localization and phosphorylation of HP1 proteins during the cell cycle in mammalian cells. *Chromosoma*, **7**, 220–234.

Mischo, H.E. & Proudfoot, N.J. (2013) Disengaging polymerase: terminating RNA polymerase II transcription in budding yeast. *Biochim. Biophys. Acta*, **1829**, 174–185.

Mizuguchi, G., Xiao, H., Wisniewski, J., Smith, M.M., & Wu, C. (2007) Nonhistone Scm3 and histones CenH3-H4 assemble the core of centromere-specific nucleosomes. *Cell*, **129**, 1153–1164.

Moazed, D. (2001) Common themes in mechanisms of gene silencing. *Mol. Cell*, **8**, 489–498.

Mohrmann, L., Langenberg, K., Krijgsveld, J., Kal, A.J., Heck, A.J.R., & Verrijzer, C.P. (2004) Differential Targeting of Two Distinct SWI/SNF-Related Drosophila Chromatin-Remodeling Complexes. *Mol. Cell. Biol.*, **24**, 3077–3088.

Morency, E., Sabra, M., Catez, F., Texier, P., & Lomonte, P. (2007) A novel cell response triggered by interphase centromere structural instability. *J. Cell Biol.*, **177**, 757–768.

Motamedi, M.R., Hong, E.-J.E., Li, X., Gerber, S., Denison, C., Gygi, S., & Moazed, D. (2008) HP1 proteins form distinct complexes and mediate heterochromatic gene silencing by nonoverlapping mechanisms. *Mol. Cell*, **32**, 778–790.

Motamedi, M.R., Verdel, A., Colmenares, S.U., Gerber, S. a, Gygi, S.P., & Moazed, D. (2004) Two RNAi complexes, RITS and RDRC, physically interact and localize to noncoding centromeric RNAs. *Cell*, **119**, 789–802.

Muchardt, C., Guilleme, M., Seeler, J.-S., Trouche, D., Dejean, A., & Yaniv, M. (2002) Coordinated methyl and RNA binding is required for heterochromatin localization of mammalian HP1alpha. *EMBO Rep.*, **3**, 975–981.

Muller, H.J. (1930) Types of visible variations induced by X-rays inDrosophila. *J. Genet.*, **22**, 299–334.

Murzina, N., Verreault, a, Laue, E., & Stillman, B. (1999) Heterochromatin dynamics in mouse cells: interaction between chromatin assembly factor 1 and HP1 proteins. *Mol. Cell*, **4**, 529–540.

Muse, G.W., Gilchrist, D. a, Nechaev, S., Shah, R., Parker, J.S., Grissom, S.F., Zeitlinger, J., & Adelman, K. (2007) RNA polymerase is poised for activation across the genome. *Nat. Genet.*, **39**, 1507–1511.

Musselman, C. a, Lalonde, M.-E., Côté, J., & Kutateladze, T.G. (2012) Perceiving the epigenetic landscape through histone readers. *Nat. Struct. Mol. Biol.*, **19**, 1218–1227.

Nagano, T. & Fraser, P. (2011) No-nonsense functions for long noncoding RNAs. *Cell*, **145**, 178–181.

Nakayama, J., Rice, J.C., Strahl, B.D., Allis, C.D., & Grewal, S.I. (2001) Role of histone H3 lysine 9 methylation in epigenetic control of heterochromatin assembly. *Science*, **292**, 110–113.

Nakayasu, E.S., Ansong, C., Brown, J.N., Yang, F., Lopez-Ferrer, D., Qian, W.-J., Smith, R.D., & Adkins, J.N. (2013) Evaluation of Selected Binding Domains for the Analysis of Ubiquitinated Proteomes. *J. Am. Soc. Mass Spectrom.*,.

Narlikar, G.J., Sundaramoorthy, R., & Owen-Hughes, T. (2013) Mechanisms and Functions of ATP-Dependent Chromatin-Remodeling Enzymes. *Cell*, **154**, 490–503.

Ng, J.M.Y., Vermeulen, W., van der Horst, G.T.J., Bergink, S., Sugasawa, K., Vrieling, H., & Hoeijmakers, J.H.J. (2003) A novel regulation mechanism of DNA repair by damage-induced and RAD23-dependent stabilization of xeroderma pigmentosum group C protein. *Genes Dev.*, **17**, 1630–1645.

Nielsen, A.L., Oulad-Abdelghani, M., Ortiz, J.A., Remboutsika, E., Chambon, P., & Losson, R. (2001) Heterochromatin formation in mammalian cells: interaction between histones and HP1 proteins. *Mol. Cell*, **7**, 729–739.

Nielsen, P.R., Nietlispach, D., Mott, H.R., Callaghan, J., Bannister, A., Kouzarides, T., Murzin, A.G., Murzina, N. V, & Laue, E.D. (2002) Structure of the HP1 chromodomain bound to histone H3 methylated at lysine 9. *Nature*, **416**, 103–107.

Nielsen, S.J., Schneider, R., Bauer, U.M., Bannister, a J., Morrison, a, O'Carroll, D., Firestein, R., Cleary, M., Jenuwein, T., Herrera, R.E., & Kouzarides, T. (2001) Rb targets histone H3 methylation and HP1 to promoters. *Nature*, **412**, 561–565.

Nishino, Y., Eltsov, M., Joti, Y., Ito, K., Takata, H., Takahashi, Y., Hihara, S., Frangakis, A.S., Imamoto, N., Ishikawa, T., & Maeshima, K. (2012) Human mitotic chromosomes consist predominantly of irregularly folded nucleosome fibres without a 30-nm chromatin structure. *EMBO J.*, **31**, 1644–1653.

Noll, M. (1974) Subunit structure of chromatin. *Nature*, **251**, 249–251.

Ogawa, H., Ishiguro, K.-I., Gaubatz, S., Livingston, D.M., & Nakatani, Y. (2002) A complex with chromatin modifiers that occupies E2F- and Myc-responsive genes in G0 cells. *Science*, **296**, 1132–1136.

Oikemus, S.R., Mcginnis, N., Queiroz-machado, J., Tukachinsky, H., Takada, S., Sunkel, C.E., & Brodsky, M.H. (2004) Drosophila atm / telomere fusion is required for telomeric localization of HP1 and telomere position effect. *Genes Dev.*, **18**, 1850–1861.

Olins, a L. & Olins, D.E. (1974) Spheroid chromatin units (v bodies). *Science*, **183**, 330–332.

Orphanides, G., LeRoy, G., Chang, C.H., Luse, D.S., & Reinberg, D. (1998) FACT, a factor that facilitates transcript elongation through nucleosomes. *Cell*, **92**, 105–116.

Ortolan, T.G., Chen, L., Tongaonkar, P., & Madura, K. (2004) Rad23 stabilizes Rad4 from degradation by the Ub/proteasome pathway. *Nucleic Acids Res.*, **32**, 6490–6500.

Pal-Bhadra, M., Leibovitch, B. a, Gandhi, S.G., Chikka, M.R., Rao, M., Bhadra, U., Birchler, J. a, & Elgin, S.C.R. (2004) Heterochromatic silencing and HP1 localization in Drosophila are dependent on the RNAi machinery. *Science*, **303**, 669–672.

Paro, R. & Hogness, D.S. (1991) The Polycomb protein shares a homologous domain with a heterochromatin-associated protein of Drosophila. *Proc. Natl. Acad. Sci. U. S. A.*, **88**, 263–267.

Pavri, R., Zhu, B., Li, G., Trojer, P., Mandal, S., Shilatifard, A., & Reinberg, D. (2006) Histone H2B monoubiquitination functions cooperatively with FACT to regulate elongation by RNA polymerase II. *Cell*, **125**, 703–717.

Perrini, B., Piacentini, L., Fanti, L., Altieri, F., Chichiarelli, S., Berloco, M., Turano, C., Ferraro, A., & Pimpinelli, S. (2004) HP1 controls telomere capping, telomere elongation, and telomere silencing by two different mechanisms in Drosophila. *Mol. Cell*, **15**, 467–476.

Phillips-Cremins, J.E. & Corces, V.G. (2013) Chromatin Insulators: Linking Genome Organization to Cellular Function. *Mol. Cell*, **50**, 461–474.

Piacentini, L., Fanti, L., Berloco, M., Perrini, B., & Pimpinelli, S. (2003) Heterochromatin protein 1 (HP1) is associated with induced gene expression in Drosophila euchromatin. *J. Cell Biol.*, **161**, 707–714.

Piacentini, L., Fanti, L., Negri, R., Del Vescovo, V., Fatica, A., Altieri, F., & Pimpinelli, S. (2009) Heterochromatin protein 1 (HP1a) positively regulates euchromatic gene expression through RNA transcript association and interaction with hnRNPs in Drosophila. *PLoS Genet.*, **5**, e1000670.

Planet, E., Attolini, C.S.-O., Reina, O., Flores, O., & Rossell, D. (2012) htSeqTools: high-throughput sequencing quality control, processing and visualization in R. *Bioinformatics*, **28**, 589–590.

Platero, J.S., Hartnett, T., & Eissenberg, J.C. (1995) Functional analysis of the chromo domain of HP1. *EMBO J.*, **14**, 3977–3986.

Powers, J. a & Eissenberg, J.C. (1993) Overlapping domains of the heterochromatin-associated protein HP1 mediate nuclear localization and heterochromatin binding. *J. Cell Biol.*, **120**, 291–299.

Proudfoot, N.J. (2011) Ending the message: poly(A) signals then and now. *Genes Dev.*, **25**, 1770–1782.

Raab, J.R. & Kamakaka, R.T. (2010) Insulators and promoters: closer than we think. *Nat. Rev. Genet.*, **11**, 439–446.

Raasi, S. (2003) Rad23 Ubiquitin-associated Domains (UBA) Inhibit 26 S Proteasome-catalyzed Proteolysis by Sequestering Lysine 48-linked Polyubiquitin Chains. *J. Biol. Chem.*, **278**, 8951–8959.

Raasi, S. & Wolf, D.H. (2007) Ubiquitin receptors and ERAD: a network of pathways to the proteasome. *Semin. Cell Dev. Biol.*, **18**, 780–791.

Raffa, G.D., Cenci, G., Ciapponi, L., & Gatti, M. (2013) Organization and Evolution of Drosophila Terminin: Similarities and Differences between Drosophila and Human Telomeres. *Front. Oncol.*, **3**, 112.

Raffa, G.D., Cenci, G., Siriaco, G., Goldberg, M.L., & Gatti, M. (2005) The putative Drosophila transcription factor woc is required to prevent telomeric fusions. *Mol. Cell*, **20**, 821–831.

Raja, S.J., Charapitsa, I., Conrad, T., Vaquerizas, J.M., Gebhardt, P., Holz, H., Kadlec, J., Fraterman, S., Luscombe, N.M., & Akhtar, A. (2010) The nonspecific lethal complex is a transcriptional regulator in Drosophila. *Mol. Cell*, **38**, 827–841.

Randles, L. & Walters, K.J. (2012) Ubiquitin and its binding domains. *Front. Biosci.*, **17**, 2140–2157.

Ransom, M., Dennehey, B.K., & Tyler, J.K. (2010) Chaperoning histones during DNA replication and repair. *Cell*, **140**, 183–195.

Rath, U., Ding, Y., Deng, H., Qi, H., Bao, X., Zhang, W., Girton, J., Johansen, J., & Johansen, K.M. (2006) The chromodomain protein, Chromator, interacts with JIL-1 kinase and regulates the structure of Drosophila polytene chromosomes. *J. Cell Sci.*, **119**, 2332–2341.

Rath, U., Wang, D., Ding, Y., Xu, Y.-Z., Qi, H., Blacketer, M.J., Girton, J., Johansen, J., & Johansen, K.M. (2004) Chromator, a novel and essential chromodomain protein interacts directly with the putative spindle matrix protein skeletor. *J. Cell. Biochem.*, **93**, 1033–1047.

Rice, J.C., Briggs, S.D., Ueberheide, B., Barber, C.M., Shabanowitz, J., Hunt, D.F., Shinkai, Y., & Allis, C.D. (2003) Different Degrees of Methylation to Define Distinct Chromatin Domains. *Mol. Cell*, **12**, 1591–1598.

Riddle, N.C., Shaffer, C.D., & Elgin, S.C.R. (2009) A lot about a little dot - lessons learned from Drosophila melanogaster chromosome 4. *Biochem. Cell Biol.*, **87**, 229–241.

Ringrose, L., Ehret, H., & Paro, R. (2004) Distinct Contributions of Histone H3 Lysine 9 and 27 Methylation to Locus-Specific Stability of Polycomb Complexes. *Mol. Cell*, **16**, 641–653.

Rogakou, E.P., Pilch, D.R., Orr, A.H., Ivanova, V.S., & Bonner, W.M. (1998) DNA Double-stranded Breaks Induce Histone H2AX Phosphorylation on Serine 139. *J. Biol. Chem.*, **273**, 5858–5868.

Ross, R.J., Weiner, M.M., & Lin, H. (2014) PIWI proteins and PIWI-interacting RNAs in the soma. *Nature*, **505**, 353–359.

Rougvie, a E. & Lis, J.T. (1988) The RNA polymerase II molecule at the 5' end of the uninduced hsp70 gene of D. melanogaster is transcriptionally engaged. *Cell*, **54**, 795–804.

Ruan, J., Ouyang, H., Amaya, M.F., Ravichandran, M., Loppnau, P., Min, J., & Zang, J. (2012) Structural basis of the chromodomain of Cbx3 bound to methylated peptides from histone h1 and G9a. *PLoS One*, **7**, e35376.

Rubertis, F. De, Kadosh, D., Henchoz, S., Pauli, D., Reuter, G., Struhl, K., & Spierer, P. (1996) The histone deacetylase RPD3 counteracts genomic silencing in Drosophila and yeast. *Nature*, **384**, 589–591.

Russell, S.J., Reed, S.H., Huang, W., Friedberg, E.C., & Johnston, S. a (1999) The 19S regulatory complex of the proteasome functions independently of proteolysis in nucleotide excision repair. *Mol. Cell*, **3**, 687–695.

Ryan, R.F., Schultz, D.C., Ayyanathan, K., Singh, P.B., Friedman, J.R., Fredericks, W.J., & Iii, F.J.R. (1999) KAP-1 Corepressor Protein Interacts and Colocalizes with Heterochromatic and Euchromatic HP1 Proteins : a Potential Role for Krüppel-Associated Box − Zinc Finger Proteins in Heterochromatin-Mediated Gene Silencing. *Mol. Cell. Biol.*, **19**, 4366–4378.

Salghetti, S.E., Caudy, a a, Chenoweth, J.G., & Tansey, W.P. (2001) Regulation of transcriptional activation domain function by ubiquitin. *Science*, **293**, 1651–1653.

Sampath, S.C., Marazzi, I., Yap, K.L., Sampath, S.C., Krutchinsky, A.N., Mecklenbräuker, I., Viale, A., Rudensky, E., Zhou, M.-M., Chait, B.T., & Tarakhovsky, A. (2007) Methylation of a histone mimic within the histone methyltransferase G9a regulates protein complex assembly. *Mol. Cell*, **27**, 596–608.

Saunders, A., Werner, J., Andrulis, E.D., Nakayama, T., Hirose, S., Reinberg, D., & Lis, J.T. (2003) Tracking FACT and the RNA polymerase II elongation complex through chromatin in vivo. *Science*, **301**, 1094–1096.

Savitsky, M., Kravchuk, O., Melnikova, L., & Georgiev, P. (2002) Heterochromatin Protein 1 Is Involved in Control of Telomere Elongation in Drosophila melanogaster Heterochromatin Protein 1 Is Involved in Control of Telomere Elongation in Drosophila melanogaster. *Mol. Cell. Biol.*, **22**, 3204–3218.

Sawarkar, R. & Paro, R. (2013) Hsp90@chromatin.nucleus: an emerging hub of a networker. *Trends Cell Biol.*, **23**, 193–201.

Schauber, C., Chen, L., Tongaonkar, P., Vega, I., Lambertson, D., Potts, W., & Madura, K. (1998) Rad23 links DNA repair to the ubiquitin/proteasome pathway. *Nature*, **391**, 715–718.

Schotta, G., Ebert, A., Krauss, V., Fischer, A., Hoffmann, J., Rea, S., Jenuwein, T., Dorn, R., & Reuter, G. (2002) Central role of

Drosophila SU(VAR)3-9 in histone H3-K9 methylation and heterochromatic gene silencing. *EMBO J.*, **21**, 1121–1131.

Sekiguchi, T., Sasaki, T., Funakoshi, M., Ishii, T., Saitoh, Y., Kaneko, S., & Kobayashi, H. (2011) Ubiquitin chains in the Dsk2 UBL domain mediate Dsk2 stability and protein degradation in yeast. *Biochem. Biophys. Res. Commun.*, **411**, 555–561.

Seum, C., Delattre, M., Spierer, A., & Spierer, P. (2001) Ectopic HP1 promotes chromosome loops and variegated silencing in Drosophila. *EMBO J.*, **20**, 812–818.

Sharma, G.G., Hwang, K., Pandita, R.K., Dhar, S., Parenteau, J., Agarwal, M., Worman, H.J., Wellinger, R.J., Tej, K., & Gupta, A. (2003) Human Heterochromatin Protein 1 Isoforms HP1 Hsα and HP1Hsβ Interfere with hTERT-Telomere Interactions and Correlate with Changes in Cell Growth and Response to Ionizing Radiation. *Mol. Cell. Biol.*, **23**, 8363–8376.

Smith, D.F., Sullivan, W.P., Marion, T.N., Zaitsu, K., Madden, B., Mccormick, D.J., & Toft, D. (1993) Identification of a 60-kilodalton stress-related protein , p60 , which interacts with hsp90 and hsp70. *Mol. Cell. Biol.*, **13**, 869–876.

Smith, E. & Shilatifard, A. (2010) The chromatin signaling pathway: diverse mechanisms of recruitment of histone-modifying enzymes and varied biological outcomes. *Mol. Cell*, **40**, 689–701.

Smothers, J.F. & Henikoff, S. (2000) The HP1 chromo shadow domain binds a consensus peptide pentamer. *Curr. Biol.*, **10**, 27–30.

Smothers, J.F. & Henikoff, S. (2001) The Hinge and Chromo Shadow Domain Impart Distinct Targeting of HP1-Like Proteins. *Mol. Cell. Biol.*, **21**, 2555–2569.

Song, K., Jung, Y., Jung, D., & Lee, I. (2001) Human Ku70 interacts with heterochromatin protein 1alpha. *J. Biol. Chem.*, **276**, 8321–8327.

Soria, G. & Almouzni, G. (2013) Differential contribution of HP1 proteins to DNA end resection and homology-directed repair. *Cell Cycle*, **12**, 422–429.

Stewart, M.D., Li, J., & Wong, J. (2005) Relationship between Histone H3 Lysine 9 Methylation , Transcription Repression , and Heterochromatin Protein 1 Recruitment. *Mol. Cell. Biol.*, **25**, 2525–2538.

Stieren, E.S., El Ayadi, A., Xiao, Y., Siller, E., Landsverk, M.L., Oberhauser, A.F., Barral, J.M., & Boehning, D. (2011) Ubiquilin-1 is a molecular chaperone for the amyloid precursor protein. *J. Biol. Chem.*, **286**, 35689–35698.

Strahl, B.D. & Allis, C.D. (2000) The language of covalent histone modifications. *Nature*, **403**, 41–45.

Su, V. & Lau, A.F. (2009) Ubiquitin-like and ubiquitin-associated domain proteins: significance in proteasomal degradation. *Cell. Mol. Life Sci.*, **66**, 2819–2833.

Sugimoto, K., Yamada, T., Muro, Y., & Himeno, M. (1996) Human homolog of Drosophila heterochromatin-associated protein 1 (HP1) is a DNA-binding protein which possesses a DNA-binding motif with weak similarity to that of human centromere protein C (CENP-C). *J. Biochem.*, **120**, 153–159.

Sun, B., Hong, J., Zhang, P., Dong, X., Shen, X., Lin, D., & Ding, J. (2008) Molecular basis of the interaction of Saccharomyces cerevisiae Eaf3 chromo domain with methylated H3K36. *J. Biol. Chem.*, **283**, 36504–36512.

Sun, Y., Jiang, X., Xu, Y., Ayrapetov, M.K., Moreau, L. a, Whetstine, J.R., & Price, B.D. (2009) Histone H3 methylation links DNA damage detection to activation of the tumour suppressor Tip60. *Nat. Cell Biol.*, **11**, 1376–1382.

Tagami, H., Ray-gallet, D., & Nakatani, Y. (2004) Histone H3.1 and H3.3 Complexes Mediate Nucleosome Assembly Pathways Dependent or Independent of DNA Synthesis. *Cell*, **116**, 51–61.

Talbert, P.B. & Henikoff, S. (2010) Histone variants--ancient wrap artists of the epigenome. *Nat. Rev. Mol. Cell Biol.*, **11**, 264–275.

Thiru, A., Nietlispach, D., Mott, H.R., Okuwaki, M., Lyon, D., Nielsen, P.R., Hirshberg, M., Verreault, A., Murzina, N. V, & Laue, E.D.

(2004) Structural basis of HP1/PXVXL motif peptide interactions and HP1 localisation to heterochromatin. *EMBO J.*, **23**, 489–499.

Trempe, J.-F. (2011) Reading the ubiquitin postal code. *Curr. Opin. Struct. Biol.*, **21**, 792–801.

Tycowski, K.T., Shu, M.-D., Kukoyi, A., & Steitz, J. a (2009) A conserved WD40 protein binds the Cajal body localization signal of scaRNP particles. *Mol. Cell*, **34**, 47–57.

Tzeng, T.-Y., Lee, C.-H., Chan, L.-W., & Shen, C.-K.J. (2007) Epigenetic regulation of the Drosophila chromosome 4 by the histone H3K9 methyltransferase dSETDB1. *Proc. Natl. Acad. Sci. U. S. A.*, **104**, 12691–12696.

Vakoc, C.R., Mandat, S. a, Olenchock, B. a, & Blobel, G. a (2005) Histone H3 lysine 9 methylation and HP1gamma are associated with transcription elongation through mammalian chromatin. *Mol. Cell*, **19**, 381–391.

Veraksa, A., Bauer, A., & Artavanis-Tsakonas, S. (2005) Analyzing protein complexes in Drosophila with tandem affinity purification-mass spectrometry. *Dev. Dyn.*, **232**, 827–834.

Verma, R., Oania, R., Graumann, J., & Deshaies, R.J. (2004) Define a Layer of Substrate Selectivity in the Ubiquitin-Proteasome System. *Cell*, **118**, 99–110.

Vermaak, D., Henikoff, S., & Malik, H.S. (2005) Positive selection drives the evolution of rhino, a member of the heterochromatin protein 1 family in Drosophila. *PLoS Genet.*, **1**, 96–108.

Vermaak, D. & Malik, H.S. (2009) Multiple roles for heterochromatin protein 1 genes in Drosophila. *Annu. Rev. Genet.*, **43**, 467–492.

Verschure, P.J., Kraan, I. Van Der, Leeuw, W. De, Vlag, J. Van Der, Carpenter, A.E., & Belmont, A.S. (2005) In Vivo HP1 Targeting Causes Large-Scale Chromatin Condensation and Enhanced Histone Lysine Methylation In Vivo HP1 Targeting Causes Large-Scale Chromatin Condensation and Enhanced Histone Lysine Methylation †. *Mol. Cell. Biol.*, **25**, 4552–4564.

Volpe, T. a, Kidner, C., Hall, I.M., Teng, G., Grewal, S.I.S., & Martienssen, R. a (2002) Regulation of heterochromatic silencing and histone H3 lysine-9 methylation by RNAi. *Science*, **297**, 1833–1837.

Wada, T., Takagi, T., Yamaguchi, Y., Watanabe, D., & Handa, H. (1998) Evidence that P-TEFb alleviates the negative effect of DSIF on RNA polymerase II-dependent transcription in vitro. *EMBO J.*, **17**, 7395–7403.

Wade, S.L. & Auble, D.T. (2010) The Rad23 ubiquitin receptor, the proteasome and functional specificity in transcriptional control. *Transcription*, **1**, 22–26.

Wade, S.L., Poorey, K., Bekiranov, S., & Auble, D.T. (2009) The Snf1 kinase and proteasome-associated Rad23 regulate UV-responsive gene expression. *EMBO J.*, **28**, 2919–2931.

Wakimoto, B. & Hearn, M. (1990) The effects of chromosome rearrangements on the expression of heterochromatic genes in chromosome 2L of Drosophila melanogaster. *Genetics*, **125**, 141–154.

Wang, C., Li, S., Januschke, J., Rossi, F., Izumi, Y., Garcia-Alvarez, G., Gwee, S.S.L., Soon, S.B., Sidhu, H.K., Yu, F., Matsuzaki, F., Gonzalez, C., & Wang, H. (2011) An ana2/ctp/mud complex regulates spindle orientation in Drosophila neuroblasts. *Dev. Cell*, **21**, 520–533.

Wang, F. & Higgins, J.M.G. (2013) Histone modifications and mitosis: countermarks, landmarks, and bookmarks. *Trends Cell Biol.*, **23**, 175–184.

Wang, G., Ma, a, Chow, C.M., Horsley, D., Brown, N.R., Cowell, I.G., & Singh, P.B. (2000) Conservation of heterochromatin protein 1 function. *Mol. Cell. Biol.*, **20**, 6970–6983.

Wang, H., Lim, P.J., Yin, C., Rieckher, M., Vogel, B.E., & Monteiro, M.J. (2006) Suppression of polyglutamine-induced toxicity in cell and animal models of Huntington's disease by ubiquilin. *Hum. Mol. Genet.*, **15**, 1025–1041.

Wang, K.C. & Chang, H.Y. (2011) Molecular mechanisms of long noncoding RNAs. *Mol. Cell*, **43**, 904–914.

Wang, Y., Zhang, W., Jin, Y., Johansen, J., & Johansen, K.M. (2001) The JIL-1 tandem kinase mediates histone H3 phosphorylation and is required for maintenance of chromatin structure in Drosophila. *Cell*, **105**, 433–443.

Watkins, J.F., Sung, P., Prakash, L., & Prakasht, S. (1993) The Saccharomyces cerevisiae DNA Repair Gene RAD23 Encodes a Nuclear Protein Containing a Ubiquitin-Like Domain Required for Biological Function. *Mol. Cell. Biol.*, **13**, 7757–7765.

Weake, V.M. & Workman, J.L. (2008) Histone ubiquitination: triggering gene activity. *Mol. Cell*, **29**, 653–663.

Weake, V.M. & Workman, J.L. (2010) Inducible gene expression: diverse regulatory mechanisms. *Nat. Rev. Genet.*, **11**, 426–437.

Widom, J. & Klug, A. (1985) Structure of the 300A Chromatin Filament : X-Ray Diffraction from Oriented Samples. *Cell*, **43**, 207–213.

Wilkinson, C.R., Seeger, M., Hartmann-Petersen, R., Stone, M., Wallace, M., Semple, C., & Gordon, C. (2001) Proteins containing the UBA domain are able to bind to multi-ubiquitin chains. *Nat. Cell Biol.*, **3**, 939–943.

Williams, S.P., Athey, B.D., Muglia, L.J., Schappe, R.S., Gough, A.H., & Langmore, J.P. (1986) Chromatin fibers are left-handed double helices with diameter and mass per unit length that depend on linker length. *Biophys. J.*, **49**, 233–248.

Wood, A., Schneider, J., Dover, J., Johnston, M., & Shilatifard, A. (2005) The Bur1/Bur2 complex is required for histone H2B monoubiquitination by Rad6/Bre1 and histone methylation by COMPASS. *Mol. Cell*, **20**, 589–599.

Wyce, A., Xiao, T., Whelan, K. a, Kosman, C., Walter, W., Eick, D., Hughes, T.R., Krogan, N.J., Strahl, B.D., & Berger, S.L. (2007) H2B ubiquitylation acts as a barrier to Ctk1 nucleosomal recruitment prior to removal by Ubp8 within a SAGA-related complex. *Mol. Cell*, **27**, 275–288.

Wysocka, J., Reilly, P.T., & Herr, W. (2001) Loss of HCF-1 − Chromatin Association Precedes Temperature-Induced Growth Arrest of tsBN67 Cells Loss of HCF-1 – Chromatin Association Precedes Temperature- Induced Growth Arrest of tsBN67 Cells. *Mol. Cell. Biol.*, **21**, 3820–3829.

Yahi, H., Fritsch, L., Philipot, O., Guasconi, V., Souidi, M., Robin, P., Polesskaya, A., Losson, R., Harel-Bellan, A., & Ait-Si-Ali, S. (2008) Differential cooperation between heterochromatin protein HP1 isoforms and MyoD in myoblasts. *J. Biol. Chem.*, **283**, 23692–23700.

Yamamoto, K. & Sonoda, M. (2003) Self-interaction of heterochromatin protein 1 is required for direct binding to histone methyltransferase, SUV39H1. *Biochem. Biophys. Res. Commun.*, **301**, 287–292.

Yang, J. & Corces, V.G. (2012) Insulators, long-range interactions, and genome function. *Curr. Opin. Genet. Dev.*, **22**, 86–92.

Ye, Q. (1997) Domain-specific Interactions of Human HP1-type Chromodomain Proteins and Inner Nuclear Membrane Protein LBR. *J. Biol. Chem.*, **272**, 14983–14989.

Yuan, G. & Zhu, B. (2012) Histone variants and epigenetic inheritance. *Biochim. Biophys. Acta*, **1819**, 222–229.

Yunis, J.Y. & Yasmineh, W.G. (1971) Heterochromatin , Satellite DNA , and Cell Function. *Science*, **174**, 1200–1209.

Zarebski, M., Wiernasz, E., & Dobrucki, J.W. (2009) Recruitment of heterochromatin protein 1 to DNA repair sites. *Cytometry. A*, **75**, 619–625.

Zeitlinger, J., Stark, A., Kellis, M., Hong, J.-W., Nechaev, S., Adelman, K., Levine, M., & Young, R. a (2007) RNA polymerase stalling at developmental control genes in the Drosophila melanogaster embryo. *Nat. Genet.*, **39**, 1512–1516.

Zeng, W., Ball, A.R., & Yokomori, K. (2010) HP1: heterochromatin binding proteins working the genome. *Epigenetics*, **5**, 287–292.

Zhang, D., Chen, T., Ziv, I., Rosenzweig, R., Matiuhin, Y., Bronner, V., Glickman, M.H., & Fushman, D. (2009) Together, Rpn10 and Dsk2

can serve as a polyubiquitin chain-length sensor. *Mol. Cell*, **36**, 1018–1033.

Zhang, D., Wang, D., & Sun, F. (2011) Drosophila melanogaster heterochromatin protein HP1b plays important roles in transcriptional activation and development. *Chromosoma*, **120**, 97–108.

Zhang, P., Du, J., Sun, B., Dong, X., Xu, G., Zhou, J., Huang, Q., Liu, Q., Hao, Q., & Ding, J. (2006) Structure of human MRG15 chromo domain and its binding to Lys36-methylated histone H3. *Nucleic Acids Res.*, **34**, 6621–6628.

Zhao, K., Hart, C.M., & Laemmli, U.K. (1995) Visualization of chromosomal domains with boundary element-associated factor BEAF-32. *Cell*, **81**, 879–889.